STUDIES ON VOLUME CHANGE MOVEMENTS IN HIGH PI CLAYS FOR BETTER DESIGN OF LOW VOLUME PAVEMENTS

by

THAMMANOON MANOSUTHIKIJ

Presented to the Faculty of the Graduate School of
The University of Texas at Arlington in Partial Fulfillment
of the Requirements for the Degree of

DOCTOR OF PHILOSOPHY

THE UNIVERSITY OF TEXAS AT ARLINGTON

August 2008

ACKNOWLEDGEMENTS

The efforts of many have led to the successful completion of this dissertation and my time at the University of Texas at Arlington. I would like express my sincere appreciation to my advising professor, Dr. Aanad J. Puppala, for his excellent guidances and encouragements through out this research study. His intelligence and immeasurable effort always inspire me. In addition, his support, patience and most of all his friendship throughout this research are truly cherished.

I would also like to convey my gratitude to Dr. Laureano R. Hoyos for his suggestions, guidance and friendship through the research. I also would like to extend my gratitude to Dr. Ali Abolmaali, Dr. Mohammad Najafi, and Dr. Chein-Pai Han for accepting to be on examination committee. I would also like to thank the above faculty for introducing me to various fields of study and my interactions during course works.

This research is supported by TxDOT under the project no. 0-5430. The author is grateful for the research assistantship granted. Author would like to acknowledge Dr. Soheil Nazarian, Imad Abdallah, Yaqi Wanyan and Anup Sabnis from University of Texas at El Paso for excellent cooperations throughout the research.

Appreciations are broadened to all the members of Department of Civil and Environmental Engineering staff, Ms. Barbara Wallace, Ms. Ginny Bowers, Ms. Sarah, Ms. Diane Copeman, Mr. Lewis, and Mr. Paul Shover for their unconditional help in various aspects during my course of study at UTA.

I like to extend my sincere appreciations to my colleagues Chakkrit Sirivitmitri, Thornchaya Wejrangsikul, Ekarut Archeewa, Artit Laikram, Raja Sekhar Madhyannapu, Baska Chittoori, Samuel Rosenberg, Srujan chikyala and Mehdi for their sincere supports, encouragement and contribution in laboratory and field studies of this research work. The value of their friendship will not be forgotten. My special thanks are due to Napat Intharasombat for his support and help at the time of my application process for Ph.D admission.

Finally, I would like to extend my utterly appreciation to my father, Chana Manosuthikij who never departed from my heart, my beloved mother, sisters and brothers. I could never thank you enough for your support and understanding during my years of schooling. The supports and love of my family throughout this process kept cheering me up. You are the best family that I can dedicate my life to.

July 10, 2008

ABSTRACT

STUDIES ON VOLUME CHANGE MOVEMENTS IN
HIGH PI CLAYS FOR BETTER DESIGN OF
LOW VOLUME PAVEMENTS

Thammanoon Manosuthikij, PhD.

The University of Texas at Arlington, 2008

Supervising Professor: Anand J. Puppala

Numerous low- to medium-volume roads such as Farm Market (FM) roads constructed on expansive clay subgrades, especially in the eastern and central Texas, encounter severe pavement cracking and premature loss of serviceability. The maintenance costs, in some cases, are greater than the initial construction costs. The roads built on problematic expansive soils often become distressed due to volume changes associated with seasonal moisture content fluctuations. This dissertation research was attempted to evaluate models that predict volume changes movements of

the expansive or highly plastic soils and also develop new models that could provide better prediction of volume change movements in expansive clays.

In this research, laboratory investigations and field studies were conducted on soils from four different locations in which highly plastic and expansive clays were encountered. These sites were located in Fort Worth, San Antonio, Paris and Houston. Laboratory tests conducted included basic soil properties, chemical and clay mineralogy and engineering soil tests. All studied soils exhibited a high degree of volumetric expansion (more than 15%). Field monitoring programs composed of elevation surveys for various environmental conditions, soil moisture and soil suction monitoring, and identifying the new cracking in pavements at all four sites.

Results showed the site environment conditions such as climate, large trees and drainage ditch have strong influence on expansive soil movements and pavement cracking. The details of the environmental effects including moisture conditions at which pavement cracks can be initiated are discussed.

Finally, pavement elevation changes monitored from each sites were compared with various heave analytical type prediction models proposed by previous researches. In addition, a Finite Element Method (FEM) model with the incorporation of soil water characteristic data was used to predict heaving the test sections. Comparisons with measured data showed that the numerical FEM model predicted swell potentials close to the field monitored soil movements, explaining the significance and effectiveness of the numerical modeling of swelling behavior of unsaturated soils. Other regression correlations for improved predictions of soil movements are also included.

TABLE OF CONTENTS

LIST OF ILLUSTRATIONS

LIST OF TABLES

CHAPTER 1

INTRODUCTION

1.1 Introduction

A number of districts, especially in east and central Texas, construct their low-volume roads on clays with high plasticity index (PI). Observations by the district transportation officials and engineers indicate that a large number of these roads do not last as long as they are designed for. A significant amount of repair work is required to maintain and rehabilitate these roads. Repair costs alone are close to a few millions of dollars annually. It is therefore imperative to improve the design and laboratory procedures to address subsoil conditions and then design pavements accordingly to extend the life expectancy of these roads.

The numerous available prediction models for volume changes of expansive soils need to be reviewed as these volume changes are attributed to majority of the distress recorded on the low volume roads built on high plastic soils. These models and their predictions should be compared with the measured data from the field sites which need to be selected and then monitored for volume changes.

The narrow width of the low-volume roads, locations of large trees as well as the poor surrounding drainage conditions accelerates the intrusion of water and as such shortens pavement life span by inducing softening of shrinkage crack induced

subgrades. In the summer months, the soil will dry out with time. Such loss of moisture results in significant increase in the strength and modulus of the clay which has a positive impact on the life of the pavement. However, the increase in stiffness results in the increase in the brittleness of the clay. The loss of moisture also contributes to the shrinkage cracking known as desiccated cracking in the clay. This tendency of clay to shrink along with the increase in the brittleness will cause cracks, which will propagate towards the surface of the road. These cracks, sometimes an inch or more wide, act as conduit for water to penetrate more rapidly in the subgrade, causing a vicious circle of continuous damage to pavement structures (Dar et al., 2007).

The consensus among researchers and practitioners with considerable experience in the area of high-PI clay is that the most important factor is to maintain the moisture content of the clay as constant as possible (Chen et al., 2004). Impacts of parameters such as widening the right of way, locations of trees and vegetations, appropriate drainage design, and other appropriate measures for maintaining the moisture content of the subgrades should be thoroughly studied and included in the present dissertation work. Also, ways of retarding the cracking of the pavement (e.g., the use of geosynthetics or reflective crack relief membranes/layers or encapsulated layers or vertical cutoff systems to maintain same moisture levels), though is not of focus of this dissertation, should be studied comprehensively.

1.2 Research Objectives

The premature failure of low volume roads on high plastic clays using the current design procedures and construction methods is significantly impacting the pavement maintenance division of Texas Department of Transportation or TxDOT and other public work groups. In order for better understanding of the causes of this pavement distresse, this dissertation research is attempted with the following specific objectives:

1. To identify the most significant soil parameters directly related to the volume changes movements of the proposed expansive and high plastic soils.

2. To propose simple and cost effective laboratory test procedures that simulate field conditions to quantify the parameters that are linked to volume changes of the above mentioned soils.

3. To review, evaluate and recommend prediction models that are effectively used for predict swell-shrinkage both in the laboratory and in the field conditions.

4. To quantify the impact of environmental-related and site-related parameters that is detrimental to the stable moisture regime in the subgrades by instrumenting field pavement sections with the advanced moisture, and suction instrumentation.

5. To understand the moisture content variations and moisture content levels as well as total suction levels that contribute to subgrade and eventual pavement cracking.

6. Develop numerical and analytical models that can provide better predictions of volume changes of subsoils in both swell and shrinkage environment.

The results from this study should provide tools and recommendations for an improved pavement design procedure that will provide more realistic layer thicknesses as well as minimize rehabilitation and maintenance of roads while in service.

1.3 Organization of the Dissertation

This dissertation consists of eight chapters.

Chapter 1 provides an introduction, background history explaining the significance of the project, research objectives, and organization to provide a framework of the completed research.

Chapter 2 presents a literature review on expansive soil behaviors, properties and their swell prediction models. Environmental conditions for example climate, drainage ditches, vegetations and road conditions that affected premature cracking of pavement and different maintenance remedies currently used are also discussed in this chapter.

Chapter 3 covers laboratory testing program designed to determine the properties relating to volume change behavior of expansive soil samples. The experimental program includes basic soil properties tests, chemical and mineralogy tests, and engineering tests on the soils from these locations. A summary of the laboratory procedures, equipments used and results as well as a ranking analysis are presented in this chapter.

Chapter 4 deals with the analysis of the laboratory results and also laboratory predictions of the degree of shrinking and swelling of soils. Statistics analysis is also introduced as a simple technique to identify and predict the volume changes. Empirical correlations of swell and shrinkage movements are also introduced based on the present soil test database.

Chapter 5 presents an overview of field studies that necessary for analyzing environmental impacts on pavement conditions including environmental site conditions, site selection, site information, field instrumentations systems, and field conditions monitoring.

Chapter 6 presents information pertaining to results of the field studies. Such information includes the effects of soil moisture fluctuations, soil matric suctions, environmental site conditions such as rainfall characteristics, location of roadside trees and drainage ditches.

Chapter 7 focuses on conducting investigations on swell-shrinkage movements in the field for each soil type by utilizing both analytical and numerical prediction models. Both types of models included laboratory swell-shrinkage data, soil matric suctions with corresponding moisture changes and field overburden pressures into account in the analysis.

Chapter 8 presents the important conclusions of the experimental and field research studies and future recommendations.

CHAPTER 2

LITERATURE REVIEW

2.1 Introduction

Natural expansive soils have been found in many places around the world. Expansive soils undergo large volumetric changes due to moisture fluctuations from seasonal variations. These volumetric changes cause swell and shrinkage movements in soils, which in turn will inflict severe damage to structures built above them (Nelson and Miller, 1992). Examples of expansive clays include high plasticity or high PI clays, over consolidated clays rich with montmorillonite clay minerals, and shales.

It was reported that the expansive soils damages to structures, particularly light buildings and pavements that are much greater than the damages caused by other natural disasters like earthquakes and floods (Jones and Holtz, 1973). Several countries in the world, including the United States, Israel, India, South Africa, and Australia, have reported infrastructure damage problems caused by the movements of expansive soils. These damages are estimated to cost several billions of dollars annually (Nelson and Miller 1992).

Numerous roads constructed on expansive clay subgrades especially in the east and central Texas, though over-designed, still encounter severe pavement cracking with short serviceability life. The maintenance costs, in some cases, are even more than their

construction costs. Pavements or roads that are constructed on soft and problematic soils have frequent maintenance problems. Brown (1996) presented a state-of-the-art paper on the use of soil mechanics principles in pavement design that is a great basis for the project at hand. He reviewed the response of clays in the context of the requirements for design. The subgrade soils, in particular expansive soils, should be better accounted for both during design and construction of the roads.

Total or differential volume movements caused by swell or shrinkage strains of expansive soils can cause damage to the highways (Chen, 1988). Differential movements induce large changes in moments and shear forces in the structures, which lead to failure in both rigid and flexible pavements. It is because these forces are not accounted for the rigid pavement design practice and flexible pavement materials that are weak in flexural strength. These soil movements in highway environment are attributed to subgrade moisture variation conditions that include the widening of the right of way, vicinity of trees close to pavement systems. The latter condition will draw more moisture from the underneath pavements, resulting in the shrinkage problems in soils, lack of adequate roadside ditches for drainage, and poor drainage conditions.

Damages sustained by the pavements include distortion and cracking of pavements in all directions as well as heave related bumps which cause ride discomforts. The cracks developed in pavements will further allow intrusion of moisture to subsoils, which results in the weakening of subsoils and loss of foundation support to pavements. Figure 2.1 and Figure 2.2 present various types of heave related to distresses noted in pavements. Overall, the magnitude and extent of damages to pavement

structures can be extensive, impairing the usefulness of the roads, and practically making them uncomfortable for riding. Maintenance and repairs requirements can be extensive that often result in excessive capitol costs.

The factors influencing the shrink-swell potential of a soil can be categorized in three different groups: soil characteristics (clay mineral, plasticity, soil suction and dry density), environmental factors (climate, groundwater, vegetation and drainage) and state of stress (Nelson and Miller, 1992).

Figure 2.1 Heaving problems

Figure 2.2 Pavement distresses from expansive soil movements

2.2 Swelling and Shrinkage Variations

2.2.1 Swell Strain Properties

In conventional engineering practice, majority of laboratory swell tests are conducted in Oedometer type apparatus with low seating pressures. Swell properties such as swell strain and swell pressure of expansive soils are dependent on three factors: (i) soil properties such as compaction or natural moisture content variation, dry density, and plasticity index, (ii) environmental conditions including temperature and humidity conditions and (iii) natural overburden pressure conditions. Because of the influence of these factors, several expansive soil characterization methods were developed in the literature (Puppala et al., 2004). These methods are mainly based on (1) swell strain

and pressure measurements, (2) plasticity properties, and (3) other correlations using activity and compaction properties.

These characterization methods often create dilemmas for practitioners since swell strain measurements and swell prediction models developed for certain conditions are not appropriate for other conditions. Rao and Smart (1980) evaluated four different correlations using ten different soils and he showed that none of the correlations were able to match the values. Snethen (1984) reported similar experiences by testing 20 highly expansive soils based on 17 models published in the literature. Despite these limitations, the models can still be used prehensively and independently verified for the conditions encountered in the state of Texas.

Formulated by the researchers at The University of Texas at Arlington (UTA), a three-dimensional free swell test did not only provide a reasonable representation of the soil maximum volumetric swell potential but also yield the reliable and repeatable test results (Punthutaecha et al., 2006). This test was conducted to investigate the maximum vertical, radial and volumetric swell potentials. In the testing, a specimen of 4.1-in. diameter and 4.5-in. height was placed between two porous stones at the top and bottom, covered by a rubber membrane, fully inundated with water at both ends and monitored for the vertical and radial swell movement until there was no further significant swell (Figure 2.3). The radial swell movement was simply measured by using Pi tape at the times of recording. Test results were expressed as the percentage of swell strain versus time. Details of these procedures are presented in the chapter 3.

Figure 2.3 Three-dimensional free swell test setup

2.2.2 Shrinkage Properties

In the present practice, expansive soils are mainly characterized based on swell characterization tests instead of shrinkage tests that are limitedly used in practice. However, it is well known that the shrinkage cracking of expansive soils in the dry environments lead to increased heaving in wet conditions. It is because surficial shrinkage cracks will allow much more moisture ingress into the underlying expansive soils and have further heaving occurred. Poor (1974) noted expansive soils that are located in regions where prolonged hot dry periods are followed by cooler and wet periods would have maximum distress to pavements and structures. Also, Wray and Ellepola (1994) described that significant large lateral stresses is anticipated when the high PI clays are shrinking. Hence, when characterizing expansive subgrades, it is

equally important to understand volumetric shrinkage strain potentials and shrinkage induced pressures of soils along with their swell potentials.

Researchers and practitioners currently use linear shrinkage strain and Atterberg Limit tests to measure and interpret shrinkage strain potential or cracking behavior of soils. These methods are considered poor since they test low amounts of soils, measure linear strains in rigid wall boxes that restrain warping movements in soils, and they do not address or simulate compaction moisture levels in the field.

Due to limitations in the linear shrinkage bar test, researchers propose a new test method. It is developed at UTA of using cylindrical compacted soil specimens for subjecting them to drying process and then measuring the volumetric, axial and radial shrinkage strains using digital imaging technology. This test offers several advantages over conventional linear shrinkage bar test such as reducing interference of boundary conditions on shrinkage, allowing larger amount of soil being tested, and simulating the compaction states of moisture content - dry density conditions. This method is recently published in ASTM geotechnical testing journal (Puppala et al., 2004), signifying the importance of this method being accepted by the researchers and practitioners. Details of these procedures are presented in the chapter 3.

2.2.3 Swell Pressure

The swell pressure of expansive soils is commonly determined by restraining the soil specimen from undergoing any volume changes under fully soaked conditions (under constant volume method). The surcharge loads added to the soil specimen to keep it under constant volume conditions is determined. The swell pressure value is estimated from the information of surcharge loads and sample dimensions. There are different test methods that can be used to measure swell pressures: (i) Conventional consolidation test procedure which yields an upper bound value; (ii) Method of equilibrium void ratio at different consolidation pressures, which gives the least swell pressure; and, (iii) Constant volume method (CV method), which yields an intermediate value. Further details on these test methods are available in Ohri (2003).

Soils with swell pressures below 0.4 ksf are regarded as low swelling soils. Soils with swell pressures 7.9 ksf or higher are classified as high swelling soils. Soils with swelling pressures values higher than 40.3 ksf are occasionally encountered in real field conditions (Peck et al., 1974). The characterization of swell pressure also depends on the overburden pressure conditions from the infrastructure. The swelling pressure of expansive soils decreases with an increase in the overburden pressure and there will be no heave in expansive soils if the overburden pressure is equal to the swell pressure of the expansive soil.

Hence, it is important to consider swell pressures in the design of structures including pavements. For example, while evaluating the stability of rigid pavement systems, it is important to take into account the swell pressures if an expansive soil is

encountered as a foundation material. Currently, TxDOT does not have a standard test procedure for swell pressure estimation. Hence, an attempt was made in this research to determine the swell pressure potentials of expansive subsoils encountered in the state of Texas. Details of these procedures are presented in the chapter 3.

2.2.4 Soil Suction

2.2.4.1 Overview

Expansive soils, which are primarily unsaturated soils, are also influenced by environmental conditions including temperature and humidity variations. These variations influence swell potentials by changing the suction potentials of unsaturated expansive soils. Hence, suction measurements are recently used to better characterize heave potentials of expansive soils. Soil suction is a macroscopic property which indicates the degree of affinity of the soil towards water. The suction changes associated with the movement of water in the liquid and vapor phases are called matric suction and osmotic suction, respectively. The total suction is equal to the sum of matric and osmotic suction.

$$\psi = (u_a - u_w) + \pi \qquad (1)$$

Where

ψ = Total suction

u_a = Pore-air pressure

u_w = Pore-water pressure

π = Osmotic suction

2.2.4.2 Matric Suction

By definition, matric suction is a capillary component of free energy. In suction term, it is the equivalent suction derived from the measurement of the partial pressure of the water vapor in equilibrium with solution identical in composition with the soil water (Aitchison, 1965). Matric suction is generally related to the surrounding environment and it may vary from time to time. Blight (1980) illustrated that the variations in the suction profile depend upon several factors such as ground surface condition, environmental conditions, vegetation, water table and permeability of the soil profile.

Ground surface condition: the matric suction below an uncovered ground surface is affected by environmental changes. Dry and wet seasons cause variation in suction, particularly suction near to the ground surface. In the real field conditions, suction beneath a covered ground surface is more constant with time than beneath an uncovered surface (Fredlund and Rahardjo, 1993). The matric suction in the soil would increase during the dry seasons and decrease during the wet seasons. Maximum changes in soil suctions occur near the ground surface (Fredlund and Rahardjo, 1993).

Vegetation: vegetation on the ground surface has the ability to apply a tension to the pore-water up to 1-2 MPa through the evapotransiration process. Evapotranspiration results in the removal of water from the soil and an increase in the matric suction. However, the evapotranspiration rate is the function of climate, the vegetation, and the depth of the root zone (Fredlund and Rahardjo, 1993).

Water table: the depth of the water table influences the magnitude of the matric suction. The deeper the water table, the higher the possible matric suction (Fredlund and Rahardjo, 1993).

Permeability of the soil profile: the permeability of soil represents its ability to transmit and drain water. This is the ability of the soil to change matric suction as the environment changes (Fredlund and Rahardjo, 1993).

2.2.4.3 Osmotic Suction

Osmotic suction is commonly related to the salt content in the pore-water, which is present in both saturated and unsaturated soils. Aitchison (1965) defined osmotic suction as "Osmotic (or solute) component of free energy is the equivalent suction derived from the measurement of the partial pressure of the water vapor in equilibrium with free pure water."

The osmotic suction pressure has an effect on the mechanical behavior of the soil in both the saturated and unsaturated zones, but is normally neglected. Fredlund (1989, 1991), Fredlund and Rahardjo (1993) discussed its reasons for the practice. Mostly the changes in matric suction are the geotechnical problems. Consequently, if the pore air pressure is equal to the atmospheric pressure, the total pressure would become equal to the negative pore pressure. However, if salts are present in soils, then the osmotic component of suction must be taken into account.

2.2.4.4 Suction Measurements

(a) Filter Paper Method

Quantitative ash-free filter papers exhibit a consistent and predictable relationship between water content and suction (Nelson and Miller, 1992). Filter paper method have been used routinely by the Water Resources Division of the U.S. Geological Survey (USGS) for many years (McQueen and Miller, 1968).

In this method, a sample of the soil along with a calibrated filter paper is placed in a closed container constructed of non-corrosive material. The filter paper should not be in contact with the soil. The soil sample and filter paper are allowed to equilibrate for a period of at least 7 days at a constant temperature. After the equilibration period, the filter paper is removed and its water content is determined by precise weightings ($\pm$ 0.0001 g) before and after oven drying.

The filter paper method can be used over a wide range of suctions up to approximately 150,000 psi (10^6 kPa). It has been used for a number of investigations of soil water relationships and it has been found to produce good results in field investigations (e.g., McKeen, 1980; Snethen and Johnson, 1980; Hamberg, 1985).

The filter paper technique is based on the principle that the relative humidity inside the container will be controlled by the soil water content and suction. The filter paper will absorb moisture until it comes into equilibrium with the relative humidity inside the container for non-contact technique and soil water content for contact technique (see Figure 2.4). After equilibrium has been reached between the soil water, the filer paper, and the relative humidity in the container, the suction in the filter paper

will be the same value as that in the soil. The humidity in non-contact case is influenced by both the osmotic and matric components of the soil suction (Fredlund and Rahardjo, 1993). Consequently, this technique measures the total suction and not just the matric suction. On the other hand, the equilibrium water content of the filter paper corresponds to the matric suction of the soil when the paper is placed in contact with the water in the soil (Fredlund and Rahardjo, 1993). Therefore, the same calibration curve is used for both the matric and total suction measurements (Figure 2.5). Standard quantitative filter papers have a bilinear relationship between suction and water content. Calibrations have been determined for different papers, but the most commonly used paper is the Schleicher and Schnell, No. 589, White Ribbon type, or its equivalent.

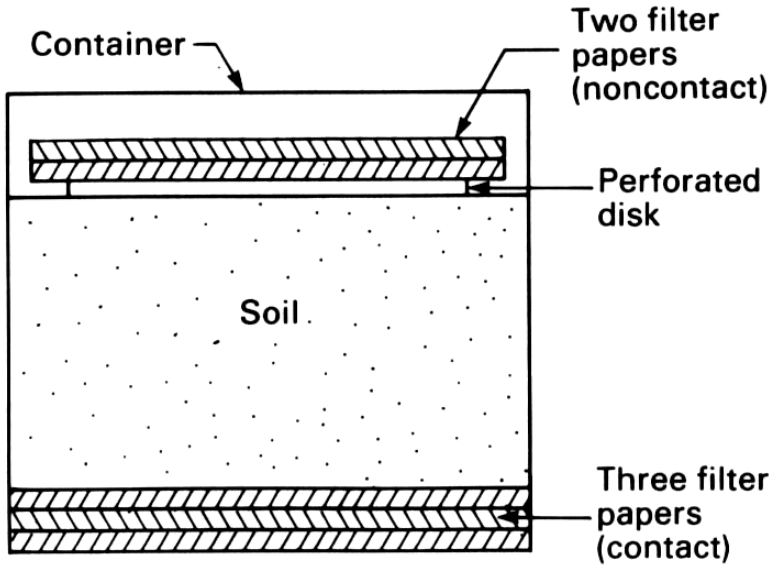

Figure 2.4 Contact and non-contact filter paper methods for measuring matric and total suction, respectively (Al-Khafaf and Hanks, 1974)

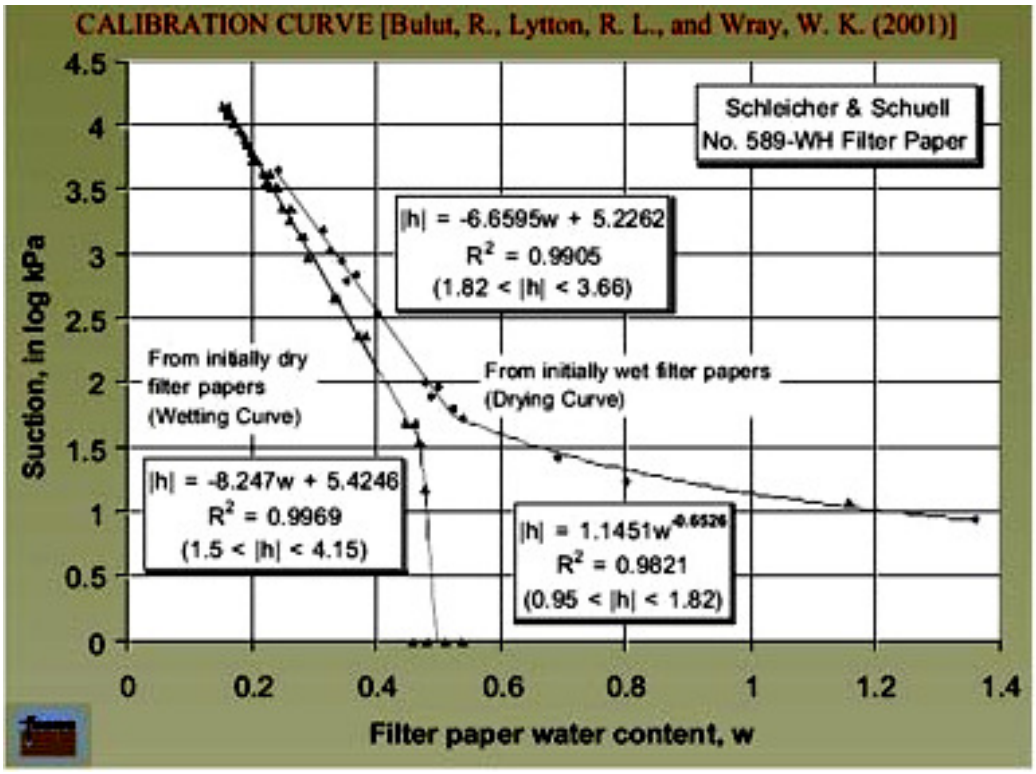

Figure 2.5 Calibration curves (Bulut, Lytton and Wray, 2001)

The advantage of the filter paper method is its simplicity and applicable usage in wide range of suctions. The disadvantage of this method is the high degree of accuracy required for weighting the filter paper (Nelson and Miller, 1992).

(b) Pressure Plates

Figure 2.6 shows the schematic of a typical pore water extraction testing setup using a pressure plate apparatus. The primary components of the system are a steel plate pressure vessel and a saturated High Air Entry (HAE) ceramic plate. As shown, a small water reservoir is formed beneath the plate using an internal screen and a neoprene diaphragm. The water reservoir is vented to the atmosphere through an outflow tube located on top of the plate, thus allowing the air pressure in the vessel and the water

pressure in the reservoir to be separated across the air-water interfaces bridging the saturated pores of the HAE material (Lu and Likos, 2004).

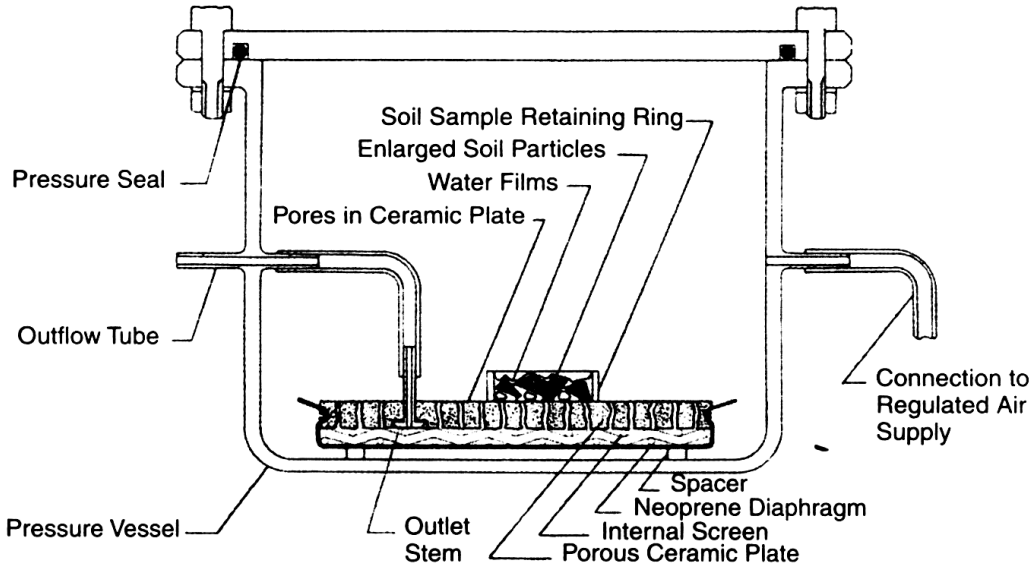

Figure 2.6 Schematic drawing of pressure plate apparatus
(Soil-Moisture Equipment Corp., 2003)

In general, specimens are initially saturated, typically by applying a partial vacuum to the air chamber and allowing the specimens to imbibe water from the underlying reservoir through the ceramic disk. Air pressure in the vessel is then increased to some desired level while pore water is allowed to drain from the specimens in pursuit of equilibrium. The outflow of water is monitored until it ceases, the pressure vessel is opened, and the water content of one or more of the specimen is measured, thus generating one point on the soil-water characteristic curve. Subsequent increments in air pressure are applied to generate addition points on the curve using the other specimen.

(c) Thermal Conductivity Sensors

Thermal properties of a soil have been found to be indicative of the water content of a soil. Water is a better thermal conductor than air. The thermal conductivity of a soil increases with an increasing water content. This is particularly true where the change in water content is associated with a change in the degree of saturation of the soil (From Fredlund and Rahardjo, 1993).

A thermal conductivity sensor consists of a porous ceramic block containing a temperature to sense element and a miniature heater (Figure 2.7). The thermal conductivity of the porous block varies in accordance with the water content of the block. The water content of the porous block is dependent upon the matric suctions applied to the block by the surrounding soil. Therefore, the thermal conductivity of the porous block can be calibrated with respect to applied matric suction (Fredlund and Rahardjo, 1993).

Thermal conductivity measurements are performed by measuring heat dissipation within the porous block. A controlled amount of heat is generated by the heater at the center of the block. A portion of the generated heat will be dissipated throughout the block. The amount of heat dissipation is controlled by the presence of water content of the block. In the other words, more heat will be dissipated as the water content in the block increases (Fredlund and Rahardjo, 1993).

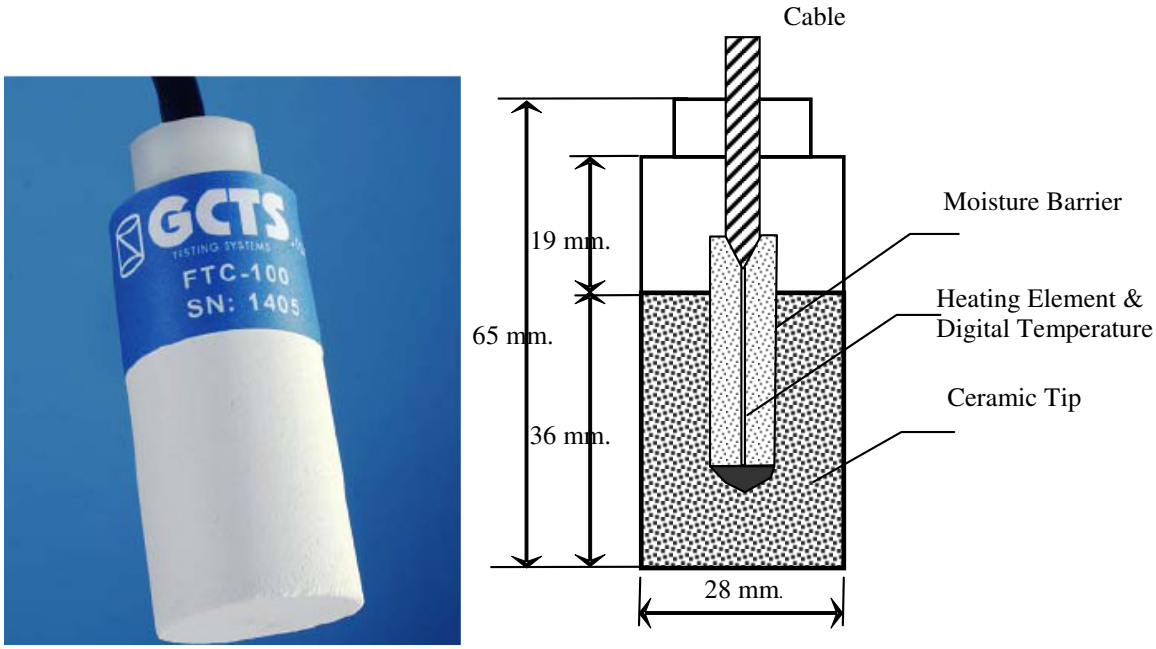

(a) (b)

Figure 2.7 (a) FTC sensor (b) FTC sensor's schematic
(From http://www.gcts.com, Accessed July 17, 2007)

The undissipated heat will result in a temperature rise at the center of the block. The temperature rise is measured by the sensing element after a specific time interval, and its magnitude is inversely proportional to the water content of the porous block. The measured temperature rise is expressed in terms of a voltage output (Fredlund and Rahardjo, 1993).

A list of suction measurement methods, the component of soil suction measured, valid ranges, and constraints associated with these methods are presented in Table 2.1. As reflected in the table, each method has its own limitations. Psychrometers are less sensitive in the low suction ranges that require frequent re-calibration and sensitive to temperature of surrounding environment that require

frequent maintenance. Filter paper measurements are difficult to automate while the tensiometers function well in the low suction range but require daily maintenance.

Table 2.1 Methods for measuring total and matric suction
*(*Rahardjo and Leong (2006); Stenke and Gallipoli (2006); Lu and Likos (2004)

Device	**Suction measured**	**Range (kPa)**	**Principal Constraints**
Standard Tensiometer	Matric	0 to 90	Required daily maintenance. Range in suction is limited by the air-entry value of ceramic.
Thermister Psychrometers	Total	100 to 10,000	Poor sensitivity in the low suction range. Frequent re-calibration is required.
Transistor Psychrometers	Total	200 to 18,000	Accuracy is very user-dependent. Highly effected by temperature changes in the surrounding environment.
Thermocouple Psychrometers	Total	100 to 7,500	Affected by temperature fluctuations and gradients. Sensitivity deteriorates with time.
Filter Paper (non-contact)	Total	400 to 30,000	Calibration is sensitivity to the equilibrium time.

Table 2.1 - Continued

Device	Suction measured	Range (kPa)	Principal Constraints
Filter Paper (in-contact)	Matric	Entire range	Automation of the procedure is difficult.
Pressure Plate (Null technique)	Matric	0 to 1500	Range of suction limited by the air-entry value of the plate. Long equilibration time for Clay.
Original Thermal Conductivity Sensors	Matric	0 to 1,000+	High failure rate. Fragile ceramic. Long-term problems associated with drift and deterioration with time.

New sensors that using thermal conductivity (TC) principles have been introduced in recent years (Lee and Fredlund, 1984). A few of these sensors include heat dissipation sensors like Fredlund thermal conductivity (FTC) sensors. However, heat dissipation sensors have certain limitations such as high failure rate in the field and the ceramic used in the sensor is fragile. Meanwhile, the FTC sensors are reported to be able to measure field suctions that are greater than 1,500 kPa reliably (Lee and Fredlund, 1984).

2.2.4.5 Soil Water Characteristic Curve (SWCC)

The soil water characteristic curve can be obtained by performing tests using pressure plate device in the laboratory following by the axis-translation technique (Hilf,

1956). In the late 1950's, soil water characteristic curve was commonly used to predict the coefficient of permeability at specific water content in terms of matric suction (Milington and Quirk, 1961). This soil-water characteristic curve is also required in the determination of water volume changes in the soil with respect to matric suction change. The coefficient of water volume change with respect to matric suction is given by the slope of the soil-water characteristic curve.

2.2.5 Swell Prediction Models

Many researchers have proposed vertical movement prediction models for expansive soils and a few of them are those developed by McDowell (1956), Snethen (1979), Mitchell and Avalle (1984), Hamberg (1985), Nelson and Miller (1992), and Lytton (2004). In this research, revisit of these models and their predictions of heave movements of soils based on laboratory tests are requisite. Other evaluations are attempted with heave movements in real subgrades, which are already obtained in this study.

2.2.5.1 Snethen's model (1979)

Snethen (1979b) reported the following model to estimate the vertical swell movement of an expansive soil. This model requires the use of soil matric suction as one of the parameters.

$$\frac{\Delta H}{H} = \frac{C_\tau}{1+e_o}\left[\left(A - Bw_o\right) - log\left(\tau_{mf} + \alpha\sigma_f\right)\right] \qquad (2)$$

Where

ΔH = vertical movement (ft.)

H = thickness of the layer (ft.)

C_τ = suction index

e_o = initial void ratio

A, B = constants from matric suction vs water content relationship

w_o = initial moisture content (%)

τ_{mf} = final matric suction (kPa)

α = compressibility factor (slope of specific volume versus moisture content curve)

σ_f = final applied pressure (kPa)

The suction index (C_τ) was not measured directly, but was calculated as follows:

$$C_\tau = \frac{\alpha G_s}{100B} \tag{3}$$

Where

B = slope of matric suction versus water content curve

G_s = specific gravity of soil.

The following equation was found to represent the suction-water content relationships for numerous clay soils with suction ranging from 100 to 5000 kPa (15 to 750 psi):

$$log\ \tau_m{}^o = A - Bw \tag{4}$$

Where

$\tau_m{}^0$ = matric suction with no surcharge (kPa)

w = gravimetric water content (%)

2.2.5.2 Hamberg's Model (1985)

Hamberg noted that any procedure for predicting potential movement in an expansive soil profile must be site specific. The Hamberg method presented here is generally applicable for the conditions which exist in much of the western U.S. and Canada. In these areas, expansive soil movements are primarily due to the volume changes of the desiccated upper layers of clays and weathered shales (Hamberg, 1985).

$$\Delta H = \sum_{i=1}^{N} \left[\frac{H_i}{(1+e_0)_i} \right] \left[C_h \cdot \Delta \log h \right]_i \qquad (5)$$

Where

ΔH = vertical movement (ft.)

N = number of layers to depth of active zone

H_i = thickness of layer i (ft.)

e_0 = initial void ratio of layer i

C_h = suction index with respect to void ratio (slope of void ratio versus soil suction in logarithmic scale)

h = soil suction (total or matric suction) (kPa)

The prediction methodology above is based on a few assumptions (Hamberg, 1985) listed as the following:

1. Volume changes are controlled primarily by the changes in soil suction stresses in the surficial, "active zone" of the soil profile.

2. Overburden and light structural loads have a small influence on the response of the soil due to suction changes.

3. Volume changes of the soil structure (represented by volumetric strain or by changes in void ratio) and associated changes in water content are directly proportional to the suction stress changes in the range of field suction variation.

4. The void ratio and water content suction indexes for wetting are equal to the suction indexes for drying.

5. Volume changes are the same in terms of either matric or total suction values.

2.2.5.3 Potential Vertical Rise (PVR)

The potential vertical rise method (PVR), developed by McDowell (1956) is widely used across the USA to the estimate the volume change behavior of expansive soils. The PVR, expressed in millimeters (inches) is the latent or potential ability of a soil material to swell at a given density, moisture, and loading condition, when exposed to capillary or surface water in which thereby increase the elevation of its upper surface along with anything resting on it (Tex-124-E). A calculation for PVR is derived from a family of universal curves developed for the relation between volumetric swell and surcharge load (McDowell 1956). Summary of assumptions together with discussions based on PVR are listed below (Lytton, 2004):

1. Soil at all depths has access to water in capillary moisture conditions.

2. Vertical swelling strain is one-third of the volume change at all depths.

3. Remolded and compacted soils adequately represent soils in the field.

4. PVR of 0.5 inch produces unsatisfactory riding quality.

5. Volume change can be predicted by the use of plasticity index alone.

Moreover, there are limitations and drawbacks in this method. For example, this method does not consider topography, vegetation and drainage effects. It is an overly conservative estimation of swell potentials for low plasticity soils and an underestimation for high PI soils (Lytton et al., 2004).

The data presented in the PVR model allows calculation for the vertical movement based on the PI of the soil. However, this method has limitations of not considering topography, vegetation and drainage effects, as well as overly conservative estimations of swell potentials. Therefore, TxDOT is currently researching an alternate approach for better swell property characterization (TxDOT Project 0-4518).

As a part of 0-4518, Lytton et al. (2004) developed an alternative method to determine the swell potentials based on suction measurements and diffusion models of soils with various scenarios. Thornthwaite moisture index, derived from the moisture balance procedure developed between rainfall and evapotranspiration (Thornthwaite 1948) can be used as a parameter to characterize climatic effects. Lytton et al. (2004) method accounts for this and other important parameters including topography and presence of localized water sources. Although this method is considered as an improvement when compared to current TxDOT practice (PVR method), it is still limited by a few problems and concerns. First, the method should be 'independently' verified for realistic estimation of swell potentials. Second, the influence or impacts of various boundary conditions on swell property variations need more investigations using the available case studies. Third and final, the method requires several empirical correlations with different degrees of correlations. Overall, such practice can lead to

compounding errors, which may limit the practicality of such expressions for routine use. Nevertheless, with thorough evaluation and modification, if necessary, this suction based method can be reliably used for estimating swell properties of site soils in the design of pavements.

2.2.5.4 Summary for Other Methods

There are usually two quantitative parameters for swelling characteristic: (1) Percentage swelling which is the vertical swelling strain under the applied load and (2) Swelling pressure which is the maximum vertical stress required to keep the soil sample at the initial volume when the sample is inundated with water and full swell occurs (Ofer and Blight, 1985).

Hussein (2001) derived a constitutive model to represent the visco-plastic behavior of an expansive soil upon wetting and drying. The model takes into account the current stress, water content and clay content as well as environmental factors. The time-dependent deformation and stress changes are associated with pore-water migration as well as the swelling and viscous nature of the material. In addition, the magnitudes of percent swell pressure are also influenced by other factors such as the following:

1. Compositional factors, which include the type and amount of clay mineral present in the soil as well as the pore fluid characteristics. Environmental factors, such as initial moisture content, initial density, initial degree of saturation, initial soil structure, stress history, availability and composition of ambient water and temperature.

2. Procedural factors in laboratory testing like size and shape of soil sample, degree of disturbance and testing procedure and techniques used.

3. Climate, depth of active zone, location and thickness of the expansive soil layer, applied loads (weight of structure and soil overburden), vegetation, site topography, surface drainage and confinement.

Budge et al. (1966) used one-dimensional consolidometer test to determine the swell characteristics of an expansive subgrade soil. This method was specifically applied to stiff and fissured clay shale that is served as subgrade. However, due to overburden removal and moisture increase, the subgrade in question has caused pavement heave in the order of several inches. In their research, new sampling equipment that contained a series of liners is designed to enable the test specimens remain confined in linear rings.

Complete lateral confinement prevents stress relief accompanied by premature expansion during the transfer of the sample into the consolidometer. The samples were loaded and unloaded in single increments to determine the expansion characteristics. The portion of total heave resulting from moisture increase was obtained in a similar swell test in which the soil was given free access to water while it was under full overburden pressure. Total surface heave was estimated from pressure release and soil moisture increase. Their validation study showed the surface heave predictions close to the field measured heave on the test pavement in the first five years since construction. This study also showed it was possible to estimate the potential heave of increments of soil at any sampling depth. But as expected, the layers of soil immediately beneath the

pavement rather than increments at greater depth contributed more heave to the pavement.

For design purposes, empirical prediction methods are generally inadequate. Holland and Cameron (1981) suggested swell testing in conventional consolidometers with a moisture correction factor provided reliable predictions. Various correlations have been suggested for predicting the swell pressure (Table 2.2) and percent swell (Table 2.3). The generalized form of the equations may be written as:

$$Log(P_0 / P_a) = a_0 + a_L(LL) + a_d(\gamma_d / \gamma_w) + a_w(w_0) \quad (6)$$

$$Log(S_0) = b_0 + b_L(LL) + b_d(\gamma_d / \gamma_w) + b_w(w_0) \quad (7)$$

Where

P_0 = swelling pressure for zero movement;

P_a = atmospheric pressure;

S_0 = percent swell for zero load (%);

LL = liquid limit (%);

γ_d = dry density of soil;

γ_w = unit weight of water;

w_0 = in situ moisture content (%);

$a_0, a_L, a_d, b_0, b_L, b_d$ are coefficients.

Table 2.2 Correlations for swelling pressure prediction
(Mowafy et al., 1985a and Nagaraj et al., 1985)

Reference	Correlations	Comments
El-Ramli (1965)	$P_s = \frac{1}{2}\gamma_d / w_s$	Does not consider the effect of initial water content
Komornik and David (1969)	$LogP_s = 2.132 + 0.0208LL + 0.000665\gamma - 0.0269w_n$	Insensitive to variations in dry density
Zacharias and Ranganatham (1972)	$P_s = -\frac{225}{6.4}(SI) + \frac{290}{6.4}(LL - w^*) + \frac{1.2}{6.4}(SI)(\frac{1}{S_r})$	Dry density is not included, only valid to dry densities ranging between 17 and 18 kN/m^3
Dedier (1973)	$LogP_s = 2.55\frac{\gamma_d}{\gamma_w} - 1.705$ $LogP_s = 0.0294C - 1.923$	Does not consider the effect of initial water content. Equations cannot be applied to soils having different initial water contents.
Rabba (1975)	For sandy-clay: $LogP_s = 2.17(\gamma_d + 0.084C) - 3.91$ For silty-clay: $LogP_s = 2.5(\gamma_d + 0.006C) - 4$	Use of equations limited to an initial water content of 8%
Mowafy and Bauer (1985a)	$Log(10.2P_s) = 1.366(10.2\gamma_d) + 8.951\times10^{-3}C - 2.179\times10^{-2}w_n - 2.840$	For soils from Nasr city, a satellite city of Cairo, Egypt

Table 2.2 - continued

Reference	Correlations	Comments
Vijayavergiya and Ghazzaly (1973)	$LogP_s = \frac{1}{12}(0.4LL - w_n - 0.4)$ $LogP_s = \frac{1}{19.5}(\gamma_d + 0.65LL - 139.5)$	Correlations developed based on 270 test results of undisturbed natural soils at shallow depth. To predict swell pressure and percent swell under 0.1 ton/ft^2.
Nagaraj and Murthy (1985)	$P_s(kPa) = 2492 - 12811.3\left(\frac{e_0}{e_L}\right)/(5.522 - \text{lc}$ $\rho = 0.0601 - 0.0297\left[\left(\frac{e_0}{e_L}\right) + \log\left(\frac{P_s}{P}\right)\right]$ $\left(\frac{e_0}{e_L}\right) = 1.122 - (0.2343 - \rho)\log P_c - \rho \log$	These three equations have three unknowns in P_s, P_c and ρ and the solutions could be obtained by iteration process.

Table 2.3 Correlations for percent swell prediction
(After dept. of the army TM 5-818-7)

Reference	Correlations	Comments
Vijayvergiya and Ghazzaly (1973)	$LogS_p = \frac{1}{12}(0.44LL - w_0 + 5.5)$ $LogS = \frac{1}{19.5}(\gamma_d + 0.65LL - 130.5)$	From initial water content to saturation for 0.1-tsf surcharge pressure
Schneider and Poor	$LogS_p = 0.9\left(\frac{PI}{w_0}\right) - 1.19$	For no fill or weight on the swelling soil to saturation
McKeen (1980)	$S_p = -100\gamma_h \log\frac{\bar{\tau}_f}{\bar{\tau}_0}$	The γ_h is found from a chart using CEC, PI, and percent clay. The weighted suction is given by $\bar{\tau} = 0.5\tau_1 + 0.3\tau_2 + 0.2\tau_3$ where τ_1 , τ_2 , τ_3 are in situ suctions measure in the top, middle, and bottom third of the active zone.
Johnson and Stroman (1976)	PI≥40 $S_p = 23.82 + 0.7346PI - 0.1458H - 1.7w_0 + 0.0025PI \times w_0 - 0.00884PI \times H$ PI≤40 $S_p = -9.18 + 1.5546PI + 0.08424H + 0.1w_0 - 0.0432PI \times w_0 - 0.01215PI \times H$	For 1 psi surcharge pressure to saturation

Note for Table 2.2 and 2.3:

P_s = swelling pressure (kg/cm^2);

γ_d = dry density (g/cm^3);

w_s = shrinkage limit (%);

LL = liquid limit (%);

w_n = natural water content (%);

SI = shrinkage index;

S_r = degree of saturation of specimen before start of test;

w^* = water content at $S_r = 100\%$;

C = clay content (%);

γ_w = density of water (g/cm^3);

P = overburden effective pressure;

$\left(\frac{e_0}{e_L}\right)$ = generalized initial state of soil;

ρ = slope of the line joining the present state to preconsolidation pressure;

S_p = percent swell (%);

PI = plasticity index (%);

w_0 = initial water content (%);

H = depth of soil (ft)

2.3 Road Conditions and Climatic Effects

Overall, both soils heaving and shrinking are influenced by clay mineral type, compaction state including moisture content and dry density conditions, environmental conditions such as rainfall and evapotranspiration, site and road conditions including road drainage slopes, location and presence of roadside drainage systems, vegetation and the presence of trees. Of all these variables, only the soil variables are well understood since they can be easily controlled in laboratory environments.

In the case of rainfall and evapotranspiration effects, researchers use different approaches. The practice in the United States is based on Thornthwaite moisture index parameter, whereas the practitioners in the South Africa often determine equilibrium moisture index that accounts for seasonal climatic effects. Both approaches require other soil properties in the final determination of suction in subgrades that is representative to soil and climactic conditions. Once such suction properties are determined, they are used in the swell property estimation, which are accounted for pavement design. Due to global warming and other seasonal moisture variations, there is a need to review current Thornthwaite index values and revise them, if necessary.

2.3.1 Influence of Drainage Ditches on Expansive Soils

Drainage systems including the ditches adjacent to pavements have a pronounced influence on expansive soil behavior. Poor designed ditches often pond the water that will raise the saturation levels in expansive subsoils. Such increase in saturation will raise the swell magnitudes and conversely increase shrinkage movements during dry spells. Hence, the presence of drainage ditches and their current conditions

will be essential in appropriate design of pavements. Stallings (1999) provided a comprehensive overview of ditches near pavements and approaches to evaluate their conditions. Similar methodology was followed in this field testing phase of the research to assess drainage ditch location and how it impacts moisture and matric suction changes in the subsoils.

2.3.2 Influence of Trees on Expansive Soils

The interaction between vegetation and available moisture in subsoils will influence swell and shrinkage in soils, which in turn can cause volume changes in inactive soils. It will eventually increase the extent of moisture-change-induced deformation in these soils.

Vegetation has several effects on available soil moisture. In addition to moisture depletion by transpiration, shading of the ground surface, buildup of organic material, retardation of precipitation runoff, and formation of water channels from root disintegration can influence soil moisture patterns (Snethen, 2001). Large trees located near to infrastructure including houses and pavements can cause the maximum change in available moisture and induce the damage to the structure. This situation generally occurs in humid or arid climates (Snethen, 2001).

Small trees, bushes, and grasses can also affect available moisture at shallow depths, particularly in arid and semi-arid climates. Total vegetation cover, as well as number, size, location, and type of trees affect soil moisture availability. In moisture-accumulation period of the year, the vegetation influence is generally unnoticed.

However, in moisture-depletion period of the year, the influence can be dramatic because drying in soils could result in damage to the structures (Snethen, 2001).

Vegetation and trees have a similar profound effect on the desiccation or drying-up of expansive soils. The presence of certain types of trees is known to cause drying in subsoils and hence induce cracking in pavements (Sillers et al., 2001; Jaksa et al., 2002). Ratios of lateral distance (D) from trees and height of plants (H) are developed for different trees near the pavements in Australia. These values are used to determine the proximity of trees to the pavements and the potential influence of trees on pavement design by properly taking the matric suction properties in subsoils into account. Similar information available on various trees or vegetation on the foundation design practices for expansive soils in Texas was reviewed and considered for the current pavement design practices on high PI clays.

Most of the available information on the trees and their influence on moisture variation are based on indirect evidence. Ward (1953) in the United Kingdom recommended safe planting distance of trees to avoid soil shrinkage settlement and damage to buildings. Ward prescribed the first "proximity rule" of distance to height of trees (D:H) equal to one. In Canada, Bozozuk (1962) demonstrated the decrease of drying settlements with distance from a row of 17 m high elm trees. In mid 70s, a severe drought in the United Kingdom caused shrinkage settlement and it was realized that a large proportion of the ground movement under footings was related to the drying effects in trees (Cameron, 2001). Further research effort was initiated in response to the widespread damage observed during the drought (e.g. Cutler and Richardson, 1981;

Driscoll, 1983). Also, the aggressiveness of different root systems of trees near to the water pipes was revealed in "root chokes" studies by the Engineering and Water Supply Department in Adelaide, Australia (Baker, 1978).

Biddle (1983, 2001) conducted studies on soil moisture deficits around specimens of certain tree species in open grassland. Five different clay soil profiles were investigated at three locations underlain by clay soils. Soil moisture was monitored with a down-hole neutron moisture meter to a maximum depth of 4 meters. Generally, it was observed that the lateral extent of drying was within a radius equal to the height of the tree. However, the depth and radius of drying, both horizontally and vertically, appeared to be species-dependent.

Tucker and Poor (1978) studied a housing estate, which was in the process of being demolished because of the extent of damage to the houses (masonry veneer walls on slabs). Tree species located near to these structures were Mulberry, Elm, Cottonwood, and Willows. Differential movements were measured and compared with D:H ratios. The data strongly indicated that tree effects were significantly reduced when D:H values were greater than one. Differential movements in excess of 120 mm were observed for trees close to the building. In New Zealand, Wesseldine (1982) demonstrated the influence of the silver dollar gum (E. cinerea) on houses. The research indicated a threshold value of 0.75 D:H for single trees and 1.0 to 1.5 for groups of these trees could cause damages. The extent of damage was not included in the correlation.

Snethen (2001) reported that climatic extremes played a major role in causing and exacerbating damage to pavements and lightly-loaded structures. The type and proximity of vegetation interacts with climatic extremes cause the problem. In all cases observed, medium to large, broad-leaf, thick canopy, and shallow-spreading-root trees in close proximity to structures (i.e., Chinese Elm and Bradford Pear), had either initiated or worsened the damage to pavements caused by the shrinking soils. These types of trees cause the greatest influence on the subsurface moisture regime. Base upon the relative average rank analysis, the most influential trees are Poplar, Elm, oak, and Ash (Bryant et al., 2001) in order. Experience and observations show that these types of trees should be planted 0.5 to 1.0 m beyond the anticipated mature drip line or the anticipated mature height of the tree from pavements or building foundations (Snethen, 2001).

In summary, types and locations of trees should be considered in landscaping decisions, particularly soils that have LL > 40 and PI > 25 (Snethen, 2001). For landscaping decisions, published information from Natural Resource Conservation Services county soil surveys and national or local geological surveys are sufficient to address such planting decisions. In this research, effects of trees and their influence on soil moisture availability and matric suction was studied and addressed.

2.4 Remediation Strategies for Expansive Soils

Ideally, the subgrade should not only be strong enough to prevent excessive rutting and shoving but it should also be sufficiently stiff to minimize resilient deflection. Due to the variety of soil types involved, their inherent seasonal variation of

strength characteristics and the influence of water availability on soil matric suction, the practical load carrying capacity of subgrade soils is most difficult to evaluate. Although seasonal deflection patterns may seem regular, it is difficult to select design-bearing values for clay subgrades. On very soft soils, thick layers of granular material may solve the bearing capacity problem. In some other instances, bearing capacity improvements involve the stabilization of the foundation soils (Raymond and Ismail, 2003). For fine-grained silt and clay soils, poor strength, high volumetric instability, and freeze/thaw durability problems are predominant. For expansive soil, the volumetric change may be more severe and thus become a bigger challenge. The expansion action may result in intolerable differential heaving of pavements. The commonly used remediation methods include:

- Treat the expansive soil with lime or other additives to reduce expansion in the presence of moisture;
- Replace the expansive material with a non-expansive material to a depth below which the seasonal moisture content will remain nearly constant;
- Provide an overlaying structural section of sufficient thickness to counteract the expansion pressure by surcharge;
- Stabilize the moisture content and minimize the access water through surface and subsurface drainage by using waterproof membrane such as rubberized asphalt membrane and geosynthetics. Put moisture barrier and/or remove nearby vegetations.
- Relocate the project to a more favorable soil condition.

The following sections describe different remediation methods. For the scope of this research, relocation is not an option.

2.4.1 Admixture Stabilization

Admixture stabilization refers to mixing and blending a liquid, slurry, or powder with soil to improve soil strength and stiffness properties. One of the most commonly used method of reducing the shrinking or swelling is stabilization with calcium based stabilizer

2.4.1.1 Lime

Lime stabilization is widely used to chemically transform the unstable soils so that the soils could be used as sound foundations. Lime stabilization creates a number of important engineering properties in soils, such as the advantages of providing improved strength; improved resistance to fracture, fatigue, and permanent deformation; improved resilient properties; reduced swelling; and resistance to the damaging effects of moisture. The most substantial improvements in these properties are seen to be in moderate to high plastic soils, such as heavy clays. (Little et al., 2000)

According to Little (1999), lime stabilization can be used to either modify or stabilize clays. Modification, which provides substantial improvement to the performance of high plasticity clays, occurs primarily due to exchange of calcium cations supplied by the lime ($Ca(OH)_2$ or hydrated lime) for the normally present cations adsorbed on the surface of the clay mineral. Modification will take place as the hydrated lime reacts with the clay mineral surface in the high pH environment. The

results of the mechanisms are plasticity reduction, reduction in moisture holding capacity (drying), swell reduction, and stability improvement.

Stabilization differs from modification that a significant level of long-term strength gain is developed through a long-term pozzolanic reaction. This pozzolanic reaction is the formation of calcium silicate hydrates and calcium aluminate hydrates as the calcium from the lime reacts with the aluminates and silicates solubilized from the clay mineral surface. Lime stabilization often induces a ten-fold stiffness increase over that of the untreated soil or aggregate.

Little (1999) developed a protocol for lime mixture design based on the following steps:

1) Select a soil or aggregate that is mineralogically reactive with lime;

2) Establish optimum lime content based on pH testing and compressive strength development (accounting for the effects of moisture-density relationships);

3) Evaluate resistance to moisture-induced damage through a capillary suction test in which the surface dielectric value of the cured, lime-treated sample is measured.

Croft (1967) found that the addition of lime significantly reduces the swelling potential, liquid limit, plasticity index and maximum dry density of the soil while increases the optimum water content, shrinkage limit and strength.

Bell (1996) indicated that the optimum addition of lime needed for maximum modification of the soil is normally between 1% and 3% lime by weight, and further additions of lime do not bring changes in the plastic limit but it will increase the

strength. However, other studies reported the use of lime is normally between 2% and 8% in soil stabilization (Basma and Tuncer, 1991).

Little (1999) stated that although resilient properties are important to the assessment of the stress state in the mechanistic analysis, it is the aggregate, soil or stabilized layer shear strength that dictates resistance to deformation and stability in the pavement. Tensile strength properties that are important to predict the shrinkage cracking potential and flexural fatigue potential of lime-soil mixtures can be approximated through the strength tests.

Thompson (1966) determined that the indirect tensile strength of lime-soil mixtures is approximately 0.13 times the unconfined compressive strength. Chou (1987) stated that the flexural tensile strength of lime-soil mixtures is approximately 0.25 times the unconfined compressive strength.

Lime and lime fly ash stabilized materials cure much slower, in general, than Portland cement stabilized layers. As with strength properties, resilient properties of lime-soil mixtures are very sensitive to the level of compaction and molding moisture content. Lime-stabilization may substantially increase shear and tensile strengths. This strength increase provides a stiffer layer with improved load distributing capabilities. However, as the stiffness of the layer increases through the development of cohesion within the stabilized layer, the layer becomes more susceptible to load-induced tensile stresses. It can lead to fatigue failure unless proper design steps are taken to reduce the potential damage due to induced loads. This is generally accomplished by ensuring the layer thicknesses are such as to insure the development of acceptable flexural stresses

within the stabilized layer. Typically, the design parameter is the flexural tensile stress ratio.

2.4.1.2 Cement

Cement has been found to be effective in stabilizing a wide variety of soils, including granular materials, silts, and clays; byproducts such as slag and fly ash; and waste materials such as pulverized bituminous pavements and crushed concrete. These materials are used in pavement base, subbase, and subgrade construction (Little, 2000). It is more effective and economical to use it with granular soils due to the ease of pulverization and mixing, and the requirement of smaller cement quantities. Fine-grained soils of low to medium plasticity can also be stabilized, but not as effectively as coarse-grained soils. If the PI exceeds 30, cement becomes difficult to mix with the soil. In these cases, lime can be added first to reduce the PI and improve workability before adding the cement. (Hicks, 2002) Cement stabilization develops from the cementitious links between the calcium silicate, aluminate hydration products and the soil particles (Croft, 1967). Addition of cement to clay soil reduces the liquid limit, PI and swelling potential; and increases the shrinkage limit and shear strength (Nelson and Miller, 1992).

Puppala et al. (2004a) studied the effectiveness of sulfate resistant cement stabilizers Types I/II and V in providing better treatment of sulfate rich soils. Experiments were designed and conducted on both controlled and cement treated sulfate soils to investigate compaction relationships, Atterberg limits, linear shrinkage and free swell strain potentials, unconfined compressive strength (UCS), and low strain

shear modulus properties. Sulfate resistant cement stabilizers of Types I/II and V were used and the following tests were performed after curing: UCS (ASTM-D 2166), resonant column tests (ASTM-D 4015-92), free swell tests (ASTM-D 4546) with a little modification of using low seating pressures, and linear shrinkage bar tests (TEX-107-E). Test results indicated significant improvement of soil properties by both cement Types I/II and V while all sulfate rich soils showed similar stabilization trends. Treated soil samples compacted at wet of optimum moisture content yielded higher strength and lesser swell properties than those compacted at optimum moisture content. This was attributed to much more moisture presence in the compacted soils at wet of optimum condition, which facilitates stronger chemical reactions particularly in hydration related reactions between cement stabilizers and soils. An increase in cement content and curing period enhanced soil properties. Both free swell and Atterberg limits reach to zero magnitudes at 5% dosage with 14-day curing. Both low and high sulfate-resistant cement types provided statistically similar and significant improvements to soil properties.

Rollings et al. (1999) examined a project in Georgia that involved a cement-stabilized and sand-based course material mixed off-site at the sand borrow pit. For the examples in the Texas (Puppala et al., 2004a), sulfate-induced heave was evident within six months after construction. A preliminary investigation provided no definitive answers as to why the base course heaved. Sulfur was not present in the cement or in the sand used. Closer inspection showed that the mixing water used at the off-site mixing plant contained over 10% sulfur, and that the water was a major contributor of

calcium. When the cement was added, the pH increased to about 12 while the alumina and silica in the soil became soluble, which lead to the formation of ettringite.

2.4.1.3 Fly Ash

Fly ash is defined in Cement and Concrete Terminology (ACI Committee 116) as "the finely divided residue resulting from the combustion of ground or powdered coal, which is transported from the firebox through the boiler by flue gases." Fly ash is a by-product of coal-fired electric generating plants. Two main types of fly ash are being used: non self-cementing Class F and lime-fly ash self-cementing Class C. Stabilization of soils and pavement bases with coal fly ash is an increasingly popular option for design engineers. Fly ash decreases swell potential of expansive soils (Ferguson 1993, White et al., 2005a, b) and soils can be treated with self-cementing fly ash to modify engineering properties as well as produce rapid strength gain in unstable soils.

Ferguson (1993) noted that the decrease in plasticity and swell potential was generally less than that of lime because fly ash did not provide as many calcium ions that modify the surface charge of clay particles. Fly ash increases the CBR of fine-grained soils, and in the case of 20% fly ash addition, the CBR can be increased up to 75%. Tests results show that fly ash increases the compacted dry density and reduces the optimum moisture content. Fly ash can also dry wet soils effectively and provide an initial rapid strength gain, which is useful during construction in wet and unstable ground conditions (White et al., 2005a). Çoçka (2001) found that plasticity index and swell potential decrease with increasing fly ash contents. The fly ash addition rates greater than 20% are comparable to lime addition rates of 8% for reducing plasticity and

ultimately the swell potential in the example soil. Strength gain in soil-fly ash mixtures is dependent on cure time and temperature, compaction energy, and compaction delay (White et al., 2005a, b).

Sulfur contents can cause formation of expansive minerals in soil-fly ash mixtures, which severely reduces the long-term strength and durability. These negative reactions resulting from sulfur were reported by many researchers and practitioners. (Puppala et al., 2004a)

2.4.1.4 Evaluation and Comparison of Stabilization Methods

To select a correct stabilizing agent, soil types, climatic and drainage conditions need to be considered. Hicks (2002) suggested the following guide to select appropriate method of stabilization:

- Soil type: Particle size distribution and Atterberg limits are commonly used to gain a preliminary assessment for the type of stabilization required for a particular material. The usual range for suitability of various types is based on the #200 sieve and the plasticity index of the soil. Figure 2.8 provides the initial guidance for selecting stabilizer type.

- Climatic conditions: In wetter areas, where the moisture content of the pavement materials is high, it is important to ensure that the wet strength of the stabilized material is adequate. In these conditions, cementitious binders are usually preferred although asphalt and asphalt/cement blends would also work. Lime is suitable for cohesive soils, particularly when used as the initial agent to dry out the material. Lime can also work with silty soils if a pozzolan is added to promote the cementing

reaction. Using emulsions in cold dry climates requires using cement or lime to facilitate moisture removal from the emulsion during the stabilization process and to promote the strength.

Puppala et al. (2003) evaluated the following four types of stabilizers to enhance the strength and reduce free swell and shrinkage strain potentials of soft, expansive and sulfate-rich soils: sulfate-resistant cement, lime mixed with fibers, ground granulated blast furnace slag (GGBFS) and Class F fly ash. Sulfate-resistant cement provided the most effective treatment. Possible mechanisms for these enhancements in soil properties were ion exchange, flocculation, cementation and pozzolanic reactions. The combined lime and fibers stabilization method provided the next best effective treatment. They enhanced UCS and reduced PI, swell and shrinkage strains. The GGBFS stabilizer provided the third best performance. It reduced the swell, shrinkage and plasticity characteristics while increasing the UCS values. Nevertheless, the GGBFS- treated soils exhibited less improvement in strength, and swell and shrinkage behaviors compared to the cement and lime plus fiber treatment methods. The Class F fly ash treatment provided low-to-moderate strength improvements that could be attributed to the low amounts of calcium present in this type of fly ash. On the other hand, the fly ash stabilization method was more cost-effective than the other methods.

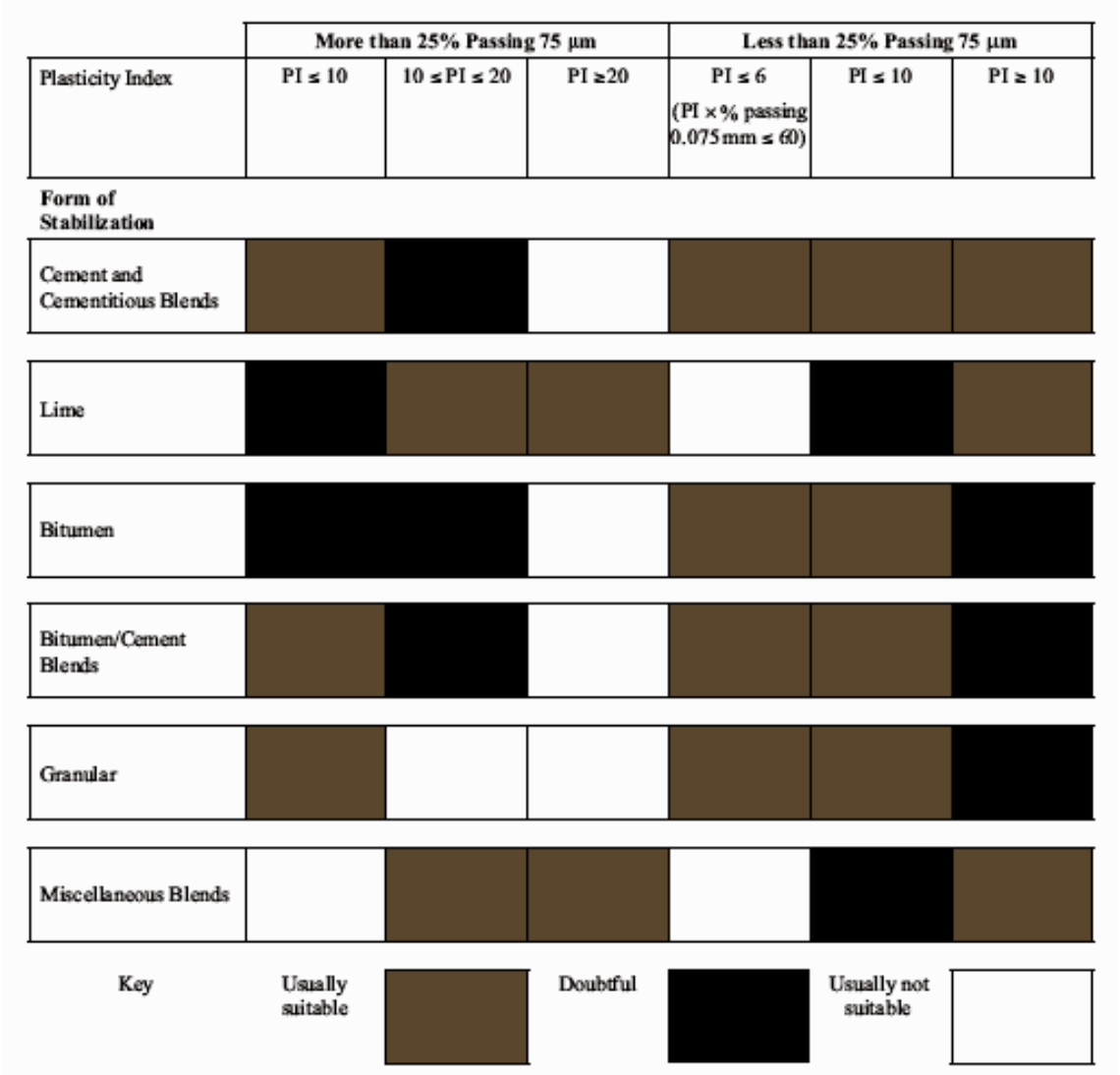

Figure 2.8 Guides to select stabilization method (Hicks, 2002)

Table 2.4 Compare the process, effects and applicable soil type of the stabilizing agents (Hicks, 2002)

Stabilization Agent	**Process**	**Effects**	**Applicable Soil Types**
Cement	Cementitious inter-particle bonds are developed.	• Low additive content (<2%): decreases susceptibility to moisture changes, resulting in modified or bound materials. • High additive content: increases modulus and tensile strength significantly, resulting in bound materials.	Not limited apart from deleterious components (organics, sulphates, etc., which retard cement reactions). Suitable for granular soils but inefficient in predominantly one-sized materials and heavy clays.

Table 2.4 - continued

Stabilization Agent	Process	Effects	Applicable Soil Types
Lime	Cementitious inter-particle bonds are developed but rate of development is slow compared to cement. Reactions are temperature dependent and require natural pozzolan to be present. If natural pozzolan is not present, a blended binder that includes pozzolan can be used.	• Improves handling properties of cohesive materials. • Low additive content (<2%): decreases susceptibility to moisture changes, and improves strength, resulting in modified or bound materials. • High additive content: increases modulus and tensile strength, resulting in bound materials.	Suitable for cohesive soils. Requires clay components in the soil that will react with lime (i.e., contain natural pozzolan). Organic materials will retard reactions.

Table 2.4 - continued

Stabilization Agent	Process	Effects	Applicable Soil Types
Blended slow-setting binders (for example: fly ash/lime, slag/lime/fly ash blends)	Lime and pozzolan modifies particle size distribution and develops cementitious bonds.	Generally similar to cement but rate of gain of strength similar to lime. Also improves workability. Generally reduces shrinkage cracking problems.	Same as for cement stabilization. Can be used where soils are not reactive to lime.

Al-Rawas et al. (2005) evaluated the effect of lime, cement, combinations of lime and cement treatment on the swelling potential an expansive soil. The liquid limit of all treated samples except for samples treated with 5% lime plus cement showed an initial increase at the addition of 3% stabilizer, followed by a gradual decrease. On the other hand, the samples treated with combinations of lime and cement exhibited an initial reduction at 3% lime + 3% cement and 5% lime + 3% cement followed by a general increase with further additions. All stabilizers caused a reduction in both swell pressure and swell percent. With the addition of 6% lime, both the swell percent and swell pressure were reduced to zero.

Kota et al. (1996) provide the following suggestions to minimize the damages caused by sulfates and calcium-based stabilizers:

Double application of lime

- Low calcium stabilizers, such as cement and fly ash
- Non-calcium stabilizers
- Geotextile or Geogrid soil reinforcement
- Stabilization of the top with non-sulfate select fill
- Pretreatment with barium compounds
- Asphalt stabilization of the sulfate bearing soils
- Compacting to lower densities

2.4.1.5 Injection of Aqueous Solution

Pengelly and Addison (2001) presented the feasibility of using an aqueous solution of potassium and ammonium ions to treat expansive clay soils. The technique

relies on reactions between the solution ions and the clay soil. All clay particles or minerals are composed of sheets of silica and alumina. The type of clay mineral associated with heave is smectite (montmorillonite). Ions such as calcium, magnesium or sodium are attracted to the surface of the clay particle in an attempt to balance the net negative charge of the clay particle. Swelling in clay is directly related to cation hydration energy (its attraction to water molecules) and the hydrated radius of the interlayer cations. The repulsive forces from hydration of above mentioned cations cause swelling. Norish (1954) and Grim (1968) recommended four commonly occurring cations with high hydration energies and low hydrated radii as the following: potassium, ammonium, rubidium and cesium.

Pengelly and Addison (2001) used potassium and ammonium as cations and mixed them in a solution of water to modify clays beneath an existing building structure. Clays treated with potassium and ammonium consistently reduced swelling at lower moisture contents. Additionally, swell caused by the introduction of an aqueous solution containing potassium and ammonium was consistently lower than that caused by water alone.

Mowafy et al. (1985b) also indicated the presence of sodium chloride in the pore fluid caused a decrease in swelling and swelling pressure. The injection of salt solutions could be a possible remediation method to overcome swelling problem if the soil permeability is sufficiently high.

Although chemical stabilization has proven successful in increasing the strength of the natural expansive soils by twenty to fifty times and is widely used throughout

Texas, situations arise where above mentioned approaches cannot be used. For example, chemical stabilization cannot be used when the temperature is below 40^{o}F and in some cases there are not enough time for curing before traffic is routed back (Hopkins et al., 2005).

2.4.2 Moisture Control

The M-E Design Guide recommended the following options to be used for conventional and deep-strength HMA pavements:

- Full-width paving to eliminate the lane/shoulder cold joint, which is a major source of water infiltration in the pavement structure.
- Provision of a granular layer between the subgrade and base course to reduce erosion, allow bottom seepage and minimize frost susceptibility that could increase pavement roughness.
- Provision of adequate side ditches with flow lines beneath the pavement structure. The edge drains should be placed under the shoulder at shallower depths.
- Install deep under drains, greater than 3 feet (1.0 meter) deep, for groundwater problems.

AASHTO (1993) provides the definitions corresponding to various drainage levels from the pavement structure as shown in Table 2.5.

Table 2.5 AASHTO definitions for pavement drainage levels

Quality of Drainage	Water Removal Within
Excellent	2 hours
Good	1 day
Fair	1 week
Poor	1 month
Very Poor	No drainage

2.4.2.1 Moisture Barriers

2.4.2.1.1 Horizontal Moisture Barriers

Horizontal moisture barriers are designed to stop rainwater from penetrating into the subgrade soils. By reducing moisture variance, soil swelling would be reduced and pavement smoothness would be better maintained. Based on a study by Browning (1999), horizontal moisture barriers neither produce a smoother ride than the unprotected pavement in the roughness tests nor reduce the moisture variance.

2.4.2.1.2 Vertical Moisture Barriers

Vertical moisture barriers have been used successfully in many cases across the United States to control movements generated from expansive soil subgrades. Sites in wet and semi-arid climates, with cracked clay soils and shallow root zones will show the greatest benefit from using vertical moisture barriers (Jayatilaka et al., 1993).

The first vertical moisture barrier trial was conducted on the IH-410 loop in San Antonio, Texas, in 1978 (Steinberg, 1992). The role of a vertical moisture barrier is to

stop the seasonal lateral migration of moisture to and from the subgrade beneath the pavement, thus preventing the subgrade from expanding during wet periods and shrinking during dry periods (Picornell and Lytton, 1986).

The main drawback is the high expense and complicated construction. Field trials to evaluate the effect of barrier depth shown the deeper barriers (8 feet) outperformed the shallow barriers (6 feet) in maintaining a more constant moisture regime, thereby further reducing vertical movements (Gay and Lytton, 1988). However, the deeper the barrier is, the more expensive the construction will become. Thus, using vertical moisture barriers has usually only been reserved for major highways.

Evans and McManus (1999) reviewed current vertical moisture barrier construction methods in the United States and developed a new economical barrier construction method for low-volume roads that consisted of a spray seal surface over low-quality base and subgrade in Australia. According to Evans and McManus (1999), moisture barriers constructed in the United States over the last 20 years has led to cheaper barriers, but still too expensive for low-volume road applications and they also have several disadvantages. The rounded gravel backfill commonly used in TX (TxDOT Special Specification No. 5431) is not an ideal material since this kind of backfill provides an "easy" moisture path to the bottom of the barrier, and thus would promote deep-seated swelling. In cases of flat terrain, where there is poor drainage, it would act like a storage reservoir next to the expansive clay subgrade. Evans and McManus's method involved the design of equipment to (1) excavate a deep and narrow slit trench (Figure 2.9); (2) install plastic sheeting into the trench without

damaging it (Figure 2.10) and (3) discharge a flowable cementitious backfill into the trench (Figure 2.11). The cost of this new barrier is about $3.10 per lineal foot.

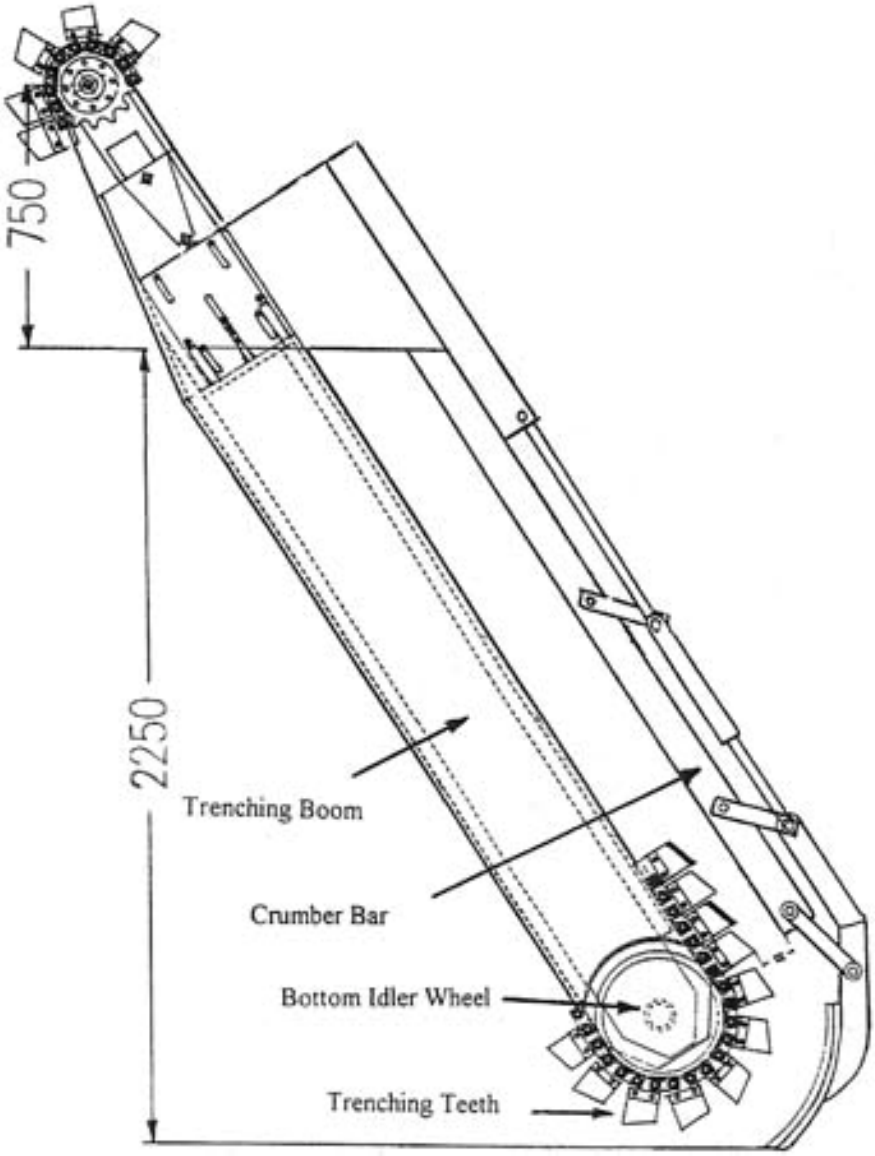

Figure 2.9 Slim-line trenching boom and crumber bar design
(Evans and McManus, 1999)

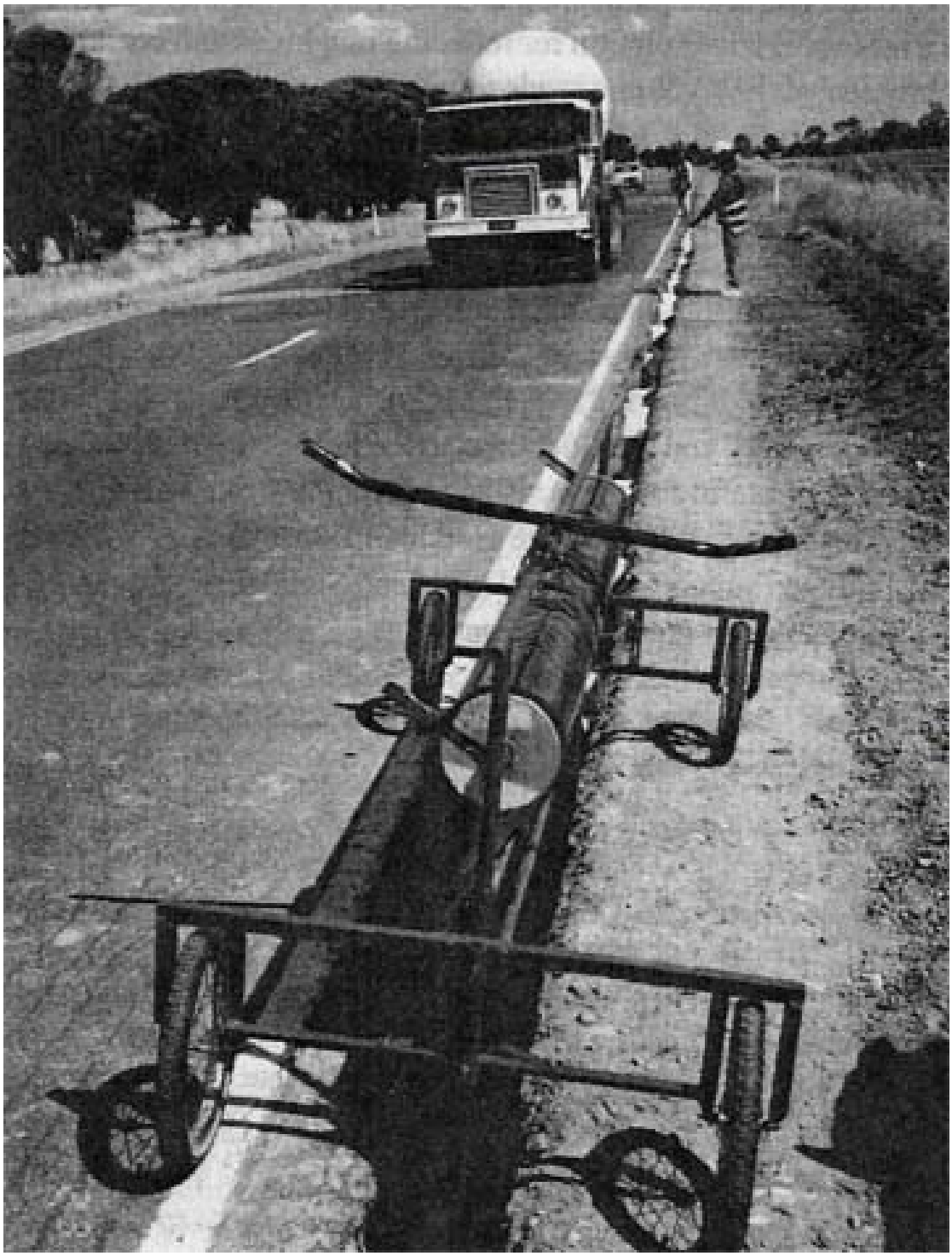

Figure 2.10 Membrane dispenser and membrane held by polystyrene wedges
(Evans and McManus, 1999)

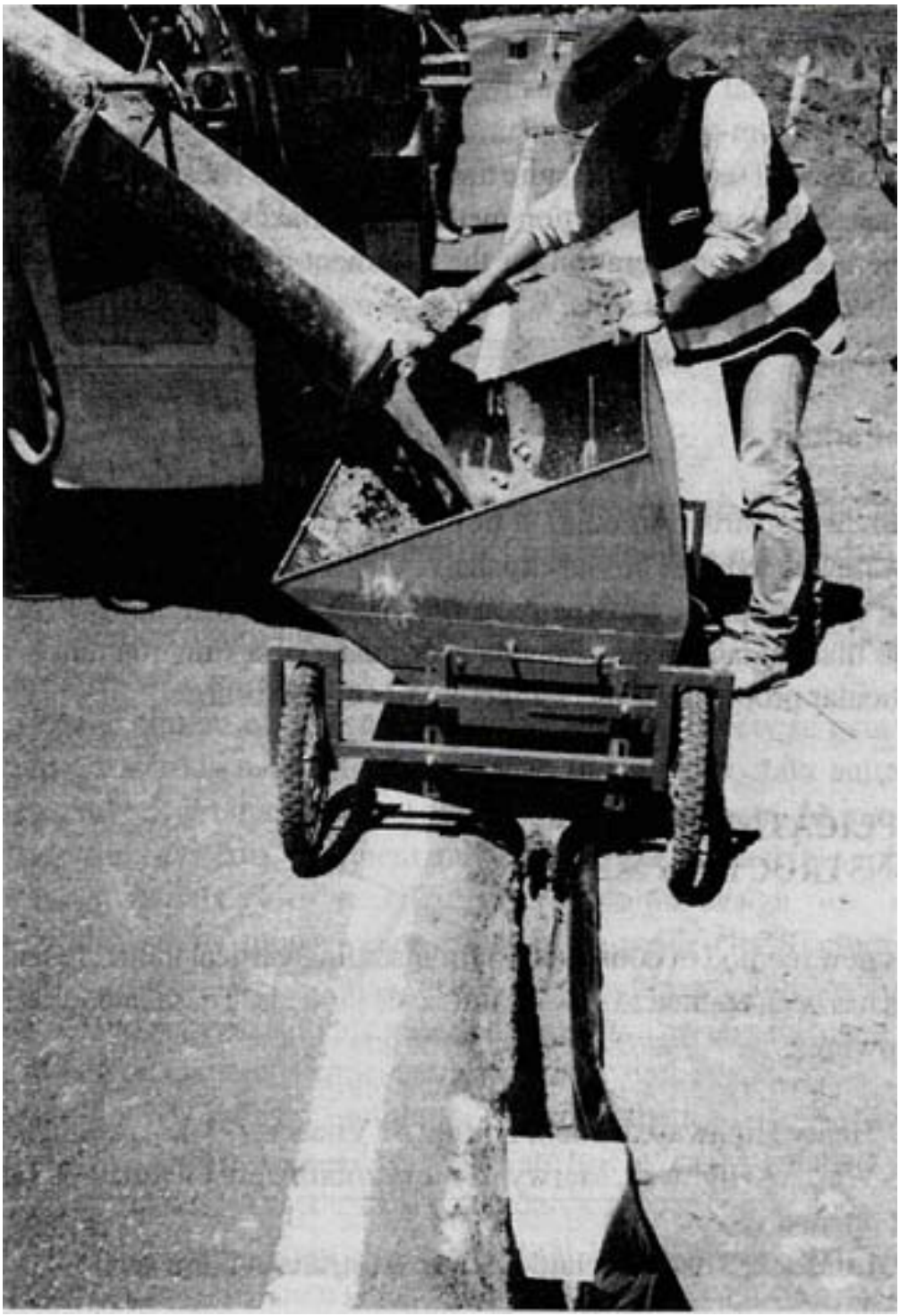

Figure 2.11 Membrane, polystyrene wedges, and placement of flowable fill (Evans and McManus, 1999)

2.4.2.2 Drainage Improvement

Subsurface drainage is recommended by the M-E Design Guide to:

- Lower the ground water level
- Intercept the lateral flow of subsurface water beneath the pavement structure, and
- Remove the water that infiltrates the pavement's surface.

Special solutions should be considered when feasible. For instance, when climate is suitable, it may be possible to place a permeable layer over a swelling soil and limit or prevent drainage from it. Moisture buildup in this layer maintains the soil in a stable and saturated condition. (Department of the Army, 1995)

Rollings and Christie (2002) noticed that the lack of adequate surface drainage is one of the critical factors leading to problems with both collapsible and expansive subgrade soils. Some obvious drainage problem signs should be monitored, such as water ponding in the drainage ditches, soft spots in the ditch, or the presence of plants and weeds that grow the best in saturated or submerged environments. They recommended drainage ditches be lined with asphalt with a protective covering of gravel to prevent leakage. In addition, cross-drains that pass through the median were also recommended so that water did not accumulate in the median prior to passing through to the other side of the roadway.

2.4.3 Geosynthetics

Adding a geosynthetic layer can increase the bearing capacity of a pavement structure by forcing the potential bearing capacity surface to develop along alternate and

higher shear strength surfaces. The geosynthetic reinforcement can absorb additional shear stresses which otherwise would be applied to the problematic subgrade. If rutting occurs, geosynthetic reinforcement is distorted and thus tensioned. Due to its stiffness, the curved geosynthetic exerts an upward force supporting the wheel load and thus the lateral restraint and/or membrane tension effects may also contribute to load carrying capacity (Hufenus et al., 2006). The inclusion of geosynthetics in flexible pavement design is difficult since number of uncertainties arise when geosynthetics is applied under distress. There are no simple rules to code a reinforced flexible pavement. The absence of an accepted design technique explains why this topic is still being researched despite the initiation usage of geosynthetics in pavement design and construction over many years ago.

There are eight types of geosynthetics (Figure 2.12): geotextiles, geogrids, geonets, geomembranes, geosynthetic clay liners, geopipe, geofoam, and geocomposties (Koerner, 2005). Geotextiles and geogrids are the most popular types of geosynthetics used in the road construction industry. Geotextiles are textiles consist of synthetic fibers rather than natural ones. These synthetic fibers have woven, non-woven, or knitted textile fabric. Geogrids are plastics formed into a very open and grid-like configuration. Geofoams are lightweight foam blocks that can be stacked and to provide lightweight fill in numerous applications. Geocomposites consist of a combination of geotextiles, geogrids, and/or other geosynthetics in a factory-fabricated unit.

Geogrids have higher tensile strengths than geotextiles. Geogrids should be used on weak subgrades with CBR values less than three (Tutumluer et al., 2005). According

to the SpectraPave2™ analysis results, the use of geogrids can effectively reduce the aggregate thickness requirements when compared to the unreinforced section results. Geogrids with higher tensile strength and high aperture stability moduli were found to give overall higher geosynthetic stiffness and hence work better than geotextiles (Giroud and Han, 2004a, b). Stiff biaxial geogrids were first used for the reinforcement of pavement in 1982 at Canvey Island, near to London, England to control reflective cracking. The use of geogrids and geotextiles is becoming more common nowadays (Austin and Gilchrist, 1996).

Expansive soils can be stabilized by maintaining volume changes in them within acceptable limits, by controlling the soil water content and also by reducing the potential of the soil to heave and shrink.

Methods to control water access to subsoils include placement of vertical moisture barriers either by grout columns or cutoff walls or geomembranes. Vertical moisture barriers placed adjacent to pavements down to the maximum depth of moisture changes can be effective in maintaining uniform soil moisture within the barrier. The use of grout columns or cutoff walls has been attempted with some success; but they can be expensive. In the case of the geomembrane barriers, Steinberg (1992) presented a case study in San Antonio where geomembranes were used for subgrade encapsulation. Although the final outcome of this research was not positive, it offered a potential method to maintain moisture variations within the barrier. Another vertical barrier used in Australian roads show a combination of inexpensive polythene layer and flowable cementatious backfill.

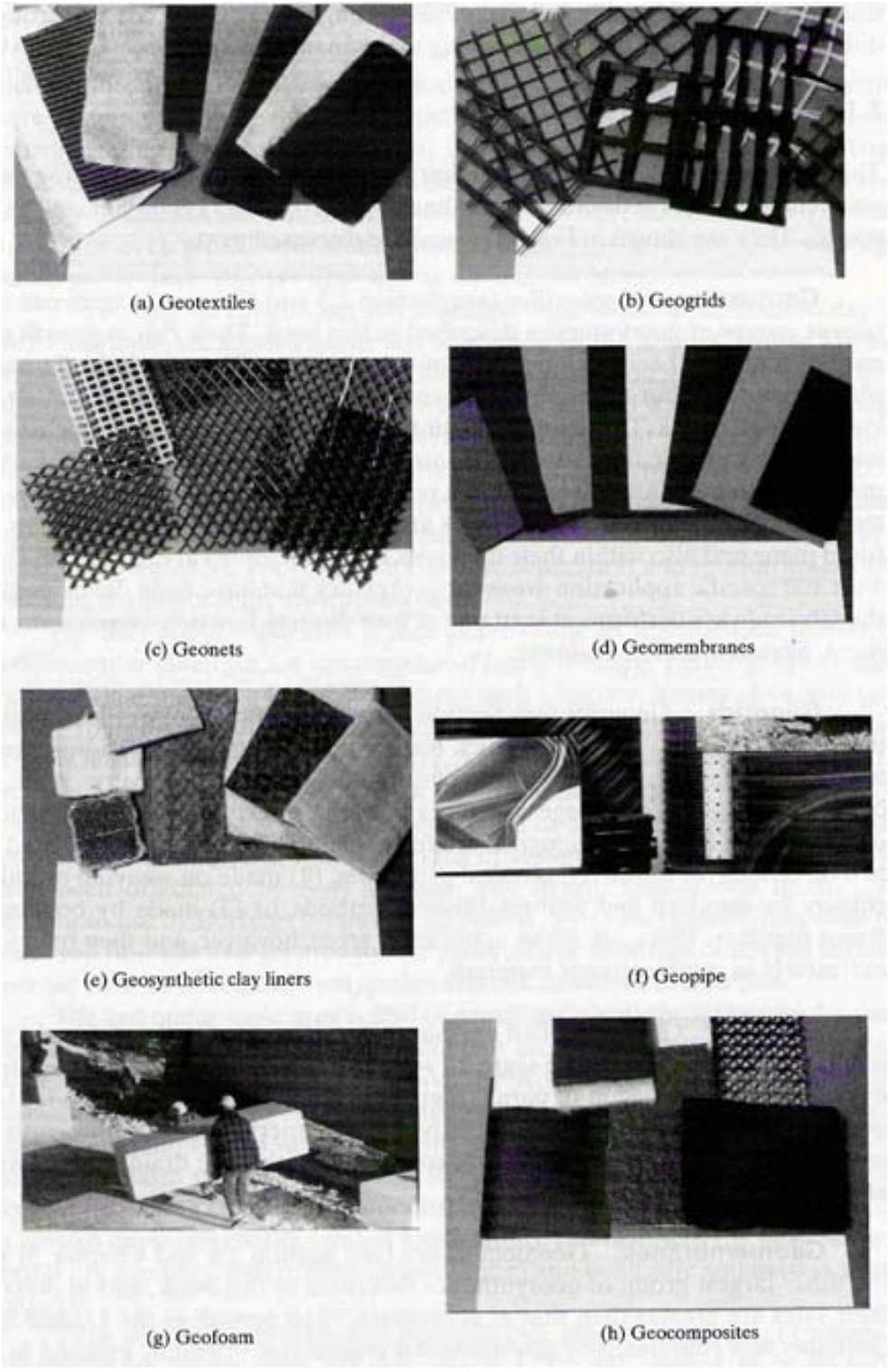

Figure 2.12 Eight types of geosynthetics (Koerner, 2005)

Other methods, including TxDOT recent research studies to stabilize expansive soils with fiber rich composts, yielded less amount of desiccation on unpaved shoulders. This resulted in less cracking in the adjacent paved shoulders. Potential stabilization with these materials can be attributed to the ability to maintain constant moisture levels and higher resistance to soil cracking through natural fiber interlocking.

In the case of stabilization methods, the intent is to reduce the heaving nature of expansive soils by chemically altering the clays. Stabilization methods for expansive soils include lime stabilization, cement stabilization and fly ash stabilization method. Stabilization mechanisms used to reduce heaving natures of soils with these treatments are well established (Hausmann, 1990). Selection of these treatment methods are currently influenced by the amount of soluble sulfates present in the subsoils and as a result, other alternate methods including sulfate resistant cement, combined lime-fiber and GGBF treatments are currently being explored (Puppala et al., 2003). All these methods and their results were reviewed and considered as the final strategy guidelines for potential stabilization of expansive high PI clayey soils.

2.4.4 Other Remediation Methods

2.4.4.1 Deep Dynamic Compaction

Almost all compacted soils have a tendency to expand and produce uplift pressures of considerable intensity when given access to water. An increase in initial moisture content will reduce the magnitude of swell and swell pressure (Mowafy et al., 1985b). In order to reduce swell and swell pressure, compaction should occur at higher

moisture content. Deep dynamic compaction is used to maximize the unit weight and density of soils. This solution may be temporary due to water infiltration.

Rollins and Christie (2002) addressed the distress problem of a 17-mile length of highway. They indicated that the problems associated with bumps, cracks and edge failures were likely associated with troubles in the subgrade soils along the alignment. Potential causes could include collapsible soil, expansive soil, compressible soil, poorly compacted fill and poor drainage. For zones with collapsible soils, deep dynamic compaction was recommended over excavation and replacement as a treatment method since the soils extended to depths of up to 20 feet below the ground surface. Deep dynamic compaction treatment was considered as one of the most economical in-situ soil improvement methods available (approximately $1 to $1.20 square foot of surface area).

Distresses related to expansive soils also existed throughout the study area. To improve the odds of success, a combination of methods were recommended: First, they recommended 3-feet excavation of the expansive material and recompaction with the same soil treated with 5% lime. Laboratory tests indicated that lime treatment would significantly reduce the plasticity of the clay (from PI of 70 in untreated to 17 in treated soils) and increase the CBR (from about 5 in untreated to 50 in treated soil). Second, they recommended a continuous rubber asphalt layer which would extend under the drainage ditches on either side of the interstate. This layer would prevent infiltration of water into the subgrade, which has occurred with the current surface drainage system. This impervious layer would need to be covered with a six-inch layer of soil to protect it

from damage. Finally, they recommended the base courses to be placed above the liner and that an asphalt wearing surface is used rather than concrete to minimize the potential for cracking.

2.4.4.2 Undercut and Backfill

The Highway Subgrade Stability Manual from Illinois DOT suggested undercut and backfill to be a popular remedial procedure for soft subgrade. The procedure is to cover the soft subgrade with a thick layer of granular material or to remove a portion of the soft material to a predetermined depth and replace it with granular material. The undercut and backfill method is a simple procedure that does not require any specialized equipment and it can be used for large scale treatments. When the backfill material is readily available, this method is relatively inexpensive (Thompson, 1982).

Ahlvin (1962) used Equation 8, developed by the Corps of Engineers to approximate the required depth of granular backfill material:

$$t = F\left[P\left(\frac{1}{8.1CBR} - \frac{1}{p\pi}\right)\right]^{1/2} \tag{8}$$

Where

t = Thickness of material layer required in inches,

P = Single or equivalent single wheel load in pounds,

CBR = CBR of underlying subgrade soil

p = Tire contact pressure, psi

F = $0.23\log C + 0.15$

C = Number of load repetitions

2.4.4.3 Decreasing Clay Content

Mowafy et al., (1985b) suggested a reduction of swelling potential can be achieved by decreasing the clay content of the problematic soil. For a given initial water content and normal pressure, there is a "critical" clay content at which the amount of swell is zero. Below the critical value the soil will shrink and above that the soil is susceptible to swelling. To accomplish the controlled clay content, the swell-susceptible clay soils could be mixed with coarse fractions of granular materials in the field.

2.4.4.4 Waterbound Macadam Base

Waterbound macadam is widely used in South Africa in 40s and 50s. The single-sized coarse aggregate is placed and compacted separately on a prepared subbase before the voids are filled with fines, and the material is then compacted and slushed (Horak, 1983). Due to the high cost and labor-intensive construction, usage of this type of construction declined. However, roads with waterbound Macadam bases have shown excellent performance and in wet regions of South Africa, this kind of bases could not only withstand destructive influence of water and heavy traffic better than other granular base, but it also can provide efficient drainage as a drainage layer. Waterbound Macadam base can provide high shear force resistance due to the coarse granular interlock (Horak and Triebel, 1986). Two conditions must be satisfied for a success use of this remediation method. First, the granular layer must be thick enough to develop acceptable pressure distribution over the problematic subgrade and second, the backfill material—coarse aggregate must be able to limit rutting under the applied wheel loads to acceptable levels (Thompson, 1979).

2.5 Summary

An attempt is made here in this chapter to review the past researches on expansive soils in various topics for example causes of expansive behaviors, volumetric changes properties and related testings, field instrumentations, swell prediction models, environmental road condition and climatic effects and remediation strategies for expansive soils. All of these presented topics will be reviewed in this research. In the next chapter, comprehensive laboratory testings and results are provided.

CHAPTER 3

LABORATORY STUDIES

3.1 Introduction

The laboratory testing program was designed to determine the properties relating to volume change behavior of expansive soil samples taken from four sites, which are located in Fort Worth, Paris, San Antonio and Houston districts in Texas. Low plasticity index (PI) soils from El Paso district are also included and compared as baseline properties. The experimental program includes basic soil properties tests, chemical and mineralogy tests, and engineering tests on the soils from these locations. A summary of the laboratory procedures, equipments used and results are presented in this chapter.

3.2 Basic Properties Tests

The tests were conducted in order to measure the basic soil properties which are carried out for most of geotechnical investigations. The tests consist of specific gravity test, sieve analysis, hydrometer test, Atterberg limits, and standard Proctor tests. The tests descriptions, and procedures are presented as follow.

3.2.1 Specific Gravity, Sieve Analysis and Hydrometer tests

Specific gravity, defined as the ratio of the mass of a given volume of solid or liquid to the mass of an equal volume of water, of testing materials was determined as

per TxDOT procedure Tex-108-E. The distribution of the grain sizes in test materials was determined using TxDOT procedure Tex-110-E. This method was also followed to determine the amount of soils finer than the No. 200 sieve opening. Finer particle size analysis was performed using hydrometer analyses.

3.2.2 Atterberg Limit Tests

Atterberg limit tests reveal properties related to consistency of the soil. These include liquid limit (LL), plastic limit (PL) and shrinkage limit (SL) and these are essential to correlate the shrink-swell potential of the soils with their respective plasticity indices. Upon addition of water the state of soil proceeds from dry, semisolid, plastic and finally to liquid states. The water content at the boundaries of these states are known as shrinkage (SL), plastic (PL) and liquid (LL) limits, respectively (Lambe and Whitman 2000). Therefore, the LL is measured as the water content at which the soil flows and the PL is determined as the water content at which the soil starts crumbling when rolled into a 1/8-inch diameter thread.

These plasticity tests are somewhat operator sensitive. The numerical difference between LL and PL values is known as plasticity index (PI) and this index characterizes the plasticity nature of the soil. Representative soil samples from regular depths are prepared following the above mentioned procedure and are subjected Atterberg limit tests to determine LL and PL following Tex-104-E and Tex-105-E, respectively. The water content of the samples during tests are measured using microwave drying method based on the repeatable data as reported by Hagerty et al. (1990).

3.2.3 Standard Compaction Tests

In order to determine the compaction moisture content and dry unit weight relationships of the soils in the present research program, it is necessary to conduct standard Proctor compaction tests on soils to establish compaction relationships. The optimum moisture content of the soil is the water content at which the soils are compacted to a maximum dry unit weight condition. Samples exhibiting a high compaction unit weight are best in supporting civil infrastructure since the void spaces are minimal and settlement will be less. Standard Proctor test method using Tex-114-E procedure was followed.

3.3 Chemical and Mineralogical Tests

3.3.1 Determination of Organic Contents

Organic contents were determined by following the ASTM D-2974-87 procedure. Ash content was determined to calculate the organic content. First, the soil was oven dried for 24 hours and the weight of the soil sample was measured and reported as 'A' grams. The soil was then taken in a porcelain dish and placed in a muffle furnace maintained at a constant temperature of 440^{o}C and held there until the specimen was ashed completely. The dish was covered with an aluminum foil and placed in a desiccator until the sample cooled down completely. The weight of this ashed sample was measured and reported as 'B' grams. The ash content was calculated as a ratio of (B/A) expressed in percentage and the organic content was calculated in percent as 100 - Ash content in percentage.

3.3.2 Determination of Soluble Sulfates Contents

The soluble sulfate in the soil is known for the cause of soil heaving when stabilized with calcium based stabilizers. Hence, it is importance to determine the sulfate levels of the studied soils to ensure that those studied soil contained low amount of sulfate since sulfate induced heaving problem is out of the scope of this research. Modified University of Texas Method (2002) formulated by Puppala et al. (2002) which is a modified standard gravimetric procedure was used for measuring the amount of soluble sulfates along with a calorimetric based TxDOT method. Further details on the sulfate gravimetric method can be found in Intharasombat (2003) and Wattanasanticharoen (2004).

3.3.3 Cation Exchange Capacity (CEC)

The CEC is the quantity of exchangeable cations required to balance the negative charge on the surface of the clay patitcles. CEC is expressed in milliequivalents per 100 grams of dry clay. In the test procedure, excess salts in the soil are first removed and absorbed cations are replaced by saturating the soil exchange sites with a know species. The amount of the known cation needed to saturate the exchange sites is determined analytically (Nelson and Miller, 1992).

CEC is related to clay mineralogy. High CEC values indicated a high surface activity. In general, swell potential increases as the CEC increases. Typical values of CEC for the three basic clay minerals are shown in Table 3.1 below.

Table 3.1 Typical values for three basic clay minerals (Mitchell, 1976).

Clay Mineral	CEC (Meq/100 g)
Kaolinite	3 -15
Illite	10 – 40
Montmorillonite	80 – 150

The measurement of CEC requires detailed and precise testing procedures that are not commonly done in most soil mechanics laboratories. However, this test is routinely performed in many agricultural soils laboratories and is inexpensive (Nelson and Miller, 1992).

3.3.4 Determination of Clay Mineralogy

Clay mineralogy is a fundamental factor controlling expansive soil behavior. Clay minerals can be identified using a variety of techniques. For this research, X-Ray diffraction, the most popular method, has been utilized. The method works on the principle that beams of X-Ray diffracted from crystals are similar to light reflections from the crystal lattice planes. X-Ray analysis is of the same order of magnitude (about 1 Å or 10^{-9} mm) as the atomic plane spacings of these minute crystals. The basal plane spacing is characteristic for each clay mineral group and gives the most intense reflections. Characteristic basal spacings are tabulated in Table 3.2.

Table 3.2 Clay mineral and basal spacing

Clay Mineral	**Basal Spacing (Å)**
Kaolinite	14.4
Illite	10.0
Montmorillonite	9.6

3.4 Engineering Tests

Engineering tests performed in this research were volumetric shrinkage test, three-dimension free swell test, pressure swell test, and matric suction measurement for all four soil types.

3.4.1 Volumetric Shrinkage Test

Due to limitations in the linear shrinkage bar test, researchers propose a new test method developed at UTA of using cylindrical compacted soil specimens for subjecting them to drying process and then measuring the volumetric, axial and radial shrinkage strains using digital imaging technology. This test offers several advantages over conventional linear shrinkage bar test such as reduced interference of boundary conditions on shrinkage, larger amount of soil being tested, and simulates compaction states of moisture content - dry density conditions. This method was published in ASTM geotechnical testing journal (Puppala et al., 2004), which signifies the importance of this method being accepted by the researchers and practitioners. Linear shrinkage bar test was also conducted to complement the volumetric shrinkage

properties and develop correlations between linear and volumetric shrinkage strains. Details of these procedures are presented in the following.

Volumetric shrinkage tests were conducted to measure the decrease in the total volume of soil specimens due to loss of moisture content from predetermined initial moisture content to a completely dry state. Three different initial moisture contents (optimum, wet of optimum and dry of optimum) were used as initial compaction conditions and tests were conducted as per the procedure outline in Puppala et al. (2004). Specimen preparations were performed by mixing the dry clay with appropriate amount of water to achieve the designed water contents, compacting the soil specimens in 2.26 in. diameter and 5 in. height mold, and measuring the initial height of the specimen. The specimens were then cured in the mold at room temperature for 12 hours and then transferred to an oven set at a temperature of 220^{o}F for 24 hours (Figure 3.1 (a) and (b)). Then, the average height and diameter of the shrunk soil specimen are manually measured. The same soil specimen is subjected to digital imaging and the images (Figure 3.2 (a) and (b)) will be used in the following equation (1) to determine volumetric shrinkage strains.

(a) (b)

Figure 3.1 Specimen (a) before oven dried and (b) after oven dried

$$V.S. = \frac{V_i - V_f}{V_i} = 1 - \frac{V_f}{V_i} = 1 - \left[\frac{A_{sf}}{A_{si}} * \frac{A_{cf}}{A_{ci}} * \frac{P_{ci}}{P_{cf}} \right] = 1 - \left(R_s * R_c * R_p \right) \quad (1)$$

Where

R_s = ratio of surface area of the soil specimen = A_{sf}/A_{si}

R_c = ratio of circular cross-section area of soil specimen = A_{cf}/A_{ci}

R_p = ratio of the circular perimeter of the soil specimen = P_{ci}/P_{cf}

V_f = final volume of the cylindrical specimen

V_i = initial volume of the cylindrical specimen

A_{sf} = area of the final surface area of specimen after shrinkage in pixels

A_{si} = area of initial surface area of specimen before shrinkage in pixels

A_{cf} = area of final circular area of specimen after shrinkage in pixels

A_{ci} = area of initial circular area of specimen before shrinkage in pixels

P_{cf} = perimeter of the final circular area after shrinkage in pixels

Pci = perimeter of circular area before shrinkage in pixels

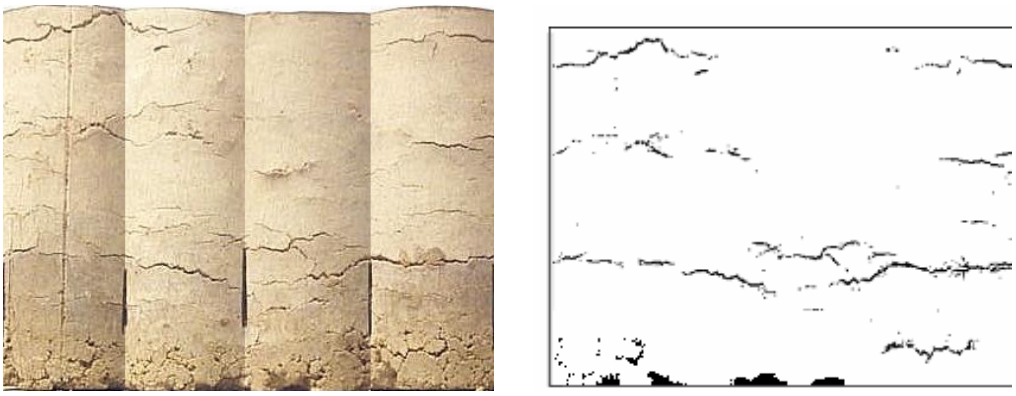

(a) (b)

Figure 3.2 (a) Typical photograph of a soil specimen surface area with cracks after test (b) Threshold image of the surface area showing only cracks

The above Equation will be used to determine volumetric shrinkage strain by capturing and analyzing digital images of surface and areal pictures of cylindrical soil specimen before and after the shrinkage test. Public-domain software, Scion, will be used in the analysis. Figure 3.2 presents surficial cracking of soil specimen after shrinkage test. As noted earlier, three proposed states of moisture conditions were simulated and studied.

3.4.2 Three-Dimensional Free Swell Testing

This test was conducted to investigate the maximum vertical, radial and volumetric swell potentials. Specimens were prepared at three different moistures conditions with corresponding densities, which are optimum, dry of optimum and wet of optimum moisture content. A specimen of 4.0-in. diameter and 4.6 in. high was

placed between two porous stones (Figure 3.3), wrapped in a rubber membrane, and was subjected to soaking by inundating it with water from both ends (Punthutaecha et al., 2003). The specimen was monitored for the vertical and radial swell movement until there was no further significant movement.

The three-dimensional free swell test investigates the maximum vertical, diametric and volumetric swell potentials for soil types. The Vertical and radial swell movement are simply measured at the times of recording by using Dial gauge and PI tape (Figure 3.3), respectively. The three-dimensional free swell test provides a reasonable representation of the soil maximum volumetric swell potential (Punthutaecha, 2006). All tests should be conducted at room temperature and three identical soil specimens should be used for each variable condition. Typical test results are expressed as a time-swell. The swelling strains for the three moisture conditions and for the 5 soils are reported in Table 3.11.

3.4.3 Swell Pressure Test

The constant swell pressure test was conducted as per ASTM D-4546 and is defined as the amount of load that should be applied over the expansive soil to resist any volume change in vertical direction. The Schematic and test set up in present study are shown in Figure 3.5 and 3.6. This test is commonly used to maximum swelling pressure of the soil specimen at which no volume change is occurred.

Figure 3.3 Three-dimensional free swell test setup

Specimens were compacted in a ring of 2.5 in. in diameter and 1.0 in. in thickness at 3 different moistures (optimum, dry of optimum and wet of optimum) conditions. The specimens were fully soaked in the standard consolidation setup. Two porous stones were placed at the top and bottom of the specimens. A dial gauge was used to monitor changes in specimen's movement. Loads were added in order to maintain original position. Testing was discontinued when the dial gauge showed no swell movement for more than two days. The total load applied to the specimen was then used to calculate its swell pressure.

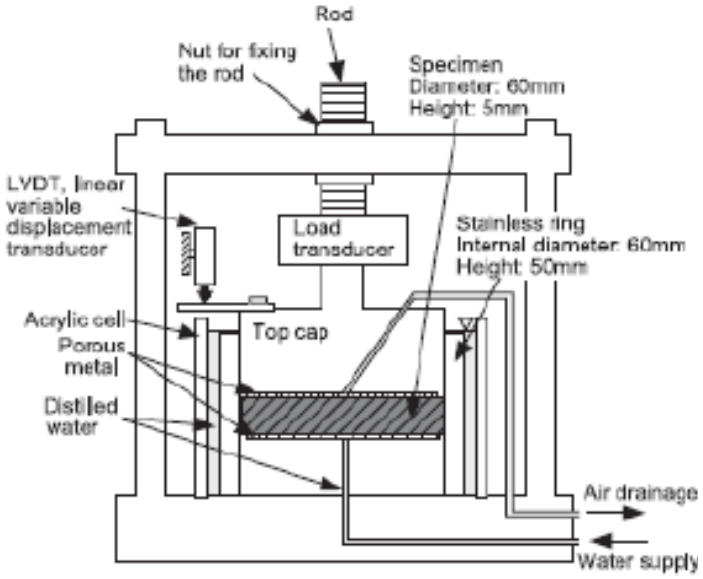

Figure 3.4 schematic of modified consolidation tests setup

Figure 3.5 Modified consolidation tests setup

3.4.4 Suction Measurements by Pressure Plate and Filter Paper Method

Several test methods including filter paper and pressure plate method are commonly used to develop Soil Water Characteristic Curves (SWCCs) of unsaturated soils studies. The limitation of the current pressure plate device at UTA is that it can measure matric suction up to only 1,000 kPa. Therefore, filter paper method was used to measure soil suction ranging more than 1,000 kPa. Hence, both pressure plate and filter paper methods were employed in the development of a complete SWCC of the present soils.

3.4.4.1 Pressure Plate Method

Figure 3.6 shows the schematic of a typical pore water extraction testing setup using a pressure plate apparatus. The primary components of the system are a steel plate pressure vessel and a saturated High Air Entry (HAE) ceramic plate. As shown, a small water reservoir is formed beneath the plate using an internal screen and a neoprene diaphragm. The water reservoir is vented to the atmosphere through an outflow tube located on top of the plate, thus allowing the air pressure in the vessel and the water pressure in the reservoir to be separated across the air-water interfaces bridging the saturated pores of the HAE material (Lu and Likos, 2004).

Specimens are initially saturated, typically by applying a partial vacuum to the air chamber and allowing the specimens to imbibe water from the underlying reservoir through the ceramic disk. Air pressure in the vessel is then increased to some desired level while pore water is allowed to drain from the specimens in pursuit of equilibrium. The outflow of water is monitored until it ceases, the pressure vessel is opened, and the

water content of one or more of the specimen is measured, thus generating one point on the soil-water characteristic curve. Subsequent increments in air pressure are applied to generate addition points on the curve using the other specimen.

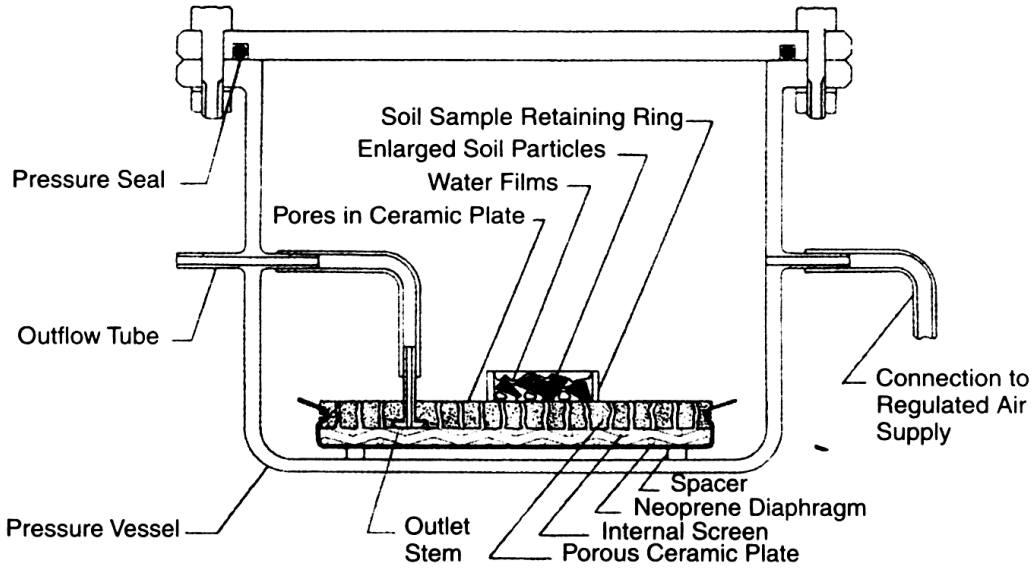

Figure 3.6 Schematic drawing of pressure plate apparatus
(Soil-Moisture Equipment Corp., 2003)

3.4.4.2 Filter Paper Method

For filter paper method, a filter paper (Schleicher & Schuell No. 589-WH type) is suspended in the headspace above the specimen such that moisture transfer occurs in the vapor phase. The equilibrium amount of water absorbed by the filter paper is a function of the pore-air relative humidity and the corresponding total soil suction. The water content of the filter paper was measured after it reached equilibrium with the soil through vapor for a period of ten days. The suction was estimated from the filter papers's moisture content using a caibratlion curve proposed by Bulut, Lytton, and

Wray (2001) (Figure 3.8). By measuring at various moisture contents, the soil water characteristic curves were obtained.

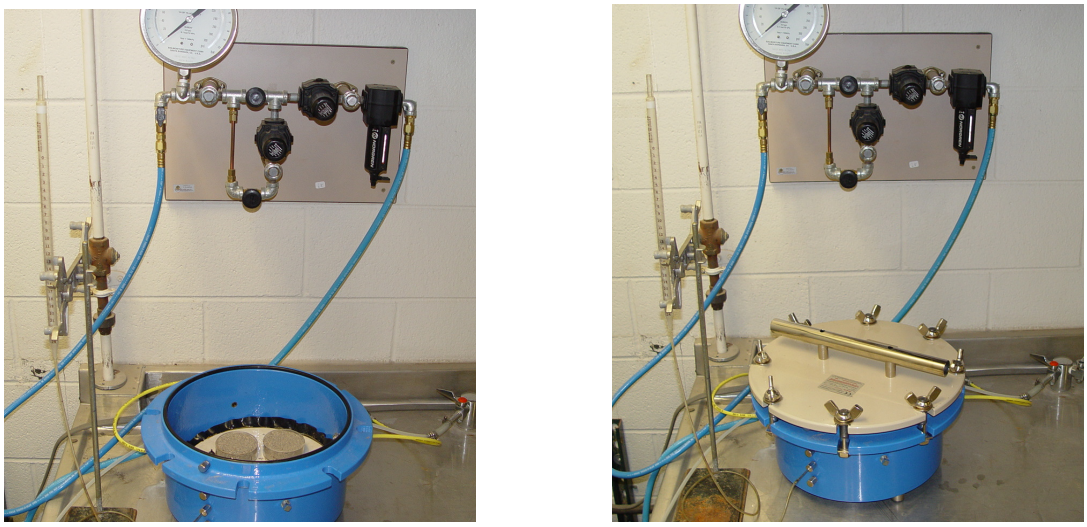

(a) (b)

Figure 3.7 Pressure plate testing (a) Initial setup of testing specimen and (b) Closed pressure vessel with air pressure applied

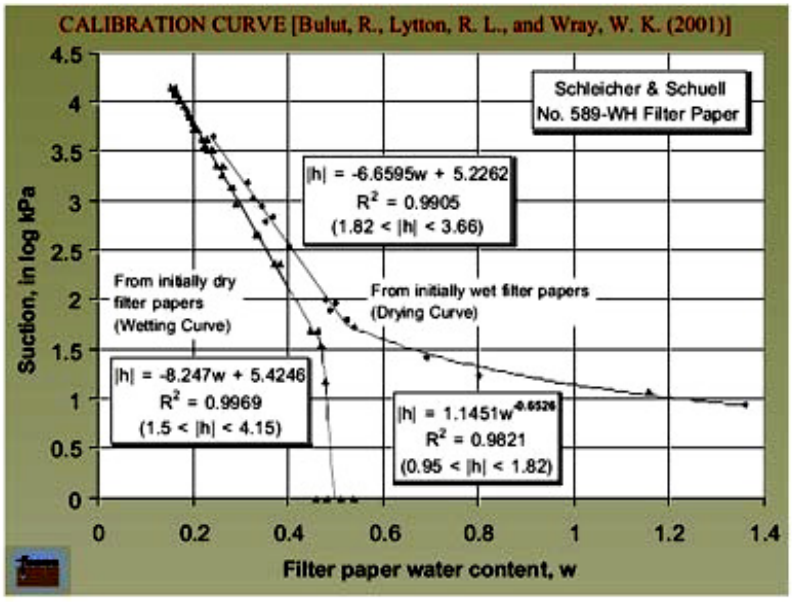

Figure 3.8 Calibration curves (Bulut, Lytton and Wray, 2001)

3.5 Laboratory Test Results

3.5.1 Basic Soil Properties Results

All representative soil samples used in this research were collected from borrow pits adjacent to paved shoulders at four sites located in Fort Worth, Paris, San Antonio and Houston, Texas. Table 3.3 presents a summary of various physical characteristics of all soils from the tests conducted on the representative samples.

Table 3.3 Basic soil properties

Property	**Soil Types**				
	Fort Worth	**San Antonio**	**Paris**	**Houston**	**El Paso**
Passing #40 (%)	100	100	100	100	100
Passing #200 (%)	85	83	81	87	88
Specific Gravity	2.7	2.7	2.7	2.7	2.7
Liquid Limit (LL, %)	61	58	60	54	30
Plastic Limit (PL, %)	24	22	23	21	14
Plasticity Index (PI, %)	37	36	37	33	16
AASHTO Classification	A-7-6	A-7-6	A-7-6	A-7-6	A-6
USCS Classification	CH	CH	CH	CH	CL

Generally, soils that exhibit plastic behavior over wide ranges of moisture content and that have high liquid limits have greater potential for swelling and

shrinking. According to expansive soil characterization information given in Table 3.4, Soils from Fort Worth, San Antonio and Paris are considered very high swelling potential whereas Houston soil is considered as only exhibiting high swelling potential. All four soils are classified as A-7-6 as per American Association of State Highway and Transportation Officials (ASSHTO) Soil Classification System and CH as per Unified Soil Classification System (USCS).

Table 3.4 Expansive soil classification based on plasticity index (Chen, 1988)

Plasticity Index	**Swelling Potential**
0 - 15	Low
10 - 35	Medium
20 - 55	High
35 and above	Very High

3.5.2 Chemical Characteristics

Chemical analysis was also introduced in this research in order to justify the causes of volume change problems. In many cases, not only the intrinsic properties of soil itself but also organic and/or soluble sulfate content plays important rules in swell/shrink behaviors. Hence, tests related soil chemical properties information and organic content were also performed. The results of the analysis are shown in the Table 3.5 below.

Table 3.5 Chemical characteristics of test materials

Property	Soil Types				
	Fort Worth	San Antonio	Paris	Houston	El Paso
Organic Content (%)	5.6	3.4	3.2	3.2	1.6
Soluble Sulfates (ppm)	358	82	136	247	1,201

As a result, all soils will not pose any problem related to organic contents. For soluble sulfates content, the test revealed that all four soil contained soluble sulfates less than 2,000 ppm which are considered as low sulfate contents.

Table 3.6 Guiding values for the classification of soils on the basis of organic content (Karlson and Hansbo, 1981)

Soil group	Organic content in % of dry material
Low organic soils	2-6
Medium organic soils	6-20
High organic soils	>20

3.5.3 Cation Exchange Capacity (CEC) and Clay Mineralogy Results

For better characterization and understanding, it is desirable to have a comprehensive understanding of the soil mineralogy as well as volume change related characteristics of the soils. Cation Exchange Capacity (CEC) is the quantity of exchangeable cations required to balance the negative charge on the surface of clay particles. High CEC values indicate a high surface activity of the clays (Nelson and Miller, 1992). In general, the swell potential increases as the CEC increases. The CEC values are reported in Table 3.7.

Clay minerals which typically cause soil volume changes are montmorillonites and some mixed layer minerals. Illite can be expansive but generally do not pose significant problem. Kaolinite is normally nonexpansive (Nelson and Miller, 1992). The test results for all soil types are shown in Table 3.8 below.

Table 3.7 Cation exchange capacity (CEC) results

Property	**Soil Types**				
	Fort Worth	**San Antonio**	**Paris**	**Houston**	**El Paso**
CEC (meq/100 g)	117	96	133	76	57
Specific Surface Area (m^2/gm)	314	269	431	236	167

Table 3.8 Mineralogy characteristics of test materials

Clay Minerals	Soil Types				
	Fort Worth	**San Antonio**	**Paris**	**Houston**	**El Paso**
% Illite	16	18	13	26	63
% Kaolinite	34	40	17	38	29
% Montmorillonite	50	42	70	36	8

Both Fort Worth and Paris clays are predominantly containing Montmorillonite clay minerals, signifying the greater volume changes problem in the fields. Although the Houston clay contains lesser amounts of Montmorillonite minerals, the value is still considerable. El Paso clay, low Plasticity Index clay, posses noticeably low amount of Montmorillonite minerals.

3.5.4 Standard Compaction Tests

Proctor Compaction tests were performed to establish compaction relationships. The optimum moisture content (OMC) of the soil is the water content at which the soil is compacted to a maximum dry density condition. Water contents at 95% of maximum dry density conditions are dry of OMC and wet of OMC which are defined in Figure 3.9 below.

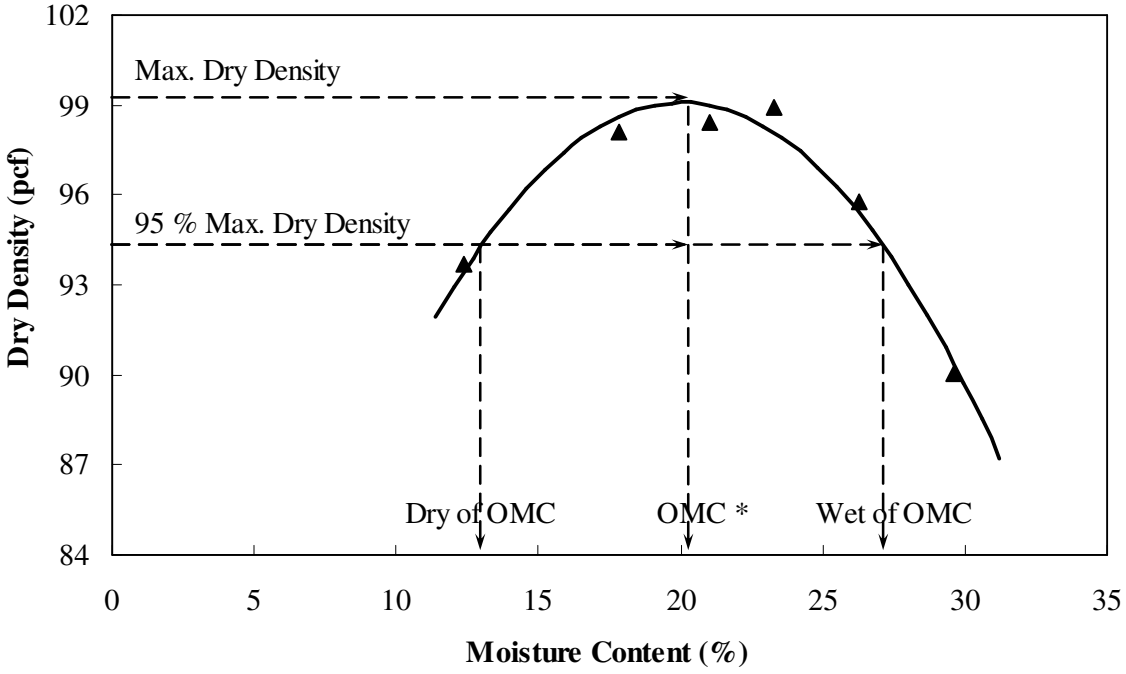

Figure 3.9 Typical standard proctor curve

Table 3.9 Proctor density tests results

		Fort Worth	San Antonio	Paris	Houston	El Paso
Moisture Content (%)	**Wet of OMC**	33.0	31.8	33.0	27.3	20.0
	OMC	24.0	21.7	23.0	20.1	16.5
	Dry of OMC	15.1	10.5	13.0	12.9	13.0
Dry Density (pcf)	**Wet of OMC**	86.9	86.9	87.5	94.1	106.4
	OMC	91.5	91.5	92.1	99.1	112.0
	Dry of OMC	86.9	86.9	87.5	94.1	106.4

From Table 3.9, El Paso clays shows the highest dry density which indicated better quality of this soil in supporting civil infrastructure whereas Houston clayey soil exhibits the highest value among high PI clay group. It should be noted that all three moisture contents conditions, wet of OMC, OMC and dry of OMC, are very important parameters which will be used as references moisture contents for the engineering tests performed in this research.

3.5.5 Volumetric Shrinkage Strain Results

Test results are expressed in term of volumetric shrinkage strain in percent values. Shrinkage strains in radial and vertical directions were first recorded and used to determine volumetric shrinkage strains. Volumetric shrinkage strain test is a better test method than linear shrinkage strain test since volumetric strain was evaluated on tests on soil samples of considerable volume.

Specimens for each soil type were prepared at least 3 samples for each moisture condition. The average shrinkage test values are presented in Table 3.10 below. These results will be used in corporate with soil movement prediction models in subsequent chapters.

Table 3.10 Volumetric shrinkage strain results

Moisture Condition	Parameter	Shrinkage Strain (%)				
		Fort Worth	San Antonio	Paris	Houston	El Paso
Wet of OMC	Vertical	8.43	9.91	8.78	5.11	4.28
	Radial	8.87	9.66	9.45	7.37	3.55
	Volumetric	23.59	26.68	24.66	18.58	10.97
OMC	Vertical	5.29	6.98	4.92	2.25	1.86
	Radial	2.47	5.33	4.91	4.57	1.77
	Volumetric	12.51	18.08	14.04	10.97	5.30
Dry of OMC	Vertical	2.17	2.81	2.41	1.44	0.36
	Radial	0.97	2.13	1.46	1.75	1.50
	Volumetric	5.22	7.55	6.15	4.85	3.33

The highest to the lowest shrinkage strain potentials are attributed to the clayey soils from San Antonio, Paris, Fort Worth, Houston, and El Paso, respectively.

3.5.6 Three-Dimensional Free Swell Test

In this testing, 3 soil samples for each moisture conditions were compacted at three different compaction moisture content conditions with their corresponding dry densities from a standard Proctor test results (Table 3.9). Table 3.11 presents the average swell strain of the test results. The typical swell characteristic graphs are shown in Figure 3.10 to 3.12 below. These results will also be used in corporate with soil movement prediction models in subsequent chapters.

Table 3.11 Volumetric swell strain tests results

Moisture Condition	**Parameter**	**Swell Strain (%)**				
		Fort Worth	**San Antonio**	**Paris**	**Houston**	**El Paso**
Wet of OMC	**Vertical**	3.63	2.99	1.43	4.14	1.47
	Radial	1.95	1.95	1.51	1.63	0.81
	Volumetric	7.71	7.04	7.50	7.56	3.11
OMC	**Vertical**	9.28	6.98	7.37	6.71	2.43
	Radial	3.46	3.80	3.60	3.81	1.27
	Volumetric	16.97	15.27	15.25	14.99	5.04
Dry of OMC	**Vertical**	14.13	14.92	14.35	11.44	4.51
	Radial	4.26	5.93	5.36	4.49	1.76
	Volumetric	24.07	28.95	26.93	21.69	8.23

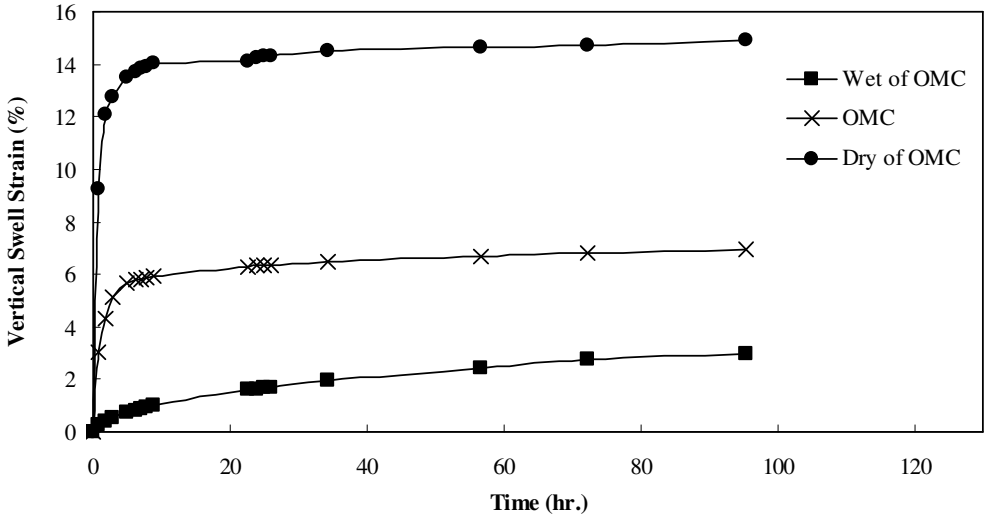

Figure 3.10 Typical vertical swell strains results from three-dimensional swell tests for three different moisture contents

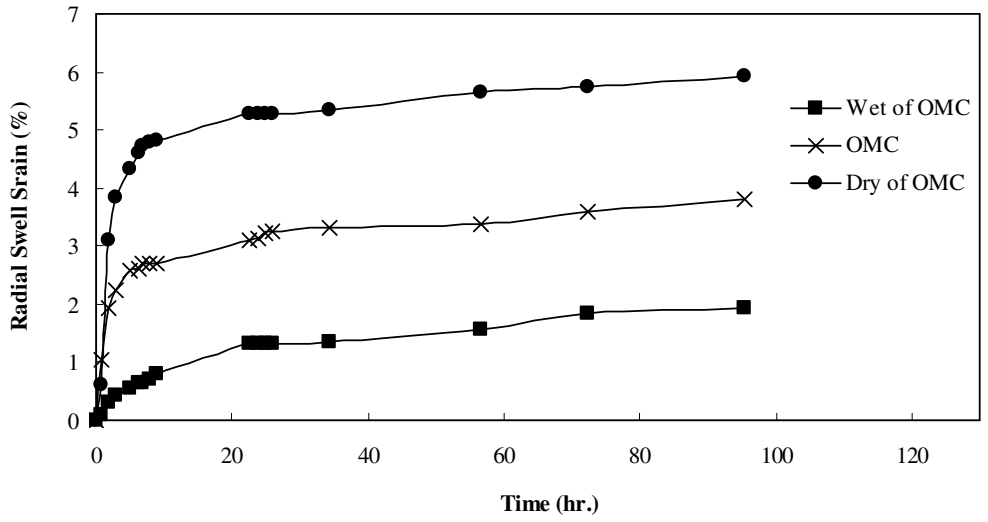

Figure 3.11 Typical radial swell strains results from three-dimensional swell tests for three different moisture contents

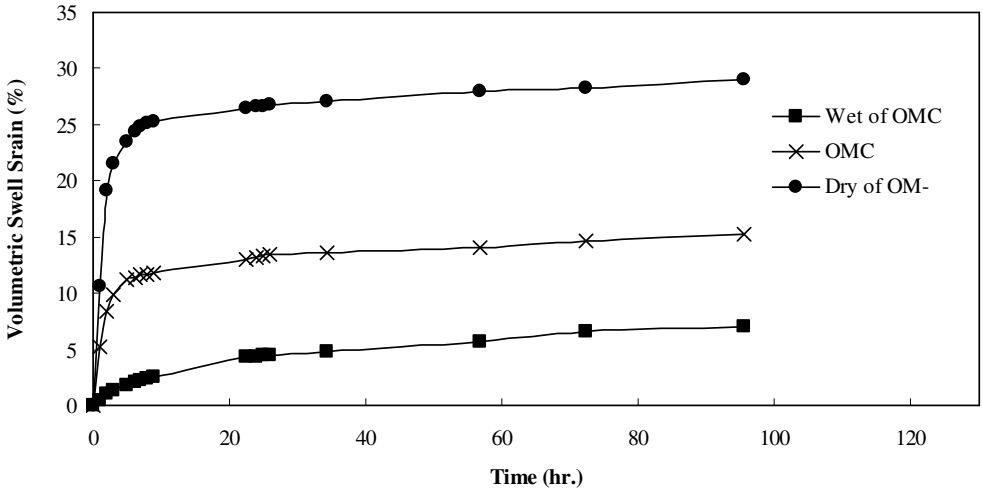

Figure 3.12 Typical volumetric swell strains results from three-dimensional swell tests for three different moisture contents

Majority of swell strains in soils was observed within the first eight hours and subsequent swell strains were continuously recorded until no swell movement was observed. Test results are expressed in terms of vertical, radial and volumetric swell strains. All four high PI soil types, Fort Worth, San Antonio, Paris and Houston soils, showed volumetric swell strain (for OMC condition) more than 10% which is considered as a very high degree of expansion (Chen, 1965). As expected, El Paso clay exhibited lowest swell strain results because El Paso clay exhibited lowest Plasticity Index, low percent of Montmorillonite clay mineral, low CEC and low specific surface area values.

3.5.7 Swell Pressure Test

The constant swell pressure tests were performed following the procedures reported by Sridharan et al. (1986) and Fredlund and Rahardjo (1993). The test was conducted in order to measure maximum loads or pressures that soils exhibit in order to maintain original volume. Swelling pressure test results were presented in term of ksf (kilopound per square foot) values. Table 3.12 presents test result for all four soils and three different moisture conditions.

Table 3.12 Swell pressure test results

Moisture Condition	**Swell Pressure (ksf)**				
	Fort Worth	**San Antonio**	**Paris**	**Houston**	**El Paso**
Wet of OMC	1.55	1.44	1.51	1.26	0.23
OMC	2.67	2.32	3.47	1.65	0.54
Dry of OMC	3.10	2.89	3.98	2.47	0.78

As expected, the swelling pressures for soils tested at wet of optimum condition exhibited low values and those at dry of optimum provided highest values. This is the reason behind numerous roads underlained by the expansive soils experience cracking when those soils are exposed to heavy rain falls following long dry periods of high temperatures. Test results revealed the same trend as other test results, showing El Paso clay exhibited lowest swell pressure values than other clays and Houston provided the

lowest values among high Plasticity Index clays. Still, the swell values measured for Houston clay are considerable to pose the problem in the field condition.

3.5.8 Matric suction Measurement by Pressure Plate and Filter Paper Method

Soil suction measurements were measured on present soils at different compaction moisture content conditions in order to establish Soil Water Characteristic Curves (SWCCs) for all soils. The SWCC describes a unique relationship between the matric suction and the moisture content of a given soils. In unsaturated soil mechanics, the SWCC is used in direct and indirect interpretations of soil strength, permeability and volume change related characteristics (Fredlund et al., 1994). The curve depends on the size and distribution of pore structures in soils, which control the permeability and amount of volume changes expected in soils (Fredlund et al., 1994).

For this research, the pressure plate method were utilized for measuring soil matric suction ranging 0 to 1000 kPa and the filter paper method were then used for the ranges more than 1,000 kPa. Although, filter paper method can evaluate both matric and total suction (total suction is a summation of matric suction and osmotic suction), only total suction measurement technique was measured.

The measured total suction is considered as matric suction because, at high total suction levels (over 1,000 kPa), the measured values are minutely affected by osmotic suction especially since the soils considered in this study contain very low amounts of salts or soluble sulfates (as shown in Table 3.5). The combined test results from pressure plate and filter paper methods are presented in the forms of SWCC as shown in Figures 3.13 to 3.16.

It should be noted that, in this suction testing, only high plasticity clays which are Fort Worth, San Antonio, Paris, and Houston are conducted.

SWCCs of all four high PI soils exhibited similar characteristics. The only noticeable difference is the saturated moisture content (at zero suction) for Houston clay, which is much lower than the other three soils. This lower value indicates less ability to hold up water or moisture, which mean that they do not undergo large swelling when hydrated.

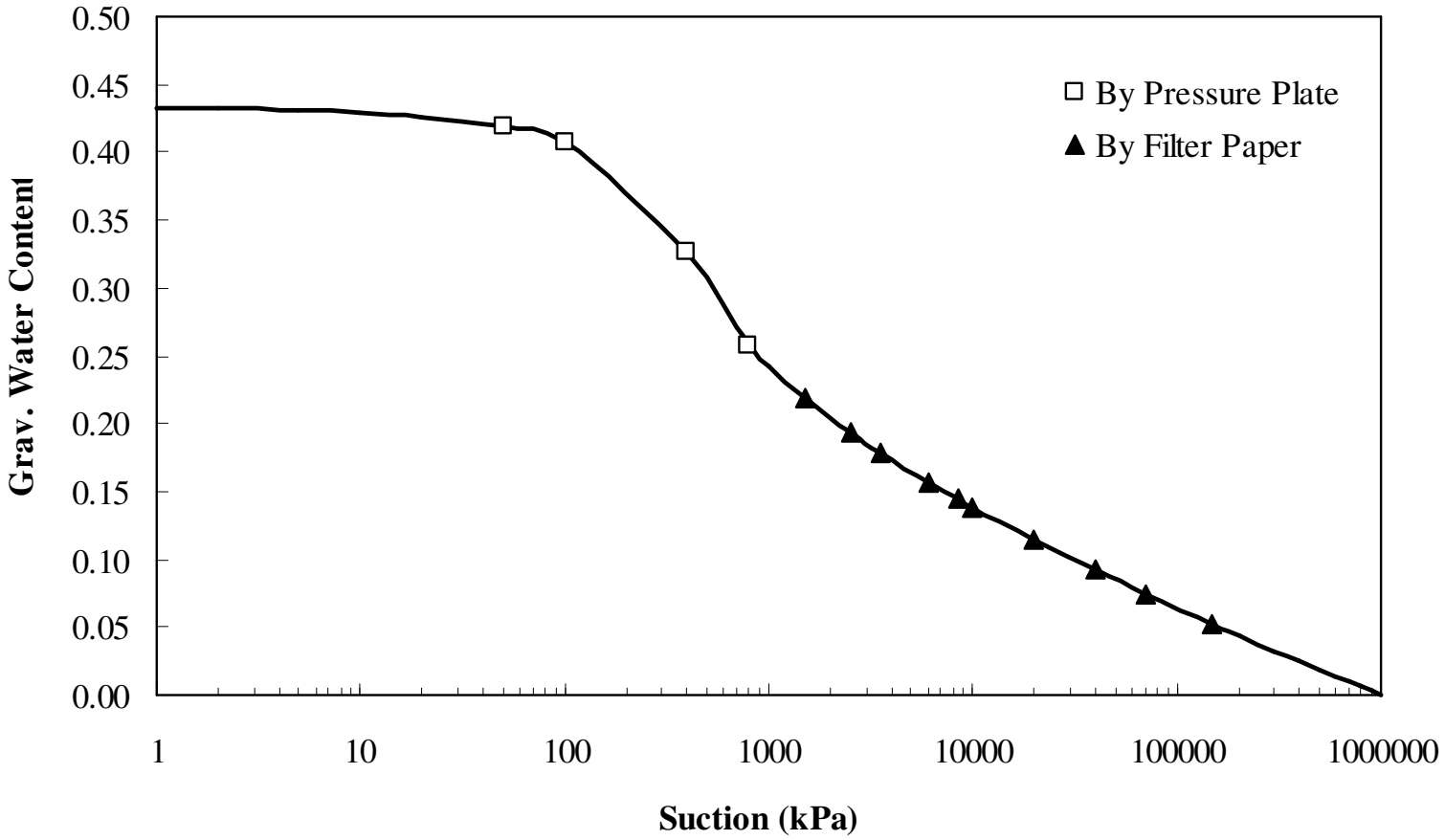

Figure 3.13 SWCC of Fort Worth clay

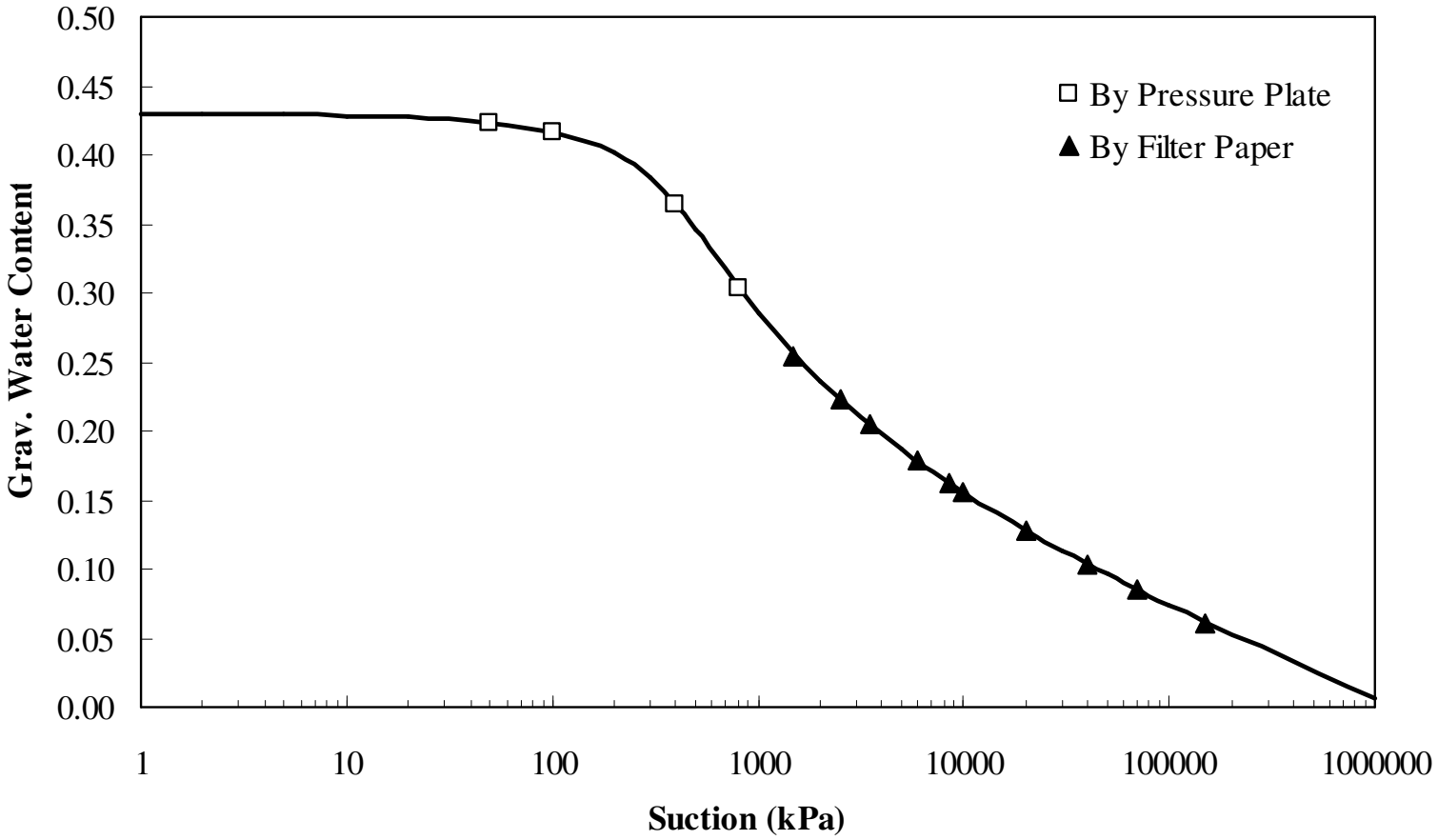

Figure 3.14 SWCC of San Antonio clay

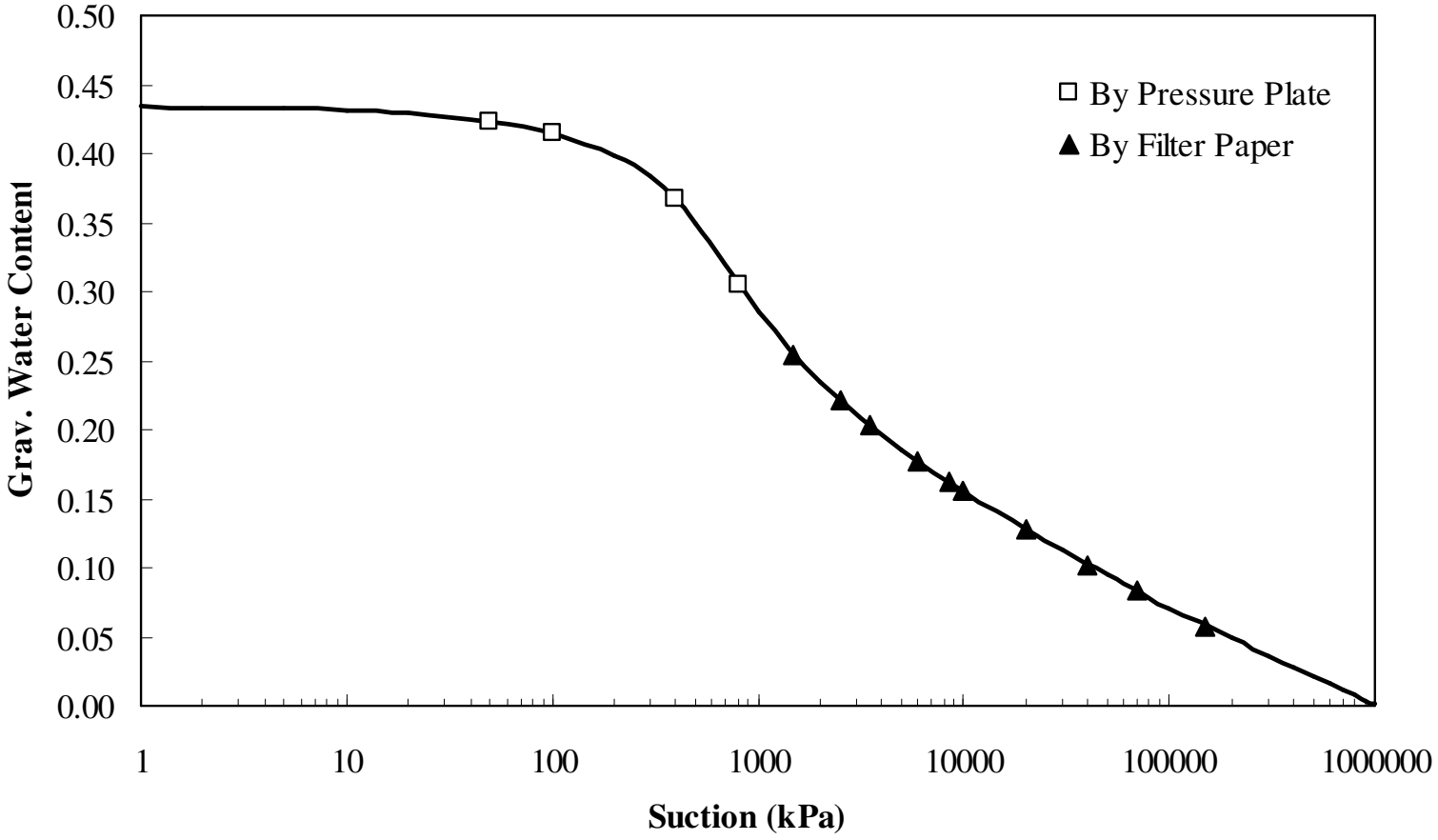

Figure 3.15 SWCC of Paris clay

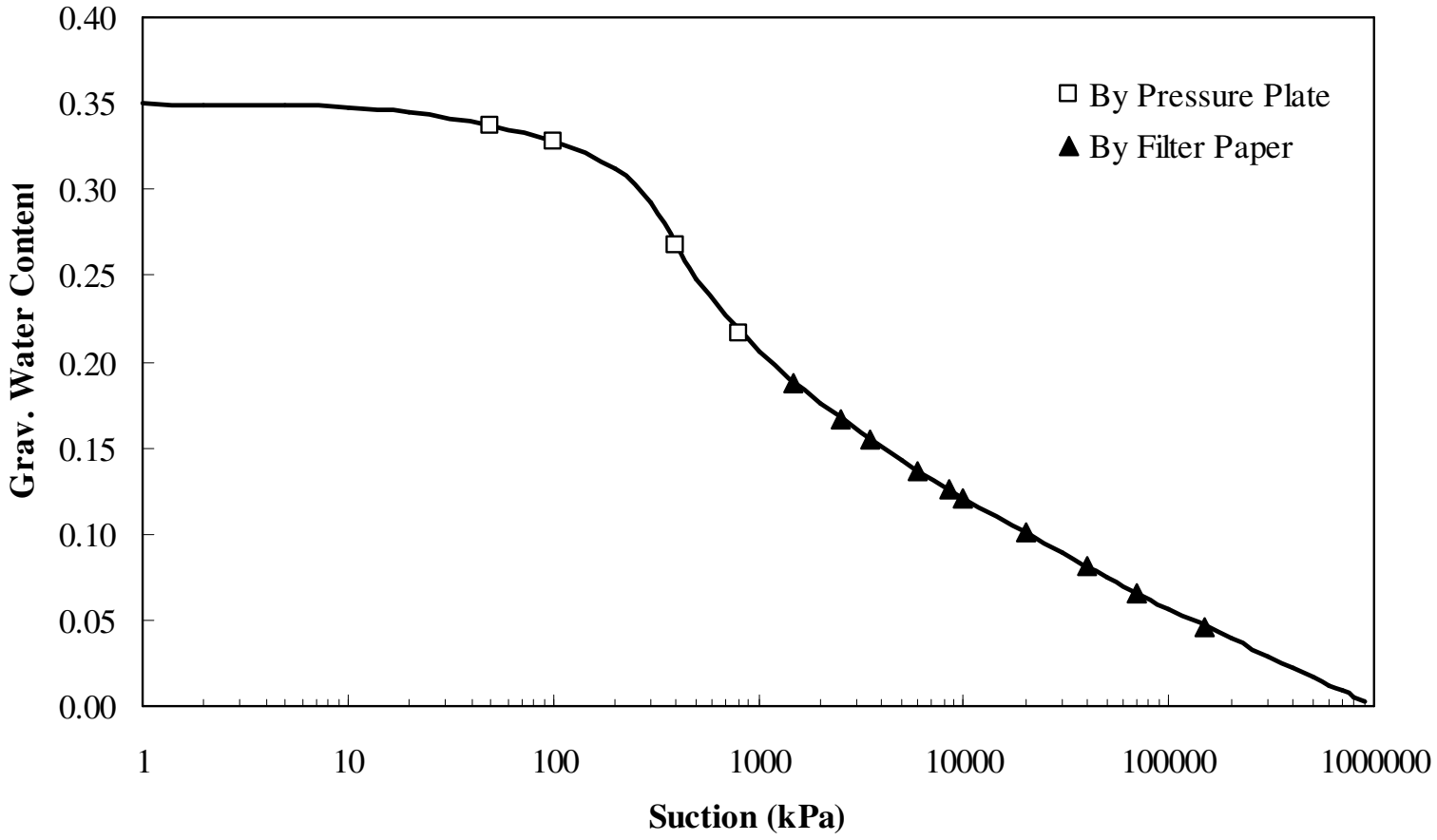

Figure 3.16 SWCC of Houston clay

3.6 Ranking Analysis

Since each clayey soil at various compaction states exhibited different shrink-swell behaviors, an attempt is made here to characterize the problematic nature of the present soils at three different moisture content conditions. The following scale system was used to characterize problematic levels from non-problematic to highly problematic levels by assigning a numerical ranking. The magnitude of ranking is based on the severity of the soil problem. The worst soil condition is given a rank of 1 and the best soil condition is given a rank of 5. In between conditions, ranks from 2 to 4, are assigned for different ranges of soil properties.

The factors that used in this ranking analysis composed of Liquid Limit (LL), Plasticity Index (PI), Volumetric Swell Strain (VSW), Volumetric Shrinkage Strain (VSH), Swell Pressure (SP), and Percentage of Montmorillonite Mineral Content (MM).

Table 3.13 gives the soil properties rank numbers based on level of degree of expansion of soils. The Overall Rank Number (ORN) is defined by the following equation.

$$ORN = \frac{1}{6}\{(PI) + (LL) + (VSW) + (VSH) + (SP) + (MM)\} \qquad (2)$$

After the Overall Rank Number (ORN) of all three moisture conditions and all soil types were evaluated, those numbers will finally be averaged in order to distinguish which soil is the worst, which soil is the best and which soils are in between.

Table 3.13 Soil characterization based in different soil properties

Degree of Expansion	**PI**	**LL**	**VSW**	**VSH**	**SP**	**MM**	**Rank**
Low	< 10	< 30	< 10	< 10	0 - 1	0 - 20	4
Medium	10 - 20	30 - 40	10 - 20	10 - 20	1 - 2	20 - 40	3
High	20 - 35	40 - 60	20 - 30	20 - 30	2 - 3	40 - 60	2
Very High	> 35	> 60	> 30	> 30	3 - 4	> 60	1

By looking at the Table 3.14, as expected, El Paso clay has the best ranking, i.e. lowest shrink-swell nature in all soils considered in this research. Among high PI clays, high to low average ranking number are soils from Houston, San Antonio, Fort Worth and Paris, respectively.

Table 3.14 Soil ranking analysis

Moisture Conditions	Soil Types	PI	LL	VSW	VSH	SP	MM	ORN	Averaged ORN
Wet of OMC	**Fort Worth**	1	1	4	2	3	2	2.2	**2.0**
OMC		1	1	3	3	2	2	2.0	
Dry of OMC		1	1	2	4	1	2	1.8	
Wet of OMC	**San Antonio**	1	2	4	2	3	2	2.3	**2.2**
OMC		1	2	3	3	2	2	2.2	
Dry of OMC		1	2	2	4	2	2	2.2	
Wet of OMC	**Paris**	1	2	4	2	3	1	2.2	**1.9***
OMC		1	2	3	3	1	1	1.8	
Dry of OMC		1	2	2	4	1	1	1.8	

Table 3.14 - continued

Moisture Conditions	Soil Types	PI	LL	VSW	VSH	SP	MM	ORN	Averaged ORN
Wet of OMC	**Houston**	2	2	4	3	3	3	2.8	**2.7**
OMC		2	2	3	3	3	3	2.7	
Dry of OMC		2	2	2	4	2	3	2.5	
Wet of OMC	**El Paso**	3	3	4	3	4	4	3.5	**3.6**
OMC		3	3	4	4	4	4	3.7	
Dry of OMC		3	3	4	4	4	4	3.7	

Remark * indicated worst average ranking number; ORN – Overall Ranking Number

3.7 Summary

A summary of laboratory methods and results for investigated clays were presented in this chapter. All four high PI soil types, Fort Worth, San Antonio, Paris and Houston soils, showed volumetric swell strain more than 10% (for OMC condition) which is considered as a very high degree of expansion (Chen, 1965). Since low amount of soluble sulfate and organic content were detected, it can be concluded that the high volume changes behaviors of studied soils were the results from their inherit soil properties which was examined from basic soil properties tests, clay mineralogy, and engineering tests conducted in this laboratory phase.

In this chapter, a ranking analysis was also presented. This analysis revealed that the behaviors of Paris, Fort Worth, San Antonio and Houston soils can be characterized as worse to better based on their volume changes measured in the laboratory studies.

CHAPTER 4

ANALYSIS OF LABORATORY TEST RESULTS

4.1 Introduction

Expansive soil is a worldwide problem and many tests and methods that include both indirect and direct measurement have been developed for estimating shrink-swell potentials of exapansive soils (Seed et al., 1962; Kormonik and David, 1969; Erguler and Ulusay, 2003). Indirect methods involve the use of soil properties and classification schemes to estimate shrink-swell potential while direct methods provide the actual physical measurements of swelling potentials in percentage values.

Soil scientists recognize that shrink-swell behavior can be best predicted by examining a combination of physical, chemical and mineralogical soil properties. These soil properties and established shrink-swell models that can be extrapolated across the same or similar parent materials are needed.

This chapter deals with the predictions of the degree of shrinking and swelling of soils. Statistics analysis is introduced as a simple technique to identify and predict the percent of volume changes. Regression analysis is used to identifying relationships between laboratory measured parameters and several correlations with

high coefficient of determination (R^2) values are determined. The R^2 is a statistical measure of how well a regression line approximates the real data points. An R^2 of 1.0 indicates that the regression line perfectly fits the data. The coefficient of determination can be defined as equation (1) below:

$$R^2 = \frac{\left(\sum_{i=1}^{n} (y_1 - \bar{y})(x_1 - \bar{x}) \right)^2}{\sum_{i=1}^{n} (y_1 - \bar{y})^2 (x_1 - \bar{x})^2} \qquad (1)$$

Where x and y are random variables.

The coefficient of determination is $0 \leq r^2 \leq 1$ and it denotes the strength of the linear association between x and y. It represents the percent of the data closest to the line of best fit. The following sections describe various correlations developed as a part of the analyses of laboratory results measured from four soil types.

4.2 Relationships between Plasticity Index (PI) and Percentage of Montmorillonite Mineral

Atterberg limit tests are traditionally used for soil classification, and the PI property indirectly gives an indication on the expansive activity of a particular soil. Montmorillonite (MM) is an expansive clay mineral with a high PI value and hence high PI soils are typically associated with the presence of expansive clay mineral such as MM (Mitchell, 1986). The PI of a pure montmorillonite soil can be as high as 514%, which is typically known as a highly expansive soil (Fahoum, 1996).

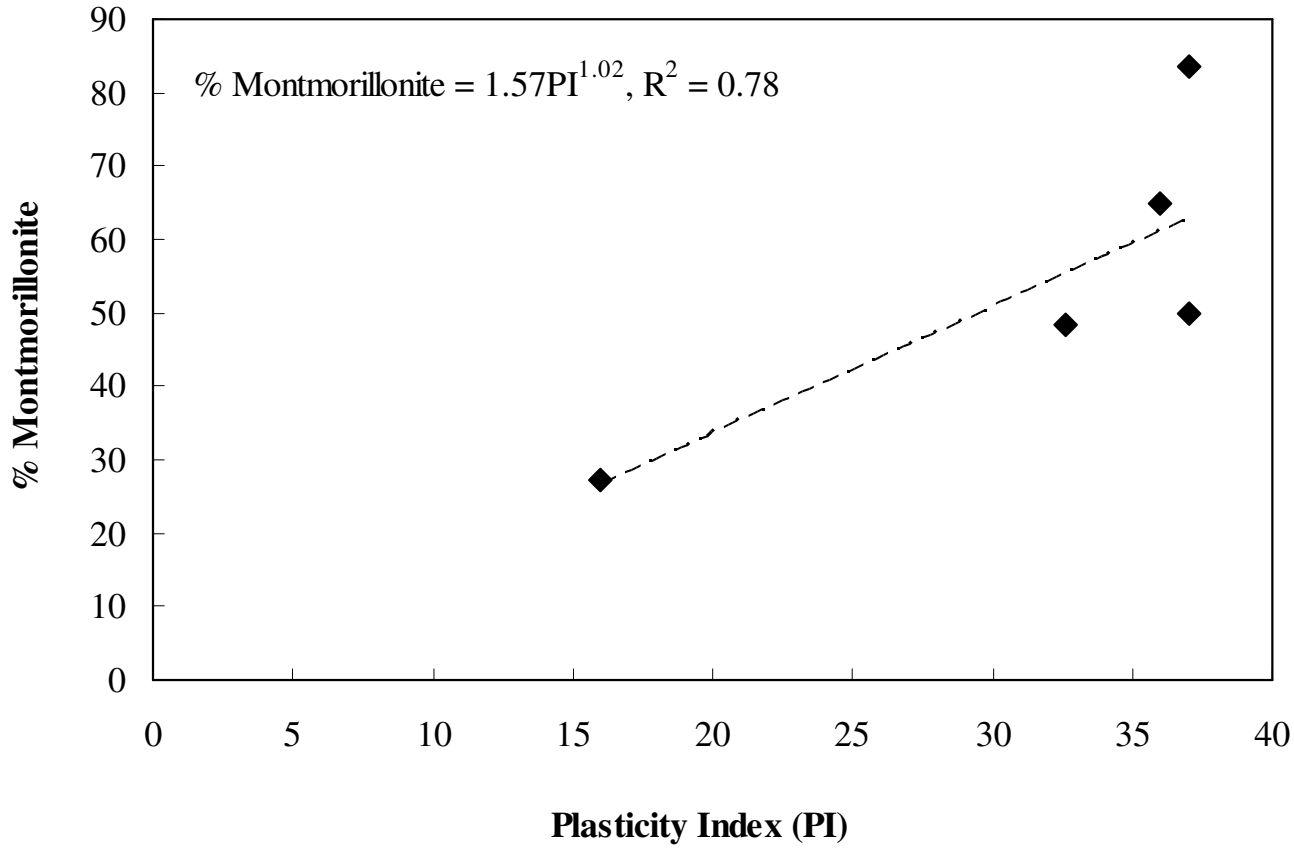

Figure 4.1 Plots between % montmorillonite mineral content and plasticity index (PI)

In this study, the variation of PI values with the percentage of montmorillonite clay mineral was investigated by comparing these values of each soil type. Results for all four clays including Fort Worth, San Antonio, Paris, Houston clays were considered along with those of El Paso clayey soil in Figure 4.1. This plot showed a strong relationship of the percent montmorillonite mineral in the clay against the plasticity index or PI value. The R^2 value of 0.77 indicates that a good correlation exists between these two parameters. This was expected as the plasticity of a clayey soil is highly dependent on moisture prone montomorillonite minerals.

4.3. Ratio of Vertical & Volumetric Strain

The following sections present various direct correlations of swell and shrinkage strains measured as a part of the experimental program.

4.3.1 Ratio of Vertical & Volumetric Swell Strain

Potential Vertical Rise (PVR) is one of the methods that is widely used across the USA to estimate the volume change behavior of expansive soils. This model was based on several assumptions and one of the assumptions is that the vertical swelling strain is equivalent to one-third of the volumetric swell strain of the soils at different depths. This assumption need to be revaluated as this PVR model is known to provide misleading results and hence this approach might not be appropriate for all soil types or at least for the medium to high PI soils studied in this research.

El Paso clay as a low PI clay was used in the initial calibration studies and hence these test results were included in the present validation studies and correlation development. Four other soils including Fort Worth, San Antonio, Paris and Houston

clays with medium to high plasticity index (PI) values and El Paso clay with a low plasticity index (PI) values were considered in the present analysis. These soils were studied using a three dimensional free swell test to investigate vertical, radial and volumetric swell potentials of each soil type. Since the test method would allow measuring swell potential in all directions, the relationship of swelling between each direction was developed. The complete test results are presented in Chapter 3.

The plots of vertical and volumetric swell strains with the PI value are presented in Figure 4.2. Most of the plots in this figure show similar slopes values (ratio between vertical and volumetric swell strain) as does the plots of El Paso soil. Figure 4.3 shows the plots of slope values obtained from plots presented in Figure 4.2 with respect to PI values of the respective clays. The data are scattered however, the average slope value is about 0.51. It is significantly different from 0.33 or $1/3^{rd}$ that is typically used in the PVR prediction models. Hence, it is possible to improve the PVR swell prediction results by modifying the ratio value used.

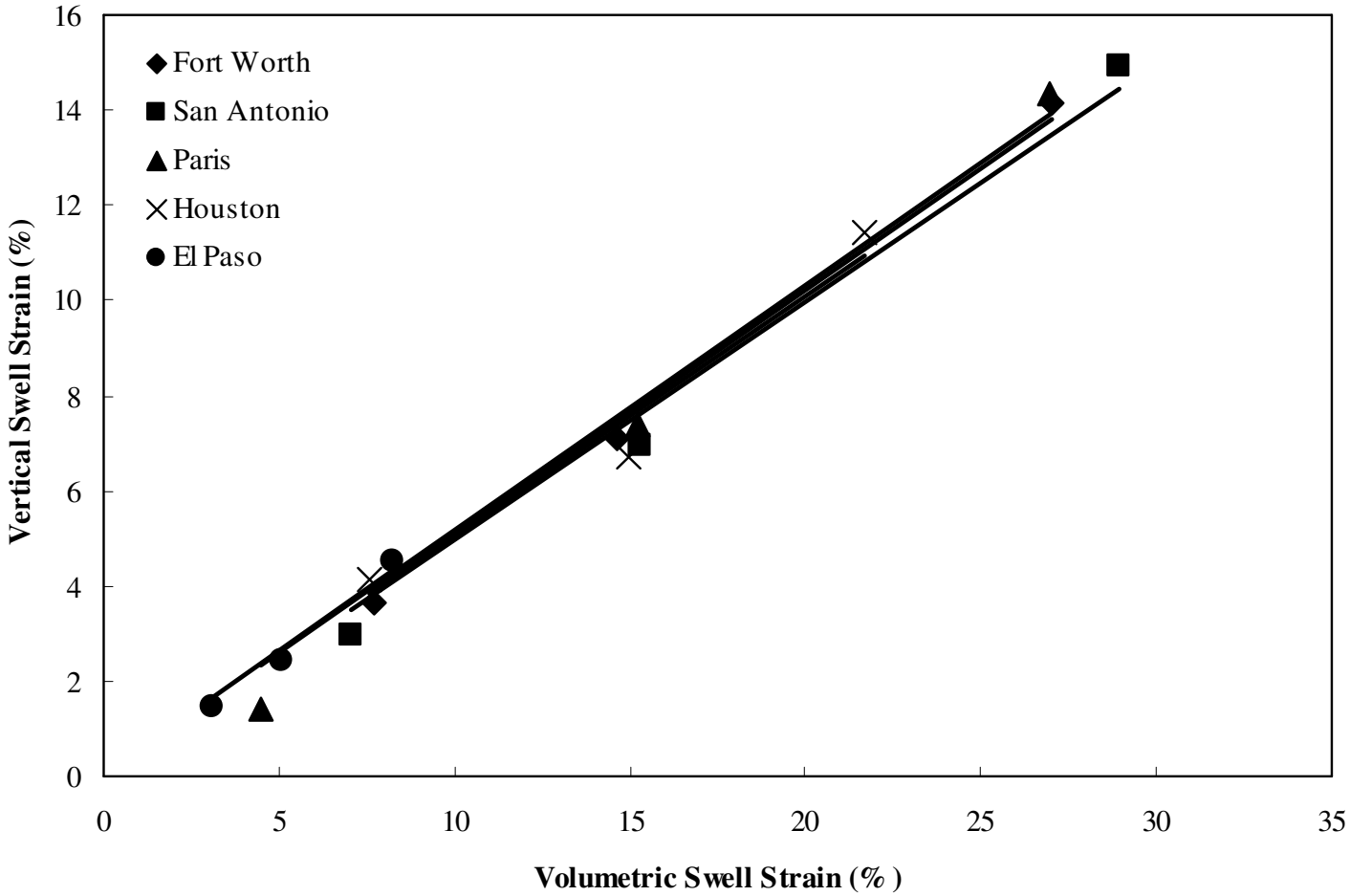

Figure 4.2 Relationships between vertical and volumetric swell strains

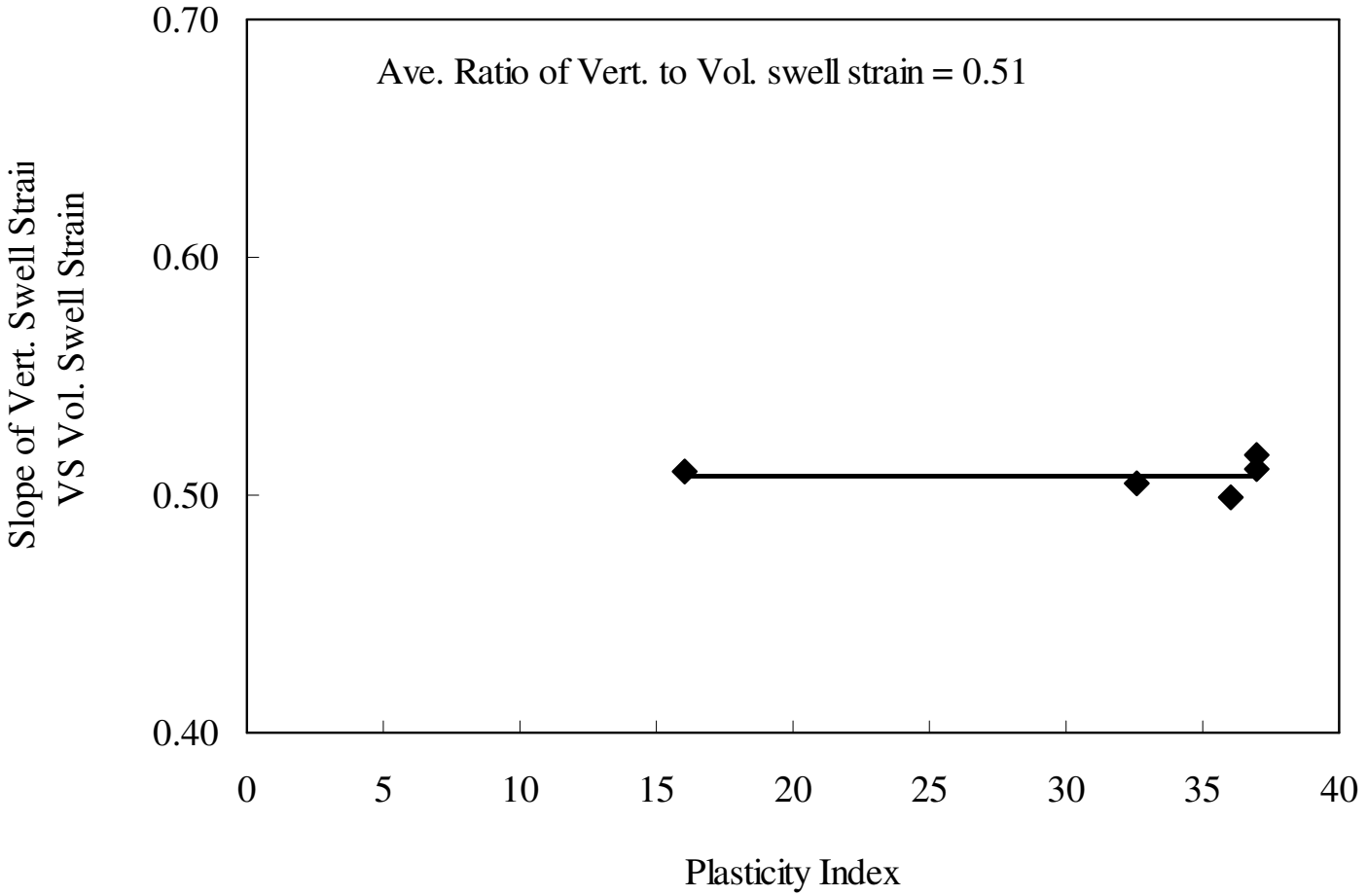

Figure 4.3 Relationships between slope of vertical and volumetric swell strain and plasticity index (PI)

4.3.2 Ratios of Vertical & Volumetric Shrinkage Strain

Volumetric shrinkage strain data was also plotted with vertical shrinkage strain in Figure 4.4. The slopes in the figure were then plotted against the PI values in Figure 4.5. In the figure, the slope values are also scattered similar to those of swell strains, but the mean value of these results is about 0.35, which is significantly less than slope of swell strain values of about 0.51.

Overall, it is shown that the radial shrinkage is more than the radial swelling for the same amount of volume changes. This explains the reasons behind pavement cracking, which often initiated in dry seasons. These cracks will get worse with an increase in the number of wetting and drying periods. Another important observation is that the slopes of shrinkage strain plots are different from slopes of swelling strain plots, indicating that the changes in volumetric strains do not follow the same trends in swell and shrinkage environment.

4.4 Empirical Correlations of Laboratory Soil Strain with Plasticity Index (PI)

4.4.1 Empirical Correlations of Laboratory Soil Swell Strain with PI

Test data from three dimensional free swell tests are again plotted with respect to the plasticity index, PI in order to develop empirical prediction models for predicting the swelling potentials of plastic soils. The present experimental data are grouped into three different moisture conditions: wet of optimum, optimum and dry of optimum moisture contents. An attempt is made to correlate vertical, radial and volumetric swell strain correlations with the PI values and these results are plotted in Figure 4.6, Figure 4.7 and Figure 4.8, respectively.

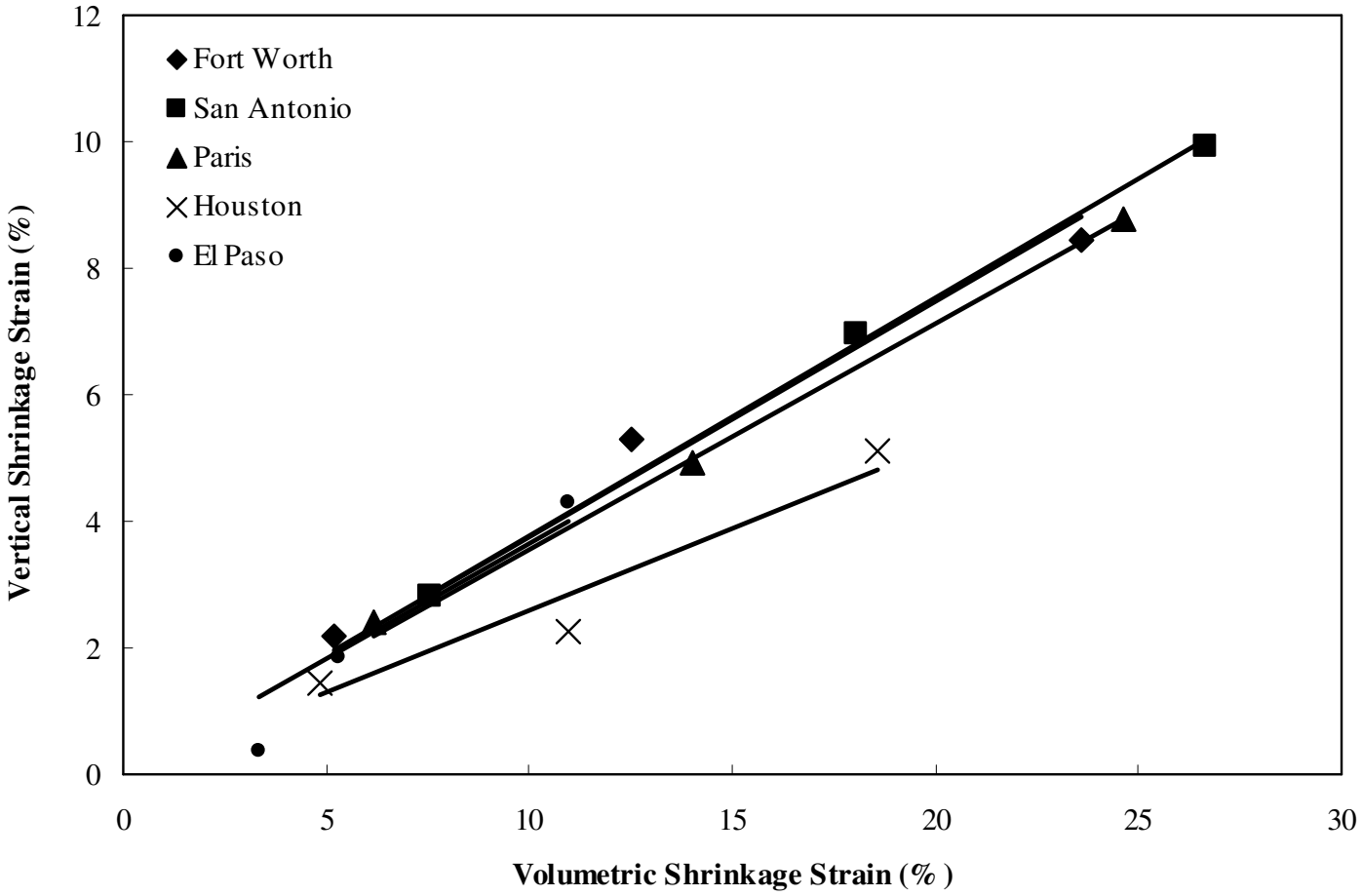

Figure 4.4 Relationships between vertical and volumetric shrinkage strains

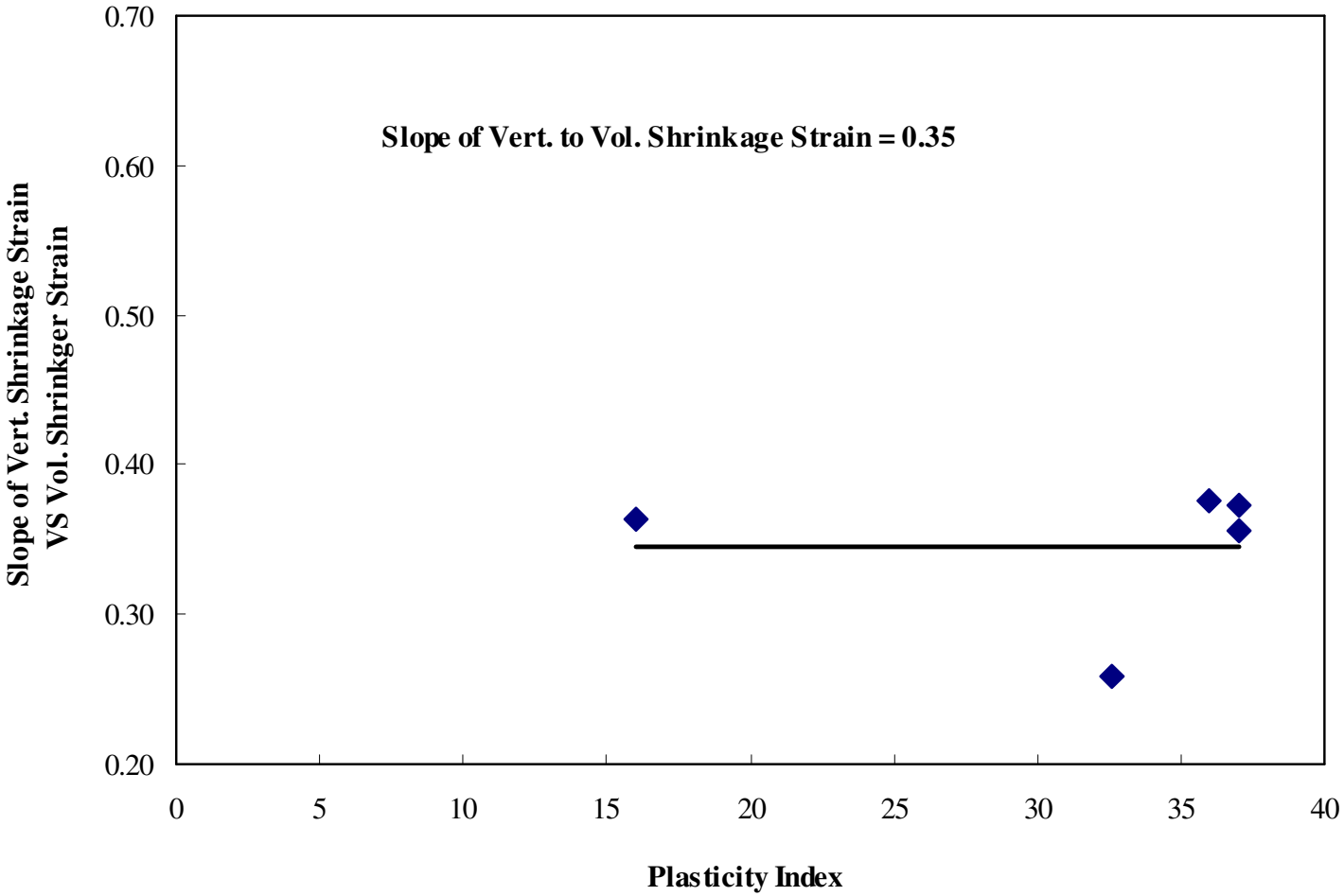

Figure 4.5 Relationships between Slope of Vertical & Volumetric Shrinkage Strain and Plasticity Index (PI)

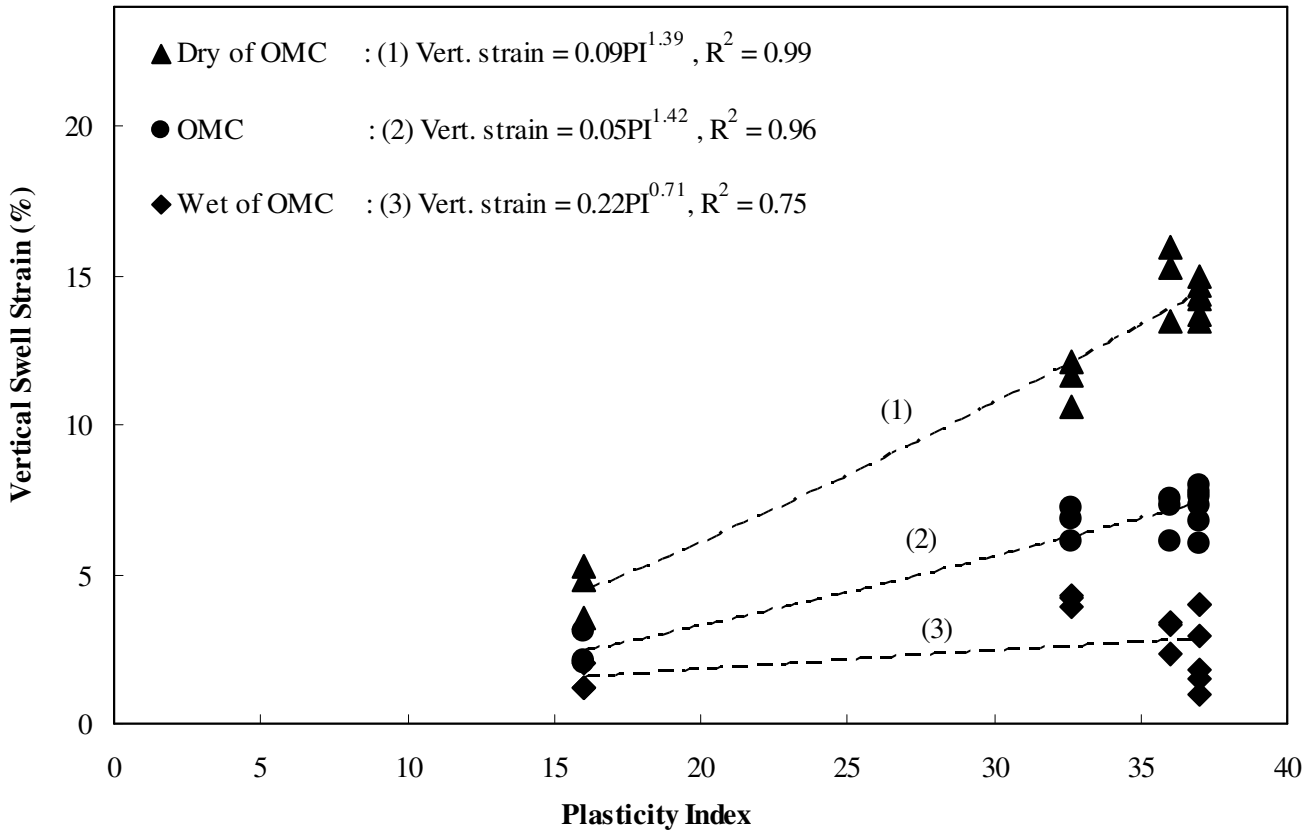

Figure 4.6 Plots of vertical swell strain with PI for different initial moisture conditions

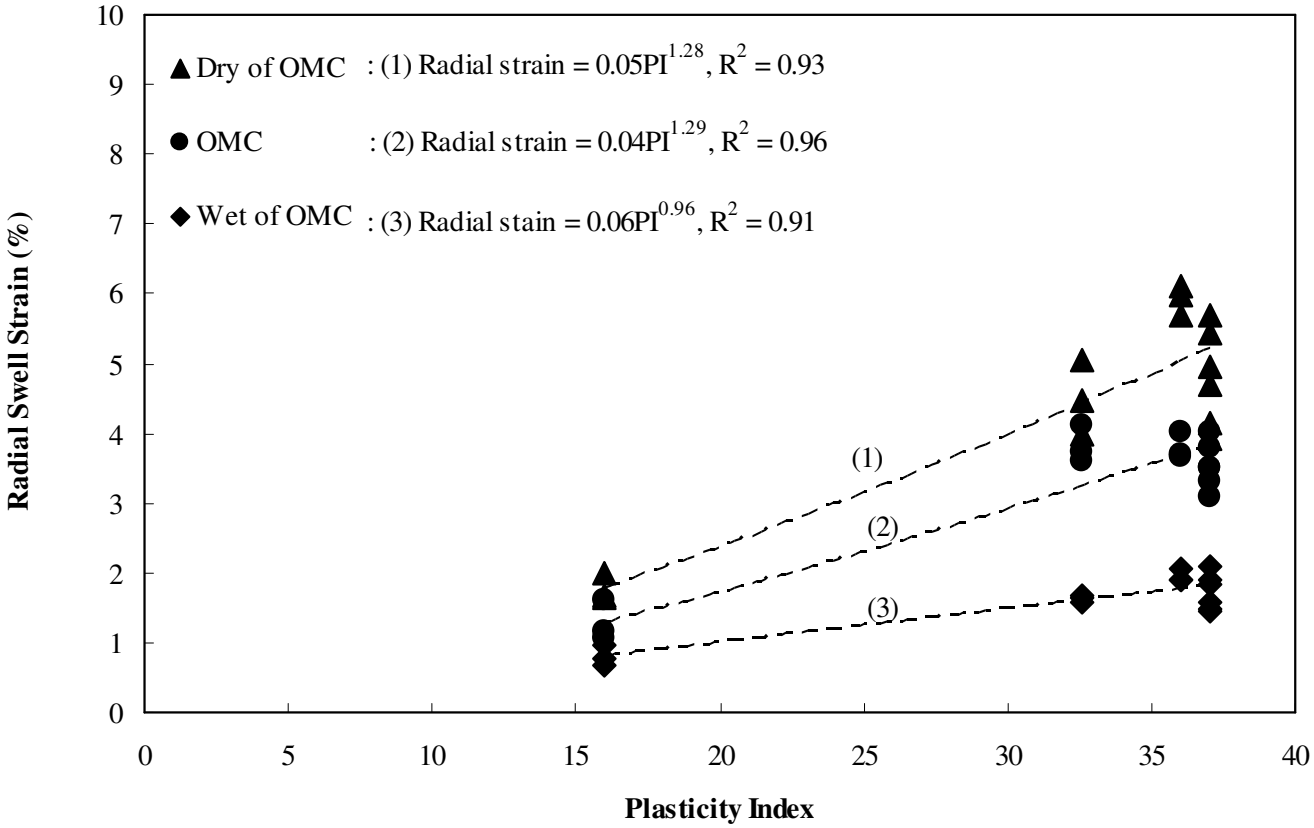

Figure 4.7 Plots of radial swell strain with PI for different initial moisture conditions

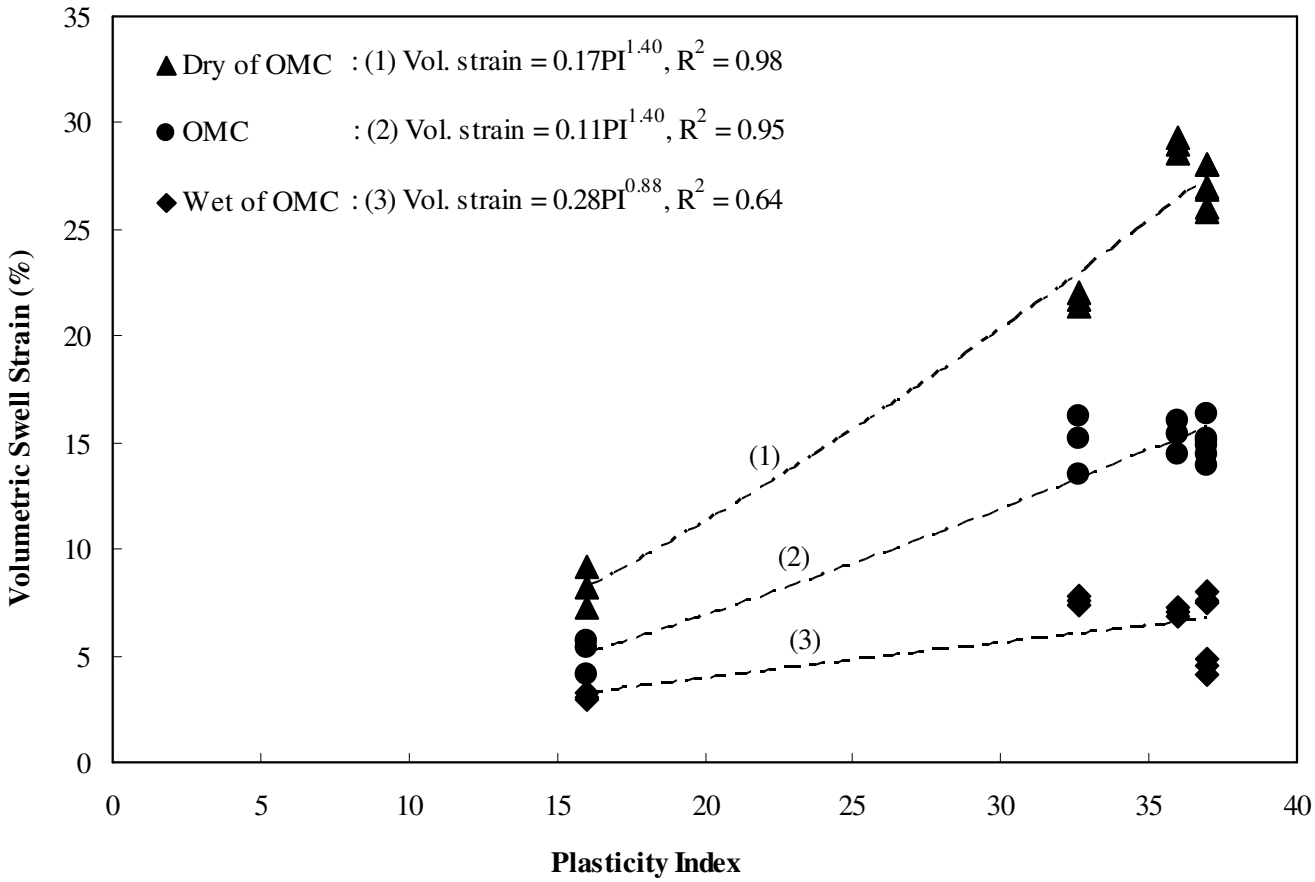

Figure 4.8 Plots of volumetric swell strain with PI for different initial moisture conditions

Most of the relationships derived in the figures show strong relationships between volumetric swell strain and PI, except at the wet of OMC condition as the coefficient of determination (R^2) at that state is 0.68. These relationships can be described by simple empirical equations as indicated in the Figures 4.6 to 4.8 above.

There are numerous laboratory swell correlations based on PI property. For example, correlations by Seed et al. (1962) and Chen (1983) are two of the frequently used correlations in the literature. These correlations are used to predict swell properties of the present soils and these results are plotted along with the present findings in Figure 4.9.

Graph No. 1 in the figure 4.9 is proposed by Seed (1962) and the equation is as the following: $Vert.Swell(\%) = 60K(PI)^{2.44}$ (2)

Where K = 3.6 x 10^5 and PI = Plasticity Index

Graph No. 2 is proposed by this research. The equation (For optimum moisture content condition) is as the following: $Vert.Swell(\%) = 0.0148(PI)^{1.4152}$ (3)

Graph No. 3 is proposed by Chen (1983). The equation is as the following:

$Vert.Swell(\%) = Be^{A(PI)}$ (4)

Where A = 0.0838 and B = 0.2558

Since the correlations proposed by those researchers did not mentioned the state of compaction or moisture condition, the optimum moisture content is assumed for soil's initial condition. As shown in Figure 4.9, the vertical swell correlation from this research shows a close agreement with those from Seed et al. (1962) and Chen (1983) models which, as a result, indicated validity of the correlation in this study.

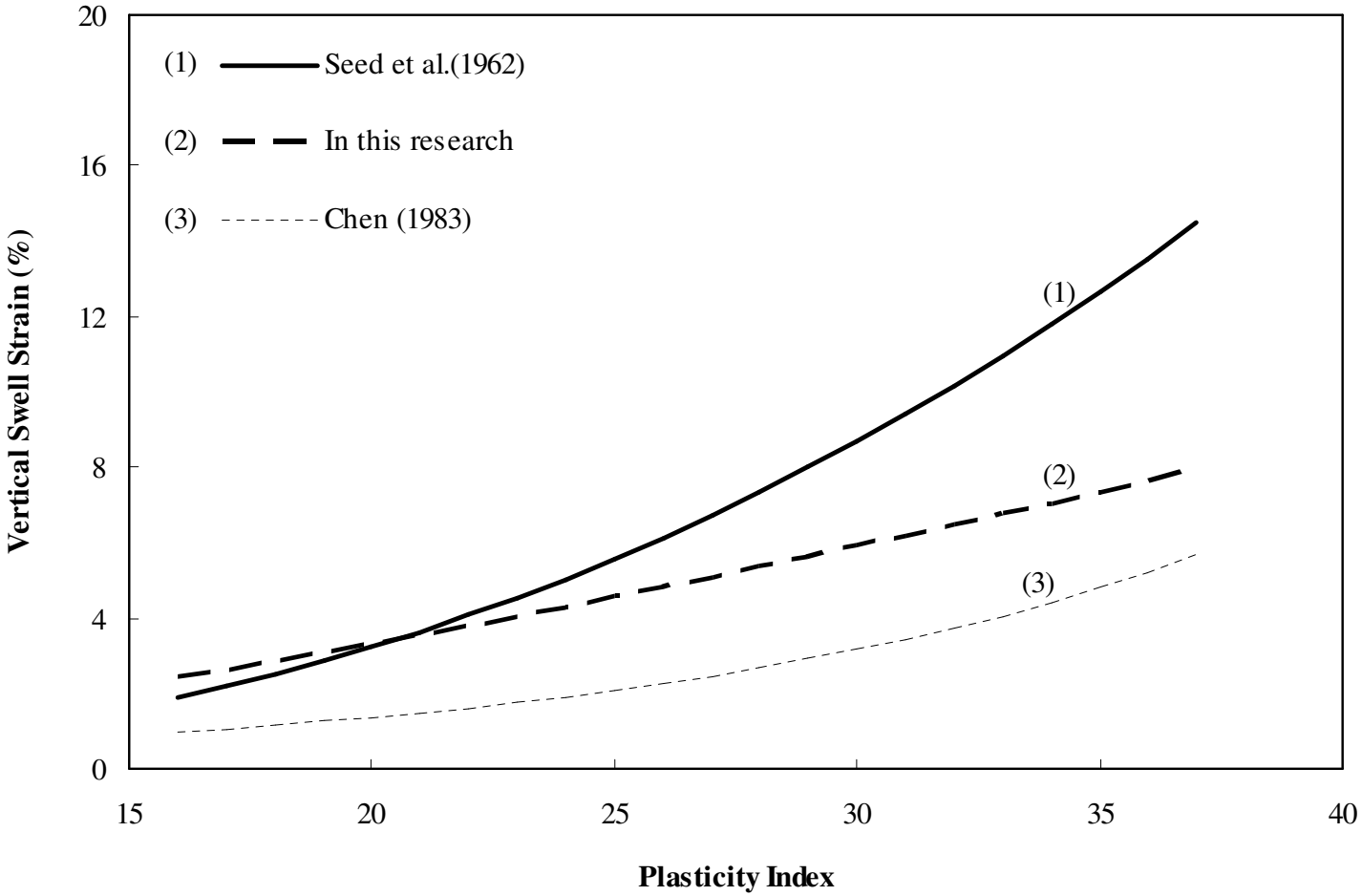

Figure 4.9 Plot of vertical swell strain with PI for different correlations

4.4.2 Empirical Correlations for Laboratory Soil Shrinkage Strain with PI

The objective of this characterization is to understand and then predict the volumetric shrinkage soil movement based on soil property (PI and initial moisture state conditions which are wet of optimum, optimum and dry of optimum moisture contents. Result plots are presented in Figure 4.10 to 4.12.

Based on the findings, only volumetric shrinkage strain has strong relationships with the PI value for all three moisture conditions (see Figure 4.12), while most of vertical and radial shrinkage strain show low to medium correlations with PI except for vertical shrinkage strain in dry of optimum condition and radial shrinkage strain in wet of optimum condition that indicated good correlations. More investigations on different clays are needed to better characterize the soil shrinkage behaviors. Based on the presented results, the following correlations derived using multiple linear regression are presented here:

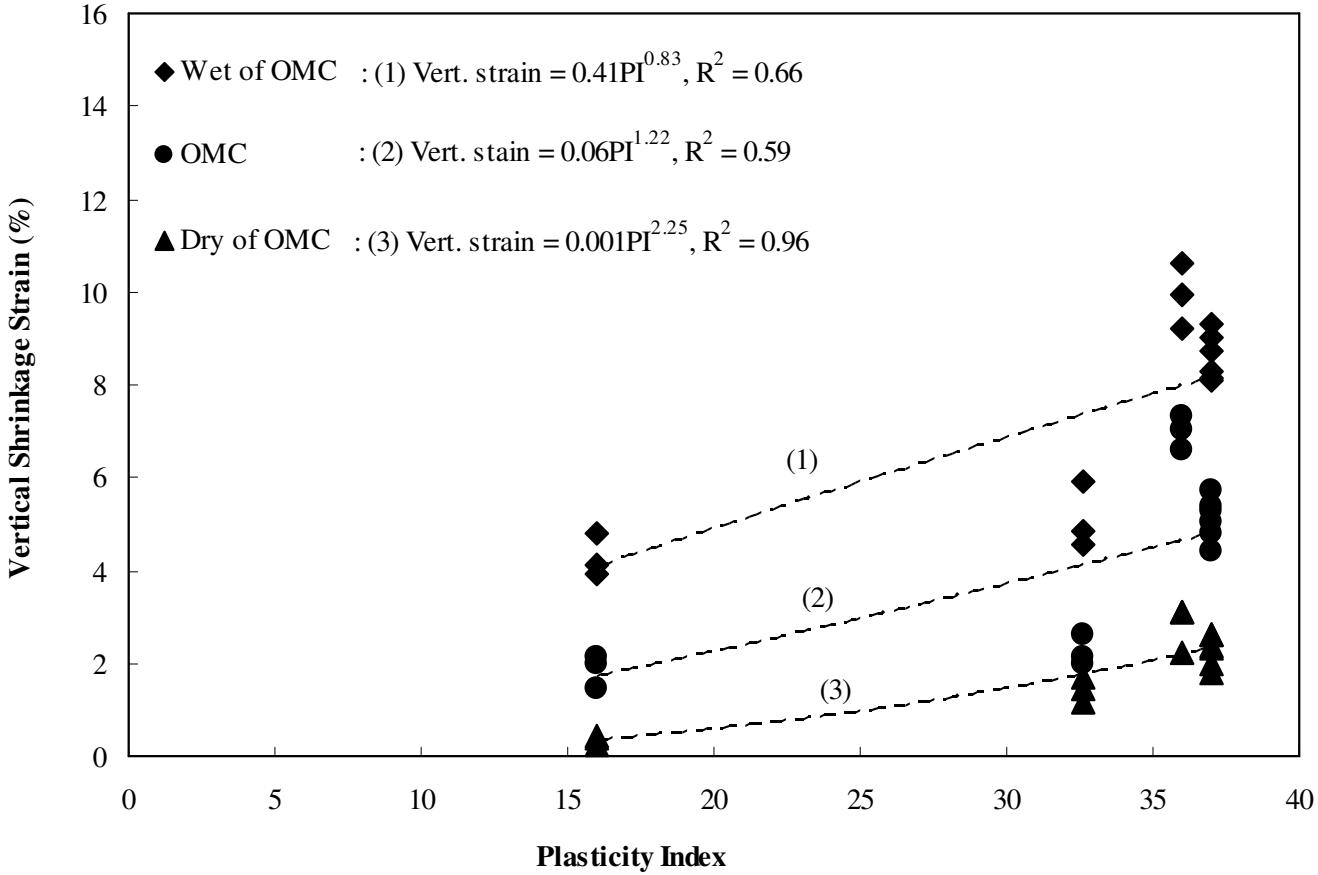

Figure 4.10 Plots of vertical shrinkage strain with PI for different initial moisture conditions

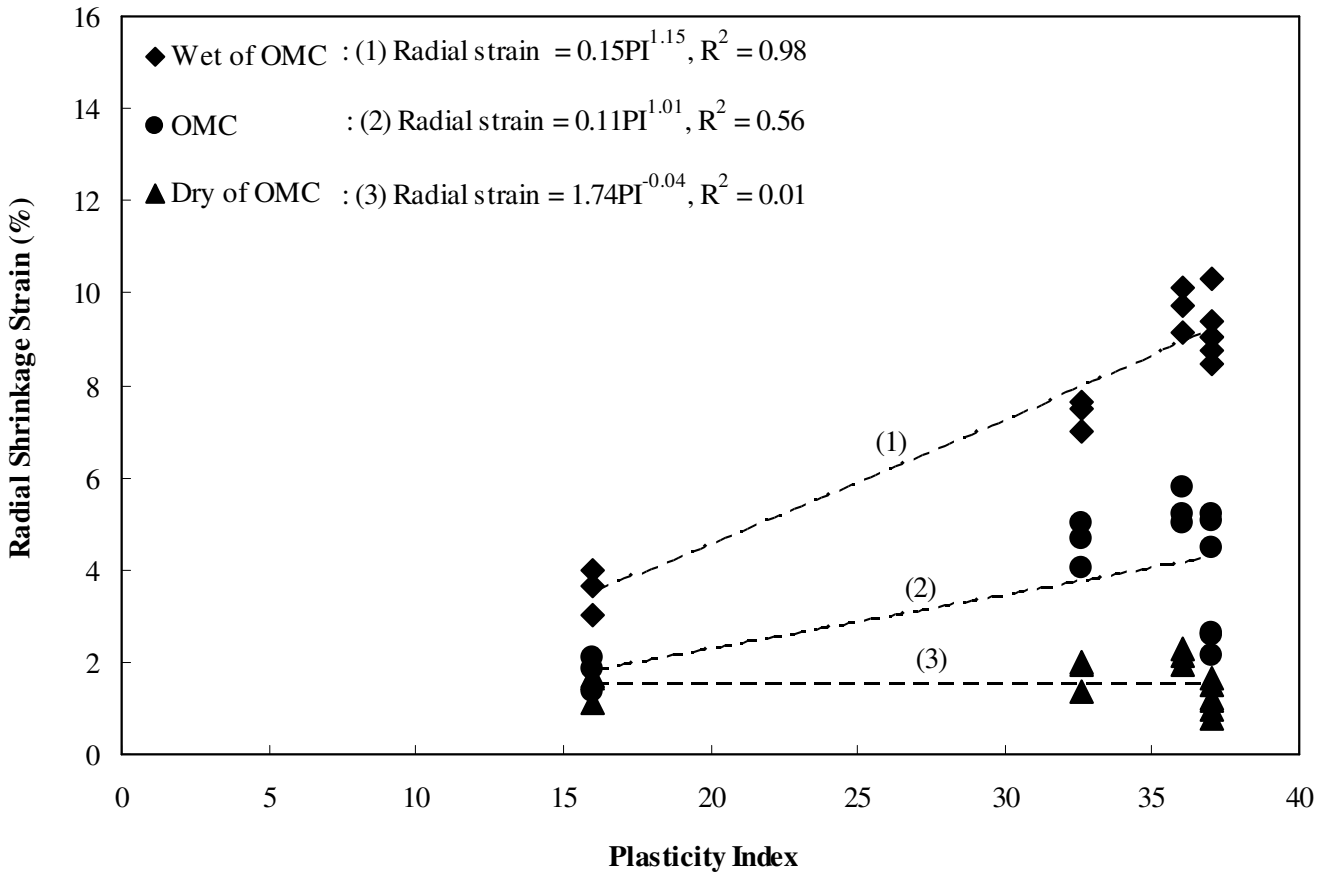

Figure 4.11 Plots of radial shrinkage strain with PI for different initial moisture conditions

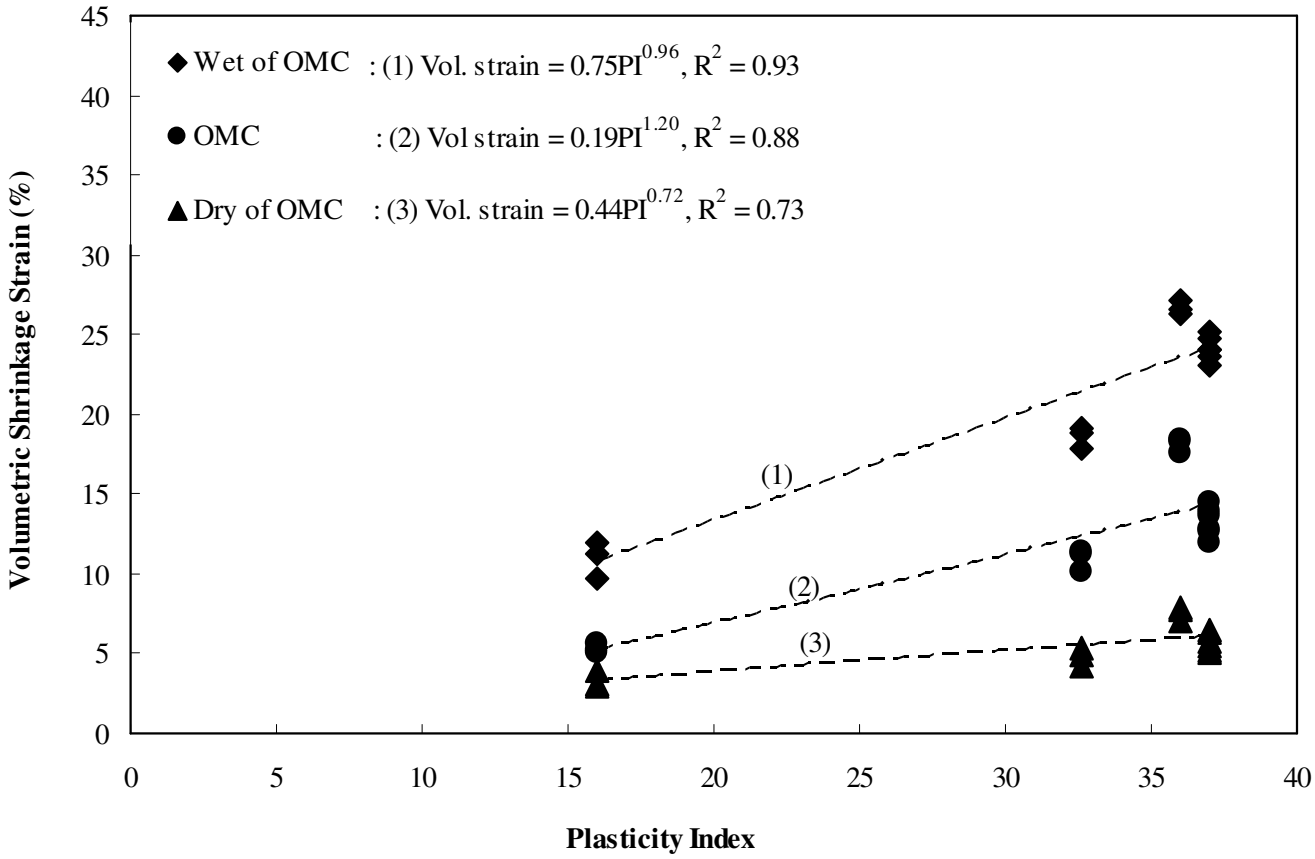

Figure 4.12 Plots of volumetric shrinkage strain with PI for different initial moisture conditions

4.4.3 Multiple Linear Regression Correlations for Laboratory Soil Shrinkage Strain

Multiple linear regression is often used when more than one soil parameter influences the independent parameter. In a multiple linear regression, the dependent variable or response is related to k independent variables. The model is $Y = \beta_0 + \beta_1 x_1 + \beta_2 x_2 + ... + \beta_k x_k + \varepsilon$. The parameter β_j, j = 0, 1… k are called regression coefficients determined from multiple linear regression analysis and k is the number of soil parameters used in this analysis (Montgomery et al., 2003). The R^2 is used as an indicator of goodness of fit between experimental data and predicted data.

In this section, the objective is to find out the best representative shrinkage correlations which posses highest R^2 and lowest number of variables. The selected soil variables, which appear to have good correlations with shrinkage potentials, were chosen as independent variables in the multiple linear regression analysis in this study. These variables consist of soil matric suction in log kPa (SU), initial soil moisture content (IMC), Plasticity index (PI) and percentage of Montmorillonite clay mineral content (MM). Generally, liquid limit (LL) is often used by many researchers, yet, in this research, liquid limits appear to be curvilinear with PI variable. This is because plastic limits (PL) for most of the studied soil are quite constant and PI is simply the difference between LL and PL. As a result, LL is discarded in the analysis.

The analyses of multiple linear regression correlations started with one variable and then the number of variables will be increased by one until all variables were included. In each number of variables, R^2 values were determined. The equations with highest R^2 would be selected as the best fit correlations for that number of variable.

Table 4.1 shows all the Volumetric Swell Strain correlations with corresponding R^2 values.

It should be noted that the correlations presented in this analysis are different from the ones in previous section (section 4.4) in that the shrinkage data were not classified in three initial moisture conditions as in the previous section. As a result, only one variable, for example PI alone might not be adequate to well represent shrinkage potential.

Table 4.1 Volumetric shrinkage strain correlations with corresponding $\mathbf{R^2}$ values.

No. of Variables	**No. of Equations**	**Values of Coefficients**					
		Constant	**SU**	**IMC**	**PI**	**MM**	**R^2**
1	1	17.385	1.505				0.030
	2*	-7.516		0.969			0.897
	3	-0.335			0.415		0.194
	4	3.215				0.165	0.174
2	1*	-13.934	1.642	1.039			0.929
	2	0.095			0.321	0.0436	0.196
	3	4.091	-9.910		1.220		0.769
	4	12.026	-6.970			0.375	0.536
	5	-10.785		0.921	0.135		0.916
	6	-9.465		0.929		0.048	0.911

Table 4.1 - continued

No. of Variables	No. of Equations	Values of Coefficients					
		Constant	**SU**	**IMC**	**PI**	**MM**	**R^2**
3	1	4.268	-9.900		1.180	0.018	0.769
	2	-16.751	3.171	1.169		0.078	0.936
	3	-10.869		0.922	0.157	-0.010	0.916
	4*	-26.628	11.696	1.857	-1.100		0.972
4	1*	-27.336	11.930	1.879	-1.048	-0.036	0.972

Remark * represents the correlation with the highest R^2 value for a particular number of variable

Noted for Table 4.1

SU = soil mtric suction in log kPa

IMC = initial soil moisture content

PI = soil plasticity index

MM = percentage of Montmorillonite clay mineral content

Best fit correlations (highest R^2) for a particular number of variables are selected from the table 4.1 and presented below.

Best fit Correlations for Volumetric Shrinkage Strain (VOS)

For one variable,

$VOS = -7.52+0.97(IMC)$ ($R^2 = 0.897$)

For two variables,

$VOS = -13.93+1.64\ (SU)+ 1.04(IMC)$ ($R^2 = 0.929$)

For three variables,

$VOS = -26.63+11.67\,(SU)+ 1.86(IMC) -1.10\,(PI)$ $(R^2 = 0.972)$

For four variables,

$VOS = -27.34+11.93(SU)+ 1.88(IMC) -1.05(PI) -0.03(MM)$ $(R^2 = 0.972)$

The above equations show the best-fit correlations of each number of variables that had been selected from the table 4.1. Apparently, initial moisture content (IMC) is best correlated with the volumetric shrinkage strain when there is only one variable included. If there are two variables, initial moisture content (IMC) and matric suction (SU) are better characterized for the correlation. For three variables, PI came into the relationship. When there are 4 variables, percentage of montmorillonite (MM) comes into the picture, however, the R^2 values are not increased. Consequently, percentage of montmorillonite (MM) might not be well correlated to the volumetric swell strain results and can also be considered as redundancies which could cause instability to the correlations.

For volumetric shrinkage strain, only three variables are adequate to characterize the volumetric shrinkage behaviors which are initial moisture content (IMC), matric suction (SU) and plasticity index (PI). By performing the same logic for vertical shrinkage strain, the best fit correlations (for a particular number of variables) are presented below.

Best fit Correlations for Vertical Shrinkage Strain (VES)

For only one variable,

$VES = -2.87+0.35(IMC)$ ($R^2 = 0.822$)

For two variables,

$VES = -5.78+0.74(SU)+0.38(IMC)$ ($R^2 = 0.868$)

For three variables,

$VES = -10.30+4.33\ (SU)+0.67(IMC)-0.39(PI)$ ($R^2 = 0.910$)

For four variables,

$VES = -9.85+4.18(SU)+0.66(IMC)+0.43(SP)-0.02(PI)$ ($R^2 = 0.910$)

Interestingly, the correlations that present the same trend of volumetric shrinkage strains used three independent variables, initial moisture content (IMC), matric suction (SU) and plasticity index (PI). Accordingly, the correlation with three variables is the best representative correlation for both volumetric and vertical shrinkage correlations since those correlations yielded the highest R^2 with lowest number of variables.

By performing the same procedures for radial shrinkage strain, the best fit correlations (for a particular number of variables) are presented below:

Best fit Correlations for Radial Shrinkage Strain (RAS)

For only one variable,

$RAS = -3.57+0.38(IMC)$ ($R^2 = 0.910$)

For two variables,

$RAS = -5.03+0.37\ (SU)+0.39(IMC)$ ($R^2 = 0.910$)

For three variables,

$RAS = -12.21+6.06(SU)+0.86(IMC)-0.62(PI)$ ($R^2 = 0.910$)

For four variables,

$RAS = -12.82+6.26(SU)+0.87(IMC)-0.58(PI)-0.03(MM)$ ($R^2 = 0.910$)

From the above analysis, apparently, only three independent variables, matric suction (SU), initial soil moisture content (IMC), and soil plasticity index (PI), are adequate to get the highest the coefficient of determination (R^2) except for radial shrinkage strain correlation which requires only initial soil moisture content (IMC) variable. In summary, the best representative correlation correlations for shrinkage behavior can be summarized as:

1. Volumetric shrinkage strain correlation

$VOS = -26.63+11.67\ (SU)+\ 1.86(IMC)\ -1.10\ (PI)$ ($R^2 = 0.972$)

2. Vertical shrinkage strain correlation

$VES = -10.30+4.33\ (SU)+0.67(IMC)-0.39(PI)$ ($R^2 = 0.910$)

3. Radial shrinkage strain correlation

$RAS = -3.57+0.38(IMC)$ ($R^2 = 0.910$)

New soil data needs to be considered for further refinements of the above correlations.

4.4.4 Correlation of Laboratory Soil Swell-Shrinkage Movements with Moisture Changes (Δw)

Kodikara (2006) showed the relationship between the volumetric shrinkage strain and the reduction in moisture content observed in drying tests that there is a remarkably linear correlation observed between the volumetric strain and the water content change (Δw) covering both slurry clay and compacted clay materials. The relationship can be expressed as:

$$\varepsilon_{sh} = \alpha \Delta w \qquad (4)$$

where α = volumetric shrinkage coefficient

Δw = moisture changes

An attempt was made in this research to correlate volumetric, vertical and radial strains in both swell and shrinkage conditions by following the above mentioned correlations. From Figures 4.13 and 4.14, it can be mentioned that the vertical swell strain is about one-half of the volumetric swell strain (as per the equations shown in Figure 4.13) whereas vertical and radial shrinkage strains are close to one-third of volumetric shrinkage strains. Good correlations for both swell and shrinkage movements of soils with moisture changes are observed. Consequently, soil volumetric, vertical and radial changes can be expressed in term of only moisture content changes regardless of the soil types and initial moisture conditions. However, some of their R^2 values are lower than those obtained from the previous sections.

Overall, several laboratory swell-shrinkage correlations were developed and included in this chapter. Predictions of soil movements can be achieved by using these

correlations and most of them require either moisture regime changes or basic soil parameters. Though high coefficients of determination are obtained, future validation with more new soil data will enhance the reliability of these correlations.

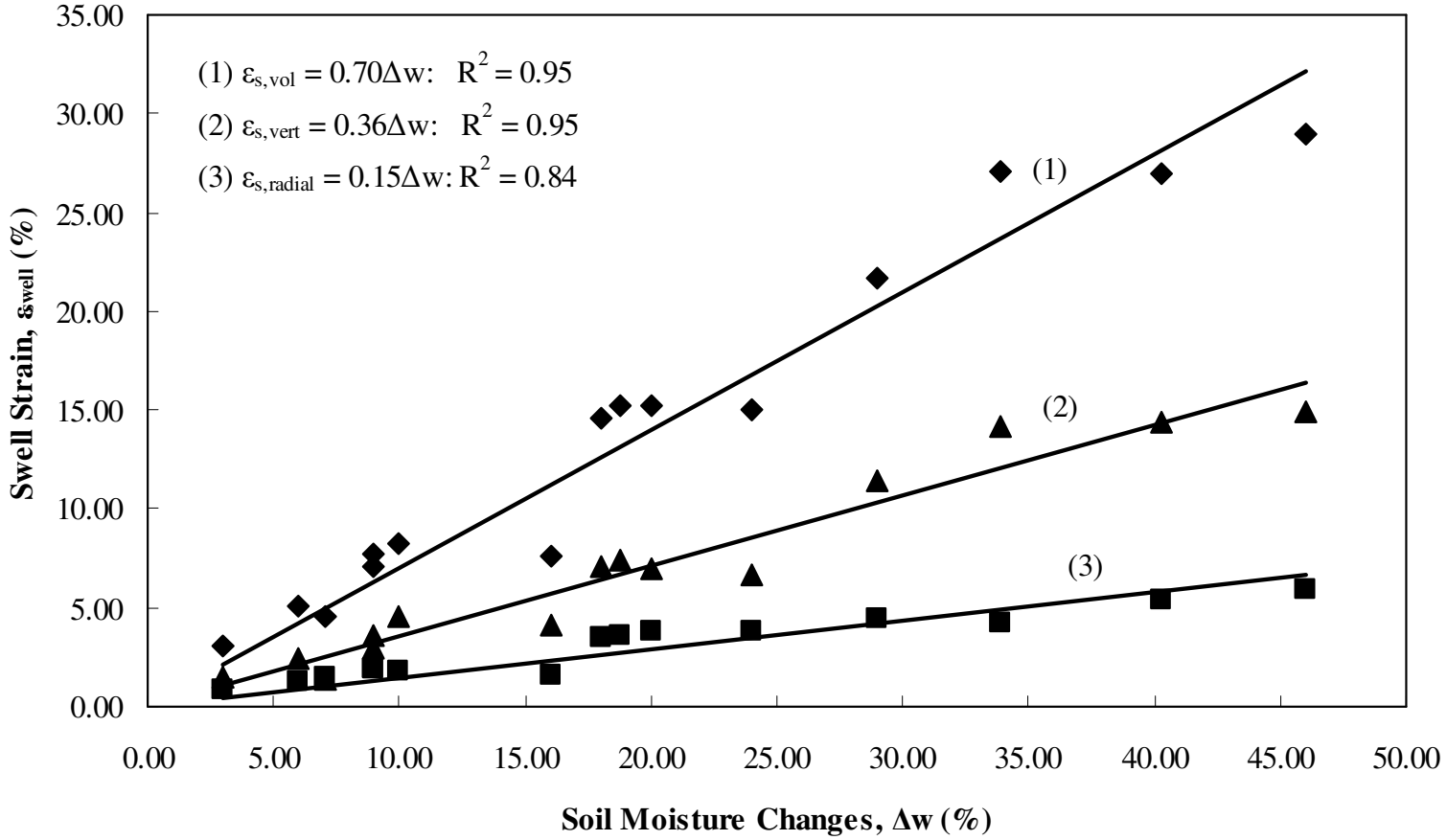

Figure 4.13 Plot of swell strain (ε_{swell}) with soil moisture change (Δw)

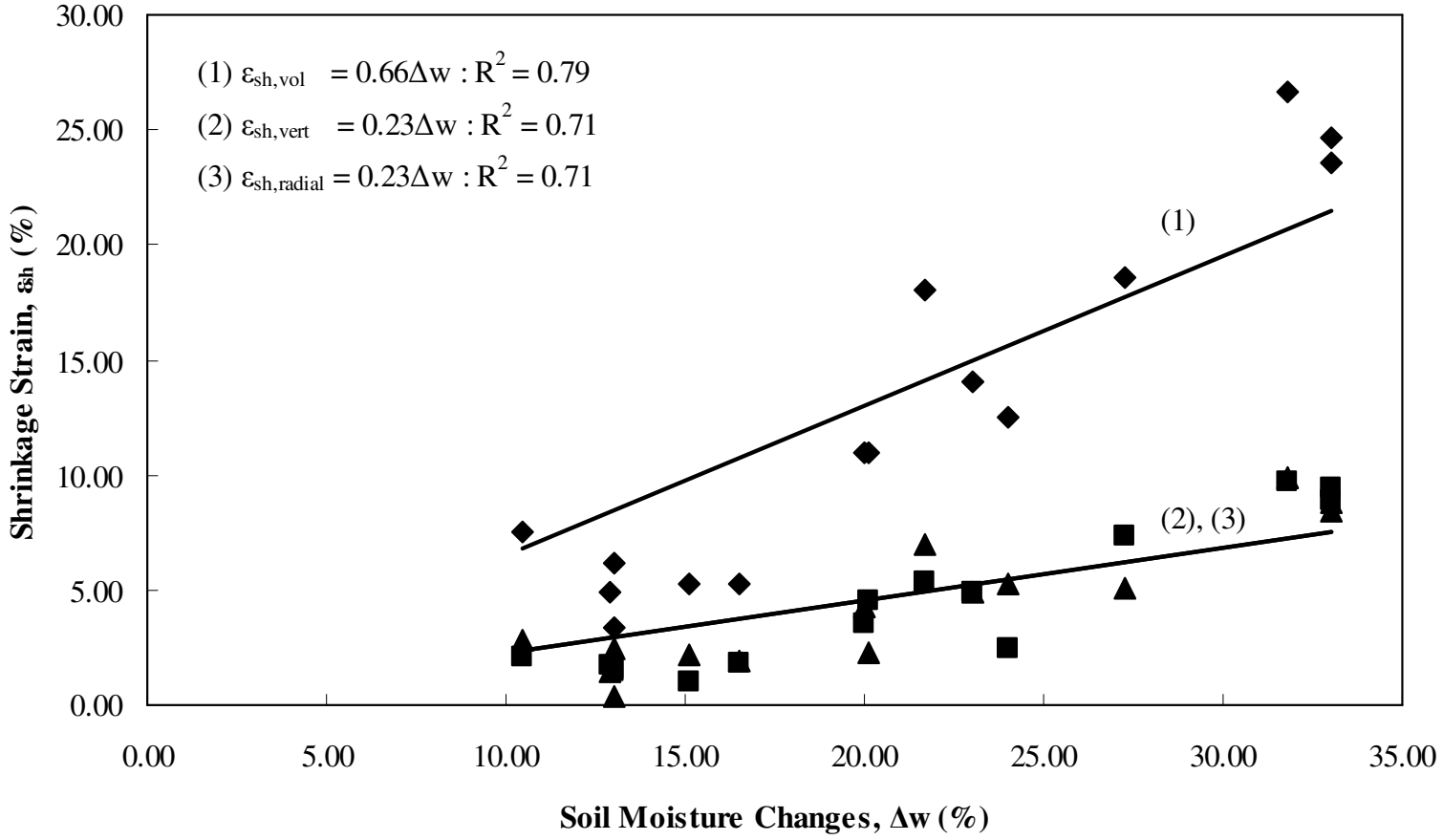

Figure 4.14 Plot of shrinkage strain (ε_{shrink}) with soil moisture change (Δw)

4.5 Summary

The following summaries are obtained from the presented analysis:

1. The presented soils showed a good correlation between PI and percentage of montmorillonite mineral content.

2. The ratio between vertical swell strain and volumetric swell strain is close to $\frac{1}{2}$. This finding indicates that the use of $\frac{1}{3}$ times the volumetric swell as vertical swell strain (as assumed in PVR model) is not valid for medium to high PI soils.

3. Laboratory vertical swell correlation from this study results via PI property showed good results since they are in close agreement with those reported by Seed et al. (1962) and Chen (1983).

4. Multiple linear regression analysis revealed that only three variables are adequate to characterize laboratory soil shrinkage behavior. Those three variables are matric suction (SU), initial soil moisture content (IMC), and soil plasticity index (PI) except for radial shrinkage strain correlation which required only initial soil moisture content. It seems that percentage of montmorillonite (%Mont) is not needed for the correlations, however it can be stated that the inclusion of PI variable indirectly accounts for clay mineralogy effects.

5. Based on the swell strain results, the Paris clayey soil experienced highest swelling whereas Houston clay has experienced low swelling.

CHAPTER 5

FIELD STUDIES

5.1 Introduction

The field monitoring data is an important part of this dissertation research to understand the moisture and soil suction variations in the field and they are assumed to be dependent on environmental boundary conditions. Unlike the laboratory data, the field data can be complicate as they are controlled by many factors in the field conditions. Yet, they are essential since they reflect the conditions in the real practical woks. In this chapter, overview of the study that necessary for analyzing environmental impacts on pavement including site conditions, site selection, site information, field instrumentations systems, and field conditions monitoring are also provided.

5.2 Overview on Environmental Site Conditions & Road Conditions

5.2.1 Vegetation and Trees

Vegetation and trees have similar intense effect on the desiccation or drying up of expansive soils (Richards, 1983). Particularly, certain types of trees are known to cause drying in subsoils in which they induce cracking on pavements (Sillers et al., 2001; Jaksa et al., 2002). As a result, ratios of lateral distance (D) from trees and height of plants (H) are developed for different trees near the pavements in Australia to determine the closeness of trees to the pavements (Ward, 1953).

5.2.2 Drainage Systems

Drainage systems including ditches adjacent to pavements have a pronounced influence on expansive soil behavior (Forstie, 1979). Poorly designed ditches often pond the water and raise the saturation levels in expansive subsoils. Such increase in saturation degree will raise the swell magnitudes and conversely increase shrinkage movements during dry spells. Hence, the influence of existing drainage ditches and their existing environmental conditions were studied in this research.

5.3 Site Selection for Baseline Study

There were four out of ten sites selected as a baseline to verify the outcomes of soils heaving and shrinking. The selection of the test sites were based on different kinds of environmental site conditions and road characteristics.

Pavement designed with chemically stabilized sulfate rich soils that cause soils heaving and shrinking are not considered and included in this research study. However, test sites with the following attributes are preferred:

- Reasonably newly constructed
- Design records are available
- Construction records are reasonably completed
- Contain some areas with typical distresses encountered due to high-PI clay
- Clay subgrade is reasonably uniform

After thorough considerations, four sites including Fort Worth, Houston, San Antonio, and Paris were selected. At the initial visit, moisture and suction sensors was installed to monitor the variations of moisture and matric suction values with respect to

time. To ascertain the soil properties, soils were first sampled and shipped to laboratories for traditional and advanced characterization for shrink and swell behaviors. These results are already covered in Chapter 3.

Throughout the project, information such as site conditions, cracking depths of pavement, soil moisture contents and soil matric suctions from these four sites were recorded and photographed during site visits which were planned once a month.

5.4 Field Instrumentations Systems

There are two types of field instrumentation systems embedded at the test sites. One type is moisture sensors together with data logger and the other one is field matric suction sensors. Both types of system were carefully placed close to each other to ensure that the data from both systems were representing the same soil conditions.

5.4.1 Moisture Sensors

The Gropoint® Moisture sensors and data logger (Figure 5.1) played an important role in understanding variation and propagation of soil moisture in this research. They work on the principle of Time Domain Transmissometry (TDT) technology to provide volumetric moisture contents.

Pulse reading is observed at the other end of transmission line from the transmitter of the sensor. The propagation time of an electromagnetic wave along a given length of transmission line is proportional to the square root of the permittivity of the medium that the transmission line immersed in. With three separate phrases of soil/water/air in the soils, the permittivity of water dominates the mixture of permittivity

and therefore the measurement is used to determine the volumetric water content of the soil mixture.

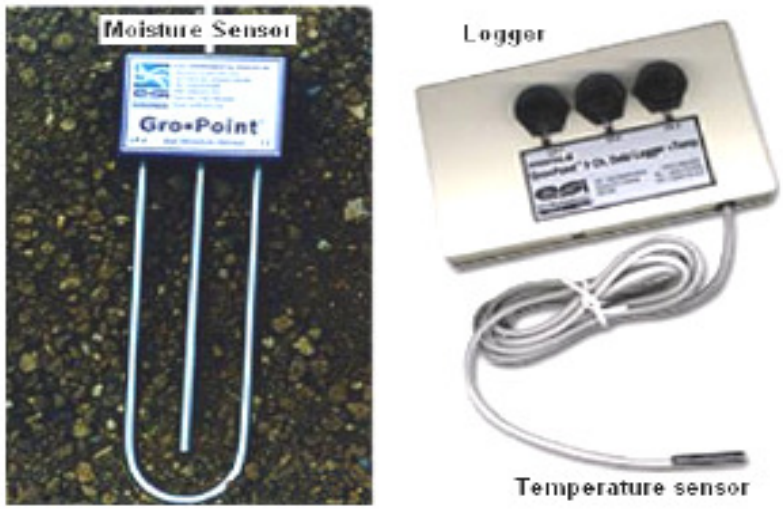

Figure 5.1 Temperature & moisture probes (left) and data logger (right)
(From http://www.esica.com/products_gropoint.php, Accessed July 17, 2007)

Volumetric moisture content is gravimetric moisture contents divided by the density of the soil medium. The relationship is shown in the following equation:

$$\theta_G = \theta_V \frac{\rho_w}{\rho_s} \quad (1)$$

θ_V = Volumetric soil moisture content;

ρ_w = Density of water

ρ_s = Bulk density of soil

On the other hand, moisture probes provide real time of volumetric moisture content data. The data was stored in a data logger stationed at each test plot, and the

data was downloaded to a computer during each site visit. A typical plot of the soil moisture data from moisture sensor collected monthly from January 2008 through March 2008 is presented in Figure 5.2. Test data collected from the entire monitoring period are provided in Chapter 6.

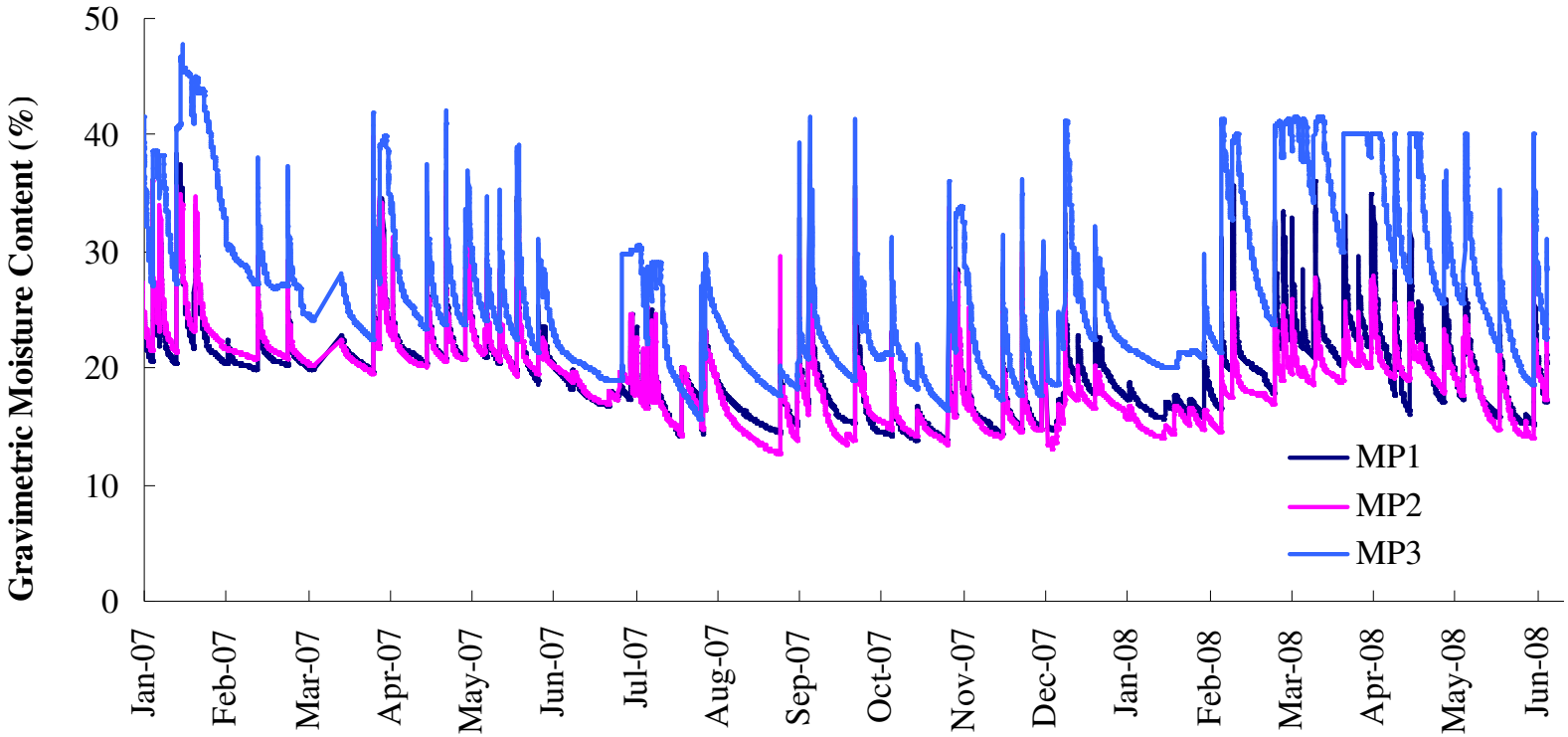

Figure 5.2 Typical plots of the moisture data from moisture sensor

5.4.2 Suction Sensors

The selection of the suction sensors is based on their accurate measurements of suction potentials more than 100 kPa. New types of suction sensors using thermal conductivity (TC) principles have been introduced in recent years. Few of these sensors include heat dissipation sensor, such as the Fredlund thermal conductivity (FTC) sensor was used in this research. Although FTC sensors have certain limitations like high failure rate in the field and the fragile ceramic used in the sensor, they are reported to be able to measure field suctions that are greater than 1,500 kPa reliably.

The FTC sensor consists of a cylindrical porous block containing a temperature sensing element and a miniature heater (Figure 5.3). The heater at the center of the porous block converts electrical energy to thermal energy. The temperature sensor measures the temperature rise as a function of the elapsed heating time. Since water has a much higher thermal conductivity than air, the rate of dissipation of the thermal energy within the porous block will increase with the increase in water content in the porous block. Thus, higher water content will result in a lower temperature rise at the center of the porous block, and, consequently, a lower voltage output of the temperature sensor. Since the water content is corresponding to the matric suction in the surrounding soil, the voltage output of the temperature sensor (i.e., the output of the suction sensor) is calibrated to determine the matric suction (Feng et al., 2002). Example of reading from the FTC suction sensor is presented in Figure 5.4.

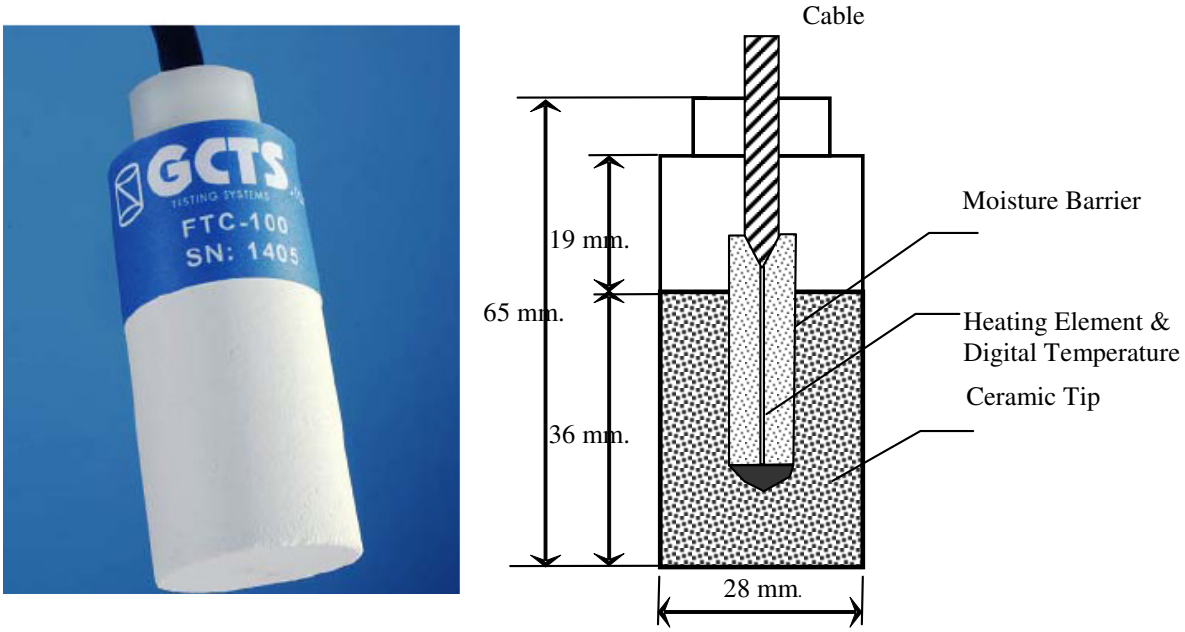

Figure 5.3 (a) FTC sensor (b) FTC sensor's schematic
(From http://www.gcts.com, Accessed July 17, 2007)

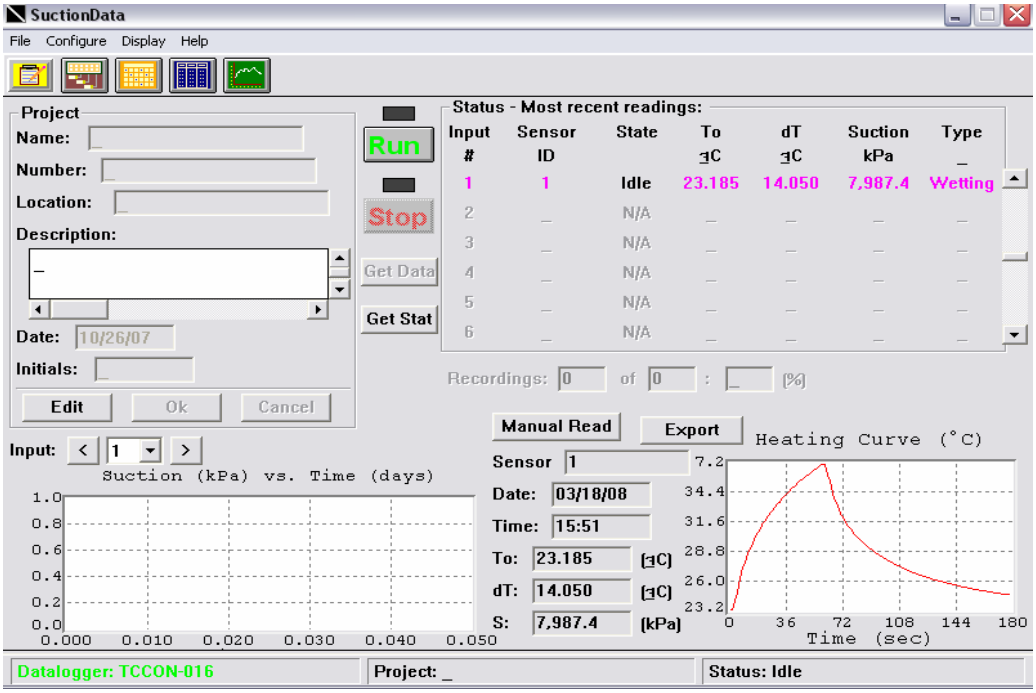

Figure 5.4 Typical reading from FTC suction sensor

5.4.3 Instrument's Calibration Study

Before the installation of instrument in the field, the moisture and FTC suction sensors were tested and calibrated in the laboratory, by placing them in a compacted Fort Worth soil mass housed in a plastic container (Figure 5.5). The variations in gravimetric moisture content and matric suction with respect to time are shown in Figure 5.6. The calibration was achieved by placing a plastic wrap on the soil in the plastic container, in order to maintain its moisture content at a constant value. The FTC matric suction values were then observed until they were constant. It would normally take about one month to reach initial equilibrium with the surrounding soil.

Then, the soil moisture content gradually decreased over the time and the variation of FTC matric suction values were also observed. As expected, a decrease in the moisture content of soil mass is associated with an increase in the matric suction that started to strike up after 150 hours later.

Figure 5.5 Clay sample in a plastic container with instrumentations

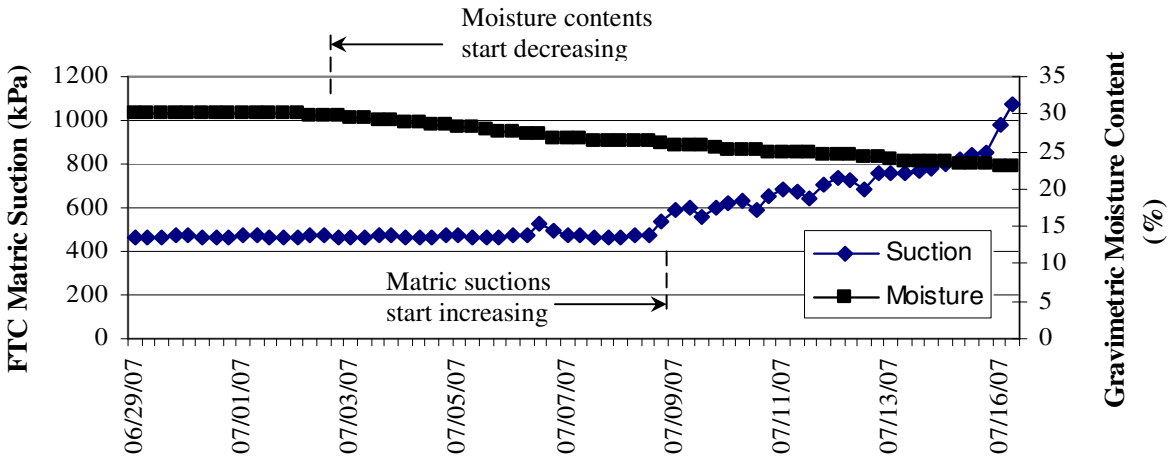

Figure 5.6 Gravimetric moisture content and matric suction measurements of clay fom Fort Worth

To evaluate the reliability of the FTC measurements, soil samples were collected from the setup shown in Figure 5.7 and were tested to measure their suction using the filter paper method. The raw matric suction measurements of the FTC sensor are compared with the suction measurements with the filter paper method shown in Figure 5.7a. The data shows that the measurements by the sensor and the filter paper method are parallel to one another when suction exceeds 500 kPa.

Figure 5.7b presents the data with the approximate 150 hours of shift factor. The shift correction recommended by Nichol et al. (2003) was used. It accounts for the equilibration of thermal conductivity sensor. This equilibration is attributed through the pore particles of the ceramic block used in the sensor and to the low saturation levels in subsoils.

As shown in Figure 5.7 (b), the use of a shift factor resulted in a close match between the two measurements. The suction sensor was capable of measuring matric suctions ranging from 400 kPa to 1400 kPa in the laboratory environment, which

indicates that this sensor is capable of providing representative results in high-suction environments.

Nichol et al. (2003) reported that the shift factor for correcting the suction data by the TC type sensors is not the same at all different suction levels. They mentioned that the TC sensors may need 30 to 70 hours of shift adjustment for sensor equilibrium to reach a change in matric suction between 0 and 7 kPa, 20 to 100 hours for a change between 55 and 103 kPa, and 100 to 200 hours for a change between 200 and 400 kPa. This observation corresponds with the present data, in which a shift of 150 hours resulted in a better match for high suction data measured by the FTC and the other one by the filter paper method.

Another important finding is that the FTC sensor was able to measure the matric suctions that ranged from 400 kPa to 1400 kPa. This reconfirms the need to use a sensor that can measure high suctions in the expansive subgrades. Furthermore, at high suction level, the differences between matric and total suctions are small, indicating the osmotic suction can be neglected for practical considerations.

Lessons learned from the laboratory calibration studies were followed during the installation of the sensors in the field. Care was taken to ensure both sensors were in good contact with the surrounding soil to obtain the reliable reading values.

5.4.4 Field Data Assessment Study

Field data assessment study was carried out after the installation of moisture and suction sensors at Fort Worth site. Figure 5.8 shows the variations of field moisture content and raw data (before applying the shift factor) of matric suction with respect to

time, measured in March 2007 and April 2007. The increasing field matric suction on event A corresponds to the increasing moisture content at the site on March 27, 2007. The FTC sensor's response time to this event lags is around 6 days (144 hours, close to 150 hours), significantly longer than the moisture sensor's lag time that is almost the real time.

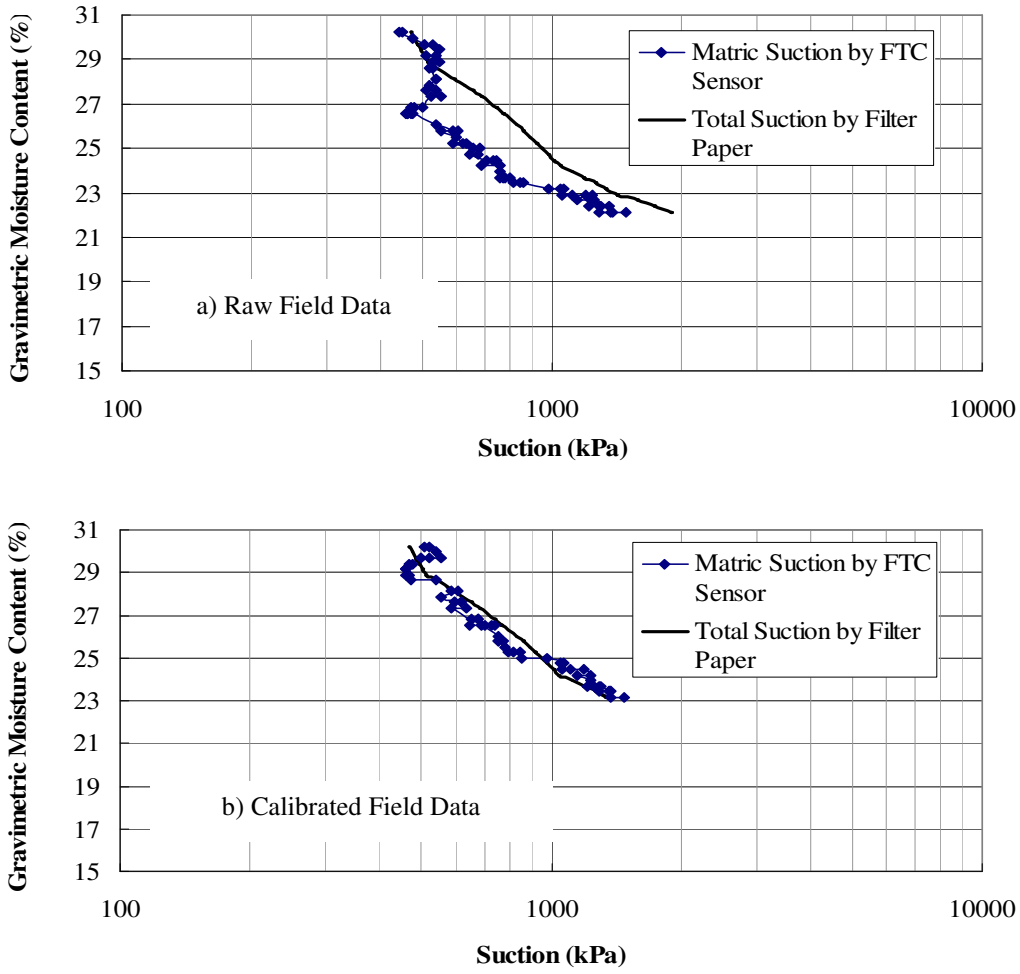

Figure 5.7 Variations of moisture content with respect to matric suction by FTC sensors and filter paper method

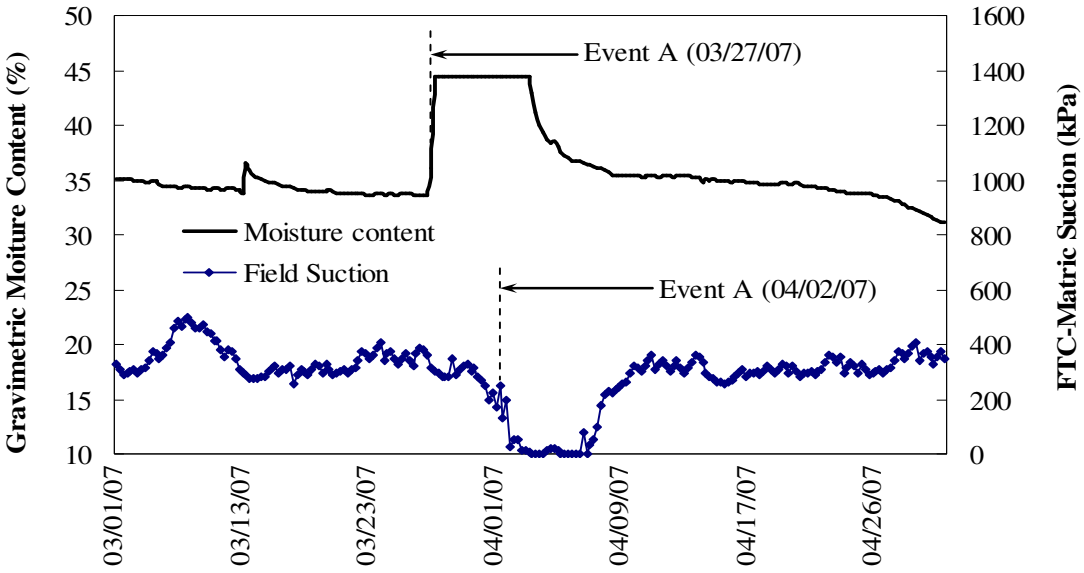

Figure 5.8 Gravimetric moisture content and raw field matric suction at Fort Worth site

The field matric suctions and corresponding moisture contents were compared with those measured in the laboratory by filter paper method, shown in Figure 5.9. As mentioned before, osmotic suctions of this soil type were very low (less than 20 kPa) based on matric and total suction measurements from both pressure plate and filter paper test methods. Sulfates and salt in the soil was very low. Hence, FTC measurements were directly compared with filter paper methods. A shift factor of 150 hours was applied to the field data. A reasonably good match was observed between the field and laboratory SWCC results. This indicates that the FTC sensors used here are capable of accurately measuring the high suctions expected in the compacted subgrades, provided the sensors are installed and calibrated carefully.

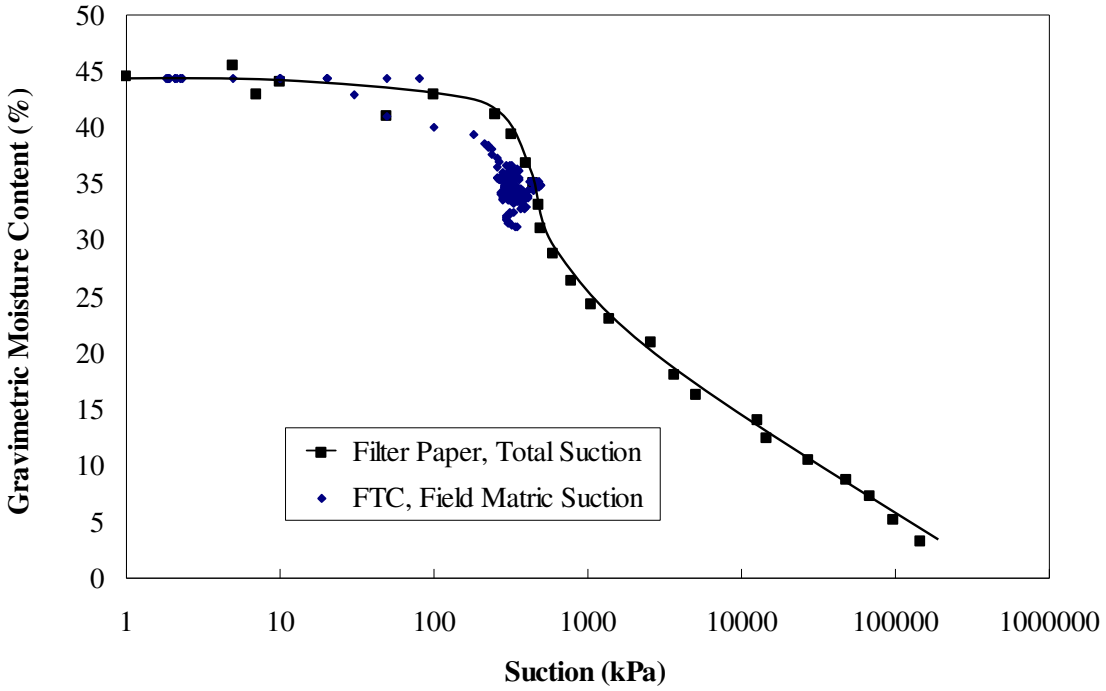

Figure 5.9 Comparisons of field and laboratory soil water characteristic curves

The measurement of matric or total suction in the field is a challenging task due to certain limitations, such as laborious installation, tedious test procedures, and high cost of current available equipments. As a result, several other sensors were not considered.

The laboratory SWCC profiles from filter paper based total suction measurements, showed a good correspondence with the field matric suctions measured from the FTC sensor. However, a correction related to response time was needed to obtain a good match. This correction factor for initial calibration studies was noted during the studies of laboratory-controlled sample.

Certain precautionary measures were taken care of when installing FTC sensors. It was to ensure a good contact between the probe and the surrounding soil for better

data collection. Overall, the FTC sensors provided satisfactory performance in measuring the field matric suction data. However, there were some limitations of this FTC sensor. The ceramic is fragile that it can be easily broken due to mishandling and the data acquisition unit was bulky.

5.5 Field Installation

A large square hole was excavated in order to accommodate all moisture sensors, suction sensors and the data acquisition unit. A data acquisition unit was placed for the continuous and real time data monitoring and collection in the field. All the sensors were embedded 1.0 to 1.5 feet below the ground surface. Moisture and suction sensors were carefully placed in a line configuration as shown in Figure 5.10, Figure 5.11 and Figure 5.12. Prior to the placements, a small 0.5 inch of depression was made at the bottom of the hole, in which the sensor was carefully placed so that there were no air gaps between the sensor and soil. The excavated soil was then filled onto the hole and compacted in the approximate 4-inch short lifts. Extreme care was taken to ensure the compaction was similar to the adjoining subsoils.

Figure 5.10 Placement of both moisture and suction sensors

Figure 5.11 Placement of suction sensors

Figure 5.12 Placement of moisture probes

Figure 5.13 Compacting after installation

Once installation work was completed, the sensors were activated by connecting them to a laptop computer. Data collections were made every two months (each site visit). A visual pavement distress survey was also carried out in each site visit.

5.6 Site Information

5.6.1 Fort Worth Site

The test site in Fort Worth is located at FM 157, about 380 feet from the east side of US Post Office at Venus, Texas (Figure 5.14). Severe longitudinal and transverse cracking with local pavement settlement were already observed at the first visit of the site (Figure 5.15). The side slope is about one vertical to four horizontal (1:4) and covered with grass on both sides of the road. There is no presence of drainage ditch on both sides of the pavement. The area next to the pavement shoulder is farmland. The site schematic is shown in Figure 5.16.

Figure 5.14 Location of the test site in Fort Worth

Figure 5.15 Longitudinal and transverse cracking

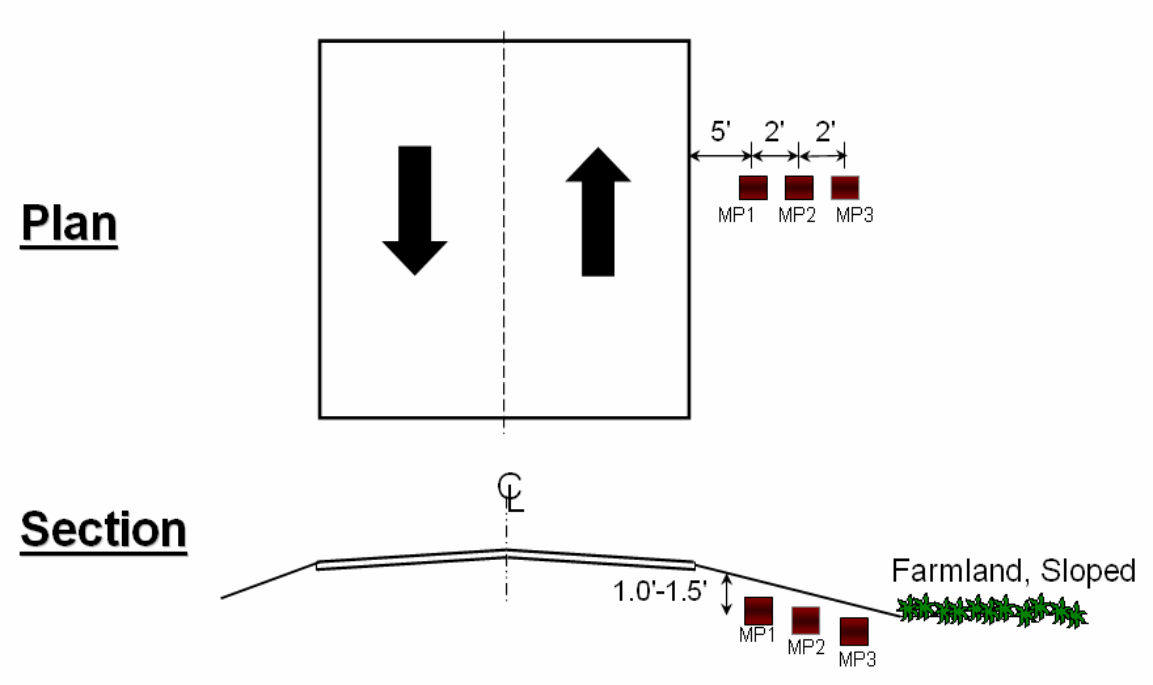

Figure 5.16 Site schematic - Fort Worth site

5.6.2 San Antonio Site

The test site in San Antonio is located at FM 1052, about 2.8 miles from the city of Uvalde, Texas (Figure 5.17). No pavement crack was observed at the first visit (Figure 5.18, 5.19). Pavement shoulder is almost leveled and covered slightly with grass on its both sides. There is no presence of drainage ditch next to the pavement shoulders. The area next to the pavement shoulder is supposedly farmland. However, no vegetation was observed during any site visits. The site schematic in Figure 5.20 depicted the main feature of this site.

Figure 5.17 Location of San Antonio site

Figure 5.18 Location of instrumentations

Figure 5.19 San Antonio Site conditions

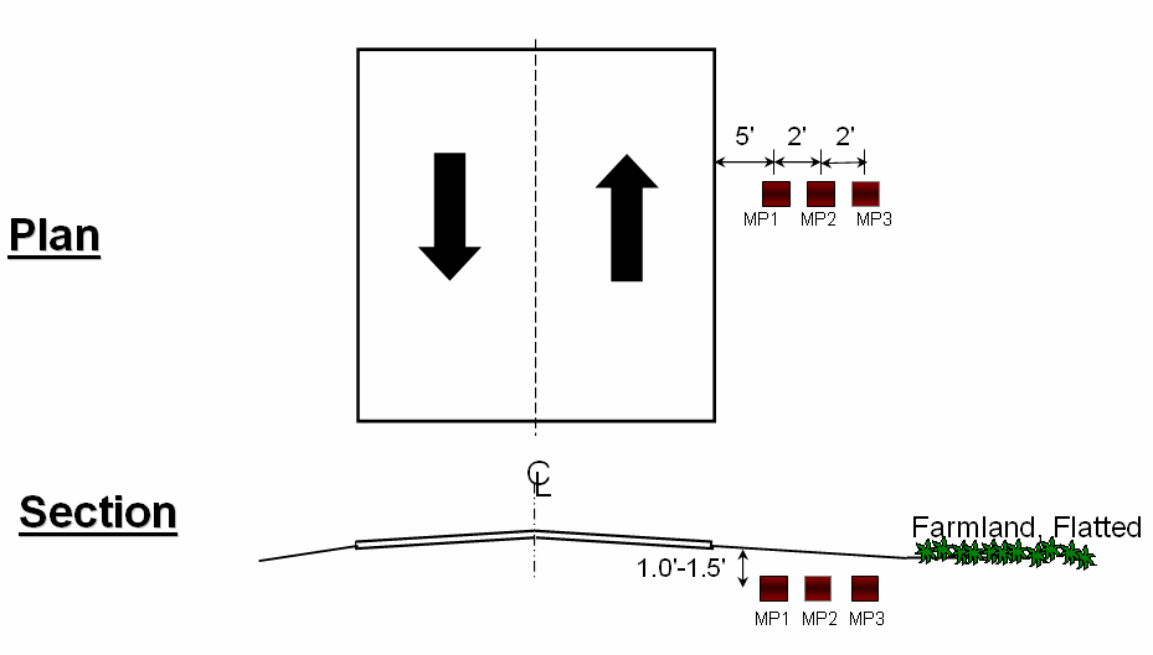

Figure 5.20 Site schematic - San Antonio site

5.6.3 Paris Site

The test site in Paris is located at FM 911, about 2.5 miles from city of Clarksville, Texas (Figure 5.21). The side slope is about one vertical to four horizontal (1:4). There were presence of large cracks and dipping on the pavement at the first visit as shown in Figure 5.22, Figure 5.23 and Figure 5.24. Soil slope next to the pavement shoulder also exhibited severe cracking and numerous holes that were about 1 to 2-inch diameter and 1 to 3-foot depth along the section. Consequently, highly expansive soil behavior can be expected in this area. This site can be considered as the worst site conditions, since it does not only have the poor soil properties but there are also the presence of poor drainage ditches and large trees along the road (Figure 5.24) that may increase soils heaving and shrinking. The site schematic in Figure 5.25 presents the main feature of Paris site.

Figure 5.21 Paris site location

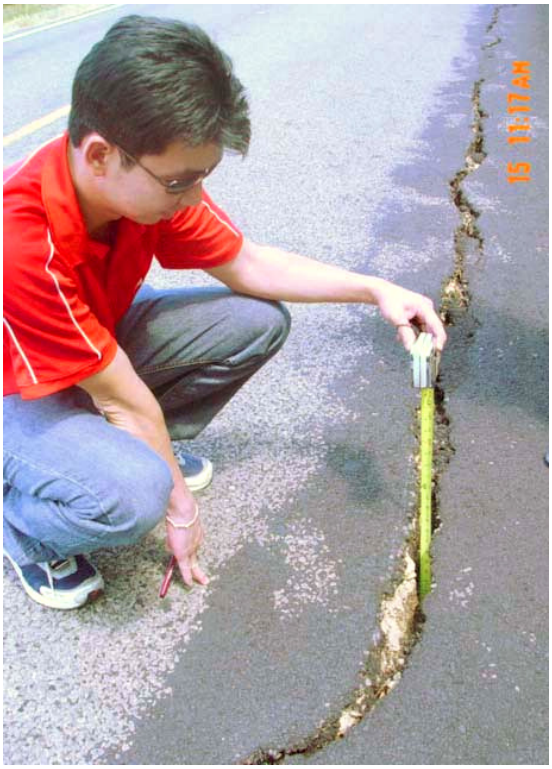

Figure 5.22 Measuring of the large cracks on the pavement

Figure 5.23 Measuring of desiccation cracks

Figure 5.24 Longitudinal and traverse cracking

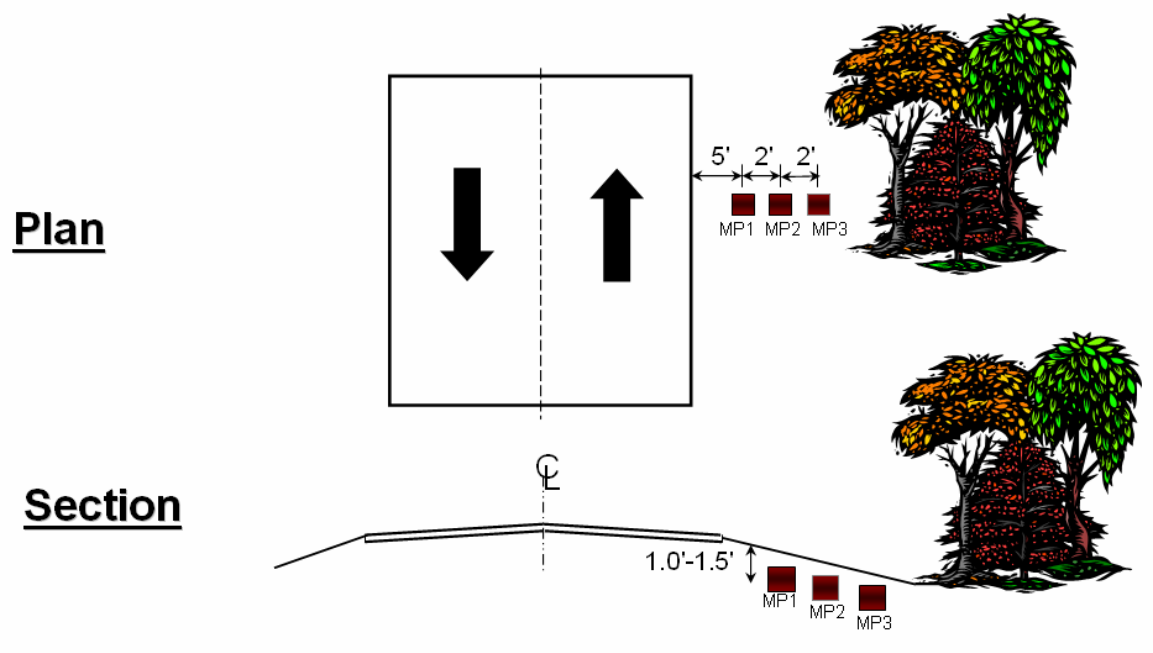

Figure 5.25 Site schematic - Paris site

5.6.4 Houston Site

Houston test site is located at FM 1236, about 0.5 mile from the intersection between FM 1236 and FM 422, Needville, Texas (Figure 5.26). There are presences of severe longitudinal cracking at the first visit (Figure 5.27). The side slope is about one horizontal to five vertical (1:5) and covered heavily with grass on both sides of the slopes. On one side of the road, there is also a poor drainage ditches (Figure 5.28). It may increase the seasonal fluctuation in the moisture content and yield the problem of soils heaving and shrinking that eventually result in cracking on the pavement. The site schematic in Figure 5.29 shows the main feature of Houston site.

Figure 5.26 Site location – Houston site

Figure 5.27 Severe longitudinal cracking

Figure 5.28 Poor drainage ditches

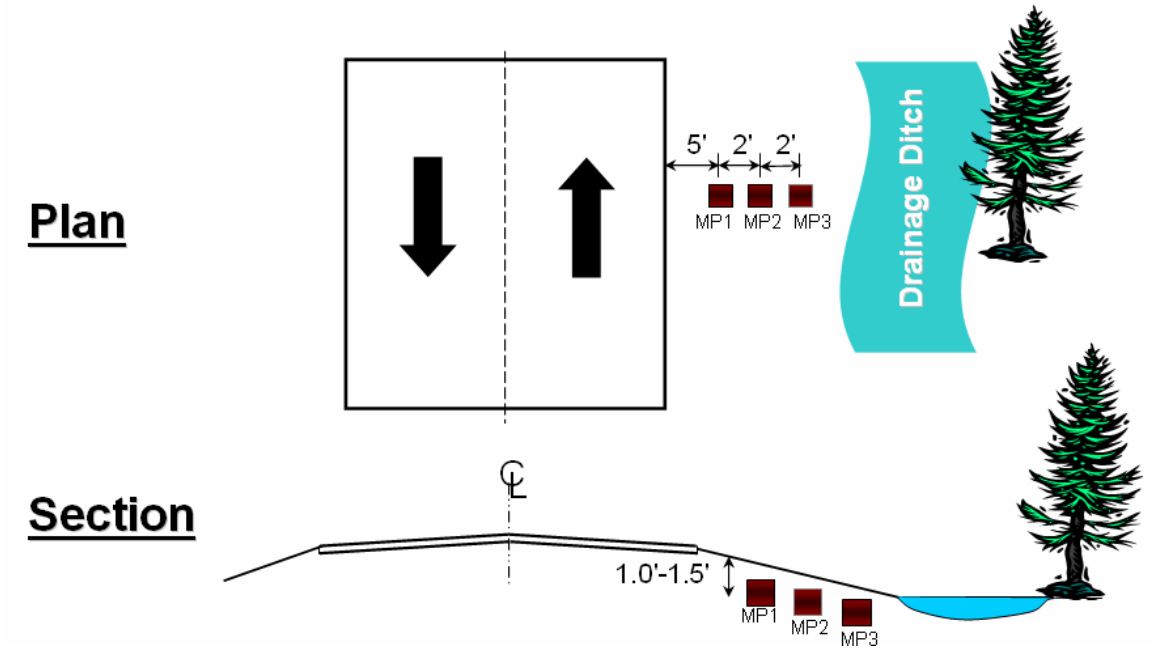

Figure 5.29 Site schematic – Houston site

5.7 Site Elevation Surveys

Topographic surveys were periodically conducted during moisture and matric suction data collection in the field, and then these results were used to evaluate vertical movements (swell/shrinkage volume changes) along the test sections (Figure 5.30). In each site, data for elevation survey were recorded at seven points with a distance of 20 feet apart from one another as shown in Figure 5.30 and 5.31.

The vertical displacements were calculated by subtracting the elevation of each spike from an initial elevation survey reading, which was established at the beginning of the monitoring process immediately after the instrumentation. Example of surveying data and plot of elevation changes are shown in Table 5.1 and Figure 5.32, respectively.

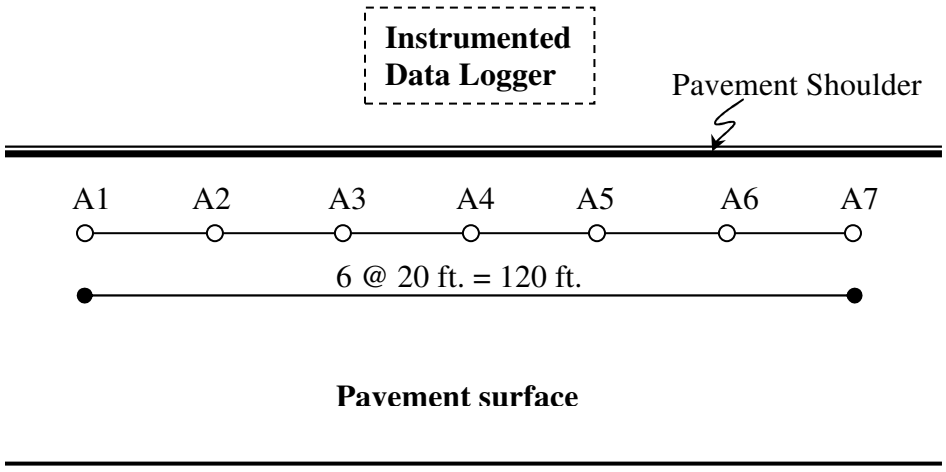

Figure 5.30 Schematic of elevation survey section

Figure 5.31 Markers for elevation survey

Table 5.1 Typical surveying data

Station		Elevation Difference (ft.)					
		03/05/07	**04/15/07**	**05/24/07**	**07/03/07**	**08/06/07**	**09/28/07**
A1	**0+60**	0.00	0.00	0.00	-0.07	-0.13	-0.04
A2	**0+40**	0.00	-0.01	-0.01	-0.09	-0.19	-0.12
A3	**0+20**	0.00	-0.01	-0.01	-0.04	-0.08	-0.12
A4	**0+00**	0.00	0.03	-0.01	-0.04	-0.10	-0.20
A5	**0-20**	0.00	0.03	0.02	0.01	-0.15	-0.27
A6	**0-40**	0.00	0.08	0.06	0.06	-0.06	-0.22
A7	**0-60**	0.00	0.00	-0.01	-0.02	-0.12	-0.28

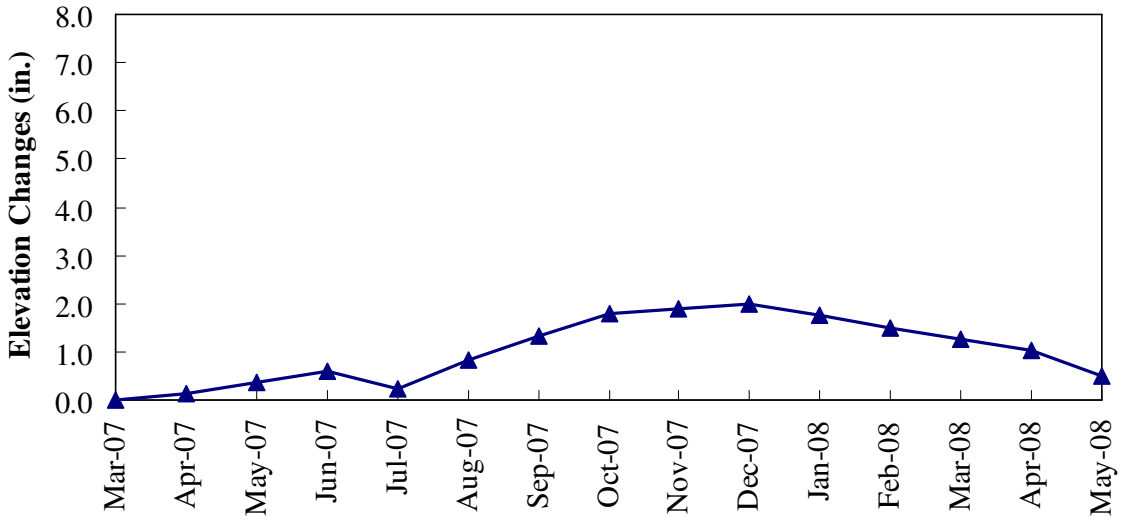

Figure 5.32 Typical plot of elevation changes at point A4
(Closest to the Data Logger) in different time period

5.8 Cracking of Paved Shoulder

Free swell analysis strain tests are often used in geotechnical practice to characterize expansive soils. However, shrinkage or desiccation strains are considered equally important because they initiate the failure mechanisms (cracks) in expansive soils that may expose large volumes of soil surface area at varying depths to saturation. If this problem is not immediately remediated, shrinkage strains in soils induced by dry environments can lead to crack propagation in both lateral and longitudinal directions. As a result, large volumes of expansive subgrades near shrinkage cracks will have moisture access during rainy seasons and will start expanding once they are saturated.

In order to distinguish between the new and old cracks on the adjoining pavement, digital photos of the paved shoulder were periodically taken. Old cracks that had been crack were sealed with the bitumen product and these could be seen in the

digital photos shown in Figure 5.33. As the paved shoulder began to deteriorate, cracks would appear and continue to propagate as well as widen. By comparing the photos at the same location, the severity of cracking can be estimated.

(a)

(b)

Figure 5.33 Photos shown the longitudinal cracking taken on (a) 04/15/07 and (b) 09/28/07

5.9 Summary

This chapter summarizes various necessary field monitoring tasks performed in this research for evaluating soil and pavement conditions. Since field instrumentation has provided very important data for monitoring soil moisture and matric suction, laboratory testing and calibrating are imperative to understand the nature of the instruments before their installation in the field. Site elevation surveys were conducted to address shrink and swell behavior of the pavement. Imaging is also one of the very effective tools for addressing pavement cracking in the test sites in different time period. More importantly, distinctive site's information and characteristics included in this chapter are the main features that can explain subsoil and pavement distress as well.

CHAPTER 6

FIELD MONITORING RESULTS

6.1 Introduction

In most cases, both heaving and shrinking of expansive soils are caused by significant fluctuation of moisture contents and matric suctions in these soils from seasonal changes. Variation of soil moisture contents and matric suctions are also influenced by pavement compaction states, environmental site conditions such as rainfall characteristics and the location of roadside trees as well as drainage ditches. Information pertaining to results of these factors is addressed in this chapter.

6.2 Field Monitoring Results

Soil moisture content data was collected by downloading from embedded data loggers for every site visit. It should be noted that matric suction data, formerly planned to collect the same manner as soil moisture content data, was gathered manually by measuring at the site instead of downloading from the data loggers. The researcher decided not to embed the data acquisition unit for suction sensors as they are expensive and highly affected by the moisture conditions in the surroundings. Hence, direct manual readings were taken while visiting the site. Elevation surveys, photographing of pavement cracks and recording of any field conditions including ponding details were also collected.

For the completeness of data, the monthly rainfall data was also included in the research in order to compare with average monthly soil moisture contents and pavement elevation changes. The data were collected from National Environmental Satellite, Data and Information Service (NESDIS) homepage (http://www.ncdc.noaa.gov/oa/climate/stationlocator.html). Since the local weather stations may not be available near the site's exact locations, the closest ones with availability of completed data were selected (Table 6.1).

Table 6.1 List of stations and distances from the site location

Cities	**Station**	**Distance between station and the sites (mi.)**
Fort Worth	Midlothain	7.9
San Antonio	Garner Field Airport	3.3
Paris	Clarksville Red River Airport	1.6
Houston	Richmond	18.4

Field results for each site are presented in the form of plotting of soil moisture contents, monthly average soil moisture contents, monthly rainfalls, and pavement elevation changes against monitoring time periods (Figure 6.2). Also, those data is correlated with any changes of pavement cracks at the site.

6.2.1 Fort Worth Site

As informed in the previous chapter, numerous transverse and longitudinal cracks were observed at the site since the initial visit (Figure 6.1). Even though, no new crack was detected, several old cracks were noticeably appeared and amplified on late September'07 site visit as shown in Figure 6.2. Figure 6.3 to 6.6 present the data collected in the field from the test location.

Figure 6.1 Longitudinal pavement cracking (Taken on April'07)

(a)

(b)

Figure 6.2 (a) Widened longitudinal cracking (b) Differntial swelling (Taken on Sept'07)

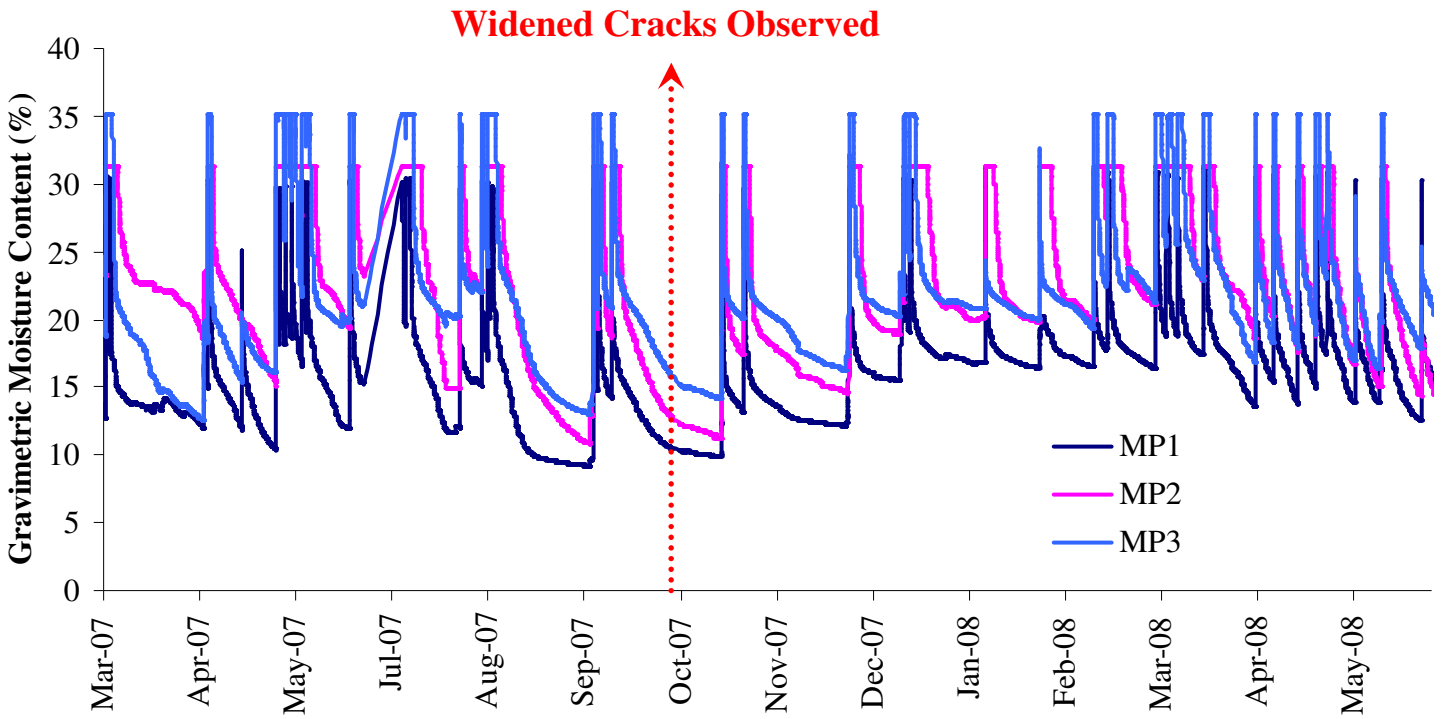

Figure 6.3 Plots of gravimetric moisture contents at Fort Worth site

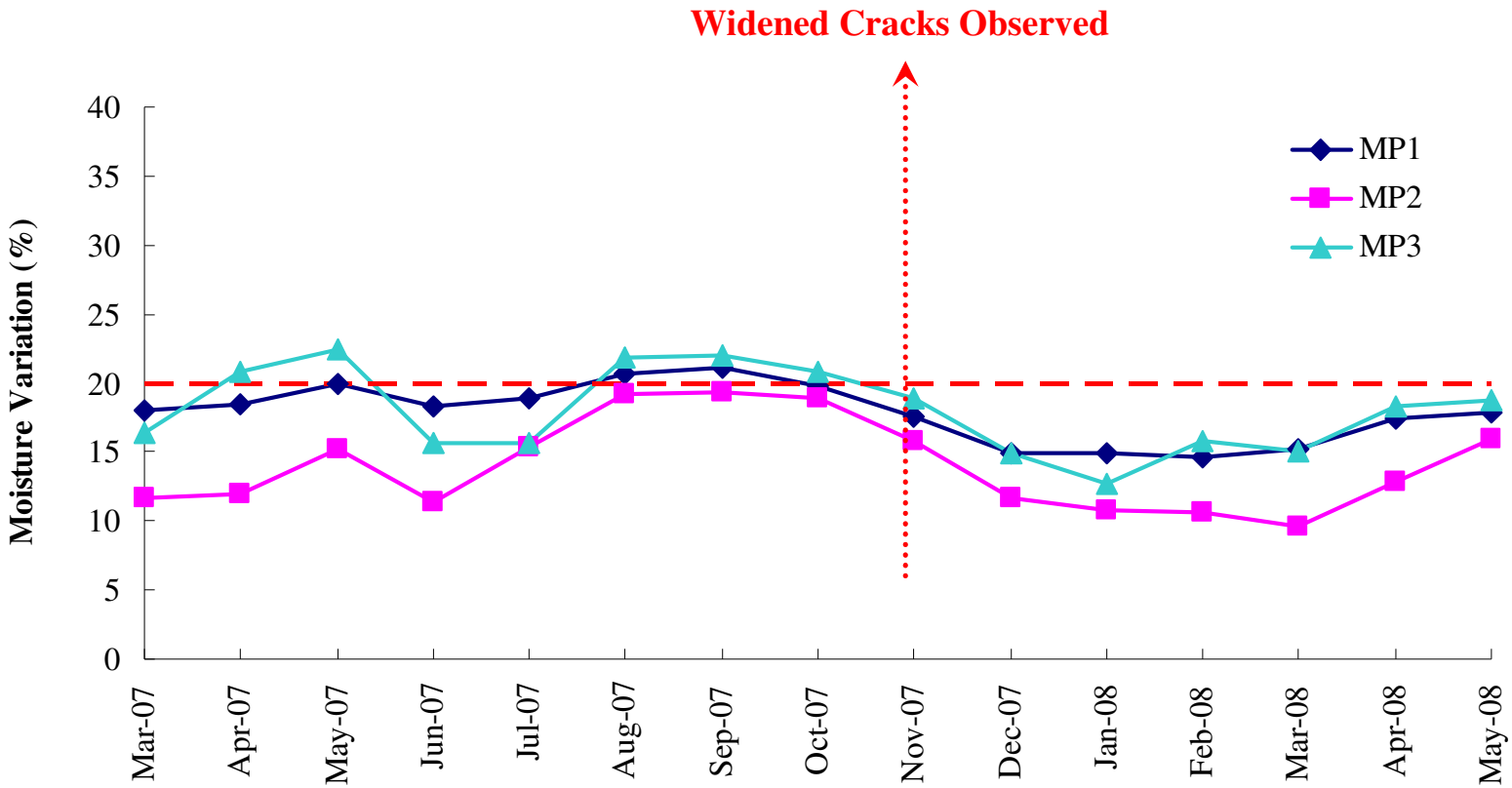

Figure 6.4 Plots of moisture variations at Fort Worth site

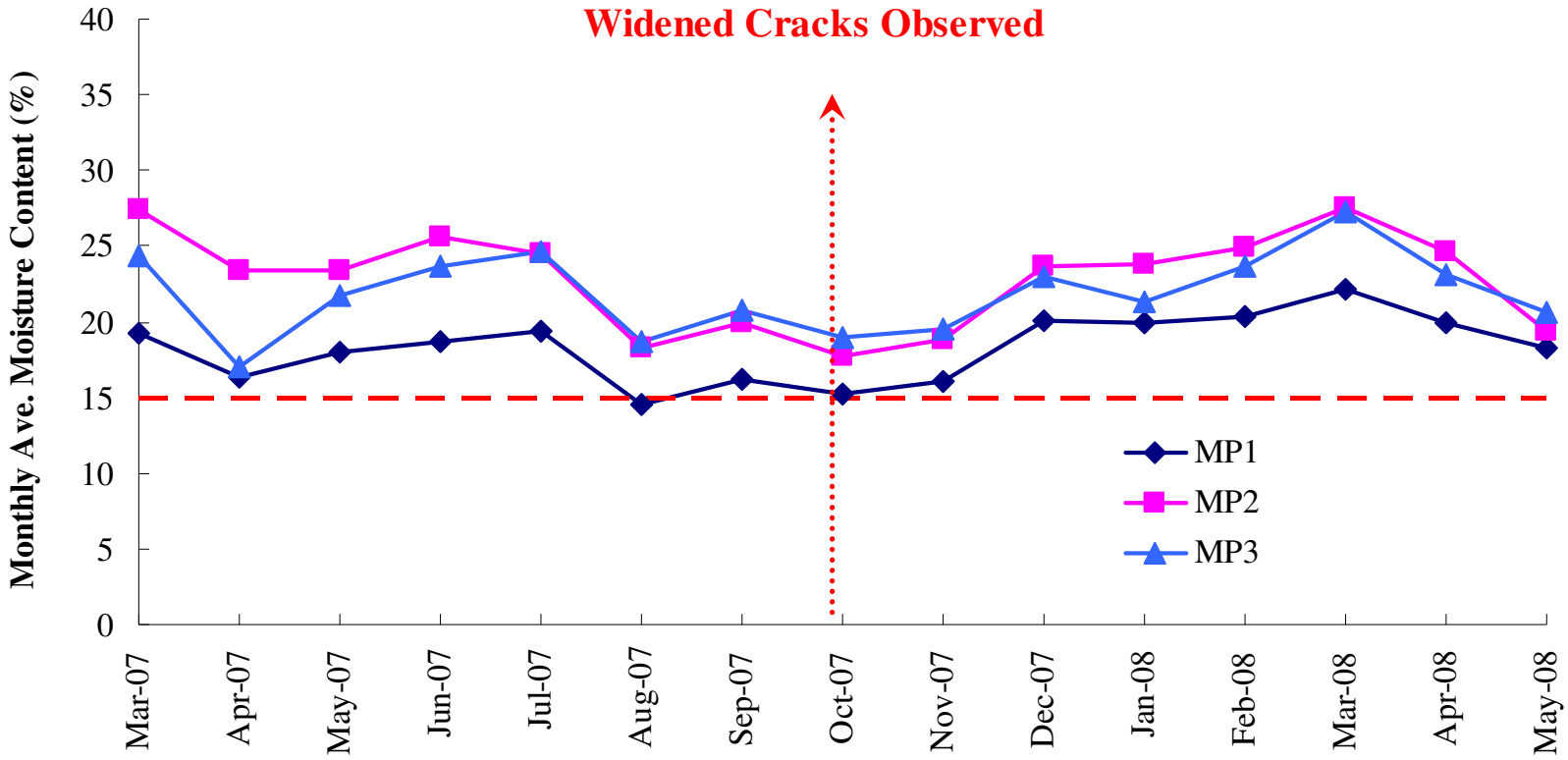

Figure 6.5 Plots of monthly average gravimetric moisture contents at Fort Worth site

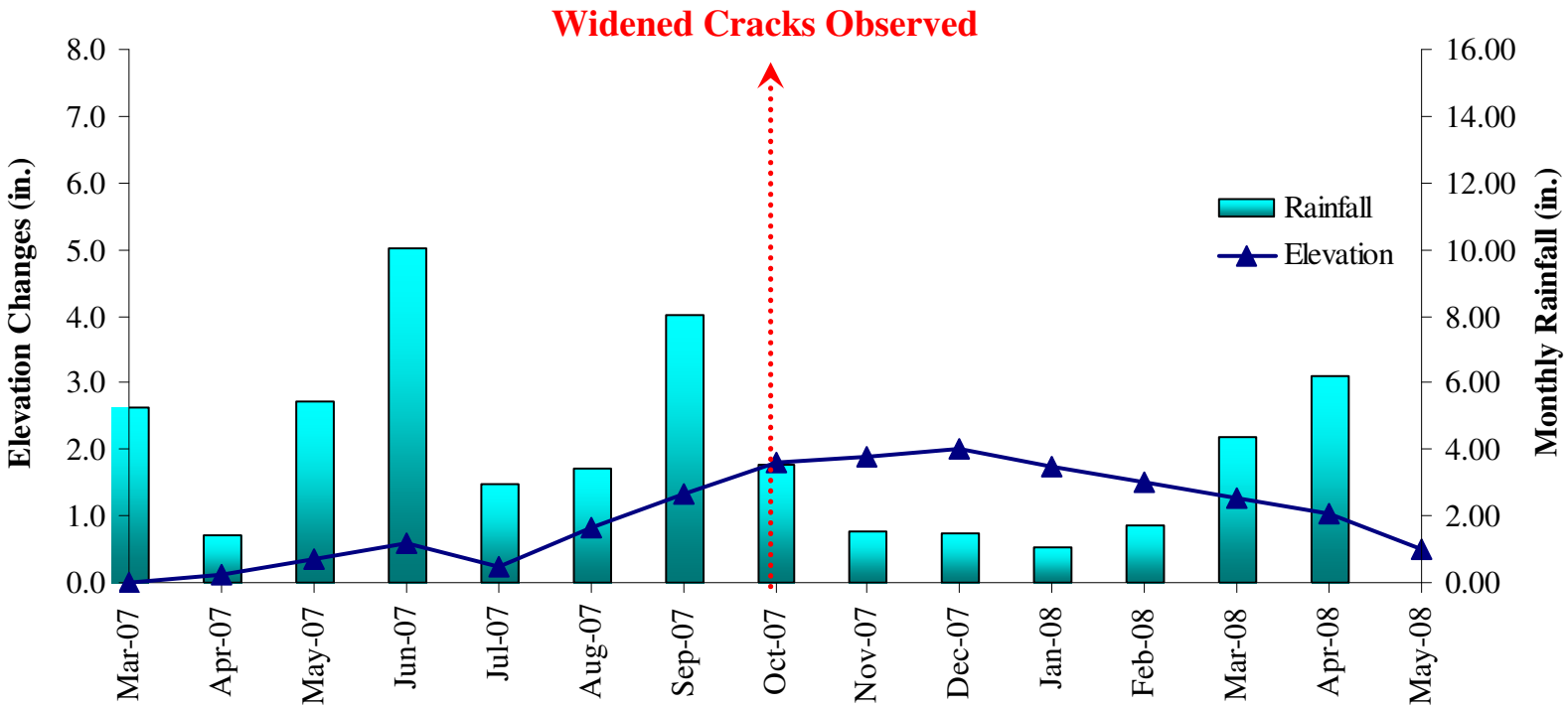

Figure 6.6 Plots of pavement elevation changes and monthly rainfall data at Fort Worth site

A term “moisture variation” is defined as the differences between maximum and minimum moisture content values in a particular month. By considering the moisture content profile in Figure 6.3, the moisture content variation data was determined and these results are presented in Figure 6.4. It is noticeable that, between the August to October’07, soil moisture variation from all three sensors were more than 20% (Figure 6.4) which is considered to be high moisture content changes that could cause expansive soil subgrade to undergo swell and shrink in short period of time. Accordingly, several existing cracks had been appearing in late September’07 visit and they are becoming wider with time.

Generally, pavement cracks usually showed up when the soil shrank in dry weather condition. However, the observed cracks were exhibited while the pavement elevation was increasing (as seen in Figure 6.6) which means the soil under the pavement was swelling. This might be the contribution of the existing cracks since those cracks will allow moisture content to migrate in and out of the subsoil faster than the areas with no cracking. As a result, differential moisture contents and also differential swell/shrink of the nearby soil occurred and this was leading to aggravate the crack development.

By reviewing the field matric suction from Table 6.2, the matric suction readings in August and September’07 were quite high indicating high potential of soil swell/shrink behavior. It should be notified that the presented values in the Table 6.2 are close to the maximum values since they were measured in high temperature conditions in a during one of the site visits.

Table 6.2 Field matric suction reading at Fort Worth site

Month	Field Matric Suction (kPa)
Mar-07	291
Apr-07	288
May-07	491
Jul-07	337
Aug-07	1,635
Sep-07	1,098
Dec-07	502
Mar-08	278
Jun-08	857

6.2.2 San Antonio Site

Since the road was relatively new, no new pavement cracks in both longitudinal and transverse directions had been detected in the earlier visits. Later, several longitudinal cracks along the pavement shoulder were noted on the site visit on November'07 and the subsequent visits on December'07 and March'08 (Figure 6.7 and 6.8). The cracks were observed not only at the pavement sections but also at the soil adjacent to the pavement and shoulders (Figure 6.7). Those cracks were quite wide and deep indicating highly shrinking nature of the soil at this site.

Figure 6.7 Crack on soil adjacent to pavement shoulder (Taken on November'07)

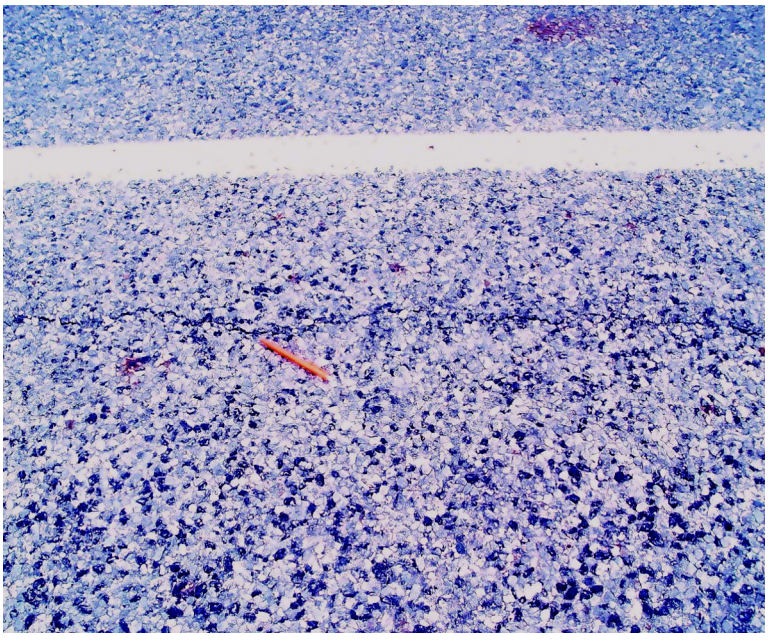

Figure 6.8 Longitudinal pavement crack (Taken on November'07)

A post mortem data analysis was done by reviewing the data closely, in particular those monitored before December'07. As shown in Figure 6.9, it is noticeable that monthly rainfall data is very low at this site since September'07. Similar to monthly low rainfall amounts, soil moisture content variation averaged per month during September'07 to March'08 is also relatively low which is less than 15% (Figure 6.10). Hence, it is reasonable to assume that this dry weather condition of this site with very low rainfall might have contributed to the pavement cracking since the cracks were first appeared on the months with lowest rainfall and low averaged soil moisture contents.

From Figure 6.11, a plot of amount of rainfall and pavement elevation changes, it is also possible that the crack might start to develop between September and October'07 and became apparent on the pavement surface only in November'07.

From Table 6.3, the field matric suction readings on August and September'07 were quite high values which are 1,361 and 2,209 kPa, respectively. However, the highest reading value is 7,987 kPa on March'08 which is the result from long period of dry spell. It should be noted that the matric suction reading could not be achieved since the sensor was malfunctioned. Thus, new spare sensor was buried on next site visit which was in December'07. Since the sensor need time at least three weeks to equilibrate with surrounding soil, no reading can be made during the site visit in December'07.

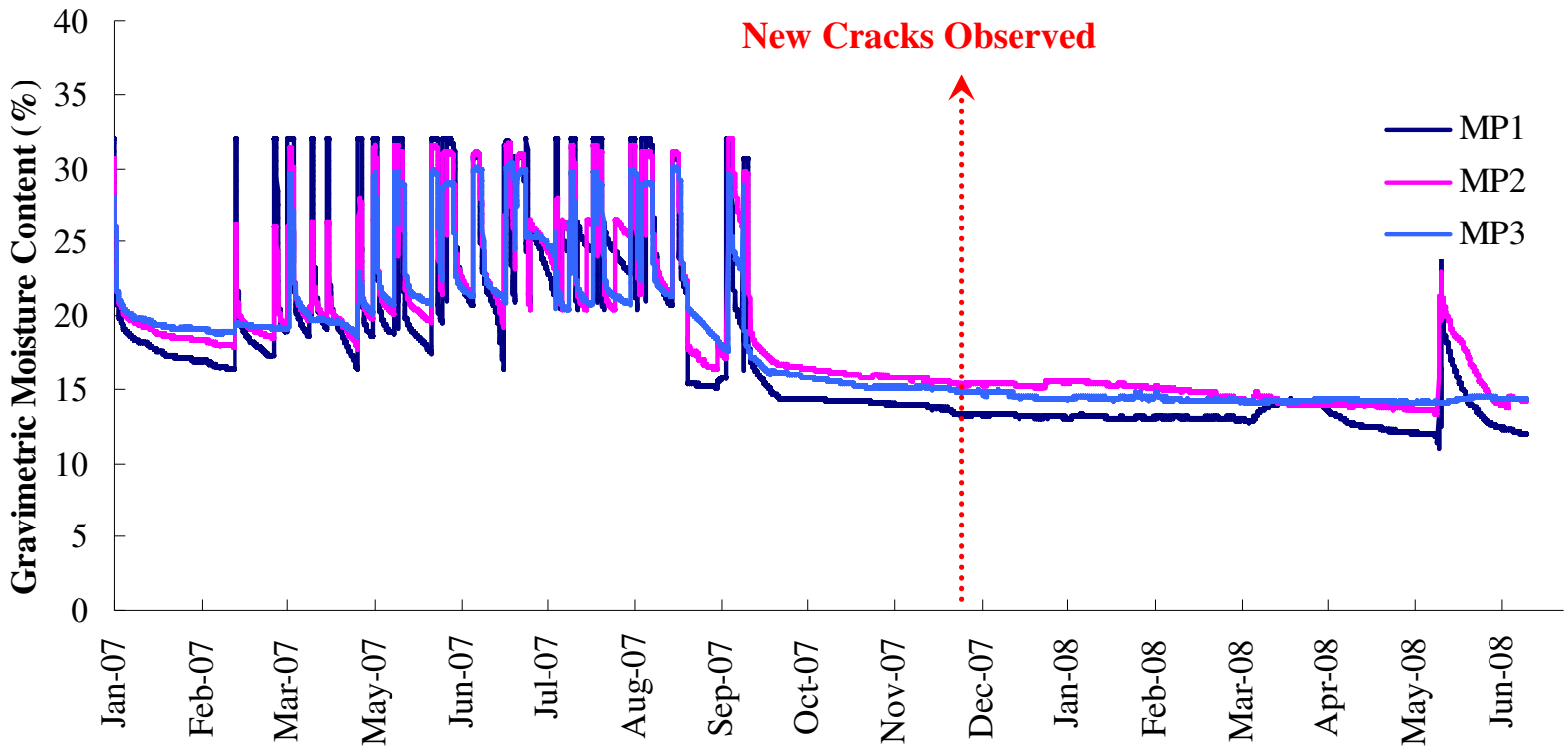

Figure 6.9 Plots of gravimetric moisture contents at San Antonio site

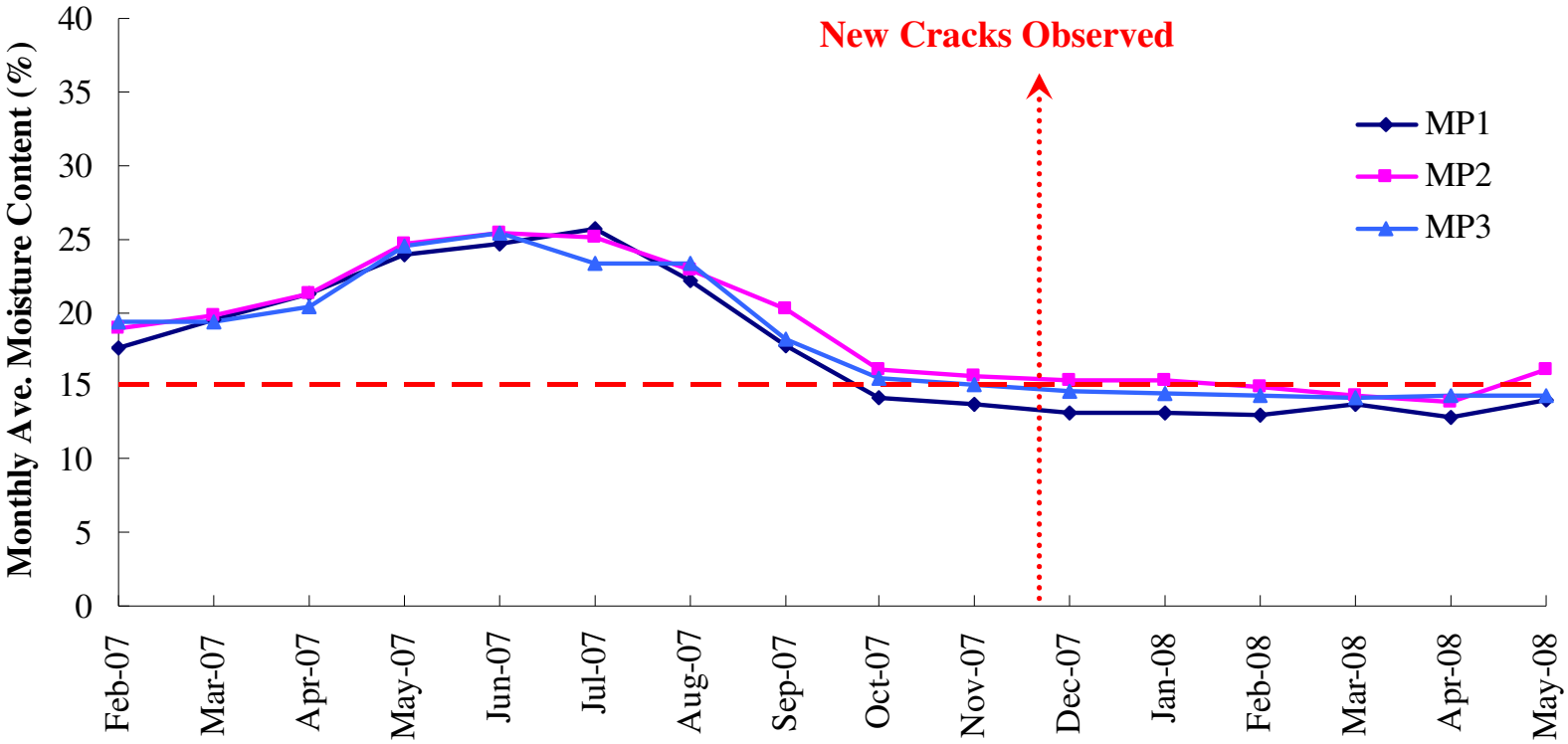

Figure 6.10 Plots of monthly average gravimetric moisture contents at San Antonio site

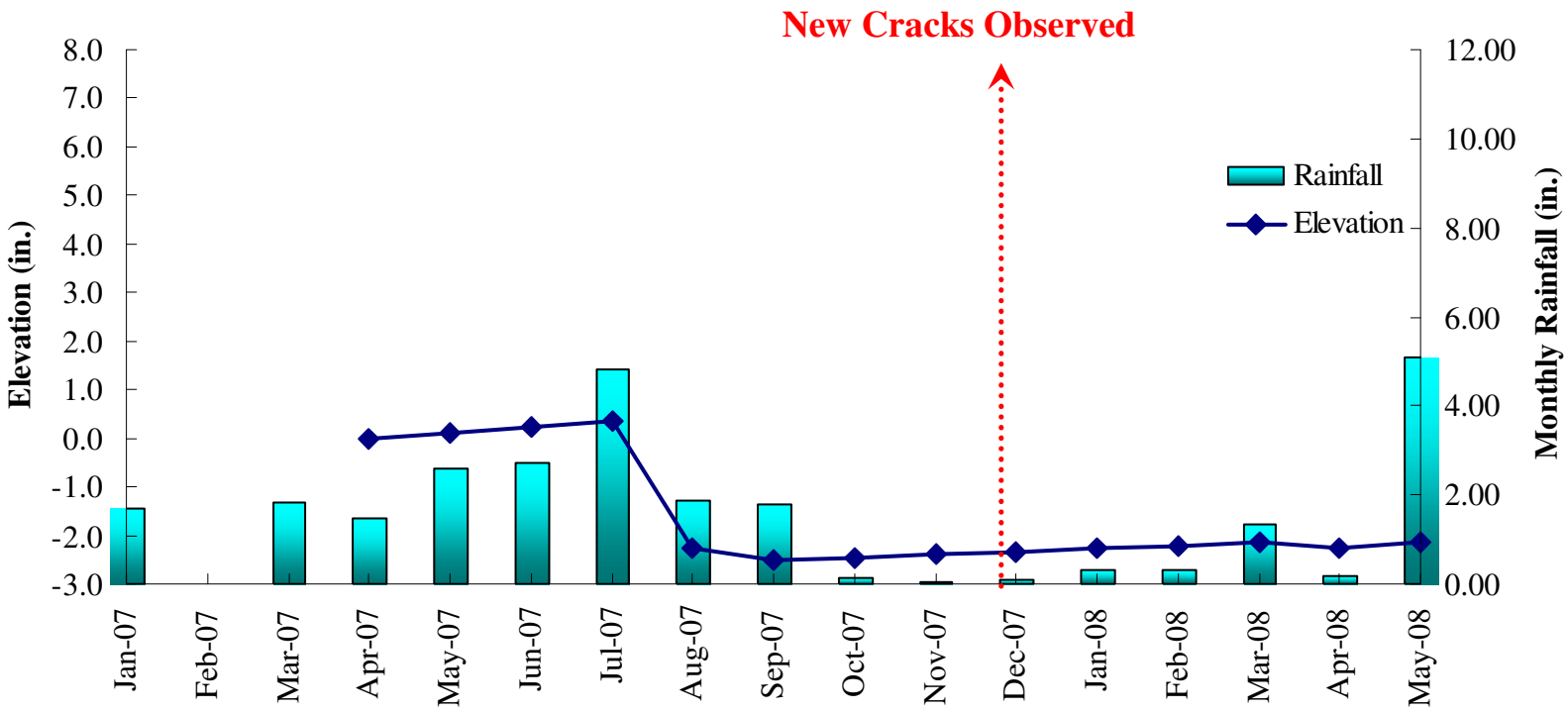

Figure 6.11 Plots of pavement elevation changes and monthly rainfall data at San Antonio site

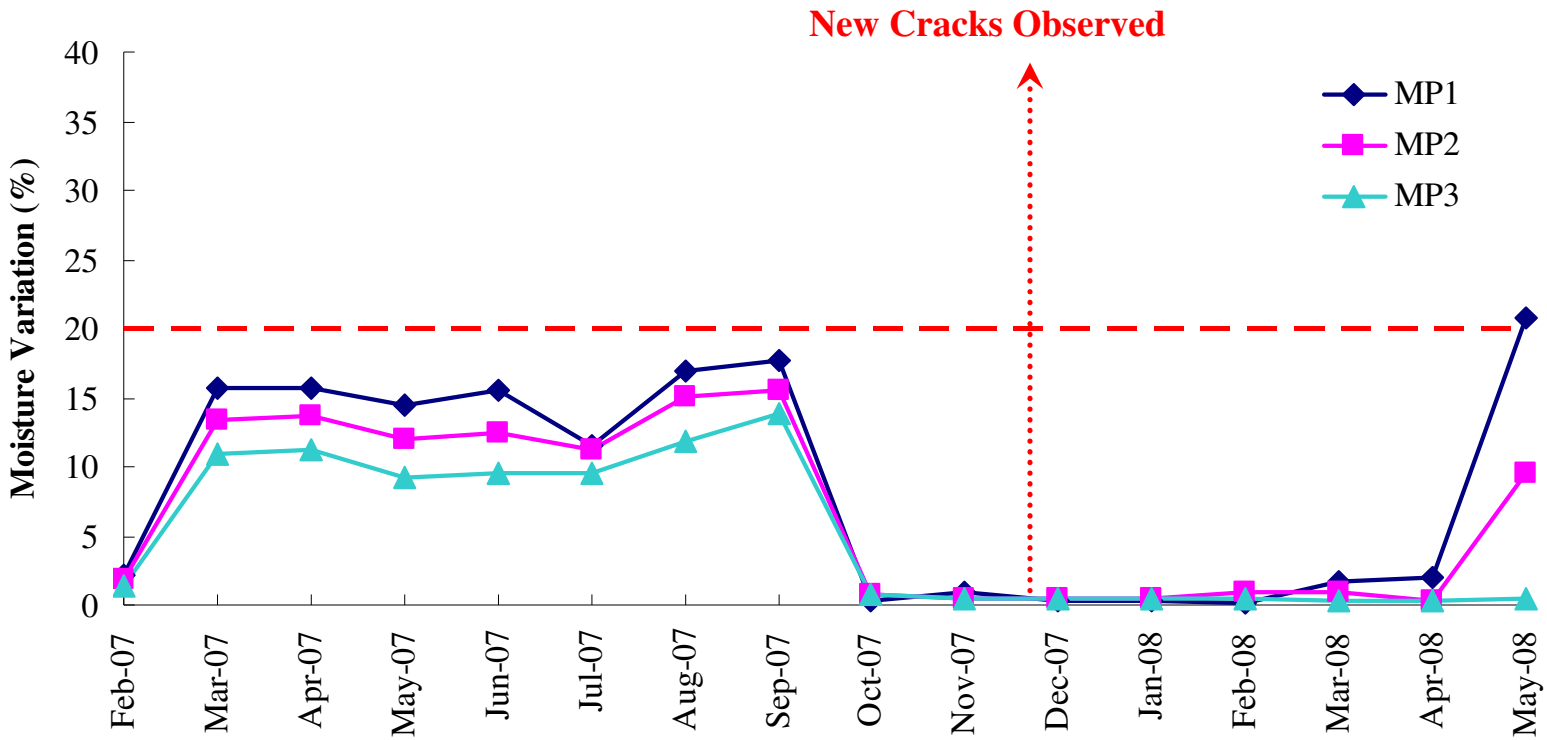

Figure 6.12 Plots of moisture variations at San Antonio site

Table 6.3 Field matric suction reading at San Antonio site

Month	**Field Matric Suction (kPa)**
May-07	639
Jun-07	600
Aug-07	1,361
Sep-07	2,209
Nov-07	N/A
Dec-07	N/A
Mar-08	7,987
Jun-08	3,425

6.2.3 Paris Site

This site was selected to study the influence of a poor drainage ditch and large trees near the pavement section and their impacts on pavement cracking. As mentioned in the earlier Chapter 5, this site is considered to have the worst pavement condition since the cracks were not only large but also long and deep. As observed by the researcher, this road had been overlayed several times during summer periods of April'07 and July'07, however, the cracks still appeared on the pavement shortly after these overlays.

Figure 6.13 are series of photographs that were taken at the same location at different time periods. It is noticeable that the cracks evidently showed up on 09/29/07 during the site visit which was the same time that all moisture variations from three sensors exceeded 20% (Figure 6.14 and 6.15). This percentage of this moisture variation is interestingly the same as Fort Worth site that resulted in the appearance of cracking. Thus, moisture variation might be one of the key contributions to the occurrences of the cracking.

Several cracks were amplified during the site visit on September'07 which is interesting since soil moisture content from MP 1 and MP 2 sensors was close to 15% (dry side) and the moisture variations of all three moisture sensors was more than 20% (Figure 6.15 and 6.16). These numbers are similar to those monitored in both Fort Worth and San Antonio sites. These are providing guidelines for threshold values for further studies on this topic.

Figure 6.13 Photographs taken on (a) 04/15/07, (b) 07/03/07, (c) 08/08/07 and (d) 09/29/07

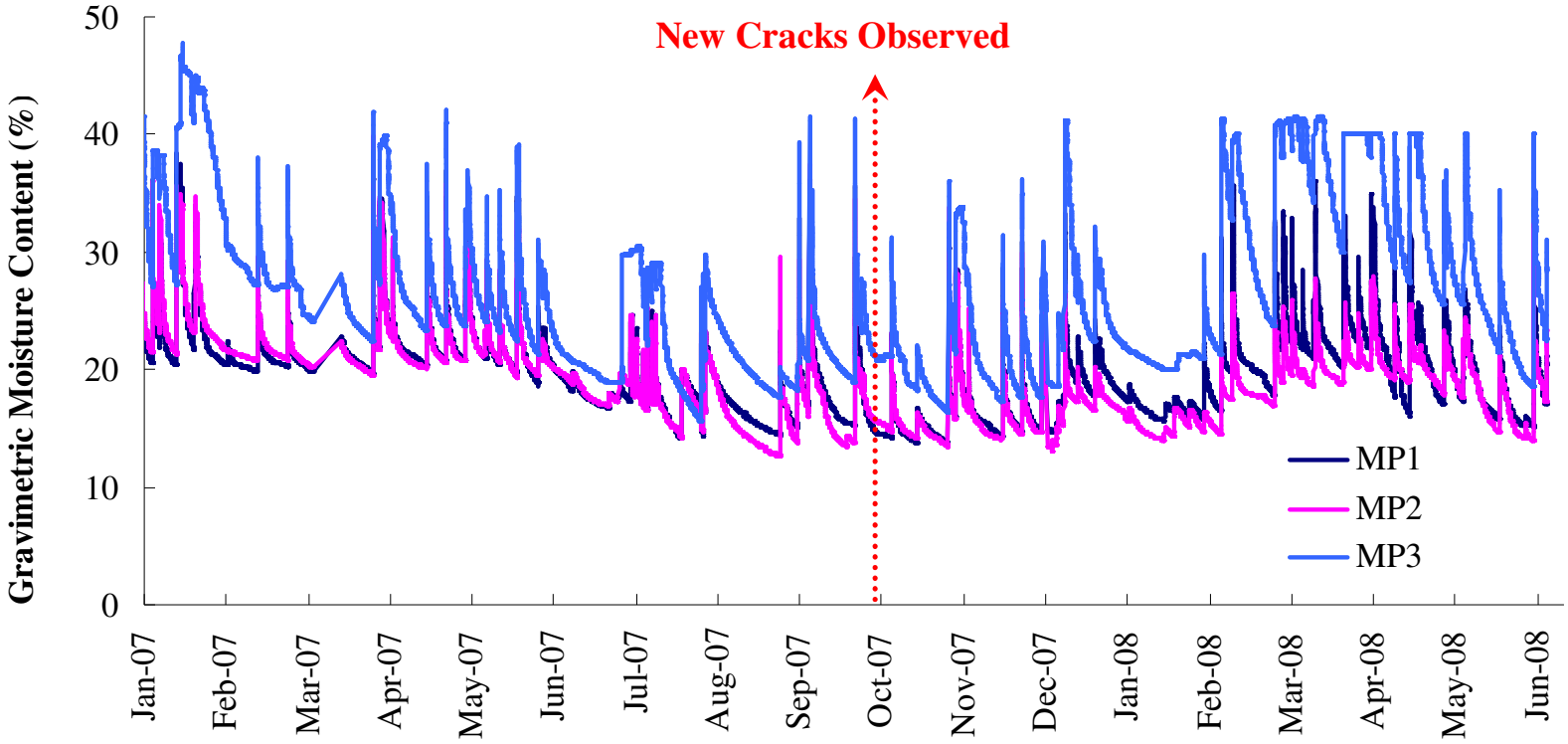

Figure 6.14 Plots of gravimetric moisture contents at Paris site

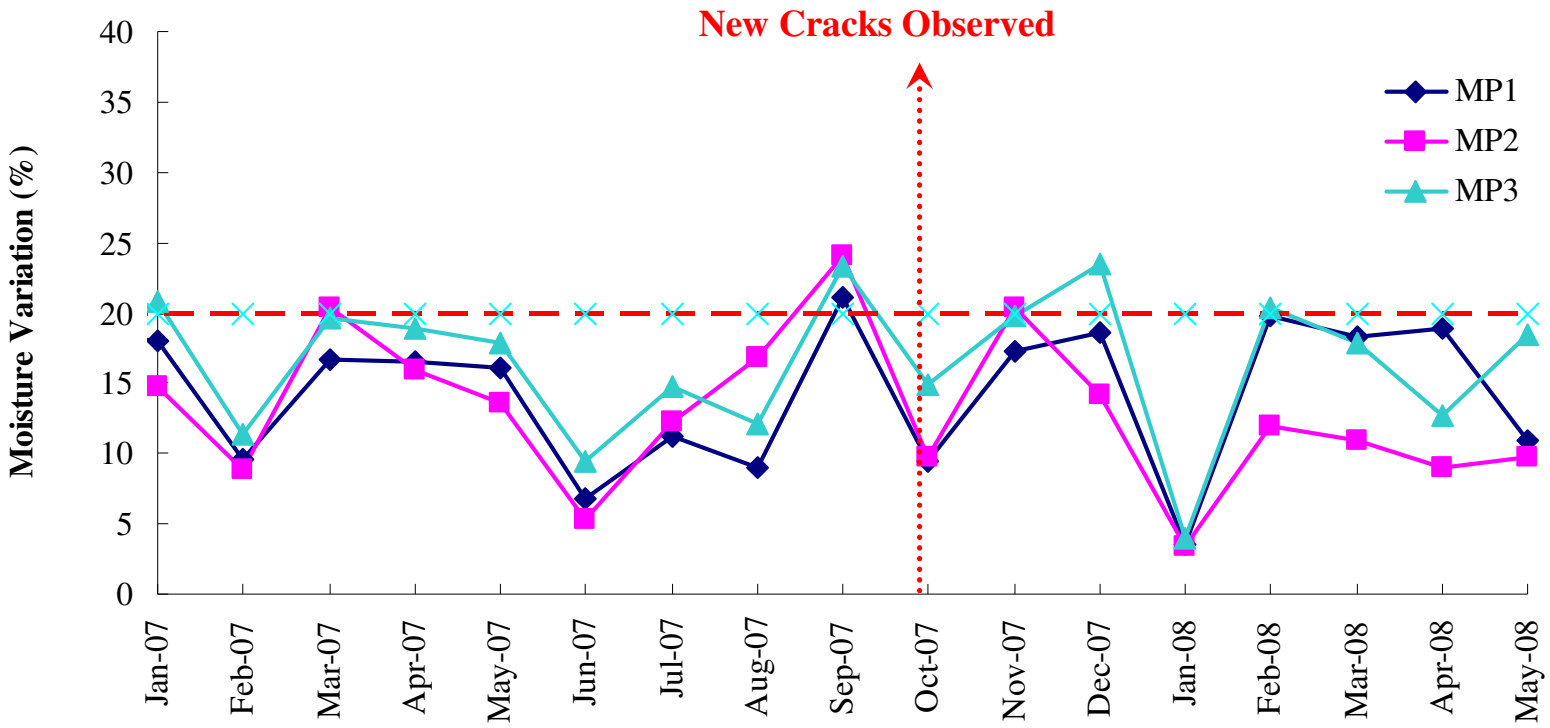

Figure 6.15 Plots of moisture variations at Paris site

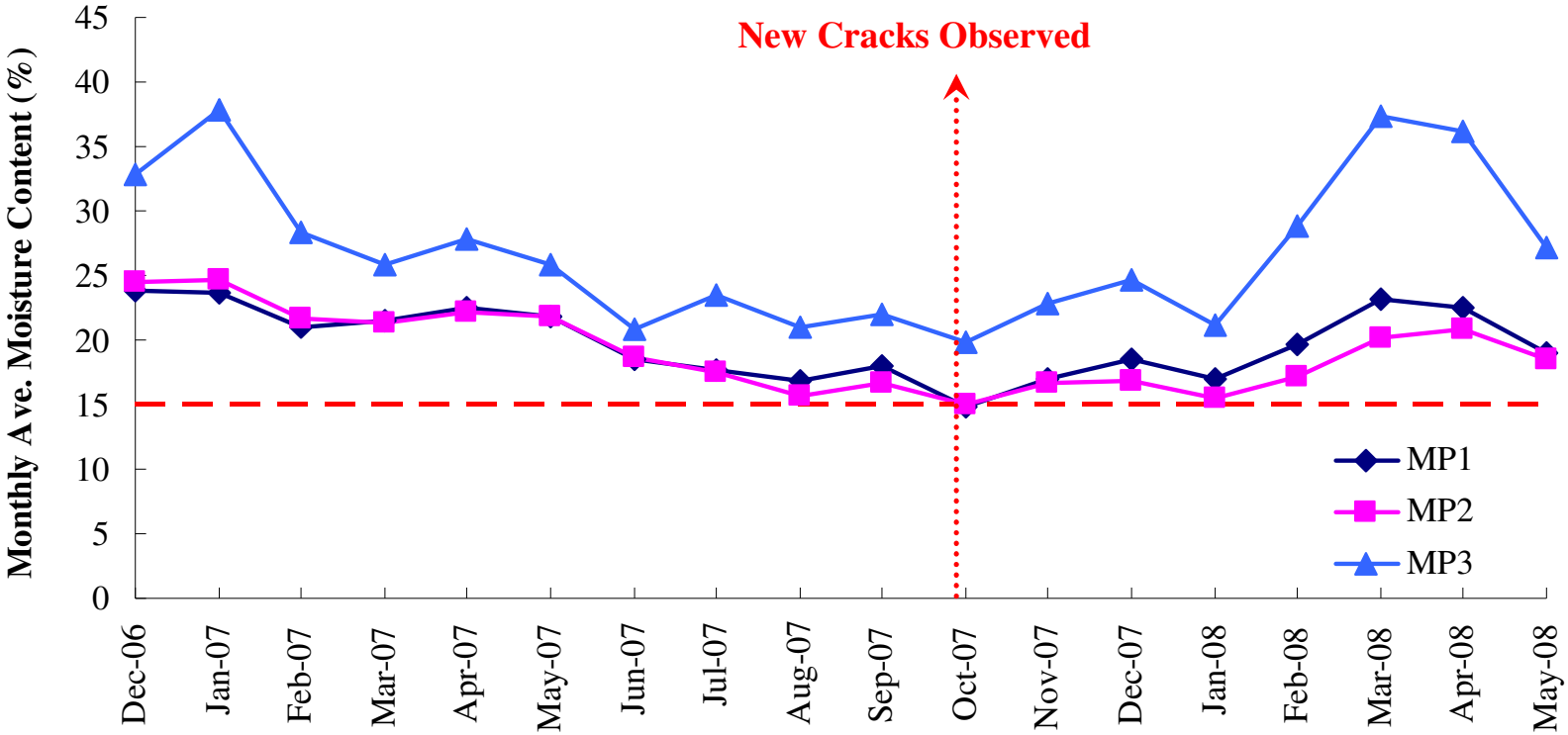

Figure 6.16 Plots of monthly average gravimetric moisture contents at Paris site

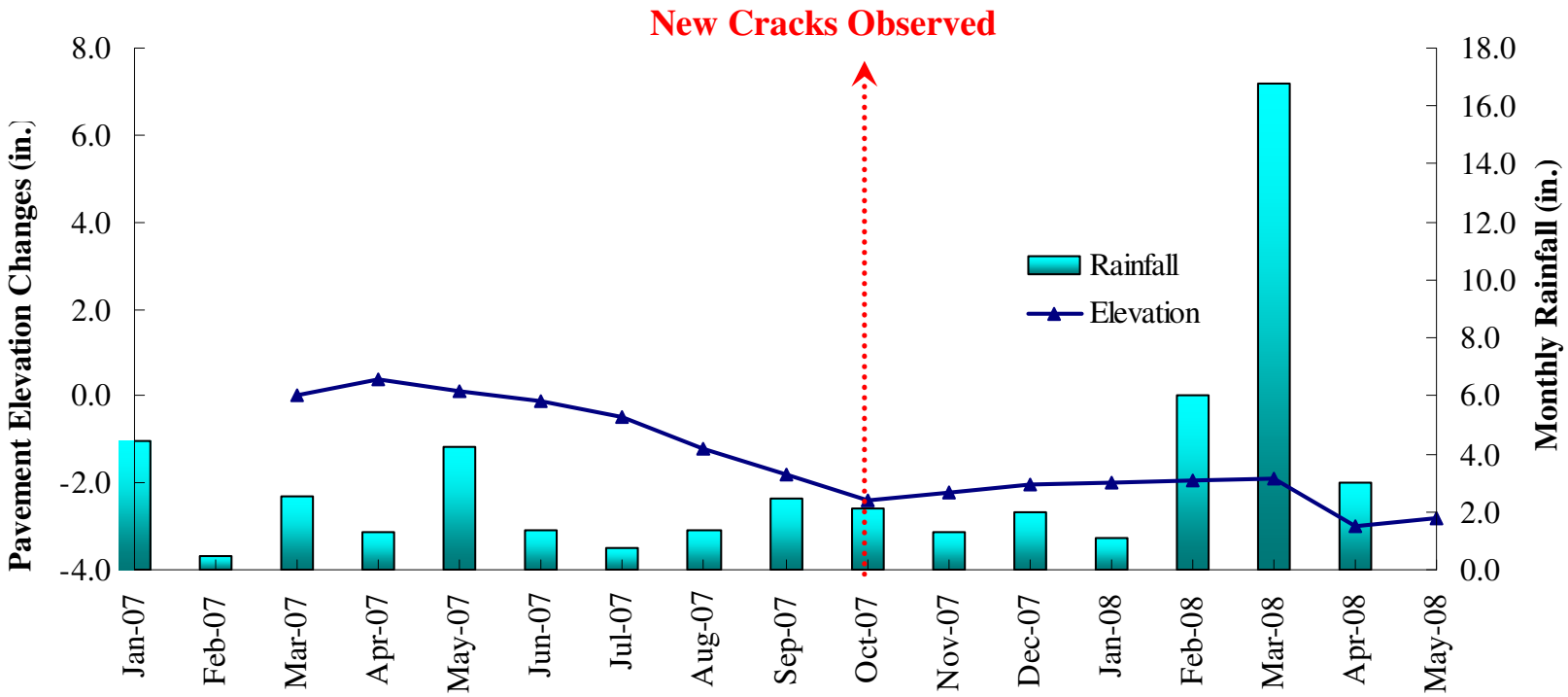

Figure 6.17 Plots of pavement elevation changes and monthly rainfall data at Paris site

From elevation survey data (Figure 6.17), the elevation readings were gradually decreasing on the period of crack initiating indicating shrinkage behavior of the soil. Consequently, the new cracks were showed up.

From Figure 6.14 and 6.16, soil moisture content from MP3 was always highest since MP3 is located at the bottom of the soil slope and also nearest to large trees (Figure 6.18). However, it is interesting to know that soil moistures near MP3 possess not only the highest moisture contents but also the highest rate of moisture changes as well. This can be seen in Figure 6.19, which is presenting the differences in values of MP3 and MP1 (MP3 – MP1) with time period.

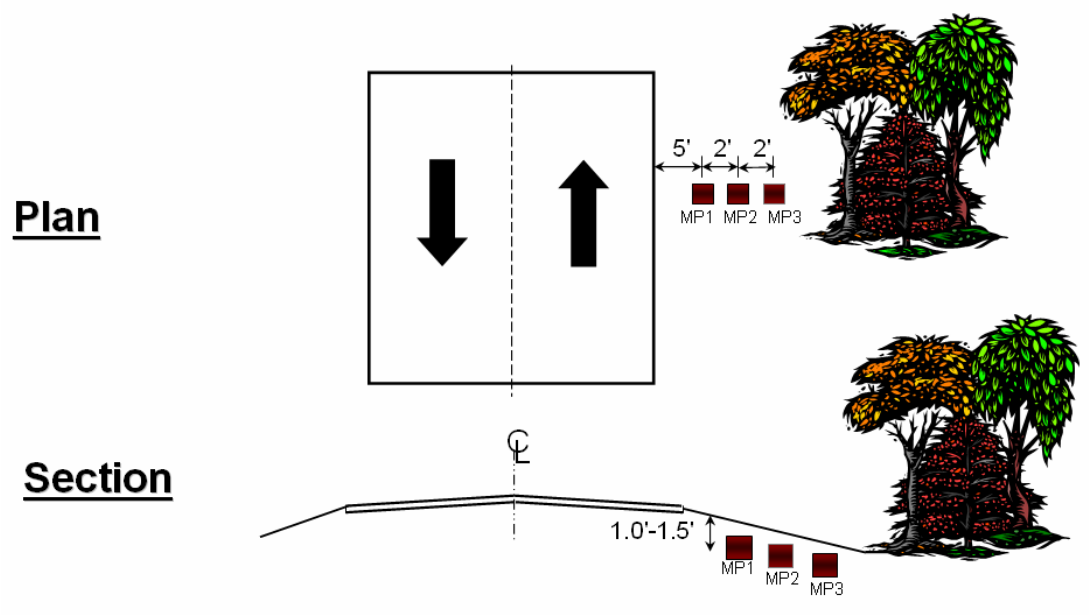

Figure 6.18 Site schematic - Paris site

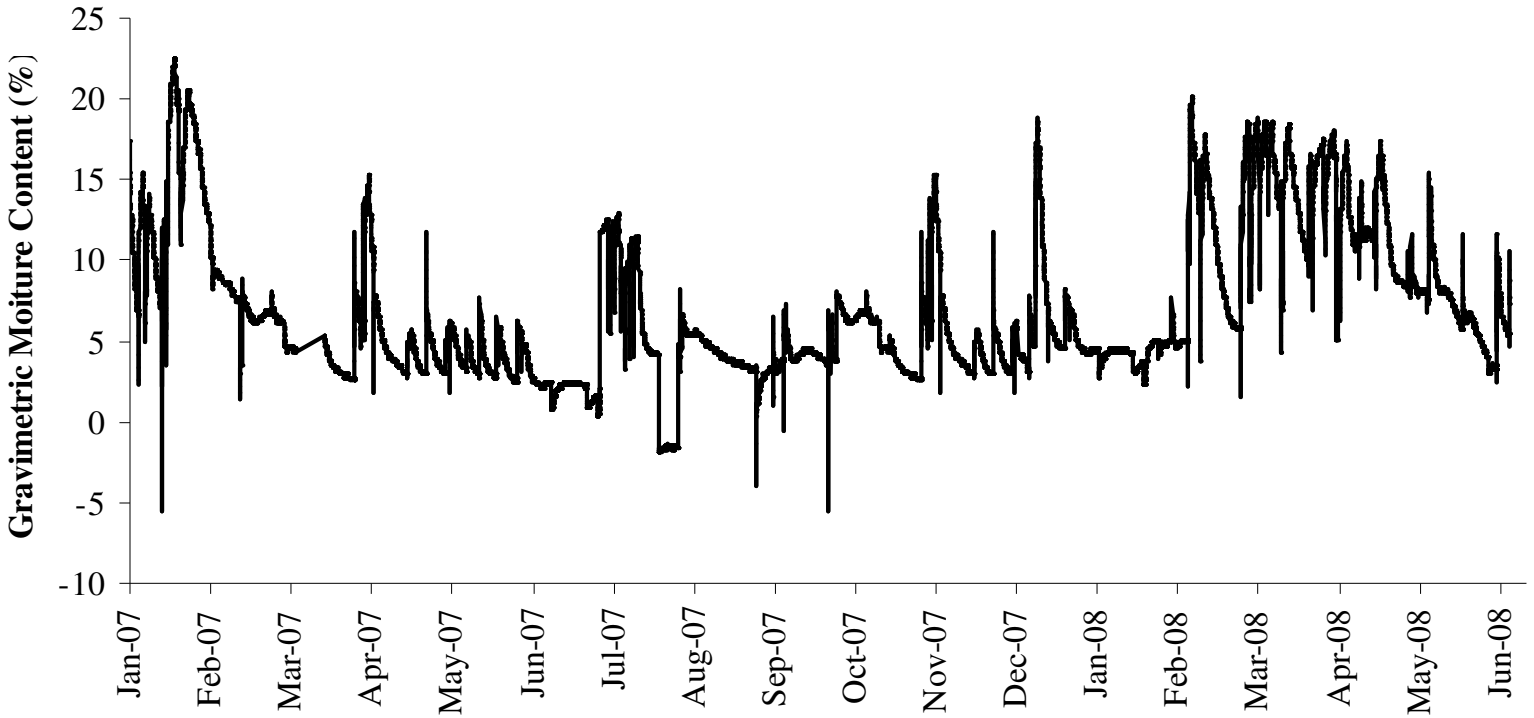

Figure 6.19 Plot of differences of moisture contents of moisture probe (MP) no. 3 and moisture probe no. 1 (MP 3 – MP 1) with time period

From Figure 6.19, the slopes of the graph are mostly negative which denote that MP3 were increasing slower than MP1. Conversely, it can also state that MP 3 readings were decreasing faster than MP 1 readings, which is possible because MP 3 situated near the large trees and tree roots can absorb the moisture in a faster period. It has been reported by many researchers that location of large tree is very critical to the stability of the structures situated on expansive soils since their roots absorb water or moisture and this can result in moisture depletion in the soil which may lead to settlement of soil underneath the structures.

Ward (1953) in the UK recommended safe planting distance of trees to avoid soil shrinkage settlement and damage to buildings. He prescribed the first "proximity rule" of D:H (D is referred distance of structure from the tree and H referred to height of tree) equal to one. In UK in the mid 70's, a severe drought caused much shrinkage settlement and it was realized that a large proportion of the ground movement under footings was related to the drying effects of trees (Cameron et al., 2006).

However, the averaged height of trees at the Paris site and distance from the trees to the existing cracks are about 42 ft. and 38 ft., respectively (see Figure 6.20 and 6.21). As a result, the D/H reading of the Paris site is around 0.9 which is closed to 1.0 as proposed by Ward (1953).

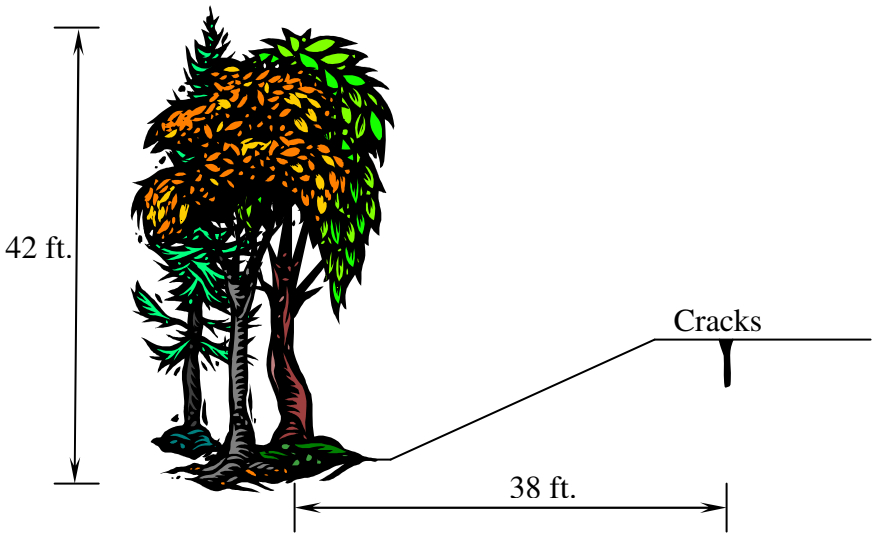

Figure 6.20 Site schematic of location of trees and existing cracks

Figure 6.21 Paris site conditions

Table 6.4 Field matric suction reading at Paris site

Month	Field Matric Suction (kPa)
Mar-07	1,986
Apr-07	1,712
May-07	N/A
Jul-07	N/A
Aug-07	0
Sep-07	2,137
Dec-07	1,932
Mar-08	20
June-08	120

The matric suction readings at this site were quite high on July and December'07 which are 2,137 and 1,932 kPa, respectively. No data available on May and June'07 because the system was damaged by moisture intrusion into the system. It should be noted that by the time of site visit on August'07 and March'08, rainfall was intense and soil slope was almost saturated and hence zero suction readings were measured.

6.2.4 Houston Site

Although there are many longitudinal pavement cracks on this site prior to starting of this field monitoring study, there are no new cracks observed so far at this site since the monitoring. The site was located near Houston close to coastal gulf of Mexico, the weather is usually humid and the rainfall was steady as shown in Figure 6.22 and 6.23.

From Figure 6.23, the monthly average of soil moisture contents from moisture sensor probes no. 1 and 2, showed a steady values while data from probe no. 3 showed about 10-15% higher during the high rainfall intensity period. This was expected as the moisture contents of this probe to be high since this probe was located closer to the drainage ditch.

Figures 6.26 and 6.27 show a schematic of field instrumentation and actual site condition at Houston test site. In general, water from the drainage ditch can propagate to the surrounding soil which can cause soil to swell and lose it's strength thus leading to pavement failure. In this case, since the drainage ditch is about 35 ft. away from the pavement shoulder, the effect of this drainage condition to pavement behavior was not apparent so far. From Figure 6.28, unlike the moisture contents from MP3, soil moisture contents of probes 1 and 2 (MP1 and MP2) were not affected by the location of the drainage ditch. Therefore, it can be concluded that the influence distance of this local drainage ditch can reach only to MP3 which is about 3.7 ft. and 24 ft. vertically and along the slope, respectively (Figure 6.26).

Distance from the source of water not only from capillary raise of the moisture in the ditches, but also moisture ingress due to geometry of the slope as well. Based on the present site conditions, it can be mentioned that both good drainage condition at the site and farther location of the ditch along with relative high humid and rainfall conditions at the site, soil cracking was not highly apparent that may have resulted in the cracking of the pavement shoulders and travel lane section. In future, it would be ideal if more sites with different slopes and distances from the ditch are considered for similar type of monitoring.

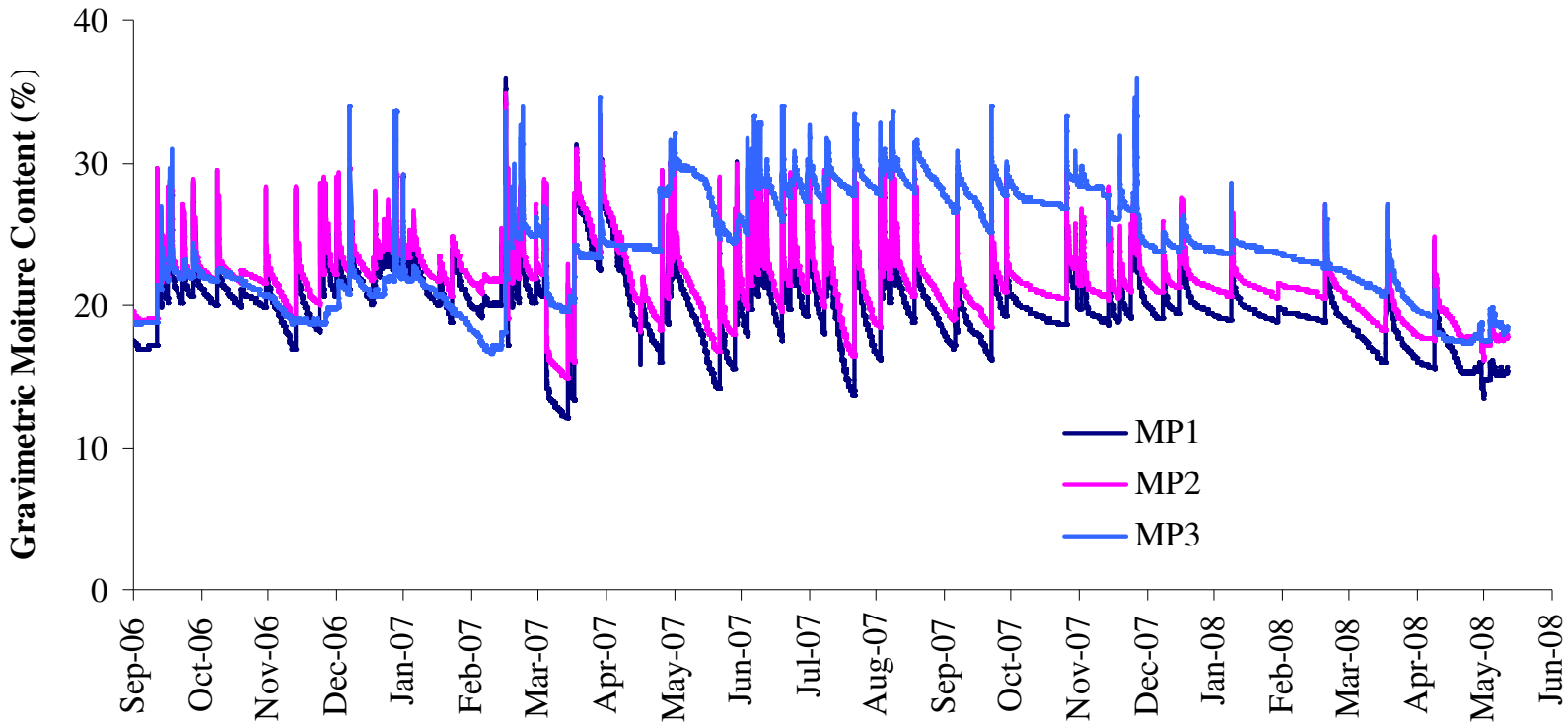

Figure 6.22 Plots of gravimetric moisture contents at Houston site

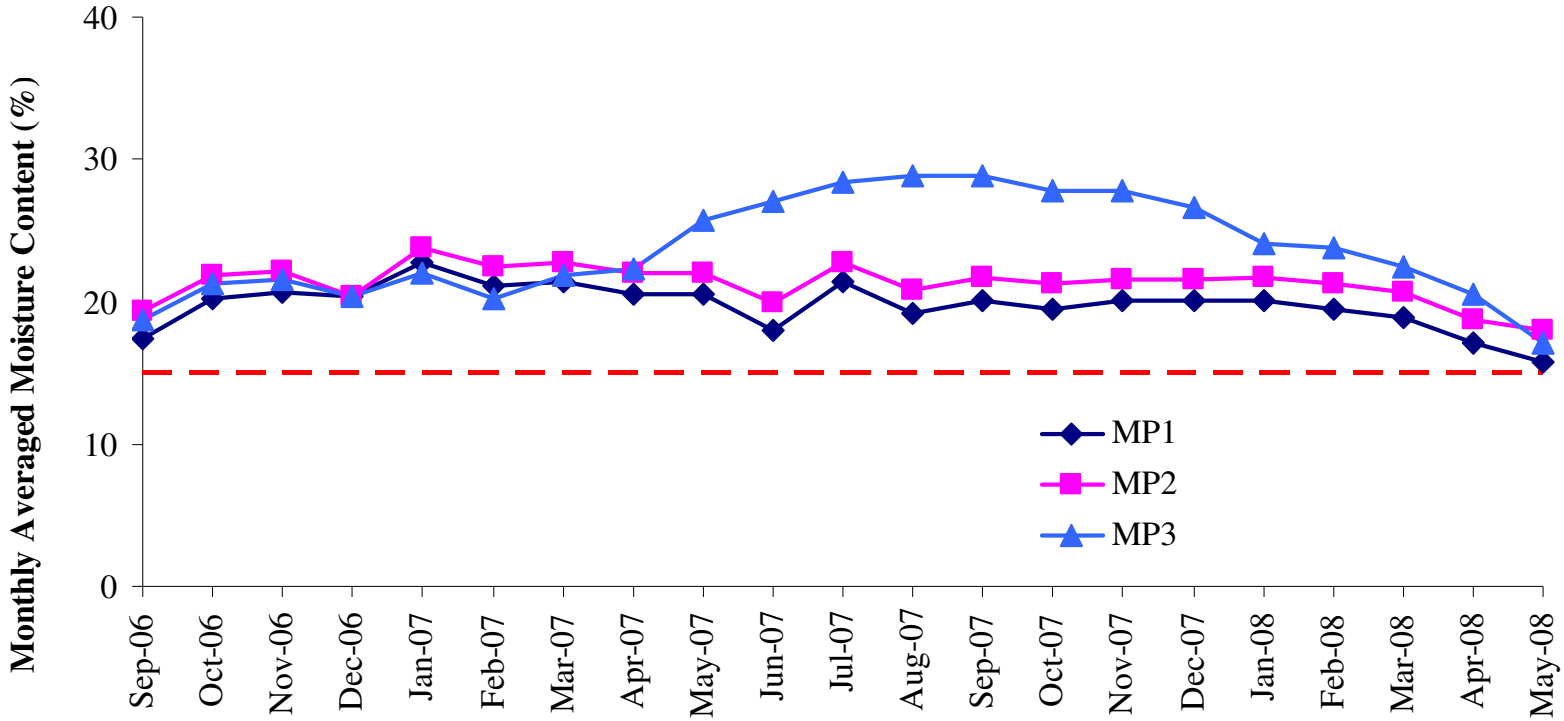

Figure 6.23 Plots of monthly average gravimetric moisture contents at Houston site

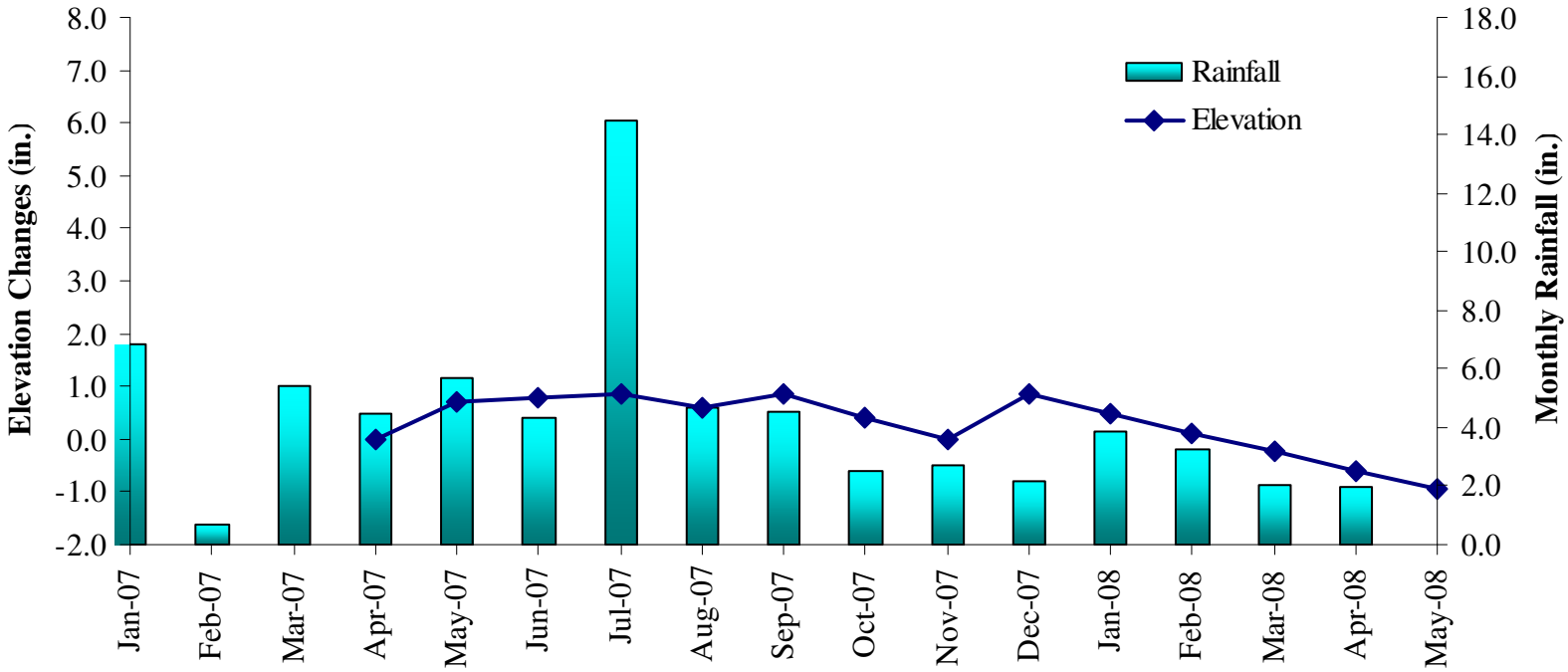

Figure 6.24 Plots of pavement elevation changes and monthly rainfall data at Houston site

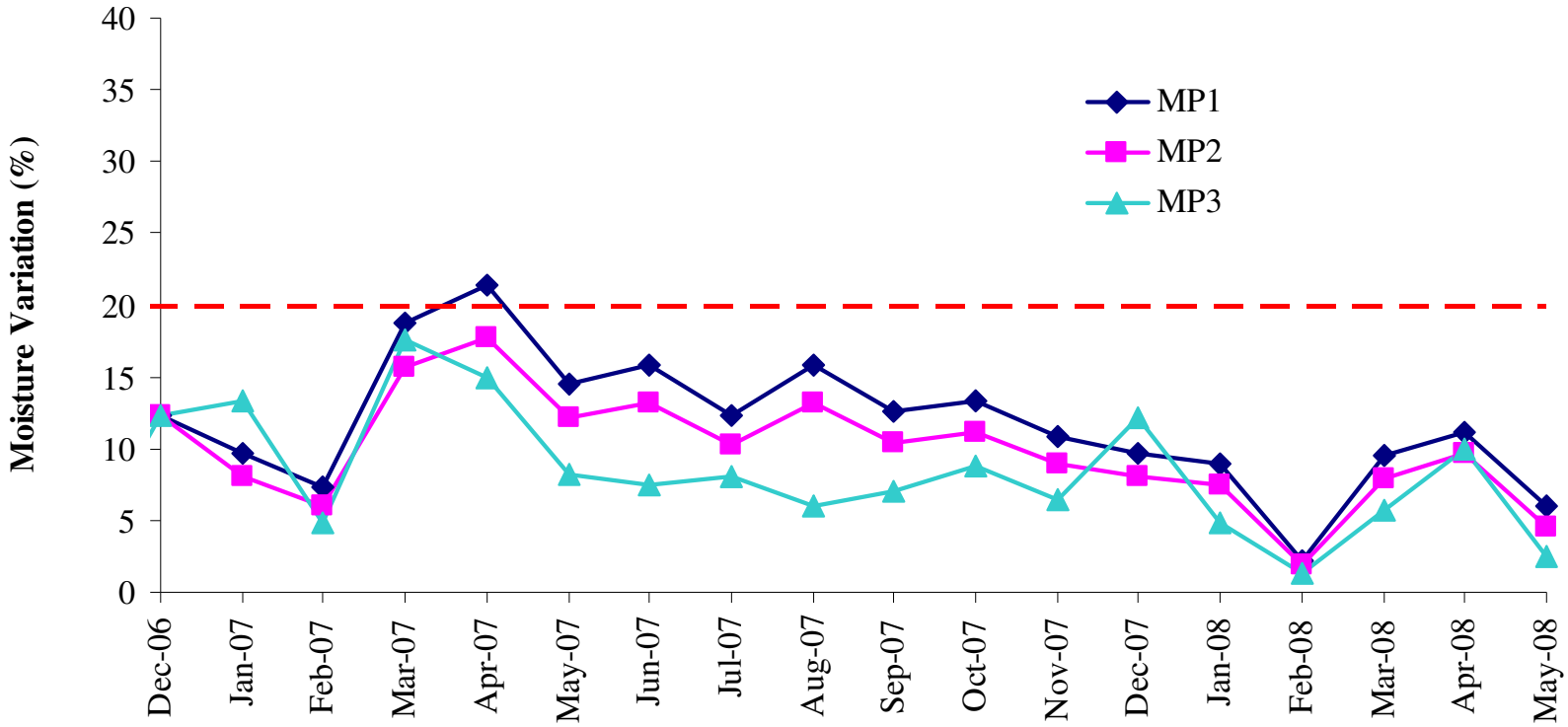

Figure 6.25 Plots of moisture variations at Houston site

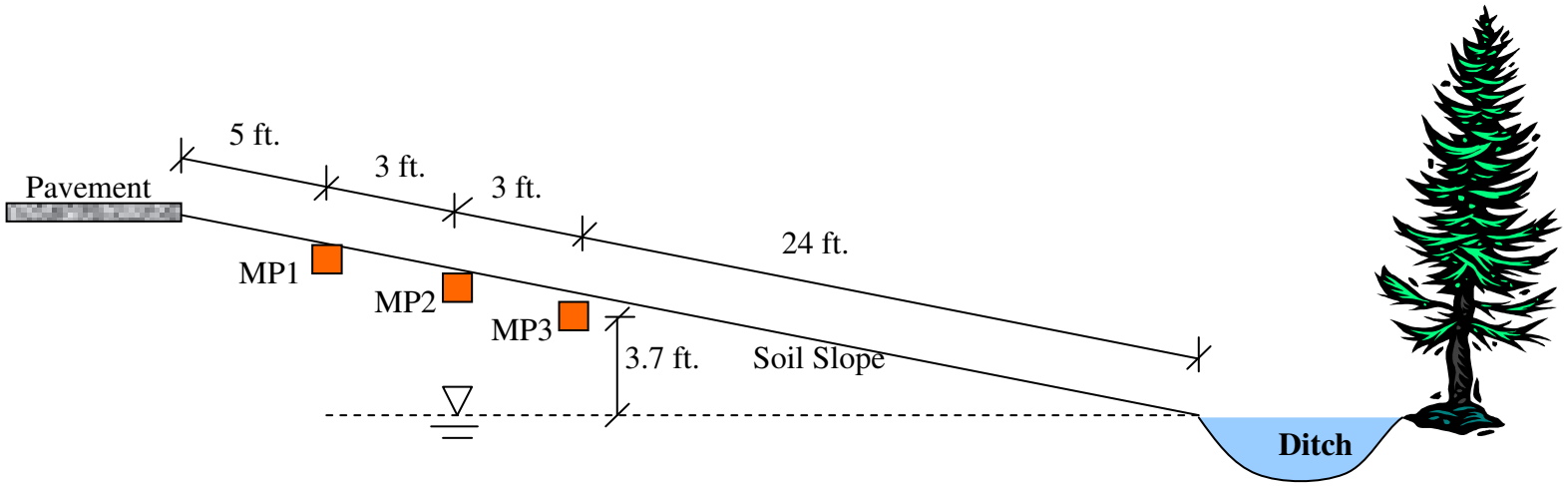

Figure 6.26 Schematic of slope at Houston site

Figure 6.27 Houston site condition (in dry season)

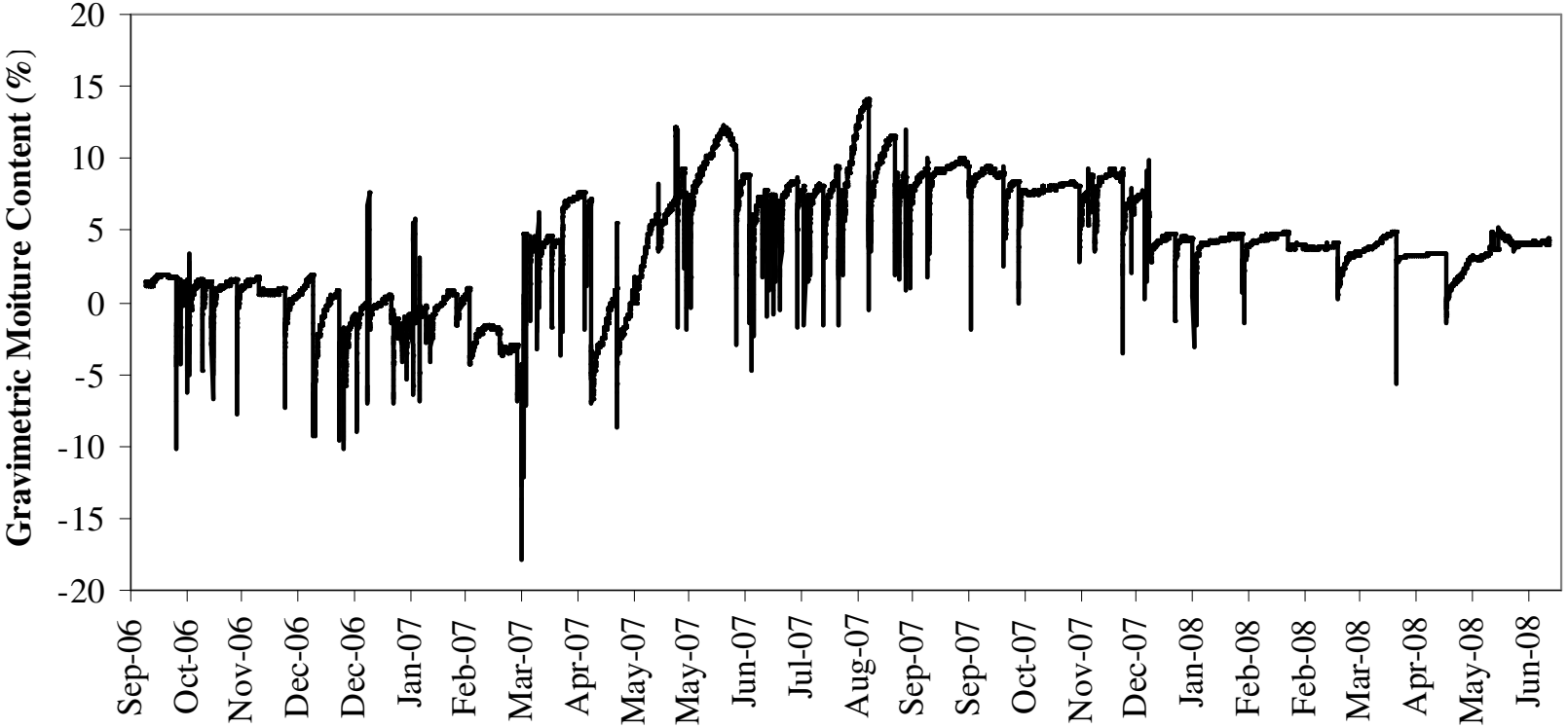

Figure 6.28 Plot of difference of moisture contents of moisture probe (MP) no. 3 and moisture probe no. 1 (MP 3 - MP 1)

Unlike the MP3 readings at Paris site, moisture contents from MP 3 at Houston are steady. Figure 6.12 showed a plot of moisture differences between MP 3 and MP 1 (MP 3 – MP 1). Slopes of the plot are mostly positive which means that MP 3 is increasing faster than MP1. Conversely, it can be mentioned that MP 3 readings decreased slower than MP1 readings which is true because MP 3 situated near the drainage ditch while MP1 located on top of the slope. As a result, the moisture content of MP 3 is more stable than the same from MP 1.

Table 6.5 Field matric suction reading at Houston site

Month	**Field Matric Suction (kPa)**
Apr-07	754
May-07	550
Jul-07	502
Aug-07	551
Sep-07	539
Oct-07	446
Dec-07	474
May-08	N/A
Jun-08	884

Matric suction readings in this site were relatively low since the weather is always humid and the rainfall precipitation is steady along the monitoring period. Since

there are no new cracks observed at the site, it could be mentioned that the moisture data collected so far showed that the site conditions and soils underneath the pavement did not show any major movements that could trigger cracking of pavements in both directions. It is important to understand what might have transpired at these sites that resulted in severe cracking along the test locations prior to the start of this monitoring period.

6.3 Summary

This chapter includes details of field results of all four sites. The results clearly showed that site environment conditions such as large trees and drainage ditch have strong effects on pavement cracking. The effects will be even more exaggerated if the subsoil is expansive in nature.

As mentioned by many researchers, large trees definitely have a strong influence to the propagation of soil moisture since they attract water toward themselves. Consequently, soil lost moisture and hence shrinkage cracking initiated. At Paris site, the ratio of D:H (D is referred distance of structure from the tree and H referred to height of tree) equal to 0.9.

Fort Worth and Paris sites shares the common pavement cracks triggered value which is about 20% for the moisture variation and averaged moisture contents were around or less than 15%. San Antonio site also exhibited cracks after a long dry spell causing averaged moisture content value of about 15% more than 2 months. At Houston site, there is no new crack observed and soil moisture contents were quite steady. The local drainage ditch affected the surrounding soil moisture contents but only for a

certain distance. For Houston site, the effected distance is about 3.7 ft. in vertical direction and 24 ft. in horizontal direction. Summary of the field observations are presented here in Table 6.6 below.

From Table 6.6, it can be concluded that

1. New cracks can be generated under 2 conditions;
   - Moisture variation more than 20% and Monthly mean moisture contents less than 15% at least a month. The type of condition was revealed at Fort Worth and Paris Site.
   - Monthly mean moisture contents are less than 15% for more than 2 months. This condition was presented at San Antonio site.

2. Although moisture variation is more than 20%, new cracks might not be observed if mean moisture are more than 22% as seen in Houston site.

3. Since the collected field matric suctions were not continuous data, the matric suctions corresponding to particular moisture contents might are difficult to correlate. However, in Chapter 5, Soil Water Characteristic Curves (SWCCs) showed good matches with the measured matric suction from the FTC sensors (after applied shift corrections). As a result, the matric suction corresponding to 15 % moisture content can also be reasonably estimated by SWCC results (Figure 3.13 to 3.16) from Chapter 3. The soil matric suctions presented in the Table 6.7 shows quite high values indicating high potential of soil volume changes.

Table 6.6 Summary of field observations

Sites	**Site Features**	**New Cracks**	**Rainfall**	**Monthly Mean Moisture Content less than 15%**	**Moisture Variation* more than 20%**	**Month that New Cracks Observed**
Fort Worth	Farmlands, Sloped Terrain	Yes	Sporadic Rainfall	Aug'07 to Nov'07	Aug'07 to Oct'07	Sept'07
San Antonio	Farmlands, Flat Terrain	Yes	Long Dry Spells	Sept'07 to March '08	-	Nov'07
Paris	Large Trees, Sloped terrain	Yes	Steady Rainfall	Aug'07, Sept'07, Oct'07, Jan'08	Sept'07,Nov'07, Dec'07,Feb'08	Sept'07
Houston	Poor Drainage Ditch, Sloped terrain	No	Steady Rainfall	April' 07	-	-

Table 6.7 Matric suctions values corresponding to 15% moisture content (based on SWCCs)

Soil Types	**Matric suction corresponding to 15% moisture content (kPa)**
Fort Worth	7,300
San Antonio	11,500
Paris	11,300
Houston	4,050

CHAPTER 7

SWELL PREDICTION AND NUMERICAL MODELS OF SOIL MOVEMENTS IN THE FIELD

7.1 Introduction

Numerous researchers proposed different swell prediction models in order to indicate amount of soil movements and severity of soil conditions. In this chapter, analytical models of vertical swell prediction models developed by Snethen et al. (1977), Hamberg (1985), PVR Method developed by McDowell (1956), and Lytton et al. (2004), and a numerical model utilizing Finite Element Method (FEM) were investigated and compared with the results from both in the field and laboratory to evaluate model's validations.

7.2 Soil Swelling Strains Based on Field and Laboratory Results

7.2.1 Soil Swelling Strains Based on Field Results

The swelling strains from the field test sections are estimated from the maximum elevation changes observed over the entire monitoring period divided by assumed active depth of 6 ft. of subsoil. Some of these assumptions are needed and they are not farther from reality as active depths of the sites vary from 3 to 10 ft. Hence an average depth of 6 ft is considered reasonable.

Figure 7.1 shows example of the maximum difference of elevation changes that observed in the field. This number will be used to calculate the total soil vertical strain

(%) which will be compared with various swell prediction models later on in this chapter.

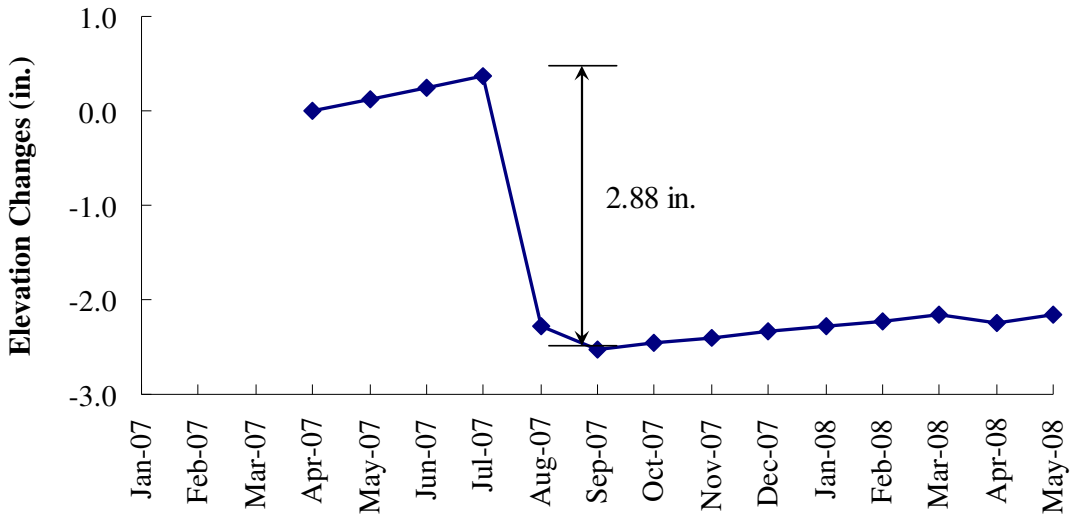

Figure 7.1 Plot of elevation changes in San Antonio site

7.2.2 Soil Swelling Strains Based on Laboratory Results

According to soil swell and shrinkage empirical correlations (as shown in Figure 4.13 and 4.14 in chapter 4) based on laboratory results, vertical soil movements in laboratory environment can be readily calculated from amount of moisture changes as defined by the equations below:

$$\varepsilon_{swell,\ vert} = 0.36\Delta w \quad (1)$$

$$\varepsilon_{shrink,\ vert} = 0.23\Delta w \quad (2)$$

In order to compare with field vertical soil movement, a range of soil moisture changes (Δw) in the field were used to estimate the vertical soil movement values. The result of the estimated soil movements and field moisture contents are presented in Table 7.1. Since the initial and final soil moisture in the field were assumed to be in

optimum moisture and saturation state, respectively, only equation (1) was required. The total movements were presented in the table below.

Table 7.1 Soil swelling movements results from the laboratory empirical correlations

	Fort Worth	**San Antonio**	**Paris**	**Houston**
Optimum Moisture Content (%)	24.0	21.7	23.0	20.0
Saturated Moisture Content (%)	43.3	43.0	43.3	35
Estimated Swell Movement (%)	6.9	7.7	7.3	5.4

7.3 Analytical Field Swelling Prediction Models

Four different models proposed by the past researchers were briefly reviewed and evaluated in this section. All of the selected models take soil matric suction parameters into account except for PVR method. Although, PVR method does not consider soil suction, it is worth investigating since it is regularly used by Texas Department of Transportation (TxDOT) to evaluate swell potential of soil in Texas area.

7.3.1 Snethen's Model (1977)

Snethen et al. (1977) proposed the following equation to predict potential heave of the expansive clay:

$$\frac{\Delta H}{H} = \frac{C_\tau}{1+e_0}\left[\left(A - Bw_0\right) - \log\left(\tau_{mf} + \alpha\sigma_f\right)\right] \qquad (3)$$

Where

H = stratum thickness (ft);

C_τ = suction index, $C_\tau = \frac{\alpha G_s}{100B}$

G_s = specific gravity

e_0 = initial void ratio;

w_0 = initial moisture content (%)

τ_{mf} = final matrix soil suction (tsf)

α = compressibility factor. In the absence of measured data, α can be roughly estimated from the PI by: $PI < 5, \alpha = 0;$

$$PI > 40, \alpha = 1;$$

$$5 < PI < 40, \alpha = 0.0275PI - 0.125$$

σ = final applied pressure (overburden plus external load) (tsf)

A, B = constants of matric suction vs. water content relationship, in the absence of

measured data,

A and B can be estimated using following equations (Lytton et al., 2004):

$$A = 5.622 + 0.0041(\%FineClay) \quad (4)$$

$$B = \left| -20.29 + 0.1555(LL) - 0.117(PI) + 0.0684(\%\#200) \right| \quad (5)$$

7.3.2 Hamberg's Model (1985)

Hamberg (1985) evaluated available testing procedures for characterizing expansive soils. He developed a method for predicting total heave on specified sites with shallow depth moisture changes and light structural loading. The relationships are in the form of the following equations:

$$\Delta H = \sum_{i=1}^{n} \left[\frac{H_i}{(1+e_0)} \right] \cdot \left(C_h \cdot \Delta \log h \right)_i \quad (6)$$

$$\Delta H = \sum_{i=1}^{n} \left[\frac{H_i}{(1+e_0)} \right] \cdot \left(C_w \cdot \Delta w \right)_i \quad (7)$$

Where

ΔH = vertical movement;

N = number of layers to depth of active zone;

H_i = thickness of layer i;

e_0 = initial void ration of layer i;

C_h = suction index with respect to void ratio (slope of void ratio verses soil suction in logarithmic scale)

h = soil suction (total or matric)

C_w = modulus ratio (slope of void ratio versus water content)

Δw = change in water content

This prediction methodology is based on the following assumptions (Hamberg, 1985).

1. Volume changes are controlled primarily by changes in soil suction stresses in the surficial, “active zone” of the soil profile.

2. Overburden and light structural loads have a small influence on the response of the soil to suction changes.

3. Volume changes of the soil structure (represented by volumetric strain or by change in void ratio) and associated changes in water content are directly proportional to the suction stress changes in the range of field suction variation.

4. The void ratio and water content in suction indexes for wetting are equal to the suction indexes for drying.

5. Volume changes are the same in terms of either matric or total suction values.

7.3.3 Potential Vertical Rise (PVR)

The potential vertical rise method (PVR) is widely used in Texas for the estimation of volume change behavior of expansive soils. The PVR is the latent or potential ability of a soil material to swell at a given density, moisture, and loading condition, when exposed to capillary or surface water, and thereby increase the elevation of its upper surface, along with any structure resting on it. This method is introduced by McDowell (1956).

The potential heave of each soil stratum is estimated from a family of curves using the LL, PI, surcharge pressure on the soil stratum, and initial water content. The initial water content is compared with maximum (0.47LL + 2) and minimum (0.2LL + 9) water contests to evaluate the percent volumetric change (Figure 7.2). The PVR of each stratum is determined from a chart using the percent volumetric change and the unit load bearing given in kPa (Figure 7.3).

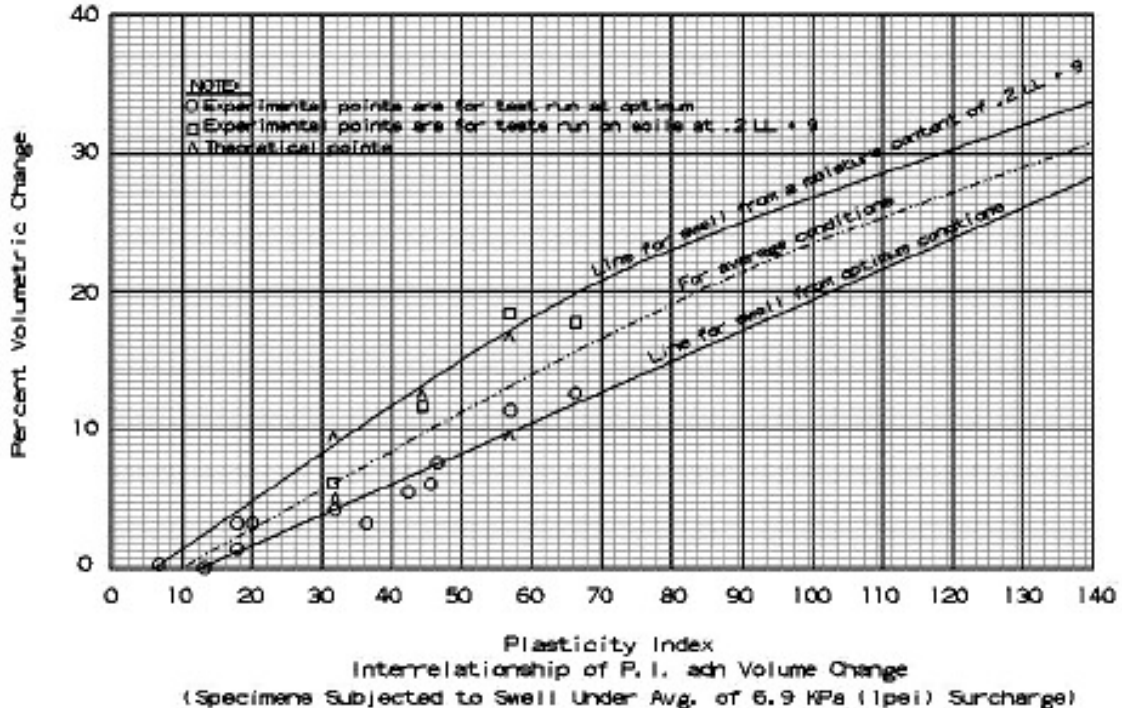

Figure 7.2 Interrelationship of PI and volume change

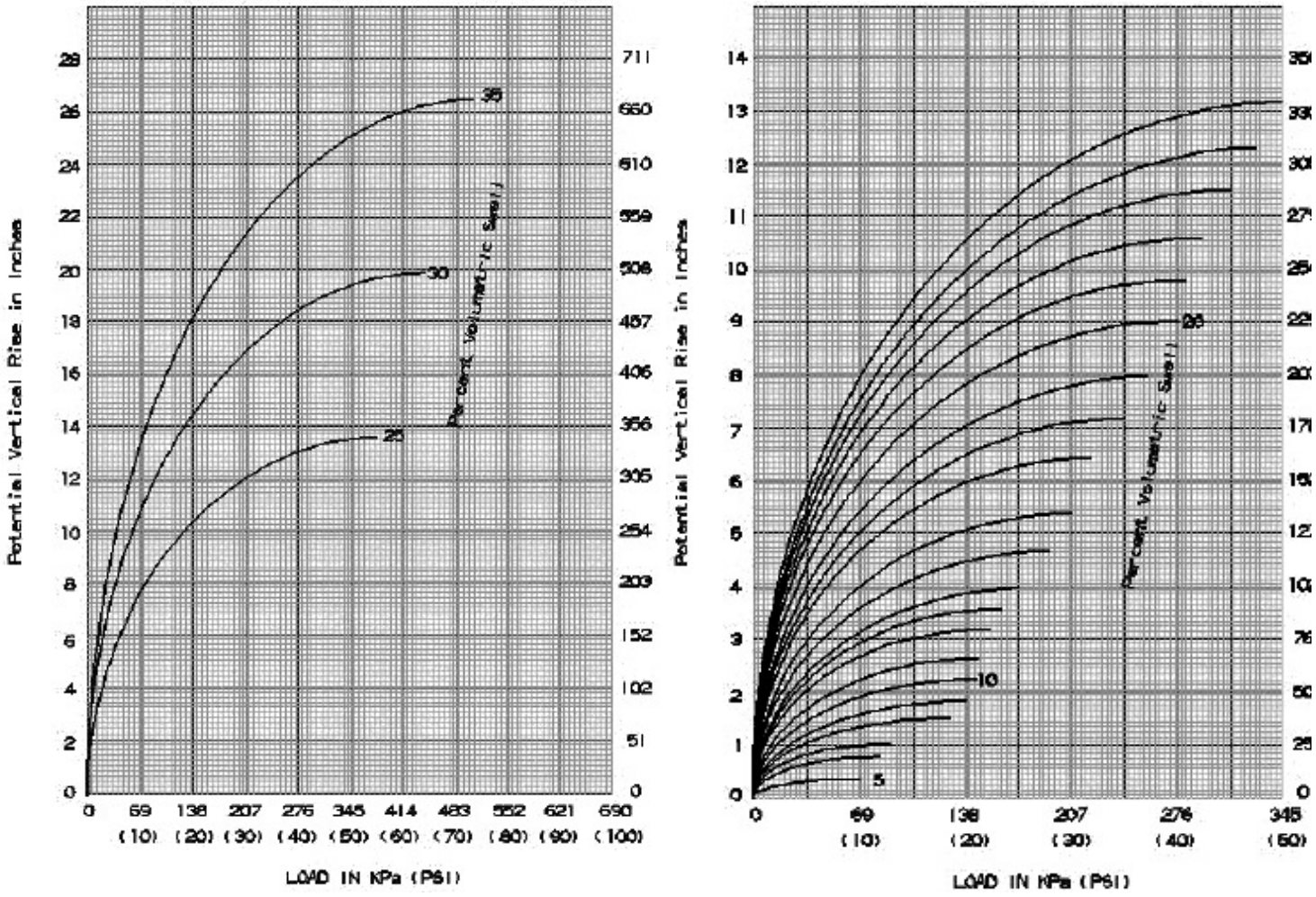

Figure 7.3 Relationships of load and potential vertical rise (PVR)

Summary of assumptions used in PVR modeling are listed by Lytton (2004) and these are:

1. Soil at all depths has access to water in capillary moisture conditions. In reality, the soil at each depth does not possess the same access to water. Mitchell (1984) showed how alpha diffusion coefficient value can be used to predict the transient changes of suction beneath a covered area like a pavement or a foundation. The determination of the alpha diffusion coefficient permits an estimate of the rate at which water will move into the soil both vertically and horizontally. It is also used to estimate the depth of the moisture active zone.

2. Vertical swelling strain is one-third of the volume change at all depths: Analysis of test results in this study shows that the ratio of vertical swelling strain and volumetric swell strain is about a half, which is not one-third as assumed by this method. Moreover, at greater depths, the ratio can also be different for each depth due to the effect of overburden pressures.

3. Remolded and compacted soils adequately represent soils in the field: Lytton et al. (2004) indicated that, from actual observation, the volume change characteristics of undisturbed soils are distinctively different than the remolded and compacted soils used by McDowell in developing his method. There is a very large database of such characteristics for over 100,000 soil samples from all over the United States that was developed over the last three decades by the U.S. Department of Agriculture's Natural Resources Conservation Service. A set of volume change coefficient charts was developed from this database and report by Covar and Lytton (2001). The data are for

undisturbed clods of soil taken from the ground and tested in their natural state with all of the cracks, roots, and wormholes as occur in the field. Those data indicated the different volume change values for remolded and undisturbed samples.

4. PVR of 0.5 inch produces unsatisfactory riding quality. Lytton et al. (1993) developed a way to both measure and predict the maximum bump height on the pavement that was based on the thousands of pavement profile data points that were collected and analyzed in the monitoring process. Both the measured and predicted bump height for serviceability indexes between 2.5 and 4.0 was in the range between 0.5 and 1.0 inch (12 to 25 mm) for all pavements (Jayatilaka et al., 1993). As a result, a bump is not the total movement, such as PVR, but instead is a differential movement and it is this movement that causes pavement roughness.

5. Volume change can be predicted by the use of plasticity index alone: Numerous researches (as shown in the previous models) have proved that in order to accurately predicted soil volume change, several variables are required for better characterized the swell potential for example soil suction, initial moisture content, initial and final void ratio, percentage of clay and clay mineral contents, etc.

Lytton et al. (2004) also stated that PVR method is an overly conservative estimation of swell potentials for low plasticity soils and underestimations for high PI soils.

7.3.4 Lytton's Model (2004)

Lytton et al. (2004) developed a procedure to determine the swell potentials based on suction measurements and diffusion models of soils with various scenarios. The Thornthwaite moisture index, which is derived from the moisture balance procedure developed between rainfall and evapotranspiration (Thornthwaite, 1948), can be used to characterize climatic effects. Also, Lytton et al. (2004) procedure accounts for other parameters, including topography and presence of localized water sources.

$$\frac{\Delta H}{H} = f\left(\frac{\Delta V}{V}\right) \tag{8}$$

Where

$\frac{\Delta H}{H}$ = vertical strain

f = the crack fabric factor, can be calculated as 0.67-0.33ΔpF ($1/3 \leq f \leq 1.0$)

$$\Delta H = \sum_{i=1}^{n} f\left(\frac{\Delta V}{V}\right)_i \cdot \Delta z_i \tag{9}$$

Where

Δz_i = the i^{th} depth increment

N = number of layers to depth of active zone

$$\left(\frac{\Delta V}{V}\right) = -\gamma_h \log\left(\frac{h_f}{h_i}\right) - \gamma_\sigma \log\left(\frac{\sigma_f}{\sigma_i}\right) \tag{10}$$

Where

ΔV = volume change;

V = initial volume;

γ_h = suction compression index (volume change coefficient);

h_i , h_f = initial and final suction;

γ_σ = compressibility constant (mean principal stress compression index)

σ_i , σ_f = initial and final mean principal stress

The suction index can be expressed as: $\gamma_h = -\dfrac{\Delta V / V_i}{\log \dfrac{h_f}{h_i}}$ (11)

Although Lytton's method is considered as a better method compared to current PVR method, it is still limited by a few problems and concerns. The influences or impacts of various boundary conditions on swell property variations require more investigation. This method also uses several empirical relationships with different degrees of coefficient of correlation. Such practice can lead to compounding of errors, which may limit the practicality of such expressions for routine use. Once it is thoroughly evaluated and modified, if necessary, this suction based method can be confidently used for estimating swell properties of site soils in the design of pavements.

7.3.5 Analytical Field Swelling Prediction Results

In order to compare between each swell prediction models, a soil stratum is needed to be assumed. In this case, all four subgrade soils which are soils from Fort Worth, San Antonio, Paris and Houston possess a six-foot depth of homogeneous active soil layer. In order to acquire the field swell prediction results, various laboratory soil parameters presented in chapter 4 were necessary. The initial and final moisture contents were assumed at optimum and saturation states, respectively. The results of the field swell prediction models are presented in Table 7.2.

Table 7.2 Swell strains (%) from four different prediction models

Soil Locations	Swell Prediction Strains (%)			
	Snethen	Hamberg & Miller	PVR	Lytton
Fort Worth	0.54	2.56	2.25	4.41
San Antonio	0.55	2.42	2.25	4.97
Paris	0.58	2.41	2.25	5.48
Houston	0.48	2.28	2.01	3.39

From Table 7.2, it can be mentioned that low to high swell strain predictions are obtained from Snethen, PVR, Hamberg and Lytton models, respectively. The swell predictions from PVR model show almost the same values for Fort Worth, San Antonio and Paris soils. This is because the PVR method depends on PI values and since these soils exhibit almost identical PI values, the interpreted PVR predictions are similar in magnitudes. Surprisingly, the PVR model which depends on Plasticity Index and Hamberg model which relies on initial void ratio and soil suction changes provide similar results for all four soils.

7.4 Numerical Swell Prediction Model Using FEM

Finite Element Method (FEM) have been successfully utilized to account for the effects of many practical conditions more realistically than theoretical solutions based on infinite slab and other idealized assumptions (Kuo, C. and Huang, C., 2006). With the introduction of three-dimensional (3D) ABAQUS software and all the promising

features, and results reported in the literature, several applications including in the areas of pavement engineering have been successfully modeled (Hammons 1998; Kim and Hjelmstad 2000).

In the swell related issues involving partially saturated soils, various complicated soil behaviors involving soil matric suction changes, volume changes of soils due to moisture fluctuations, and soil strength aspects are needed. The analysis is even more challenging when simulation involves multi-soil layer system.

The commercial software, ABAQUS® has numerous useful built-in models that are closely related to shrinking and swelling of expansive soils based on moisture changes. The models used in this study are composed of linearly elastic, moisture swelling and sorption models which require some of the experimental data presented in Chapter 3. Details of the model simulation are presented as the following.

7.4.1 Element Types

The typical three-dimensional element types C3D8R and C3D8P, which are continuum stress/displacement, three-dimensional, linear hexahedron element types with no pore pressure allowed and with pore pressure allowed, respectively, were assigned in this model for modeling asphalt pavement and soil materials (see Table 7.3). Figure 7.4 shows a mesh element discretization of the pavement section. Since, in the analysis, the section is symmetrical in all directions, only a quarter of the full test pavement section was analyzed (Figure 7.5)

Table 7.3 General input data

Element Layers	Material Types	Element Types	Thickness (in.)
Top Layer	Asphalt	C3D8R	4.0
Middle Layer	Base Course	C3D8R	8.0
Bottom Layer	Subgrade Course	C3D8P	72.0

7.4.2 Boundaries Conditions

As shown in Figure 7.5, the bottom of the section is fixed in all direction whereas the surface elements on the longer sides are fixed only in x-direction and the ones on the shorter side are fixed only in y-direction. The model was simulated hereby allowing moisture flow from both sides (shoulders) of the pavement.

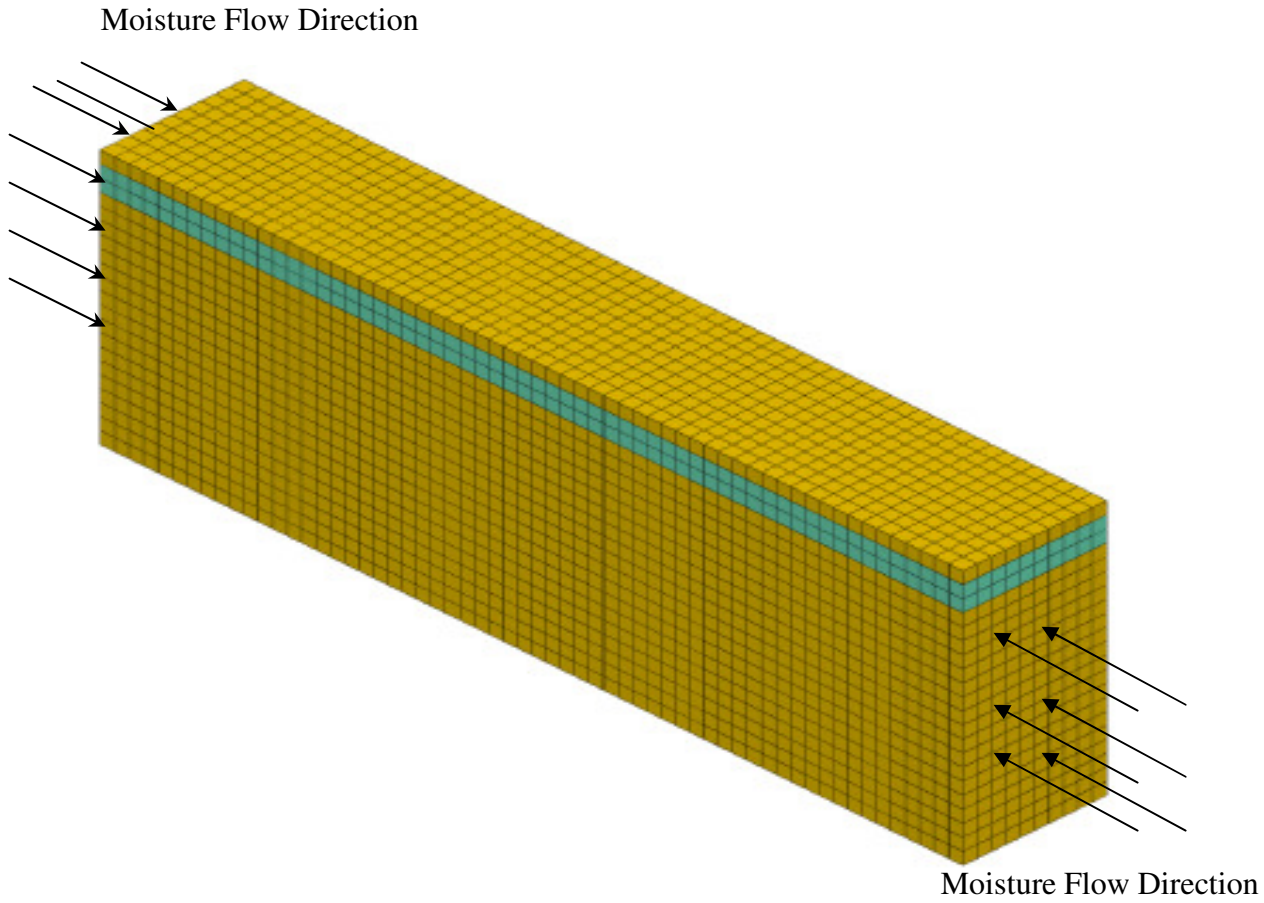

Figure 7.4 Full section of meshed elements with moisture flow direction

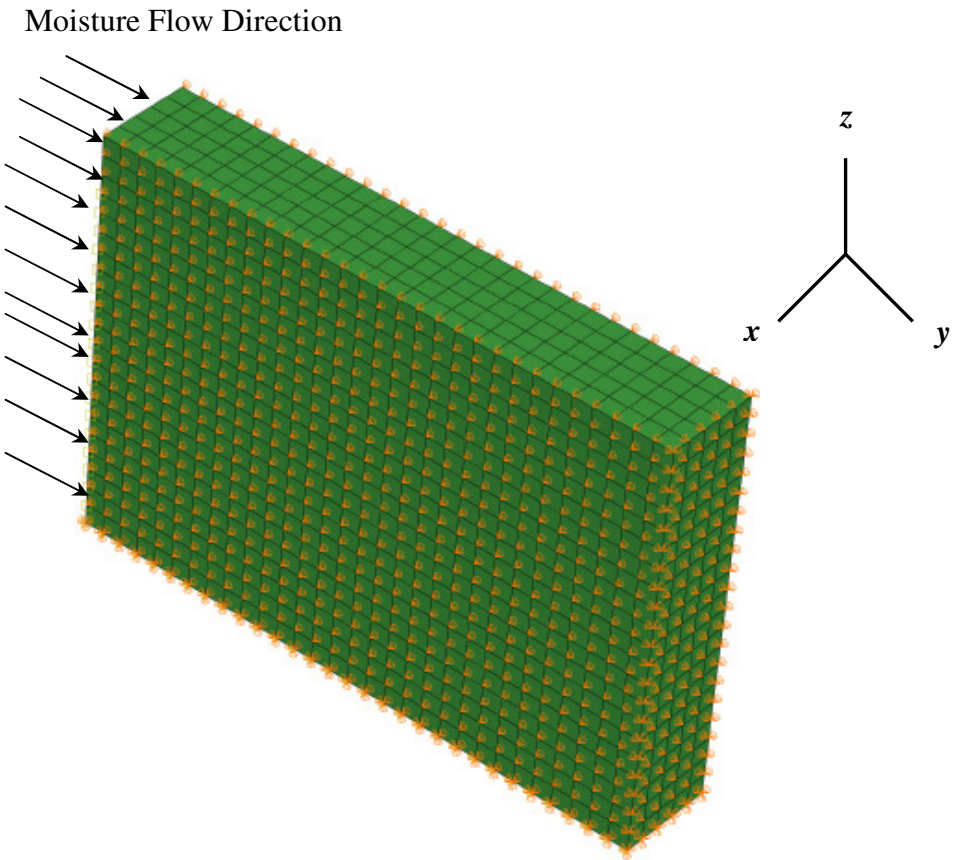

Figure 7.5 Quarter of section with moisture flow direction and boundary condition

7.4.3 Built-in Models Used in the Analysis

7.4.3.1 Linearly Elastic Model

Since swell-shrink behavior is the main focus in this research, an element with swell capabilities and linear elastic properties is used for simulating plastic clay layer. The soil element when subjected to swelling will undergo volumetric changes caused by absorbing water and this element is not expected to either fail or yield during the swelling period. Consequently, a linearly elastic property was applied for all four clay material sections of this research as shown in Table 7.4.

Table 7.4 Input data in the linearly elastic model

Soil Types		**Fort Worth**	**San Antonio**	**Paris**	**Houston**
Specific Gravity, G		2.70	2.70	2.70	2.70
Young's Modulus, E (N/m^2)		1.46×10^7	1.08×10^7	1.21×10^7	1.67×10^7
Poisson's Ratio, μ		0.30	0.30	0.30	0.30
Density of Soil (at OMC), ρ (kg/m^3)		1,465.8	1,465.8	1,475.4	1,587.6
Void Ratio, e	**At OMC**	0.84	0.841	0.83	0.70
	At Saturation	1.31	1.31	1.28	1.17

7.4.3.2 Moisture Swelling

The moisture swelling model defines the saturation-driven volumetric swelling of the solid skeleton of a porous medium in partially saturated flow conditions and can be used in the analysis of coupled wetting liquid flow and porous medium stress.

The moisture swelling model assumes that the volumetric swelling of the porous medium's solid skeleton is a function of the saturation of the wetting liquid in partially saturated flow conditions (ABAQUS ver 6.7 Online Manual). The porous medium is partially saturated when the pore liquid pressure, u_w, is negative. The swelling behavior is assumed to be reversible. The logarithmic measure of swelling strain is calculated with reference to the initial saturation such that

$$\varepsilon_{ii}^{ms} = r_{ii}\frac{1}{3}\left(\varepsilon^{ms}(s) - \varepsilon^{ms}\left(s^{I}\right)\right) \quad \text{, (no sum on } i\text{)} \tag{12}$$

Where $\varepsilon^{ms}(s)$ and $\varepsilon^{ms}\left(s^{I}\right)$ are the volumetric swelling strains at the current and initial saturations. A typical volume strain – soil saturation curve is shown in Figure 7.6 below.

In ABAQUS, the volumetric swelling strain, $\varepsilon^{ms}(s)$, can be defined as a tabular function of the wetting liquid saturation (see Table 7.4 to 7.7). The swelling strain must be defined for the range $0.0 \le s \le 1.0$. The initial saturation values can be defined otherwise the default is fully saturated conditions. For partial saturation the initial saturation and pore fluid pressure must be consistent, in the sense that the pore fluid pressure must lie within the absorption and exsorption values for the initial saturation values (ABAQUS ver 6.7 online manual).

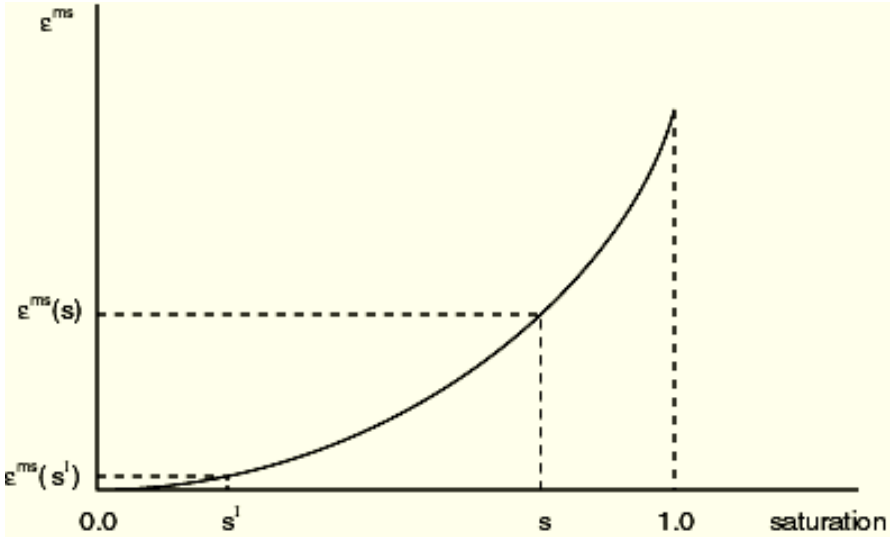

Figure 7.6 Typical volumetric moisture swelling versus saturation curve
(From ABAQUS ver 6.7 online manual, Accessed June 15, 2008)

7.4.3.3 Sorption Model

The sorption is a porous material's absorption/exsorption behavior under partially saturated flow conditions and is used in the analysis of coupled wetting liquid flow and porous medium stress. A porous medium becomes partially saturated when the total pore liquid pressure, u_w, becomes negative. Negative values of u_w represent capillary or suction effects in the medium. For $u_w < 0$, it is known that the saturation lies within certain limits that depend on the value of the capillary pressure, $-u_w$. Typical forms of these limits are shown in Figure 7.7. These limits can be written as $s^a \le s \le s^c$, where $s^a(u_w)$ is the limit at which absorption will occur (so that $\dot{s} > 0$), and $s^e(u_w)$ is the limit at which exsorption will occur (so that $\dot{s} < 0$). The transition between absorption and exsorption and vice versa takes place along "scanning" curves (ABAQUS Online

Manual). These curves are approximated by the single straight line as shown in Figure 7.7. However, only sorption was considered in this study.

Absorption and exsorption behaviors are defined by specifying the pore liquid pressure, u_w (negative "capillary tension"), as a function of saturation. By software default, the absorption and exsorption behaviors are defined by specifying u_w values as shown in Table 7.5 to 7.8 which are retrieved from the present 'Soil Water Characteristic Curves' (SWCCs) presented in Chapter 3 (Figure 3.13 to 3.16).

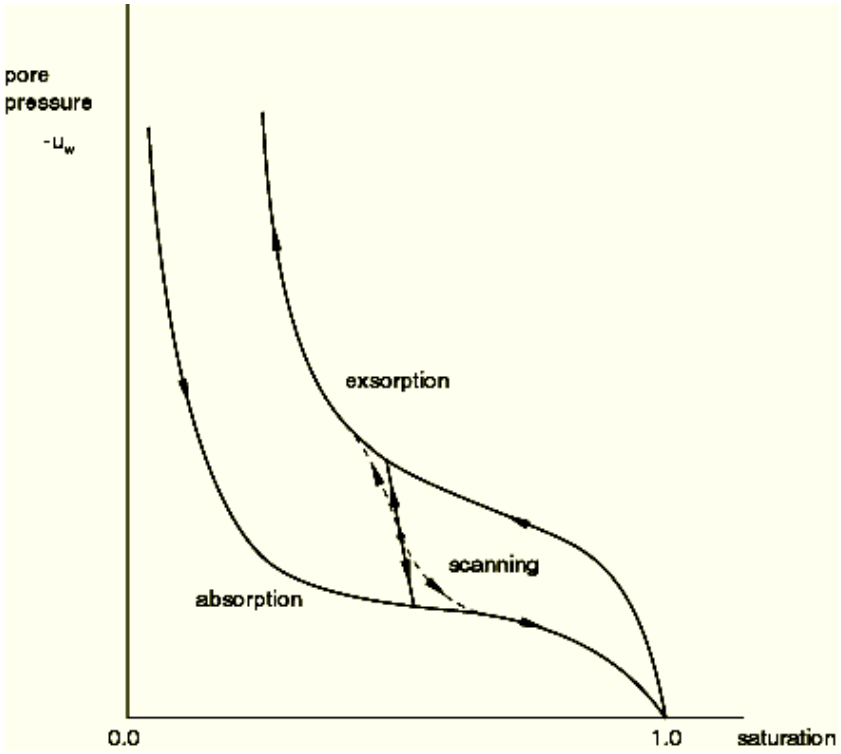

Figure 7.7 Typical absorption and exsorption behaviors
(From ABAQUS ver 6.7 online manual, Accessed June 15, 2008)

Table 7.5 Input data for moisture swelling and sorption models for Fort Worth clay

Moisture Conditions	Saturation	Strain (Moisture Swelling)	Suction, Pa (Sorption)
OMC	0.77	0.071	-1.0×10^{6}
Wet of OMC	0.95	0.1636	-3.8×10^{5}
Saturation	1.00	0.2407	0.00

Table 7.6 Input data for moisture swelling and sorption models for San Antonio clay

Moisture Conditions	Saturation	Strain (Moisture Swelling)	Suction, Pa (Sorption)
OMC	0.70	0.1368	-2.0×10^{6}
Wet of OMC	0.91	0.2197	-6.0×10^{5}
Saturation	1.00	0.2895	0.00

Table 7.7 Input data for moisture swelling and sorption models for Paris soil

Moisture Conditions	Saturation	Strain (Moisture Swelling)	Suction, Pa (Sorption)
OMC	0.75	0.117	-2.0×10^{6}
Wet of OMC	0.96	0.224	-6.0×10^{5}
Saturation	1.00	0.269	0.00

Table 7.8 Input data for moisture swelling and sorption models for Houston clay

Moisture Conditions	Saturation	Strain (Moisture Swelling)	Suction, Pa (Sorption)
OMC	0.78	0.067	-1.0×10^{6}
Wet of OMC	0.93	0.1413	-3.8×10^{5}
Saturation	1.00	0.2169	0.00

7.4.4 Numerical Swell Prediction Model (using FEM) Results

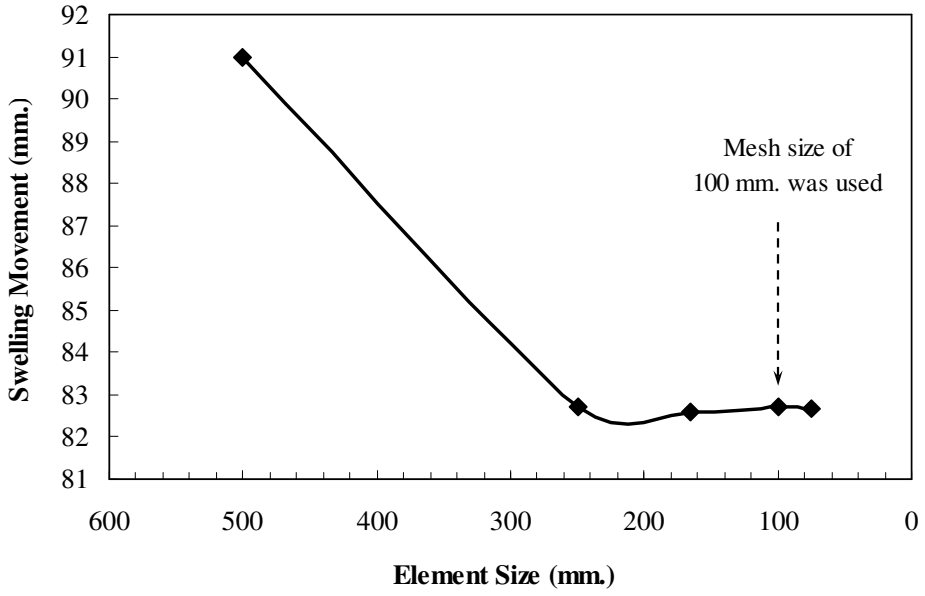

Figure 7.8 Convergent analysis results

The finite element method will converge toward the correct answer as the element size is decreased, provided that the interpolation equation gives a constant value throughout the element when the nodal values are numerically identical (Segerlind, 1976). Convergence analysis was also performed by investigating the size of elements

with output results. Figure 7.10 shows swelling movement results were converged when the element size was reduced to 100 mm. Hence, the element size of 100 mm. was used in this study.

The deformed mesh of the discretized pavement section built on Paris clay is presented in Figure 7.10a to 7.10c. The movements in the deformed mesh are attributed to moisture changes from an initial compaction condition of optimum moisture content to a saturation moisture value. As seen in Figure 7.10b, the swell movements can be clearly seen on the elements near the shoulder. The maximum swell movement recorded here is 61.7 mm, which upon conversion will yield to 3.43 % of strain. The soil swell predictions for all soil types are presented in Table 7.9.

Table 7.9 Soil swell predictions from numerical modeling using FEM

Soil Types	**Soil Swell Movements (%)**
Fort Worth	2.83
San Antonio	2.75
Paris	3.43
Houston	2.57

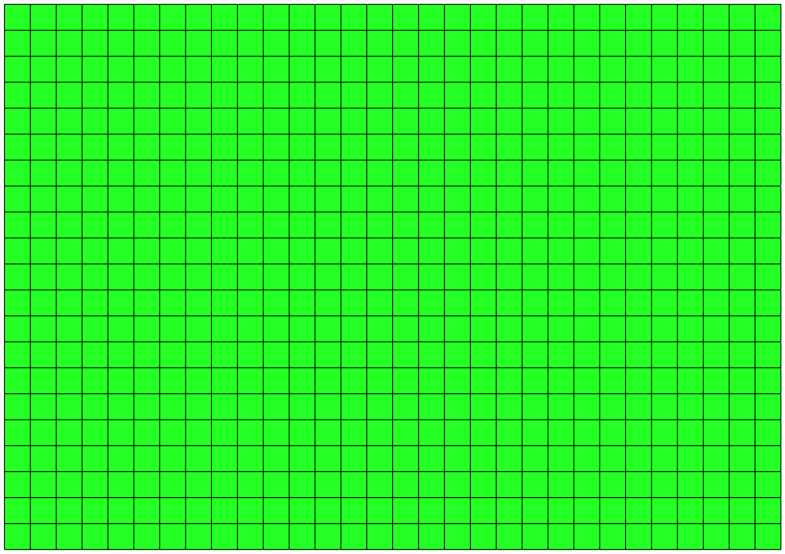

(a)

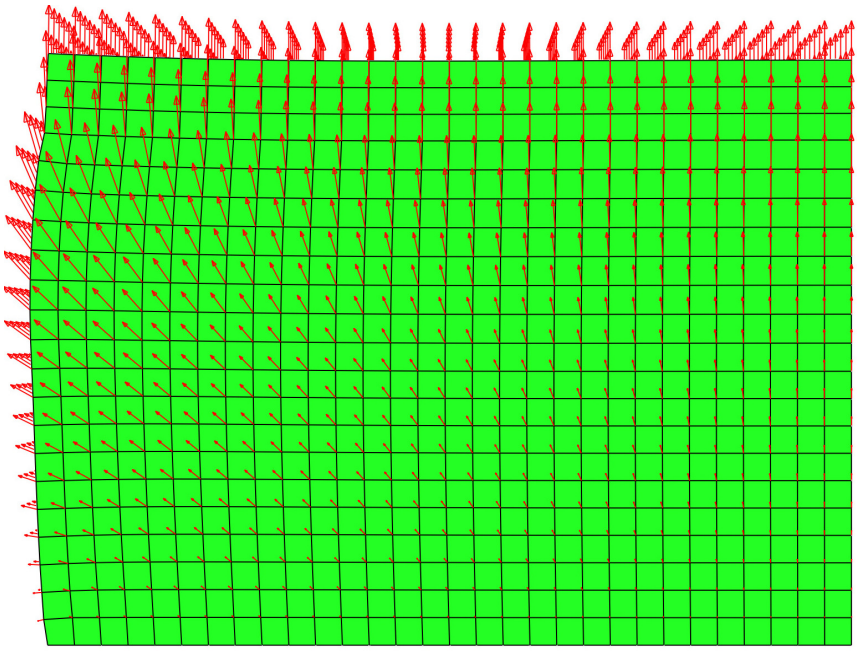

(b)

Figure 7.9 2-D views of quarter section of (a) Meshed elements before executed and (b) Deformed elements with displacement vectors after executed of Paris soil

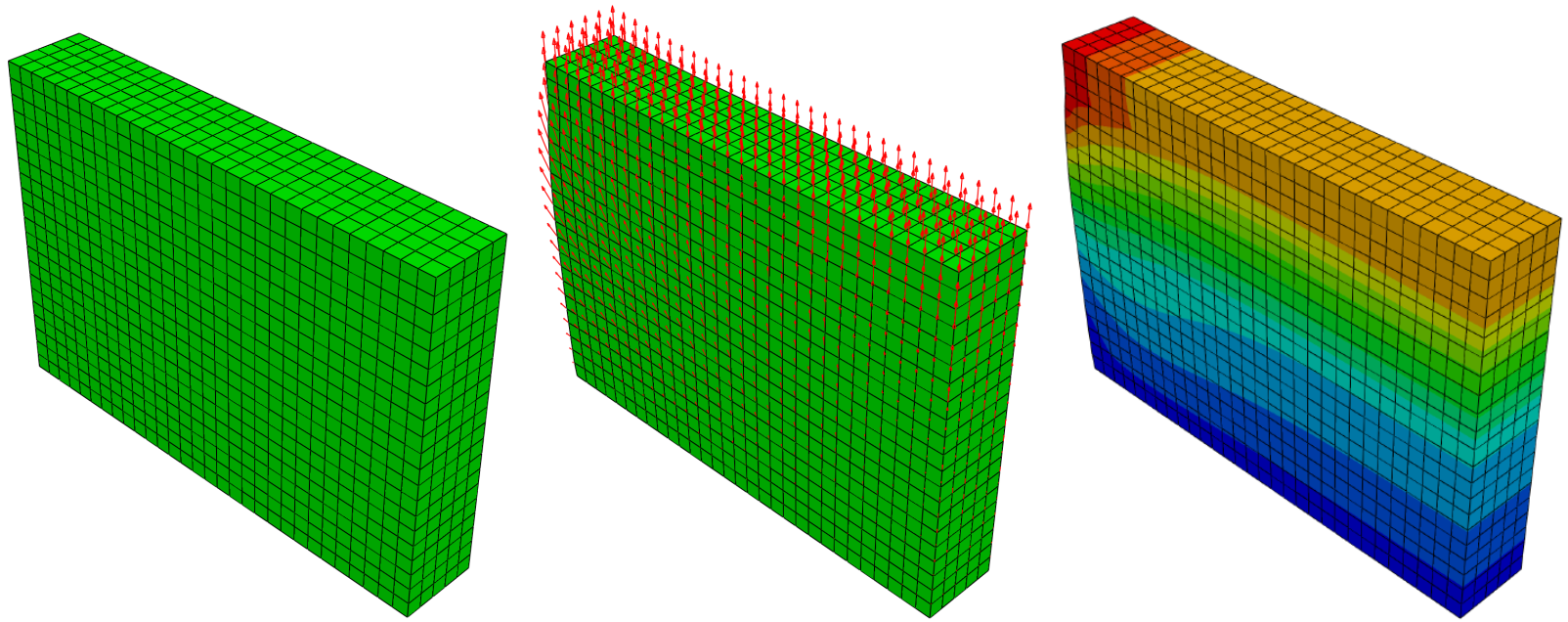

(a) (b) (c)

Figure 7.10 Typical 3-D views of quarter section of (a) Elements before executed, (b) Deformed elements with displacement vectors after executed and (c) Deformed elements with vertical displacement contours after executed

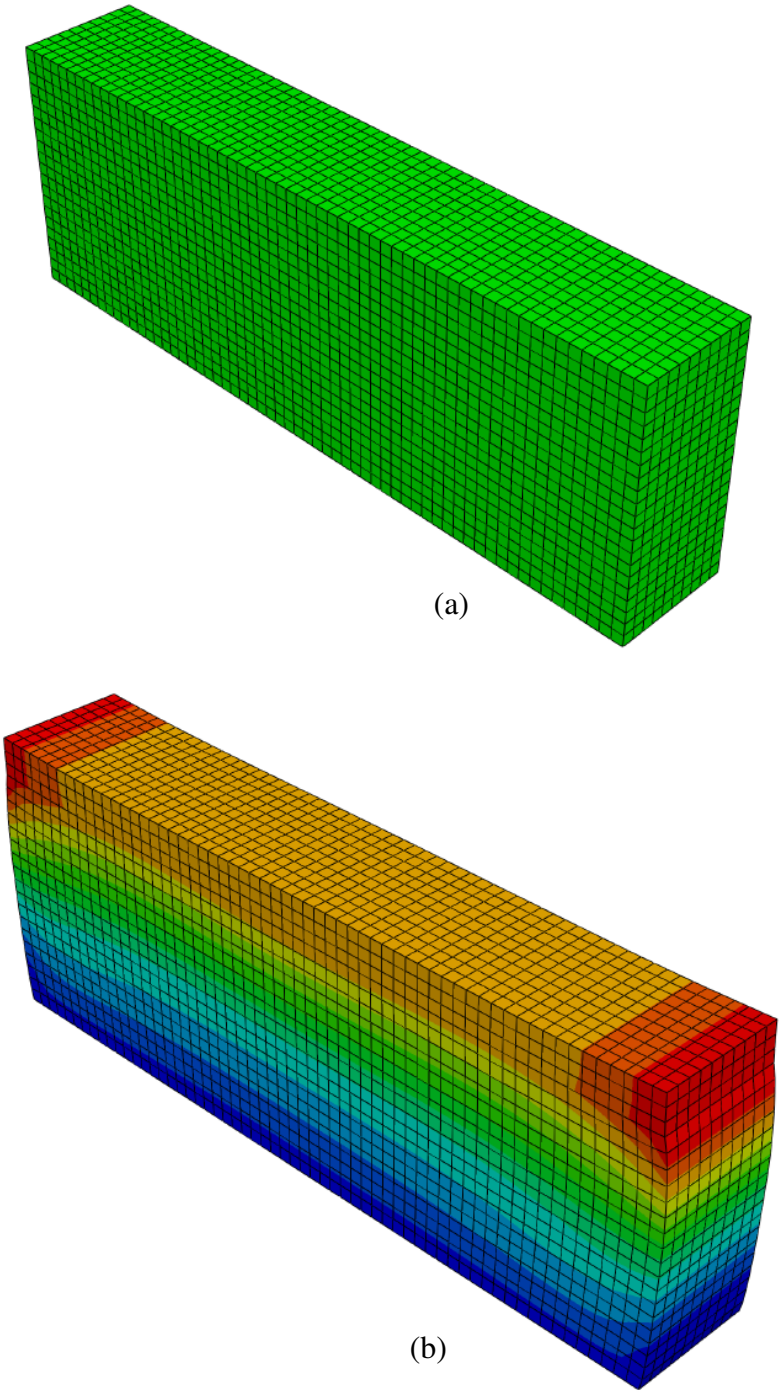

Figure 7.11 Typical vertical displacement contours of the full section of element meshes (3-D view) (a) Before and (b) After executed the model

In this analysis, the soil conditions for all depths are assumed similar. However, in reality, confinement influences, soil moisture fluctuations and thereby related volume changes are different. It is possible that more soil layers with different soil swell properties can be assumed if more accuracy is needed. However, due to lack of SWCC data at different confinements, such modeling is not considered here. Nevertheless, considering the shallow subgrades simulated in the numerical modeling, such accuracy may not be needed.

7.5 Comparisons of Swell Prediction Results

Table 7.10 and Figure 7.12 present comparison between swell prediction results and measured swell strain both from field elevation survey and laboratory testing. As expected, swell strains based on three-dimendional free swell test are the highest since it did not consider overburden pressure effects into account. Tests at free swell conditions are extrapolated for confine depths of 6-ft and hence high values are recorded in these interpretations. Based on the swell strain results, the Paris clayey soil experienced highest swelling whereas Houston clay has experienced low swelling.

The swell movements recorded from the field monitoring lied between PVR and Lytton models which indicated that both methods can be simply used to predict both lower bound and upper bound predictions of the swell movements in the field. However, more sites need to be instrumented and elevation changes from these sites will further corroborate the present findings.

The values predicted from the present numerical modeling show similar trends as those observed in the field and are closer to field elevation survey data than any other

models. This explains the importance of numerical modeling for better simulation of volume changes expected in the underlying subsoils. This also enhances the confidence of using numerical models for better prediction of soil movements associated with pavement infrastructure.

7.6 Summary

This chapter presents the reviews of swell prediction model developed by past researchers and also details of finite element modeling analysis by using a commercial 3-D finite element ABAQUS® software. The built-in models used in the FEM analysis composed of linearly elastic, moisture swelling and sorption models.

From comparison of field observations with model predictions, it is observed that swell movements recorded from the field monitoring lie between PVR and Lytton models indicating that both methods can be used to predict both lower bound and upper bound predictions of the swell movements whereas numerical modeling predictions are the closest to field monitored soil movements. Thus, explaining the significance of the numerical modeling of swelling behavior of unsaturated soils. However, more sites are needed to be instrumented and monitored for further corroborating the present findings.

Table 7.10 Comparison of predicted swell strains with measured swell strains

Soil Types	Predicted Swell Strains (%)					Measured Swell Strains (%)	
	Swell Prediction Models by Past Researchers				Numerical Method (FEM)	Field Elevation	3-D Swell Testing*
	Snethen	Hamberg & Miller	PVR	Lytton			
Fort Worth	0.54	2.25	2.56	4.41	2.83	2.78	6.91
San Antonio	0.55	2.25	2.42	4.97	2.75	4.00	7.73
Paris	0.58	2.25	2.41	5.48	3.43	4.67	7.37
Houston	0.48	2.01	2.28	3.39	2.57	2.50	5.42

Note: * 3-D Swell data from laboratory

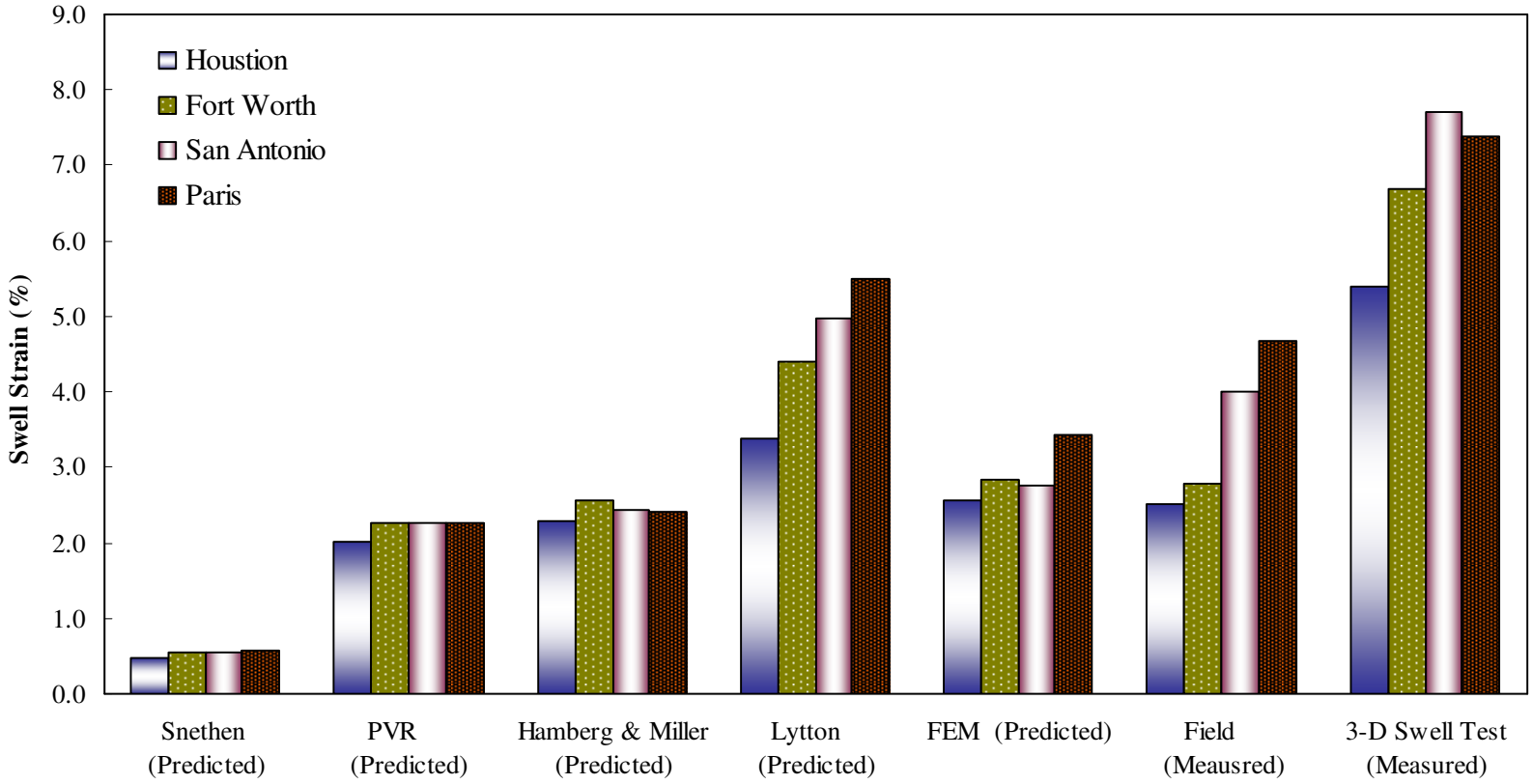

Figure 7.12 Comparison of predicted swell strains with measured swell strains

CHAPTER 8

SUMMARY OF FINDINGS AND FUTURE RESEARCH DIRECTIONS

8.1 Introduction

Expansive soils are commonly present in subsoils of various districts in Texas. Due to seasonal related moisture content fluctuations, swell and/or shrinkage related movements occur in the subgrade soils underneath pavement shoulders. These differential subsoil movements often cause pavement cracking and result in the poor performance of the pavements. This type of problem is more evident in the case of low volume roads where pavement layers such as subbases are not present.

The main objective of this research is to better understand the volumetric movements of plastic soils in both shrinkage (dry) and swell (wet) environments as well as in laboratory and field conditions. This objective was fully accomplished and several important findings were resulted. Current swell prediction models were evaluated along with the development of new volumetric swell and shrinkage strain prediction models. Field sections with different boundary conditions were selected and instrumented. Field data was studied to understand the causes of soil movements and pavement cracking patterns. Numerical modeling was attempted to simulate the soil movements from moisture fluctuations and understand their impacts on the infrastructure.

The following conclusions are developed from the analyses results presented in Chapters 3 to 7. These conclusions are based on the majority of the trends noted in the present data. These conclusions may be valid for other similar types of soils, with a few validation studies.

8.2 Summary of Findings

The following lists the major conclusions obtained from this research.

1. All four high Plasticity Index (PI) soils, Fort Worth, San Antonio, Paris and Houston soils, showed volumetric swell strain more than 10% (for OMC condition) which is considered as a very high degree of expansion. Since these soils contain low amounts of soluble sulfates and organic contents, it can be concluded that the high volume changes behaviors of studied soils can be attributed to the inherent soil properties which can be examined from basic soil properties tests, clay mineralogy, and engineering tests presented in this research. A ranking analysis based on soil property magnitudes revealed that all clayey soils from Paris, Fort Worth, San Antonio and Houston exhibited high volume changes, with Houston showing the lowest amounts of movements in the present group.

2. All four soils showed a good correlation between Plasticity Index (PI) property and the amount of montmorillonite mineral content expressed in percent. This is expected since this mineral exhibits high affinity to holding moisture content, which in turn influences the plasticity nature of the soil.

3. Ratios between the present measured vertical swell strain and volumetric swell strain of all test soils is close to ½ or 0.5. This finding indicates that the use of ⅓

or 0.33 to convert the volumetric swell strain into vertical swell strain (as assumed in PVR model) is not accurate. This also explains one of the reasons for PVR model to predict higher soil movements.

4. Laboratory vertical swell model with the plasticity index property from this study showed a good and close agreement with those from Seed et al. (1962) and Chen (1983) models, indicating soils from different regions behaved in a similar fashion.

5. Multiple linear regression analysis revealed that three independent soil property variables are adequate to characterize laboratory soil volume change related shrinkage behavior. Those three variables are matric suction, initial soil moisture content, and soil plasticity index. In the case of radial shrinkage strain model, initial soil moisture content alone appeared to capture the overall shrinkage movement in radial direction.

6. As a part of the evaluation of swell prediction models in this research, models by Snethen, Hamberg and Miller, PVR and Lytton indicated similar trends with predictions for Paris soil being highest and the same for Houston soil being lowest.

7. The vertical swell values from the field monitoring test sections from elevation surveys lie between PVR and Lytton models' predictions. This indicated that both these methods can be utilized to predict both lower and upper bounds of the swell movements expected in the field. More site data and movements are required to further corroborate these findings.

8. From the field monitoring data, site boundary or environmental conditions such as large trees and drainage ditches have a strong influence on pavement cracking.

These conditions will exaggerate the problems of expansive soil behavior by inducing more dry related shrinkage movements. At Paris site (where there are large trees located), the ratio of D:H (D is referred to as distance of structure from the tree and H is referred to as the height of tree) is equal to 0.9. As mentioned by many researchers, large trees have a strong influence on the propagation of soil moisture content since their roots attract water toward themselves. As a result, soil moisture will be depleted, which in turn will lead to soil shrinkage cracking. This was evident in Paris site where drying related shrinkage cracks were detected on the pavement sections as well as moisture depletion was noted from the monitored data. Hence, future pavement design should incorporate the inclusion of dry or shrink related soil movements in their soil modeling while designing pavements near the trees in expansive clay environment.

9. Local drainage ditches near the pavements affected the surrounding soil moisture contents, but only for a short distance. For Houston site, the pavement was not affected during the monitoring period since the drainage ditch is about 35 ft. away from the pavement. Analyzing the moisture sensors' data at the Houston site, the water migration effected distance is about 3.7 ft. in vertical direction and 24 ft. in horizontal direction.

10. From field observations of all test sections, new cracks appeared when the following two conditions occurred in the field:

    a. As observed from Fort Worth and Paris sites, moisture content variation (the difference between maximum and minimum moisture contents in a particular month) was more than 20% together with the

mean moisture contents at the top 2 to 3 ft of subgrade is reaching a value close to 15% at least for a month.

b. Monthly mean moisture contents are less than 15% for more than one month. This condition was observed at San Antonio site.

11. Although moisture content variation is more than 20%, new cracks were not detected in the Houston site since mean moisture content is more than 22%.

12. Numerical modeling using 3-D finite element software was used to model swelling soils by incorporating linear elastic and swelling material. Predictions by this model showed a good match with the measured field elevation data, indicating the capabilities of the numerical modeling of unsaturated expansive soils.

8.3 Future Research

1. More sites with various different environmental site conditions are needed for further validation of the findings and for the development of a database for better swell-shrinkage estimations in the field.

2. Investigations on other soil parameters which are potentially related to soil volume changes and cracking initiation are needed. Other information including shrinkage induced pressure and shrinkage induced tensile stress are needed for better understanding of cracking in the infrastructure.

3. Also, numerical modeling of pavements built on expansive subgrades with a more realistic simulation of modeling of soils at different confinement depths is needed. This will further enhance the understanding of numerical modeling of unsaturated and expansive soils.

REFERENCES

1. Ahlvin, R.G. (1962). "Flexible Pavement Design Criteria." *Journal of the Aero-Space Transport Division*, Proceedings of the ASCE.

2. Aitchison, G.D. (1965). "Moisture Equilibria and Moisture Changes in Soil Beneath Covered Areas." *A Symp. In Print, G.D. Aitchison*, Ed., Australia: Butterworths, pp. 278.

3. Al-Khafaf and Hanks, R. J. (1974). "Evaluation of the Filter Paper Method for Estimating Soil Water Potential." *Soil Sci.*, vol. 117, pp. 194 – 199.

4. Al-Rawas, A.A., Hago, A.W. and Al-Sarmi, H. (2005). "Effect of lime, Cement and Sarooj (Artificial Pozzolan) on the Swelling Potential of an Expansive Soil from Oman." *Building and Environment 40,* pp.681 – 687.

5. Austin, R.A. and Gilchrist, A.J.T. (1996). "Enhanced Performance of Asphalt Pavements Using Geocomposites." *Geotextiles and Geomembranes 14*. pp.175-186.

6. Baker, P. D. (1978). "Tree Root Intrusion into Sewers." *Progress Report No. 2*: Analysis of Root Chokes by Species." *Engineering and Water Supply Department, Sewerage Branch*, SA, Australia, August.

7. Basma, A.A., Tuncer, E.R. (1991). "Effect of Lime on Volume Change and Compressibility of Expansive Clays." *Transportation Research Board, TRR No. 1296*, Washington DC. pp. 54-61.

8. Bell, F.G. (1996) "Lime Stabilization of Clay Minerals and Soils". *Engineering Geology 42,* pp.223-237.

9. Biddle, P. G. (1983). "Patterns of Soil Drying and Moisture Deficit in the Vicinity of Trees on Clay Soils." *Geotechnique*, 33, 2, 107-126.
10. Biddle, P. G. (2001). "Trees Root Damages to Buildings." *ASCE Geotechnical Special Publication*, 115, 1-23.
11. Brown, S.F. (1996). "Soil mechanics in pavement engineering." *Geotechnique*, v 46, n 3, Sep, 1996, p 383-426.
12. Browning, G. (1999). "Evaluation of Soil Moisture Barrier." *FHWA/MS-DOT-RD-99-21 & 23; Final Report.*
13. Bozozuk, M. (1962). "Soil Shrinking Damages Shallow Foundations at Ottawa, Canada." Research Paper 163, Division Building Research, *NRCC*, Canada.
14. Budge, W.D., Sampson, E. Jr., and Schuster, R.L. (1966). "A Method of Determining Swell Potential of an Expansive Clay." *Highway Research Record.*
15. Bulut, R., Lytton, R. L., and Wray, W. K. (2001). "Soil suction measurements by filter paper." *Expansive Clay Soils and Vegetative Influence on Shallow Foundations*, 2001, p 243-261.
16. Bryant, J. T., Morris, D. V., Sweeney, S. P., Gehrig, M. D., and Mathis, J. D. (2001) "Tree root influence on soil-structure interaction in expansive clay soils." *Expansive Clay Soils and Vegetative Influence on Shallow Foundations*, 2001, p 110-131.
17. Cameron, D. A. (2001). "The Extent of Soil Desiccation near Trees in a Semi-Arid Environment Footings Group." *IE Aust SA*, 17.
18. Chen, F. H. (1983). *Foundation on Expansive Soils*, Elsevier Scientific Publishing Co., New York, USA.
19. Chen, F.H (1988). *Foundations on expansive soils 2nd Ed.*, Elsevier Science Publications, New York.
20. Chen, J., Lin, K. and Young, S. (2004). "Effects of crack width and permeability on moisture-induced damage of pavements." *Journal of Materials in Civil Engineering*, v 16, n 3, p 276-282.

21. Chou, L. (1987) “Lime Stabilization: Reactions, Properties, Design and Construction.” TRB State of the Art Report 5, *Transportation Research Board*, National Research Council, Washington D.C.

22. Covar, A.P. and Lytton, R.L. (2001). “Estimating Soil Swelling Behavior Using Soil Classification Properties.” *ASCE Geotechnical Special Technical Publication* No. 115, pp. 44-63.

23. Croft, J.B. (1967). “The Influence of Soil Mineralogical Composition on Cement Stabilization.” *Geotechnique,* vol. 17, London, England, pp.119–135.

24. Cutler, D. F. and Richardson, I. B. K. (1981). “Trees and buildings.” *Construction Press*: London.

25. Dar, H. C., and Moon, W. (2007). “Field Investigations of Cracking on Concrete Pavements.” *J. Perf. Constr. Fac*., 21, 450-460.

26. Dedier, G. (1973) “Prediction of Potential and Swelling Pressure of Soils.” *Proceeding of 8th International Society for Soil Mechanics and Foundation Engineering*, Vol. 22, 1-20.

27. Department of the Army USA (1983) “Foundations in Expansive Soils, 1 September 1983.” *Technical Manual TM, 5-818-7.*

28. Driscoll, R. (1983). “The Influence of Vegetation on the Swelling and Shrinkage of Clay in Britain.” *Geotechnique*, 33 (2), 93-105.

29. El-Ramli, A.H. (1965). “Swelling Characteristics of Some Egyptian Soils” *Journal of the Egyptian Society of Engineering*, Vol. 4, No. 1, 25-35.

30. Environmental Sensors Inc. homepage. *Product – GroPoint*. http://www.esica.com/products_gropoint.php. Accessed July 17, 2007.

31. Erguler, Z.A. and Ulusay, E. (2003). “A simple test and predictive models for assessing swell potential of Ankara (Turkey) clay.” *Engineering Geology*, Vol. 67, pp. 331-352.

32. Evans, R. P.; McManus, K. J. (1999). "Construction Of Vertical Moisture Barriers To Reduce Expansive Soil Subgrade Movement." *Transportation Research Record 1652, 7th International Conference on Low-Volume Roads*, pp.108-112.

33. Fahoum, K., Aggour, M. S. and Amini F. (1996)."Dynamic Properties of Cohesive Soils Treated with Lime." *J. Geotech. Engrg*. 122, 382.

34. Feng, M, Fredlund, D. G., Shuai, F. (2002). "A Laboratory Study of the Hysteresis of a Thermal Conductivity Soil Suction Sensor." *J Geotechnical Testing*, Vol. 25(3), 303-314.

35. Ferguson, G. (1993). "Use of self-cementing fly ashes as a soil stabilization agent." *ASCE Geotechnical Special Publication No. 36*, ASCE, New York.

36. Fredlund, D. G. (1989). "Soil Suction Monitoring for Roads and Airfields." *Sym. on the State of Art of Pavement Response Monitoring System for Roads and Airfields*, March 6-9.

37. Fredlund, D. G. (1991). "How Negative Can Pore-Water Pressure Get?" *Geotechnical News*, Vol.9, no. 3, Can. Geot. Society, pp. 44-46.

38. Fredlund, D.G. and Rahardjo (1993). *Soil Mechanics for Unsaturated Soils*, John Wiley & Sons, Inc., New York.

39. Fredlund, D.G., Xing, A., Huang, S. (1994). "Predicting the permeability function for unsaturated soils using the soil-water characteristic curve." *Canadian Geotechnical Journal*, v 31, n 4, Aug, 1994, p 533-546.

40. Forstie, D., Walsh, H., Way, G. (1979). "Control of Expansive Clays under Existing Highways." *Proceedings of the Paving Conference*, 1979, p 13-33.

41. GCTS Inc. homepage. *Fredlund Thermal Conductivity Sensor (FTC-100).* http://www.gcts.com/products.php?catid=3&menuid=7&prodid=195. Accessed July 17, 2007.

42. Giroud, J.P. and Han, J. (2004a). "Design Method for Geogrid-Reinforced Unpaved Roads. I. Development of Design Method." *Journal of Geotechnical and Geoenvironmental Engineering*, pp.775-786.

43. Giroud, J.P. and Han, J. (2004b). "Design Method for Geogrid-Reinforced Unpaved Roads. II. Calibration and Applications." *Journal of Geotechnical and Geoenvironmental Engineering*, pp.787-797.

44. Hagerty, D. J., Ullrich, C. R., Denton, M. M. (1990). "Microwave drying of soils." *Geotechnical Testing Journal*, v 13, n 2, Jun, 1990, p 138-141.

45. Hamberg, D. J. (1985). "A simplified method for predicting heave in expansive soils." *M.S. thesis*, Colorado State University, Fort Collins, CO.

46. Hammons, M. I. (1998). "Advanced pavement design: Finite element modeling for rigid pavement joints." *Rep. No. II*: *Model Development, DOT/FAA/AR-97-7*, Federal Aviation Administration, U.S. Dept. of Transportation.

47. Hicks, R.G. (2002). "Alaska Soil Stabilization Design Guide." *FHWA-AK-RD-01-6B.*

48. Hilf, J.W. (1956). "An Investigation of Pore-Water Pressure in Compacted Cohesive Soils." *Tech. Memo*. 654, U.S. Department of the Interior, Bureau of Reclamation Design and Construction Div, Denver, Colorado.

49. Holland, J.E. and Cameron, D.A. (1981). "Seasonal Heave of Clay Soils." *Civil Engineering Transactions, 1981*. pp.55-67.

50. Hopkins, T.C., Sun, L. and Slepak, M. (2005). "Bearing Capacity Analysis and Design of Highway Base Materials Reinforced with Geofabrics." University of Kentucky Transportation Center, College of Engineering, *Research Report KTC-05-21/SPR 238-02-1F*.

51. Horak, E. (1983). "Waterbound Macadam Bases." *M.E. thesis*, Department of Civil Engineering, Univ. of Pretoria, Republic of South Africa.

52. Horak, E. and Triebel, R.H.H. (1986). "Waterbound Macadam as a Base and a Drainage Layer." *Transportation Research Record 1055*. pp.48-51.

53. Hufenus R., Rueegger, R., Banjac, R., Mayor, P., Springman, S.M. and Brönnimann, R. (2006). "Full-Scale Field Tests on Geosynthetic Reinforced Unpaved Roads on Soft Subgrade." *Geotextiles and Geomembranes* 24, pp.21-37.

54. Hussein E.A. (2001). "Viscoplastic Finite Element Model for Expansive Soils." *EJGE*, paper 2001-0122.

55. Intharasombat, N. (2003). "Ettringite formation in lime treated sulfate soils : verification by mineralogical and swell testing." *M. S. Thesis*, University of Texas, Arlington, Texas, 117 pages.

56. Jaksa, M. B., Kaggwa, W. S., Woodburn, J. A., and Sinclair, R. (2002). "Influence of Large Gums Trees on the Soil Suction Profile in Expansive Clays." *Australian Geomechanics*, 71(1), 23-33.

57. Jayatilaka, R., Gay, D.A., Lytton, R.L.,and Wray, W.K. (1993). "Effectiveness of Controlling Pavement Roughness Due To Expansive Clays With Vertical Moisture Barriers." Texas Transportation Institute Research Report 1165-2F, May.

58. Johnson, L.D., Stroman, W.R.(1976). "Analysis of Behavior of Expansive Soil Foundations." *U.S. Army Engineer Waterways Experiment Station Technical Report S-76-8.*

59. Jones, D. E., and Holtz, W. J. (1973). "Expansive soils: The hidden disaster." *Civ. Eng.* (N.Y.) 43(8), 49–51.

60. Karlsson, R., & Hansbo, S. (1981). "Soil classification and identification." *Swedish council for building research*. D8: 81. Stocckholm.

61. Kim, J., and Hjelmstad, K. (2000). "Three-dimensional finite element analysis of multi-layered systems: Comprehensive nonlinear analysis of rigid airport pavement systems." *Federal Aviation Administration DOT 95-C-001, COE Rep. No. 10*, Univ. of Illinois at Urbana-Champaign, Urbana, Ill.

62. Kodikara, J.K. and Choi, X. (2006). "A simplified analytical model for desiccation cracking of clay layers in laboratory tests". *Geotechnical Special Publication*, n 147, *Proceedings of the Fourth International Conference on Unsaturated Soils*, 2006, p 2558-2569.

63. Koerner, R.M. (2005). *Design with Geosynthetics* 5th Ed. Pearson Prentice Hall, Upper Saddle River, NJ.

64. Kormonik, A. and David, D. (1969). "Prediction of swell pressure of clays." *Journal of Soil Mechanics and Foundation Division ASCE*, Vol. 95 (SM1), pp. 209-225.

65. Kota, P.B.V.S., Hazlett, D., and Perrin, L. (1996). "Sulfate-bearing soils: Problems with calcium-based stabilizers." *Transportation Research Record 1546*, pp.62-69.

66. Kuo, C., Huang, C. (2006). "Three-dimensional pavement analysis with nonlinear subgrade materials." *Journal of Materials in Civil Engineering*, v 18, n 4, August, 2006, p 537-544.

67. Lambe, T. W and Whitman, R. V. (2000). *Soil mechanics, SI version*. John Wiley & Sons, New York, 2000.

68. Lee, R. K. C. and Fredlund, D. G. (1984). "Measurement of soil suction using the MSC 6000 gauge." *Proc. 5th Int. Conf. Expansive Soils.* Adelaide, Australia. 50-54.

69. Leong, E. C., He, L., and Rahardjo, H. (2002). "Factors Affecting the Filter Paper Method for Total and Matric Sucion Measurements." *Journal of Geotechnical Testing*, Vol. 23(3), 2002, 1-12.

70. Little, D.N.(1999). "Evaluation of Structural Properties of Lime Stabilized Soils and Aggregates, Vol. I. Summary of Findings." *National Lime Association Publication.*

71. Little, D., Males, E. H., Prusinski, J.R. and Stewart, B. (2000). "Cementitious Stabilization." *79th Millennium Rep. Series, Transportation Research Board.*

72. Lu, N. and Likos, W. J. (2004). *Unsaturated Soil Mechanics.* John Wiley & Sons, New York, 2004.

73. Lytton (2004). "Introduction, design procedure for pavements on expansive soils". *Report No. FHWA/TX-05/0-4518-1*, Texas Department of Transportation, 2004, 1-32.

74. McDowell, C. (1956). "Interrelationship of load, volume change, and layer thickness of soils to the behavior of engineering structures." *Proc. Highway Research Board*, No. 35, 754-770.

75. McKeen, R. G. (1980). "Field studies of airport pavements on expansive clay." *Proc. 4th Int. Conf. on Expansive Soils,* Denver, 1, 242–261.

76. McKeen, R. G. (1981). *Design of airport pavement for expansive soils*, U.S. Dept. of Transportation, Federal Aviation Administration, Rep. No. DOT/FAA/RD-81/25.

77. Mcqueen, I. S. and Miller, R. F. (1968). "Calibration and Evaluation of a Wide Range Method of Measuring Moisture Stress." *J. Soil Sci*., Vol 106, no.3, pp. 225-231.

78. Millington, R.J. and Quirk, J.R. (1961). "Permeability of Porous Solids." *Trans. Faraday Soc*., Vol. 57, pp. 1200-1207.

79. Mitchell, J. K. (1976). *Fundamentals of Soil Behavior*. John Wiley, New York.

80. Mitchell, J. K. (1986). *Fundamentals of soil behavior*, 3rd Ed., Wiley, Hoboken, N.J.

81. Mitchell, P.W. and Avalle, D.L. (1984). "A Technique to Predict Expansive Soil Movements." *Proceedings, 5th International Conference on Expansive Soils*, Adelaide, South Australia.

82. Montgomery, D. C., Runger, G. C., and Hubele, R. N. (2003). *Engineering Statistic 3rd edition*, John Wiley & Sons, New York.

83. Mowafy, Y.M. and Bauer, G.E. (1985a). "Prediction of Swelling Pressure and Factors Affecting the Swell Behavior of an Expansive Soil." *Transportation Research Record 1032*. pp.23-33.

84. Mowafy, Y.M., Bauer, G.E. and Sakeb, F.H. (1985b). "Treatment of Expansive Soils: A Laboratory Study." *Transportation Research Record 1032*, pp.34-39.

85. Nagaraj, T.S. and Srinivasa Murthy, B.R. (1985). "Rational Approach to Predict Swelling Soil Behavior." *Transportation Research Record 1032*, pp.1-7.

86. Nelson, D. and Miller, D. J. (1992). *Expansive Soils Problems and practice in Foundation and Pavement Engineering,* John Wiley & Sons, New York, 1992., 40-80.

87. Nichol, C., Smith, L., and Beckie, R. (2003). "Long-term Measurement of Matric Suction using Thermal Conductivity Sensors." *Canadian Geotech. J*., 40, 587-597.

88. Ofer, Z. and Blight, G.E. (1985). "Measurement of Swelling Pressure in the Laboratory and In Situ." *Transportation Research Record 1032*, pp.15-22.

89. Ohri, M.L. (2003). "Swelling behavior of clays and its control." *Proc. of International Conference on Problematic soils*, Nottingham, U.K, pp 427-433.

90. Peck, R.B., Hansen, W.E., Thornburn, T.H. (1974). *Foundations Engineering*. John Wiley and Sons, New York.

91. Pengelly, A. and Addison, M. (2001). "In-Situ Modificaiton of Active Clays for Shallow Foundation Remediation." *Expansive Clay Soils and Vegetative Influences*, pp.192-214.

92. Phene, J., Hoffman, G. J. and Rawlins, S. L. (1971). "Measuring Soil Matric Potential in Situ by Sensing Heat Dissipation with a Porous Body: Theory and Sensor Construction." *Proc. Soil Sci. Soc. Amer*., vol. 35, pp. 27 – 32.

93. Picornell, M. and Lytton, R.L. (1986). "Behavior and Design of Vertical Moisture Barriers." *Transportation Research Record 1137*, pp.71-81.

94. Punthutaecha, K., Puppala, A. J., Vanapalli, S. K., and Inyang, H. (2006). "Volume change behaviors of expansive soils stabilized with recycled ashes and fibers." *J. Materials in Civil Engineering*, 18(2), 295-306.

95. Puppala, Anand J., Viyanant, C., Kruzic, A. P., Perrin, L. (2002). "Evaluation of a modified soluble sulfate determination method for fine-grained cohesive soils." *Geotechnical Testing Journal*, v 25, n 1, March, 2002, p 85-94.

96. Puppala, A.J., Wattanasanticharoen, E. and Punthutaecha, K. (2003). "Experimental Evaluations of Stabilization Methods for Sulphate-rich Expansive Soils." *Ground Improvement Vol. 7, No. 1*, 2003. pp.25-35.

97. Puppala, A.J., Griffin, J.A., Hoyos, L.R. and Chomtid, S. (2004a). "Studies on Sulfate-Resistant Cement Stabilization Methods to Address Sulfate-Induced Soil Heave." *Journal of Geotechnical and Geoenvironmental Engineering,* 130, pp.391-402.

98. Poor, A.R. (1974). ''Experimental residential foundation design on expansive clay soils.'' *Rep. No. TR-3-78*, *Final Rep.*, Construction Research Center, Univ. of Texas at Arlington, Texas.

99. Rabba, S. (1975). "Factors Affecting Engineering Properties of Expansive Soils." *M.S. Thesis*, Al-Azhar University, Cairo, Egypt.

100. Rahardjo, H. and Leong, E. C. (2006). "Suction Measurements." *Proceedings of the Fourth International Conference on Unsaturated Soils*, Carefree, Arizona, USA, p. 81-104.

101. Rao, R.R., and Smart, P. (1980). "Significance of Particle Size Distribution Similarity in Predicction of Swell Properties." *Proc. of 4th International Conference on Expansive Soils*, Denver, Colorado, pp.96-105.

102. Raymond, G. and Ismail, I. (2003). "The Effect of Geogrid Reinforcement on Unbound Aggregates." *Geotextile and Geomembranes 21*, pp.355-380.

103. Rollings Jr., R.S., Burkes, J.P., and Rollings, M.P. (1999). "Sulfate attack on cement-stabilized sand." *Journal of Geotechnical and Geoenvironmental Engineering*, *vol. 125 No.5,* pp.364-372.

104. Seed, H.B., Chan, C.K., and Lee, C.E., (1962). "Resilience Characteristics of Subgrade Soils and their Relation to Fatigue Failures in Asphalt Pavements." *Proc. of 1st International Conference on the Structural Design of Asphalt Pavements*, Ann Arbor, Michigan, pp.77-113.

105. Seed, H.B., Woodward, R.J., and Lundgren, R. (1962) "Prediction of swelling potential for compacted clays." *Journal of Soil Mechanics and Foundation Division ASCE*, Vol. 88 (SM3), pp. 53-87.

106. Segerlind, L. J. (1976). *Applied finite element analysis*. John Wiley & Sons, Inc. New York.

107. Sillers, W. S., and Fredlund, D. G. (2001). "Statistical assessment of soil-water characteristic curve models for geotechnical engineering." *Canadian Geotechnical Journal*, v 38, n 6, December, 2001, p 1297-1313.

108. Simulia support homepage. Abaqus Analysis User's Manual ver 6.7, http://aeweb.tamu.edu/v6.7/books/usb/default.htm?startat=book01.html, Accessed June 15, 2008.

109. Snethen, D. R. (1979b). "An Evaluation of methodology for prediction and minimization of volume change of expansive soils in highway subgrades." *Research Report No. FHWA-RD-79-49.*, U. S. Army Eng. Waterway Exp. Sta., Vicksburg, MS.

110. Snethen, D. R., and Johnson, L. D. (1980). "Evaluation of soil suction from filter paper." *Geotech. Lab.*, U.S. Army Eng. Waterway Exp. Sta., Vicksburg, Mississippi, Misc. Paper No. 6L-80-4.

111. Snethen, D. R. (1984). "Evaluation Of Expedient Methods For Identification And Classificaiton Of Potentially Expansive Soils." *National Conference Publication - Institution of Engineers, Australia*, n 84/3, 1984, p 22-26.

112. Snethen, D.R. (2001). “Influence of Local Tree Species on Shrink/Swell Behavior of Permian Clays in Central Oklahoma.” *Expansive Clay Soils and Vegetative Influence on Shallow Foundations*, pp.158-171.

113. Sridharan, A., Sreepada R. A., Sivapullaiah, P. V. (1986). “Swelling Pressure of Clays.” *Geotechnical Testing Journal*, v 9, n 1, Mar, 1986, p 24-33.

114. Stallings, S.L. (1999). “Roadside Ditch Design and Erosion Control on Virginia Highways.” *MS Thesis*, Virginia Polytechnic and State University, Blacksburg, Virginia, 170 pages.

115. Steinberg, M.L. (1992). “Vertical Moisture Barrier Update.” *Transportation Research Record 1362*. pp.111-117.

116. Stenke, F., Toll, D. G. and Gallipoli, D. (2006). “Comparison of Water Retention Curves for Clayey Soils Using Different Measurement Techniques.” *Proceedings of the Fourth International Conference on Unsaturated Soils*, Carefree, Arizona, USA, p. 1451-1461.

117. Thompson, M.R., (1966). “Lime Reactivity of Illinois Soils.” *Journal of the Soil Mechanics and Foundations Division, ASCE*, Vol. 92, No. SMS.

118. Thompson, M.R.(1982). “Highway Subgrade Stability Manual.” Illinois Department of Transportation, Departmental Policies, *MAT-10.*

119. Thornthwaite, C.W. (1948). “An Approach Toward a Ration Classification of Climate.” *Geographical Review*, pp.54-94.

120. Tucker, R.L. and Poor, A.R. (1978). “Field Study of Moisture Effects on Slab Movements.” *Journal of Geotechnical Engineer, ASCE*, 104(4), 403-415.

121. Tutumluer, E. and Kwon, J. (2005). “Evaluation of Geosynthetics use for Pavement Subgrade Restraint and Working Platform Construction.” *Proc. of 13th Annual Great Lakes Geotechnical/Geoenvironmental Conference on Geotechnical Applications for Transportation Infrastructure*, May 13, 2005.

122. Vijayavergiya, V. N. and Ghazzaly, O, I. (1973). "Prediction of Swelling Potential for Natural Clays." *Proc. of 3rd International Conference on Expansive Soils*, Haifa, Israel, Vol. 1, pp.227-236.

123. Ward, W. H. (1953). "Soil Movements and Weather." *Proceeding of 3rd International Conference Soil Mechanics*, Zurich, 2, 477-481.

124. Wattanasanticharoen, E. (2004). "Experimental Studies of Volume Change Behaviors of Chemically Treated Sulfate Bearing Soils." *PhD. Dissertation*, The University of Texas at Arlington, Arlington, Texas, 304 pages.

125. Wesseldine, M.A. (1982). "House Foundation Failures Due To Clay Shrinkage Caused by Gum Trees" *Transactions, Institution of Professional Engineers*, NZ, March, CE9(1).

126. White, D.J., Harrington, D. and Thomas, Z. (2005a). "Fly Ash Soil Stabilization for Non-Uniform Subgrade Soils, Volume I: Engineering Properties and Construction Guidelines." Iowa Highway Research Board Report: *IHRB Projectc TR-461; FHWA Project 4*.

127. White, D.J., Harrington, D. and Rupnow, T. (2005b). "Fly Ash Soil Stabilization for Non-Uniform Subgrade Soils, Volume II: Influence of Subgrade Non-Uniformity on PCC Pavement Performance." Iowa Highway Research Board Report: *IHRB Projectc TR-461; FHWA Project 4.*

128. Wray, W.K.; Ellepola, C.B. (1994). "Stresses Developed by Laterally Shrinking High-PI Clay." *Proc. of 8th International Conference on Computer Methods in Advanced Geomechanics*, vol. 4, p 1515-1526.

129. Zacharias, G. and Ranganatham, B.V. (1972). "Swelling and Swelling Characteristics of Synthetic Clays." *Proceedings of Symposium on Strength and Deformation Behavior of Soils, Vol. 1,* pp. 35-46.

BIOGRAPHICAL INFORMATION

Thammanoon Manosuthikij was born in Bangkok, THAILAND. He graduated from Chulalongkorn University, Bangkok, THAILAND, with a Bachelor's Degree in Civil Engineering in 1997. After working as a site and designer engineer for 4 years, he obtained Royal Thai Government Scholarship for continuing Master's Degree in Mining and Earth System Engineering at Colorado School of Mines, Colorado. After graduated in 2002, he worked as a Geological Engineer in Thai Royal Irrigation Department, Ministry of Agriculture and Co-operatives, Bangkok, THAILAND for 4 years. His works related to performing geological mapping and surveying at dam sites for rock/soil classifications and quality ratings, identifying potential types of rock/soil failures at dam sites, determining rock excavation and/or blasting methods for slopes and tunnels, and designing and inspected dam's foundations improvements by slurry grouting method.

In 2006, he pursued doctoral program in the Department of Civil and Environmental Engineering at the University of Texas at Arlington (UTA), Arlington, Texas with Geotechnical Engineering as the major area of research. At UTA, he performed research in studies on expansive soils behaviors under the guidance of Prof. Anand J. Puppala and successfully defended his dissertation in July 2008. During the course of his study, he worked in various research areas related to field instrumentation, ground improvement, soil suction testing, and expansive soils behaviors.